An improved efficiency model for ACE/SWICS - Determination of the carbon isotopic ratio $^{13}C/^{12}C$ in the solar wind from ACE/SWICS measurements

Dissertation
zur Erlangung des Doktorgrades
der Mathematisch-Naturwissenschaftlichen-Fakultät
der Christian-Albrechts-Universität
zu Kiel

vorgelegt von
Dipl.-Phys. Muharrem Köten

Kiel im März 2009

Referent/in : _____

Korreferent/in : _____

Tag der mündlichen Prüfung : _____

Zum Druck genehmigt : _____

_____
Der Dekan

Zusammenfassung

Die Element- und Isotopen-Zusammensetzung schwerer Ionen im Sonnenwind liefert wertvolle Informationen über die Zusammensetzung des präsolaren Nebels, da in der Sonne keine schwereren Elemente als Helium durch Kernfusion synthetisiert werden. Daher kann die solare Zusammensetzung als Bezugspunkt zum Nachweis eventuell vorhandener Abweichungen in unterschiedlichen Regionen des Sonnensystems verwendet werden. Besonders der Vergleich der Isotopen-Zusammensetzung extraterrestrischer Proben mit der des präsolaren Nebels liefert Hinweise über die frühe Entwicklung des Sonnensystems. Diese Arbeit befaßt sich mit dem Studium der Isotopen-Zusammensetzung des vierthäufigsten Elementes im Sonnensystem, Kohlenstoff, oder genauer, der Untersuchung des Verhältnisses der beiden stabilen Kohlenstoff-Isotope ^{12}C und ^{13}C. Hierfür haben wir Messungen von ACE/SWICS, einem linearen Flugzeit-Massenspektrometer, welches am 1. Lagrange-Punkt positioniert ist, verwendet. Zum Zweck einer detaillierten Datenanalyse haben wir ein Effizienzmodell für das Instrument entwickelt.

Da Kohlenstoff ein hochgradig volatiles Element ist, ist die relative Häufigkeit verglichen mit fraktionären Elementen auf der Erde sehr viel niedriger im Vergleich zur Element-Zusammensetzung der Sonne. Es kann davon ausgegangen werden, daß die Isotopen-Zusammensetzung der Sonne und des Sonnenwindes ähnlich der der Erde sind. Eine mögliche Abweichung zwischen der Zusammensetzung der Sonne und der des Sonnenwindes würden darauf hindeuten, daß während der Sonnenwindentstehung massenabhängige Fraktionierungsprozesse ablaufen. Bis zum heutigen Zeitpunkt existieren lediglich Publikation, in denen die Kohlenstoff-Zusammensetzung der Sonne spektroskopisch bestimmt wurde (für einen Überblick siehe *Woods and Willacy* [2009], *Woods* [2009] und *Harris et al.* [1987]). Diese Bestimmungen basieren auf Messungen von CO Absorptionslinien. Größtenteils belegen bisherige Resultate, daß der solare Wert ähnlich dem terrestrischen Wert ist, z. B. fanden *Harris et al.* [1987] einen Wert von ^{12}C/^{13}C $= 84 \pm 5$. Im Rahmen dieser Arbeit wurde erstmals dieses Isotopenverhältnis im Sonnenwind durch in-situ Messungen bestimmt mit dem Ergebnis ^{12}C/^{13}C $= 97,7^{+10.3}_{-9.3}$. Innerhalb der Fehlerbalken stimmen sowohl der hier bestimmte

Wert als auch der Wert von *Harris et al.* [1987] mit dem terrestrischen Verhältnis von etwa ^{12}C$/^{13}$C ≈ 89 überein.

Abstract

The elemental and isotopic composition of heavy ions in the solar wind is a source of information about the composition of the presolar nebula because there is no synthesis of heavy ions from helium due to nuclear burning in the Sun. Thus, the solar composition can be used as a baseline for the detection of eventual spatial deviations in the solar system. Especially the isotopic composition of different extraterrestrial samples compared to the composition of the presolar nebula can provide information about the early evolution of the solar system. The focus of this work is to study the solar isotopic composition of the fourth most abundant solar wind ion, carbon, especially the ratio of the two stable isotopes ^{12}C and ^{13}C. For that we have used measurements of ACE/SWICS, a linear Time-of-Flight mass spectrometer which is positioned at L1. For the purpose of a detailed analysis of these data we have developed an advanced efficiency model of the instrument.

Carbon is a highly volatile element and therefore, the terrestrial abundance with respect to non-volatile elements is lower than is observed for solar elemental composition. Nevertheless, it is assumed that the solar carbon isotopic composition as well as the composition of the solar wind is similar to the terrestrial one. A possible deviation between the solar and the solar-wind composition would indicate mass dependent fractionation processes in solar-wind evolution. All previous measurements of the solar carbon-isotopic ratio were accomplished via spectroscopic observations (for an overview see *Woods and Willacy* [2009], *Woods* [2009], and *Harris et al.* [1987]). These determinations are based on measurements of CO absorption lines in the solar electromagnetic radiation spectrum. Most of the previous results show that the solar value is similar to the terrestrial one, e. g. *Harris et al.* [1987] found ^{12}C/^{13}C $= 84 \pm 5$. For the first time we have determined that ratio in the solar wind by in-situ measurements and found ^{12}C/^{13}C $= 97.7^{+10.3}_{-9.3}\%$. Within the error bars both ratios are consistent with the terrestrial ratio of about ^{12}C/^{13}C ≈ 89.

Contents

1. INTRODUCTION

As the title of this thesis indicates this work deals with two topics which are connected with each other. The first part deals with the development of an efficiency model for the SWICS (Solar Wind Ion Composition Spectrometer) instrument that is used to measure the elemental and charge state composition of solar wind ions and suprathermal particles in space. SWICS is a linear Time-of-Flight mass spectrometer and one of the instruments mounted on the ACE (Advances Composition Explorer) space probe which was launched in 1997 and since then positioned at L1.

The efficiency model presented here provides two fundamental contributions for a comprehensive analysis of the ACE/SWICS data. The model allows to calculate the detection probability depending on mass, charge and velocity of the incoming particles. These efficiencies are essential to derive physical quantities which describe the properties of the solar wind ions, e.g. temperatures, densities, and absolute fluxes, from the data we get from the instrument in space. It can also be used to calculate the positions of all solar winds ion in the so called ET-matrices (see section 4.2). The data products the efficiency model delivers are presented in chapter 5 and in appendix A. The efficiency model includes all relevant components of the instrument and the interactions between the incoming particles and the different instrument components.

In chapter 3 we give an overview about the functional breakdown of the instrument. The items discussed in this context are

- the selection of the ions in the deflection system,

- the focussing effect of an ion beam due to the post acceleration,

- the energy loss of different ion species by passing the thin carbon foil,

- the energy measurement with the solid state detectors (SSD),

- the Time-of-Flight (ToF) measurement via secondary electrons which are ejected by the ions passage through the foil and its impact on the solid state detector (SSD) surface.

In chapter 4 the calibration of the instrument is described which can be split into two parts, the Pre-Flight Calibration (PFC) which is based on data measured before launch, and the In-Flight Calibration (IFC) which is based on measurements of the instrument in space. The method of the PFC is described here very shortly but in detail in *Köten* [2005]. The results presented here are not just a repetition of *Köten* [2005] but a continuation because, for the purpose of a more detailed data analysis with regard to the detection of the carbon isotopic composition, the model needed to be improved.

The second focus of this work is the determination of the isopotic ratio of the two stable carbon isotopes $^{12}_{6}C$ and $^{13}_{6}C$ in the solar wind. Why are we interested in this ratio? For that first we have to answer the question, where the carbon does come from.

Carbon is the fourth most abundant element in the solar system. It does not originate from nucleosynthesis processes in the Sun but was one of the components of the presolar nebula the

solar system originates from. Carbon is synthesized during the helium burning stage in the core of stars due to the tripe-alpha process. As the name implies in this case three helium nucleis are fused to one carbon nuclei. These stars, so-called AGB stars or red giants, can undergo periodic radial oscillations resulting in a convection of the carbon from the core to the surface and dredge the fusion products into interstellar space. On their way from the core to the surface of the star a certain fraction of these ^{12}C atoms is converted to ^{13}C due to a proton capture with a subsequent beta decay. By the way, these are the first two steps of the CNO-cycle which is described in chapter 2. However, it is not the purpose of this work to locate and quantify these presolar-time events but we can assume that there was a certain fraction of the presolar nebula consisting of ^{12}C and a much smaller fraction consisting of ^{13}C.

In general, the analysis of the isotopic composition of different samples is a source of information about the conditions which were dominating during the condensation of the respective source of the samples. Especially, the today's isotopic composition of volatile elements like H, C, N, O, and the noble gases can provide information about the history of degassing and the atmospheric evolution of planets. This brings us back to the initial question. The answer is, actually we are interested in the isotopic composition of the presolar nebula as a baseline of the starting conditions of the solar system. The composition of the outer convection zone (OCZ) of the Sun and the solar wind is assumed to represent the isotopic composition of the presolar nebula for most elements with presumably small deviations.

In this context and with regard to the analysis of the solar carbon isotopic ratio it is worth mentioning that in fact ^{13}C is produced in the core of the Sun at the expense of ^{12}C due to the CNO-cycle. However, in this process ^{12}C just serves as a catalyst and is reproduced at the end of the cycle. The intermediate ^{13}C isotopes remain in the core and do not reach the convection zone until they are destroyed and converted to ^{14}N by a proton capture.

The deviations mentioned above can be caused by two effects which have to be considered. The first is the mass-dependent gravitational settling in the OCZ. For example, current models for the calculation of the gravitational settling effects predict a fractionation of the considered carbon isotopes on the order of about 0.5 % (*Wiens et al.* [2004]). Deviations on that order of magnitude are difficult to measure because spectroscopic observations are less precise. The second effect consists of mass dependent fractionation processes during the solar wind origination and propagation. In this context the Coulomb drag effect (*Bochsler et al.* [2006]) was supposed to enrich lighter isotopes in the solar wind compared to the relative isotopic abundances in the OCZ. However, the predictions of this theory concerning the isotopic enrichment or depletion, which are on the order of about a few percent per amu, and their experimental verifications are still matter of current research and will not be discussed in this work.

There are different ways to measure the elemental and isotopic composition of the Sun or especially of the OCZ.

- spectroscopic observations of the photosphere,

- solar wind measurements from

    - Solar Wind Composition (SWC) experiments with specialized foils exposed to the solar wind as has been accomplished during the Apollo missions on the lunar surface,

    - the analysis of planetary or lunar regoliths and asteroids,

    - in-situ measurements with instruments in space

In this work we have concentrated on the analysis of the solar wind composition based on in-situ measurements of the instrument (SWICS) described above briefly and in detail in chapter 3. SWICS was originally designed to measure the elemental and charge-state composition of the solar wind and not the isotopic composition. There are similar instruments in space which were designed to measure the isotopic composition of the solar wind, e.g CELIAS/MTOF on SOHO (*Kallenbach et al.* [1997a]) or SWIMS (Solar Wind Ion Mass Spectrometer) on ACE (*Gloeckler et al.* [1998]), but these instruments have a crucial disadvantage for the measurement of the isotopic composition of carbon because the design of these instruments does not allow to distinguish between the carbon ions related to the solar wind and those ejected from a thin carbon foil which is implemented in these instruments and the incoming particles have to pass through.

In chapter 6 we present the method of the detection of both considered carbon isotopes from the ACE/SWICS data and the determination of the corresponding isotopic ratio. In this context we turn our attention to the instrumental response function and the data selection. Finally, the results are presented in chapter 7.

1. INTRODUCTION

2. THE SUN

As an introduction first we will give some basic facts about the Sun.

- Classification: The Sun is a medium scale star belonging to the calss of yellow dwarfs. With a surface temperature at the photosphere of about 5800 Kelvin, in the Hertzsprung-Russel diagram the Sun belongs to the main sequence with stellar classification G2.

- Measures and composition: The solar diameter is about 1.4 million km and its mass amounts $1.99 \cdot 10^{30}$ kg which concludes in a average density of $1400 \, \text{kg/m}^3$. It contains about 99.9 % of the mass in the solar system which consists to about 72 % of hydrogen and about 26 % of helium. The remaining fraction consists of heavy elements whose most prominent representatives are oxygen and carbon (*Prölls* [2004]).

- Rotation: The Sun rotates differentially depending on the degree of latitude resulting in a rotation period that extends from 25.4 days at the equator to about 36 days near the poles.

- Magnetic field: The orientation of the magnetic field depends on the 22-years cycle of the Sun. Every eleven years the magnetic poles change their polarity. Thus, after 22 years the magnetic field again has the start configuration. During quiet phases it can be approximated by a dipole field.

A more detailed description of the solar magnetic field, the corresponding 22-years cycle, and the inner structure of the Sun is given in *Stix* [2004].

2.1. Origin of the Sun

The Sun formed about 4.6 billion years ago from the presolar nebula, a cloud consisting to about 98 % of hydrogen and helium. The remaining fraction consisted of heavy elements beyond helium in the periodic system of the elements which were probably supernova remnants from much bigger stars than the Sun in the 'neighbourhood'. Probably, disturbances from these supernova explosions caused a gravitational collapse of the gas cloud. A part of the gravitational energy was converted to heat until the temperature in the center of the gas ball was high enough that hydrogen fused to helium. The high temperature in the core caused a pressure in outward direction which compensated the gravitational pressure inwards. The starting amount of hydrogen is enough to hold this state of equilibrium about 10-12 billion years, thus the Sun will burn further at least about 5-7 billion years.

2.2. Nucleosynthesis in the Sun

As described above the Sun is a gas ball which consists mainly of hydrogen. The source of energy are fusion processes in the core. At temperatures of about 15 million Kelvin the so-called

hydrogen-burning proceeds and helium is generated. In this case, four protons fuse to an α-particle. Comparing the involved masses before and after the fusion process respectively, shows that a certain fraction of the mass is lost and converted to energy which can be calculated by the fundamental relation $\Delta E = \Delta m \cdot c^2$. There are two ways of producing helium from hydrogen, the pp-chain and the CNO-cycle.

At temperatures which are dominating in the cores of stars, which are on the order of magnitude of the Sun and belong to the Population I stars, the dominating fusion process is the pp-chain according to *Unsöld* [2005]. This process is described very briefly in the following reaction chain:

$$^{1}\text{H} + {}^{1}\text{H} \rightarrow {}^{2}\text{D} + \text{e}^{+} + \nu$$
$$^{2}\text{D} + {}^{1}\text{H} \rightarrow {}^{3}\text{He} + \gamma$$
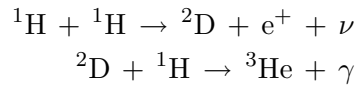
With the basic product ^{3}He there are three ways to generate ^{4}He. These different processes are called ppI ($\Delta E = 26.23$MeV), ppII ($\Delta E = 25.67$MeV), and ppIII ($\Delta E = 19.28$MeV).

$$\text{ppI}: \quad {}^{3}\text{He} + {}^{3}\text{He} \rightarrow {}^{4}\text{He} + {}^{1}\text{H} + {}^{1}\text{H}$$

$$\text{ppII}: \quad {}^{3}\text{He} + {}^{4}\text{He} \rightarrow {}^{7}\text{Be} + \gamma$$
$$^{7}\text{Be} + \text{e}^{-} \rightarrow {}^{7}\text{Li} + \nu$$
$$^{7}\text{Li} + {}^{1}\text{H} \rightarrow {}^{4}\text{He} + {}^{4}\text{He}$$

$$\text{ppIII}: \quad {}^{3}\text{He} + {}^{4}\text{He} \rightarrow {}^{7}\text{Be} + \gamma$$
$$^{7}\text{Be} + {}^{1}\text{H} \rightarrow {}^{8}\text{B} + \gamma$$
$$^{8}\text{B} \rightarrow \text{e}^{+} + {}^{8}\text{Be} + \nu$$
$$^{8}\text{Be} \rightarrow {}^{4}\text{He} + {}^{4}\text{He}$$
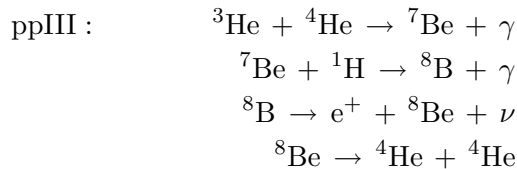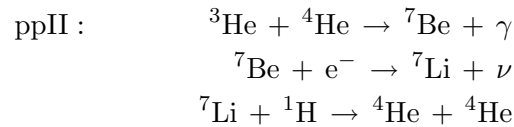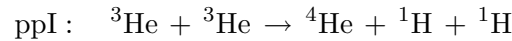
The second contribution to the mass-to-energy conversion is provided by the CNO-cycle which is described by the following reaction chain:

$$^{12}\text{C} + {}^{1}\text{H} \rightarrow {}^{13}\text{N} + \gamma \quad (1.3 \cdot 10^{7}\,\text{a})$$
$$^{13}\text{N} \rightarrow {}^{13}\text{C} + \text{e}^{+} + \nu \quad (7\,\text{min})$$
$$^{13}\text{C} + {}^{1}\text{H} \rightarrow {}^{14}\text{N} + \gamma \quad (2.7 \cdot 10^{6}\,\text{a})$$
$$^{14}\text{N} + {}^{1}\text{H} \rightarrow {}^{15}\text{O} + \gamma \quad (3.2 \cdot 10^{8}\,\text{a})$$
$$^{15}\text{O} \rightarrow {}^{15}\text{N} + \text{e}^{+} + \nu \quad (82\,\text{sec})$$
$$^{15}\text{N} + {}^{1}\text{H} \rightarrow {}^{12}\text{C} + {}^{4}\text{He} \quad (1.12 \cdot 10^{5}\,\text{a})$$
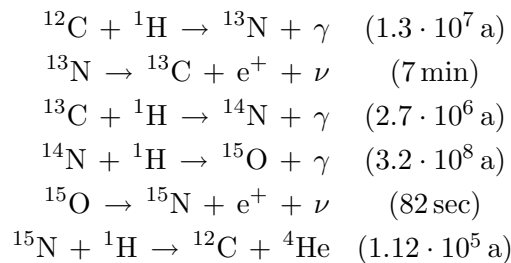
Assuming a star with the solar chemical composition but with a core temperature of about 18 million Kelvin the number of CNO-cycle processes would be on the same order of magnitude

as the pp-chain processes (*Unsöld* [2005]), but in the case of the Sun only 1.6 % of the total energy conversion is provided by the CNO-cycle. Due to the CNO-cycle the abundances of the participating nitrogen and oxygen isotopes, and ^{13}C increase at the expense of ^{12}C. In this process ^{12}C serves only as a catalyst and is reproduced at the end of the cycle. The temporarily generated ^{13}C ions remain in the core and do not reach the convection zone until they are destroyed and converted to nitrogen by a further proton capture.

This is the present status. For the sake of completeness we will describe very briefly the further burning stage which will occur in about 5-7 billion years from now. When the bigger part of the hydrogen is converted to helium the temperatures in the core will go up to about 100 million Kelvin. In that case the helium burning will be ignited where three α-particles fuse to carbon which is called the triple-α-process. Through accretion of further α-particles oxygen, neon, magnesium, and silicon can also be generated. However, the generation of trans-oxygen elements is possible but very unlikely due to quantum-mechanical reasons according to *Burbidge et al.* [1957].

Generally, there are further burning stages whose ignition depends on the mass of the star and thus which temperatures can be reached in the core according to the different periods of the lifetime of the star. For example, for the ignition of the next burning stage (the carbon-burning) the mass of the star must be four times bigger than the mass of the Sun. Thus, the Sun will end as white dwarf mainly consisting of carbon and oxygen.

Nevertheless, in the further burning stages of much bigger stars than the Sun elements up to iron are fused from lighter elements. Heavier elements than iron can only be generated in supernovae because there is a negative energy gain by fusing elements beyond iron in the periodic system of elements. The theory of the origin of heavy elements including the trans-iron elements are described in detail in *Burbidge et al.* [1957] and *Wallerstein et al.* [1997].

The abundances of heavy elements (up to Z=26 or higher) in the solar system, which do not originate from nucleosynthesis processes proceeding in the solar core, is an evidence that the solar system consists at least partially of matter remaining from considerably bigger stars than the Sun, whose life ended with supernova explosions.

2.3. Solar wind

The solar wind is a highly ionized plasma that streams radially away from the Sun. The mass loss of the Sun due to the solar wind is on the order of about a few billion kg per second. About 95 % of the particles in the solar wind ions are protons, about 5 % consist of helium, and less than 1 % consist of heavy ions with masses beyond helium in the periodic system of the elements.

Generally, there are two types of solar wind. The slow solar wind with velocities of about 400 km/s originates from regions close to closed magnetic field regions in the solar corona, whereas the fast solar wind with velocities of about 800 km/s originates from coronal holes. The mechanisms leading to the escape of the highly ionized plasma from the Sun are not understood in detail yet but it is matter of actual research. An overview of current state of theories is given in *Aschwanden* [2004] and in *Hollweg* [2006]. There are a couple of parameters which can be used to characterize the state of the solar wind. The main parameters are velocity, density and temperature of the solar wind whereas these quantities can vary for different ions and electrons and the configuration and strength of the magnetic field. Additionally, ratios of different ion abundances can be used to determine quantities like the freezing-in temperature of the solar wind plasma. As an example, Figure 2.1 shows a sample of solar wind parameters measured

with the instruments SWEPAM and SWICS on ACE in the period of time of the first 30 days in 2007.

The analysis of the elemental and isotopic composition of the solar wind is important for the understanding of the processes in the Sun, the solar atmosphere, and the interplanetary medium. Additionally, the determination of temperatures, velocities, and densities of particles escaping from the solar surface provides a large source of information about the acceleration processes in the interplanetary medium.
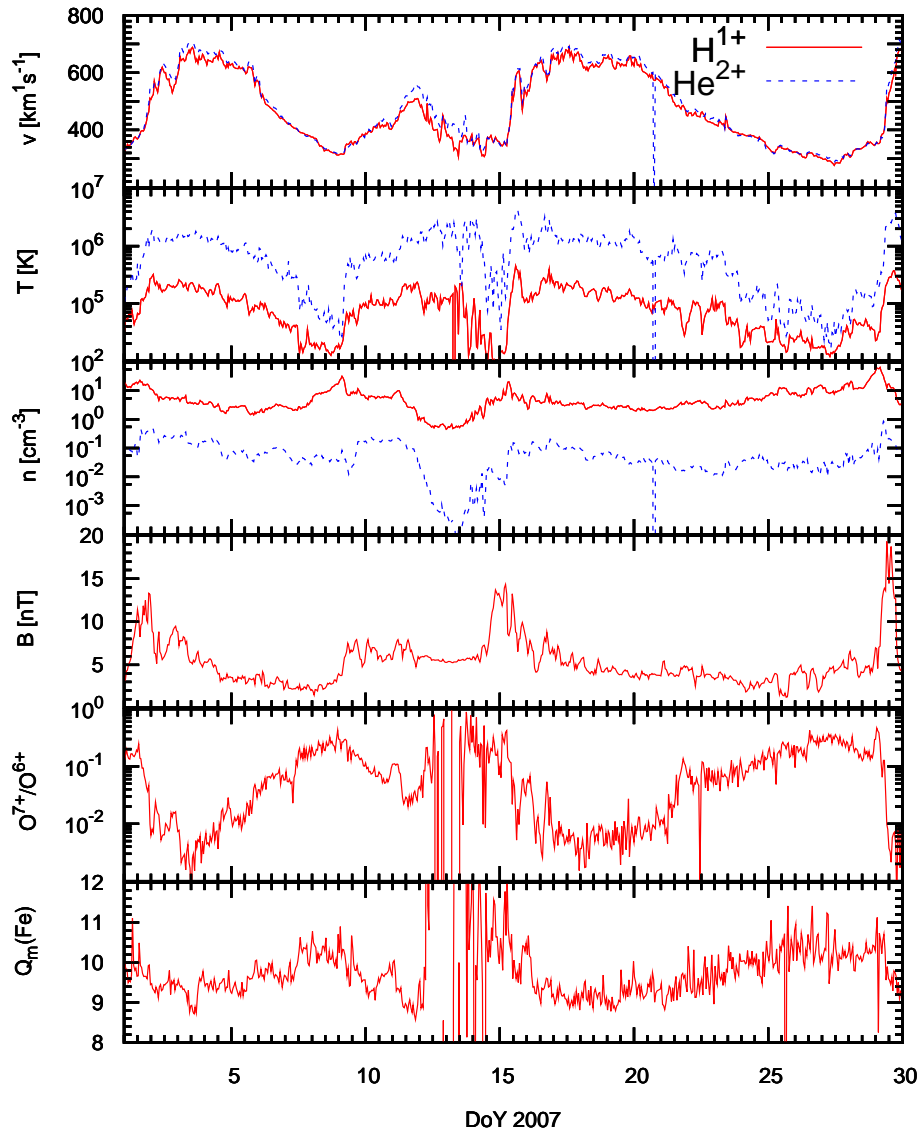
Figure 2.1.: Sample of solar wind parameters in the time-period of the first 30 days of the year 2007 measured with ACE/SWEPAM and ACE/SWICS at 1 AU. The first three panels show the solar wind speed, the ion temperature and the ion density of H^+ and He^{2+}. Periods with slow solar wind alternate with periods with fast solar wind. The density of the solar wind at 1 AU which is dominated by the most abundant ion H^{1+} is depending on the solar wind regime on the order of about $5-20/cm^3$. The fourth panel shows the strength of the magnetic field. Panel 5 shows the ratio of the fluxes of the O^{7+} and O^{6+} and panel 6 shows the mean charge-state of iron. Both are tracers for the freezing-in temperature. In this context freezing-in temperature denotes the temperature at a certain height above the corona where the coronal plasma becomes so rare that the ions do not interact with the surrounding electrons anymore and the charge-states of the ions at that moment are frozen-in.

3. ACE/SWICS

The Advanced Composition Explorer (ACE) is a NASA mission that was launched on August 25, 1997. Since then the space probe is located at L1 and therefore in a corotating orbit with the Earth around the Sun. There are various instruments on board to measure the elemental and isotopic composition of the solar wind and of particles in the heliosphere. One of them is the Solar Wind Ion Composition Spectrometer (SWICS) (*Gloeckler et al.* [1992]). It measures the elemental and charge-state composition of the solar wind and of suprathermal particles in the energy range from about 0.6 keV/e up to about 100 keV/e. SWICS is a linear Time-of-Flight (ToF) mass spectrometer with electrostatic deflection. Figure 3.1 is a picture of the instrument. A very short description of the different instrument components is given in the corresponding caption.
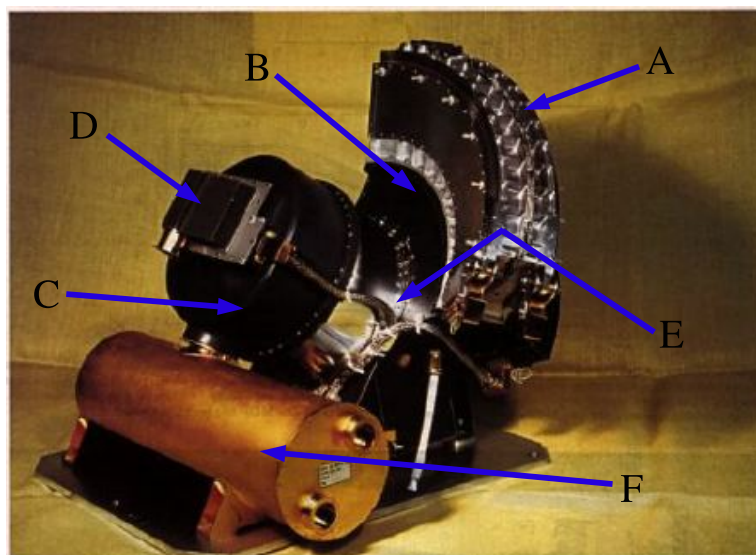
Figure 3.1.: Picture of the Solar Wind Ion Composition Spectrometer (SWICS) instrument. The top of the fan-shaped portion on the upper right (A) is the mechanical collimator with a protective cover in place (this cover swung open after launch). Immediately below the collimator is the electrostatic deflection array (B). The black cylindrical portion in the middle contains the analog and digital electronics and the sensor power supplies (C). Topping that section is the opto-coupler box that transmits signals to the DPU (Data Processing Unit) across a vacuum gap between inner and outer housings (D). Not clearly visible but indicated with the arrow (E) is the position of the Time-of-Flight section. The gold plated cylinder on the left of the instrument is the 30 kV power supply (F). The picture was taken from the internet site of the original institution *http : //space.umd.edu/umd_sensors/swics.html*.

3.1. Introduction to Time-of-Flight mass spectrometers

A single solar wind ion is fully characterized by its velocity $\vec{v} = (v_x, v_y, v_z)$, mass m, and charge q. If the flight trajectory is of less interest the full characterization is also given by the energy E, mass m, and charge q. A Time-of-Flight (ToF) mass spectrometer like SWICS is an instrument that can be used to determine these quantities. In this chapter we give a very short overview of the operational breakdown of ToF mass spectrometers. The following general description also describes similar instruments like PLASTIC (PLAsma and Suprathermal Ion Composition) on STEREO (Solar TErrestrial RElations Observatory) or CELIAS (Charge, ELement, and Isotope Analysis System)/CTOF on SOHO (SOlar and Heliospheric Observatory).

In the first step the ions are selected by their energy per charge. This is achieved by applying a defined voltage to two curved electrodes. Only those ions are selected that satisfy the condition that the centrifugal force be equal to the electric force

$$qE_0 = \frac{m|\vec{v}|^2}{r}.$$ (3.1)

E_0 is the electric field strength between the electrodes and r is the radius of curvature of the deflection system. Assuming that E_0 can be approximated locally to behave like the electric field strength between two parallel plates of a capacitor and neglecting edge effects we obtain

$$E_0 = \frac{U}{d},$$ (3.2)

and therefore the energy per charge $\frac{E_1}{q}$ of the passing particles is given by

$$\frac{E_1}{q} = \frac{m\vec{v}^2}{2q} = U\frac{r}{2d}.$$ (3.3)

Figure 3.2 shows a sketch of an electrostatic deflection system. Assuming that $\Delta r = \frac{d}{2}$ we can estimate the energy-per-charge interval $\frac{E}{q} \pm \Delta\frac{E}{q}$ of ions that pass through such a deflection system. We obtain for $\Delta\frac{E}{q}$ and $\frac{\Delta E/q}{E/q}$ respectively:

$$\Delta\frac{E}{q} = U\frac{\Delta r}{2d} = U\frac{d}{4d} = \frac{U}{4},$$ (3.4)

$$\frac{\Delta E/q}{E/q} = \frac{U\frac{\Delta r}{2d}}{U\frac{r}{2d}} = \frac{d}{2r} \approx 5\%.$$ (3.5)

After passing the deflection system the ions are accelerated by a post acceleration voltage U_{acc}. A ToF mass-spectrometer would also work without that post acceleration. The reason for the acceleration is to lift the kinetic energy of the ion above the threshold of the solid state detector for the energy measurement. For example U_{acc} in SWICS on ACE is about -25 kV. Thus, the total energy after the post acceleration E_2 is then given by

$$E_2 = E_1 + qU_{\text{acc}},$$ (3.6)

Then the ion passes through a thin carbon foil. The interaction of projectile and target material decelerates the ion and thus causes an energy loss ΔE. The total energy after the foil E_3 is then given by

$$E_3 = E_2 - \Delta E = E_1 + qU_{\text{acc}} - \Delta E$$ (3.7)
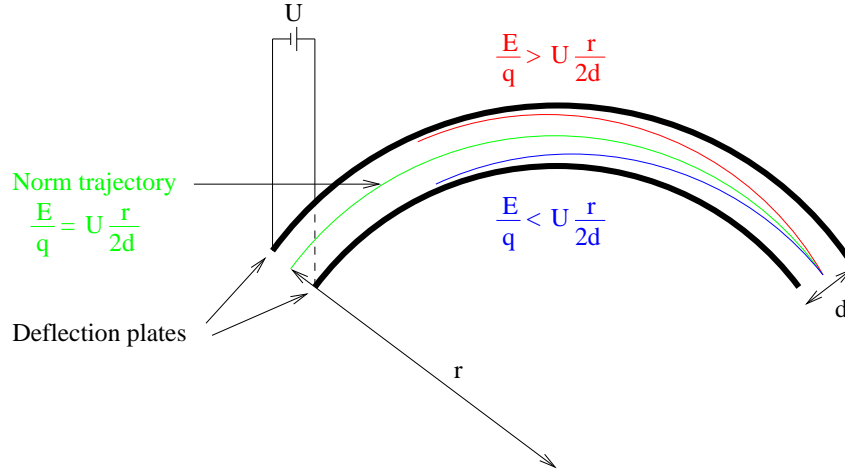
Figure 3.2.: Schematic view of a spherical electrostatic deflection system. The power supply induces a potential U between the inner and the outer deflection plate. The figure shows three trajectories which correspond to three different $\frac{E}{q}$ values. The ions enter the system from the right. The green trajectory indicates the norm trajectory of an ion that satisfies the equation 3.3 in opposite to the red and the blue curve which hit the outer and the inner deflection plate respectively.

The energy of the ion after the foil is measured with a solid state detector (SSD). The measured energy is not equal to E_3 but a fraction thereof and is given by

$$E_{\text{meas}} = \eta E_3. \tag{3.8}$$

η is a unitless value between 0 and 1 and depends on the energy and mass of the projectile and on the properties of the SSD. Between carbon foil and SSD is a more or less force-free gap, the so-called time-of-flight section. For example, the length of that distance is about 10 cm in SWICS and about 8 cm in PLASTIC.

By the ion's passage through the foil and its impact on the SSD surface the emission of so-called secondary electrons is induced. These electrons are detected by two different Micro Channel Plates (MCP) and trigger the start- and a stop-signal respectively for the time-of-flight measurement. An MCP is an electron multiplier which can be very efficiently used to detect even single electrons. The operational breakdown is schematically shown in Figure 3.3.

Summing up, the instrument makes three measurements

- Selection by energy per charge $\frac{E_1}{q}$

- Time-of-flight measurement τ

- Energy measurement E_{meas}

For a post acceleration voltage of about 25 kV, as it is applied in the SWICS instrument on ACE, *Bodmer* [1992] found an empirical formula for the energy loss in the carbon foil depending on the charge state of the ion and on the foil thickness t, given in units of $\mu g/cm^2$

$$\frac{\Delta E}{q} = (0.5 \frac{kV}{\mu g/cm^2} \pm 30\%) \cdot t. \tag{3.9}$$

13
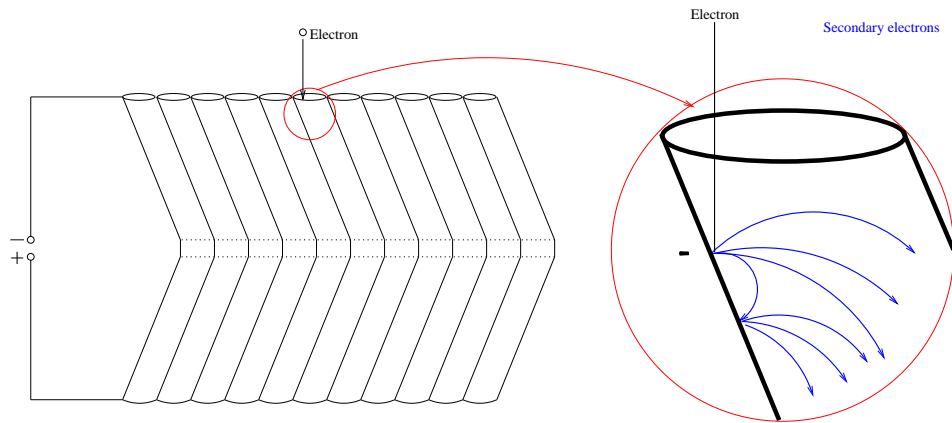
Figure 3.3.: Schematic view of a cut through an MCP stack. The electrons enter the small channels with a diameter of typically less than 10μm from the top. When they hit the inner surface secondary electrons are ejected. By an electrostatic potential gradient these electrons are accelerated to the bottom and again hit the inner surface of the tubes. Finally, the electron cascade can be detected as an electronic current to trigger the start- and the stop-signal for the ToF measurement.
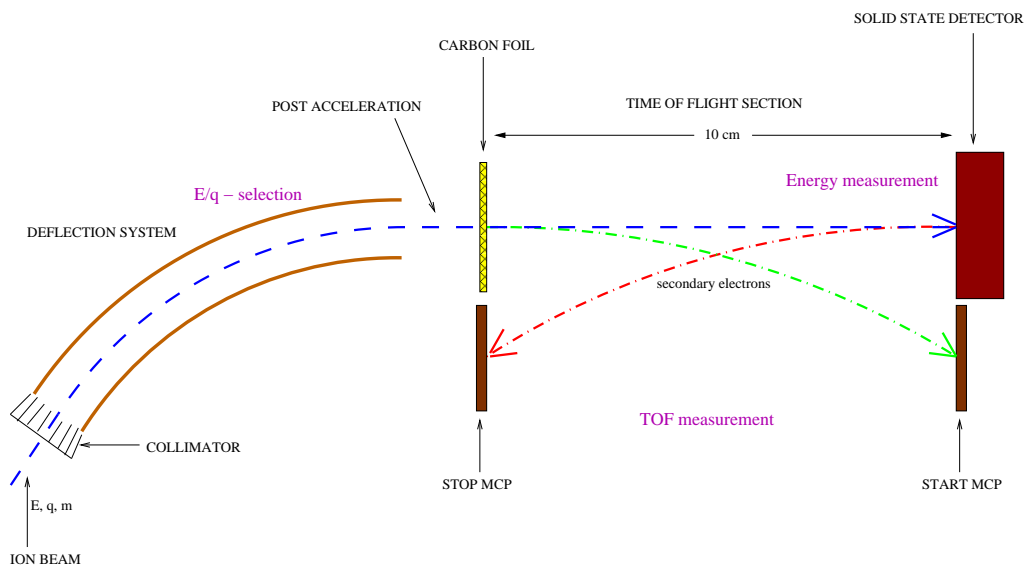
Figure 3.4.: Schematic view of the inner working of SWICS. The ions enter the instrument through the curved deflection system where they are selected by their energy per charge. Afterwards the ions become post accelerated and pass a thin carbon foil. As an example the trajectory of an ion leading to the SSD at the end of the time-of-flight section is plotted in blue. The nominal trajectories of the secondary electrons emitted from the carbon foil and from the SSD surface are plotted in green and red respectively. By the energy-per-charge selection, the time-of-flight-, and the energy measurement the ion is fully characterized in its properties energy E, mass m, and charge q

Additionally assuming that we know η as a function of mass and energy of the particle, the quantities initial energy E_1, mass m, and charge q are then given by

$$E_1 = \frac{\frac{E_1}{q} \cdot E_{\text{meas}}}{\eta \cdot (\frac{E_1}{q} + U_{\text{acc}} - \frac{\Delta E}{q})}, \tag{3.10}$$

$$q = \frac{E_{\text{meas}}}{\eta \cdot (\frac{E_1}{q} + U_{\text{acc}} - \frac{\Delta E}{q})}, \tag{3.11}$$

$$m = \frac{2q\tau^2}{s^2} \cdot (\frac{E_1}{q} + U_{\text{acc}} - \frac{\Delta E}{q}). \tag{3.12}$$

As an example for a time-of-flight mass spectrometer, Figure 3.4 schematically shows the inner working of the SWICS instrument including all relevant components.

3.2. Entrance system

The entrance system of SWICS is described in detail in *Bodmer* [1992]. The model described in this work starts its calculations after the deflection system. For the sake of completeness we will give some fundamental information about the entrance system.

Mounted right in front of the deflection system is a mechanical collimator which guarantees the selection mainly of those particles with a flight trajectory parallel to the normal of the entrance slot.
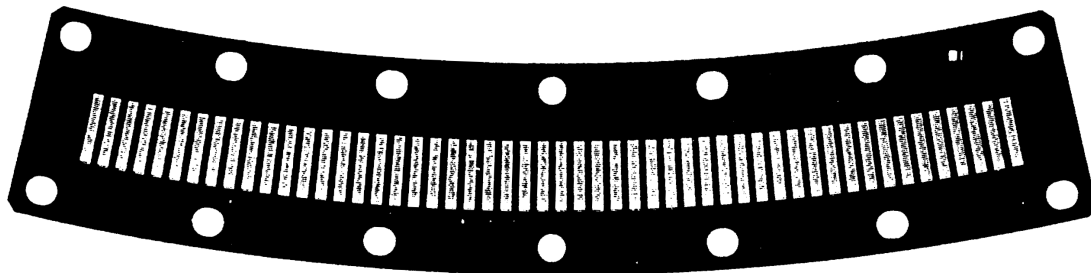
Figure 3.5.: Planed view of the front plate of the mechanical collimator. There are 52 slits (2mm each) in horizontal and 37 slits (0.18 mm each) in vertical direction.

Figure 3.5 shows an image of the surface of the collimator that consists of 52 slits in horizontal direction with about 2 mm length each and 37 slits in vertical direction of about 0.18 mm each. The extent of the collimator in the direction perpendicular to the surface is 35 mm. It consists of a stack of 18 parallel plates with a gap in-between to minimize the possible effect that ions are reflected from the inner surface of the collimator channels and enter the deflection system with a non-predictable trajectory. Additionally the plates are blackened with copper sulphide (CuS) to avoid that ultraviolet rays enter the instrument. The three-dimensional geometry of the collimator is not plane but spherical. The exact calculations described in *Bodmer* [1992] result in the following characteristic values. For each channel the angular acceptance is about 3.54° and 0.295° in horizontal and vertical direction respectively. The spherical geometry provides an angle of view of about 45° and 4° in horizontal and vertical direction respectively.

Figure 3.6 shows a side view of the deflection system including the trajectories of a sample of ions. Two significant effects can be observed considering an ion beam passing through the entrance system. First, due to the ion-optical effect of the electrostatic field between the deflection plates the ion beams are deflected. Second, the geometry of the deflection system is optimized to focus a parallel entering ion beam on a slit of 1 mm width at the end of the entrance system. Due to that focussing effect the beam profile becomes smaller. Additionally, a sample of ions, even if they pass the entrance slit with parallel trajectories, has an angular divergence at the exit slot. Among other things that property of an ion beam was analyzed in *Bodmer* [1992] depending on the trajectory while passing the entrance slit.

After the deflection system the ions become accelerated. In addition to the increase of the kinetic energy of a single particle the divergence of the beam profile is reduced. That effect is described below by means of the trajectory of a single ion that leaves the deflection system with a non-vanishing angle related to the normal of the exit slit surface.

In the example shown in Figure 3.7 the trajectory of the ion is chosen to pass the center of the exit slit with width s_1. The angle between the trajectory and the normal of the exit slit
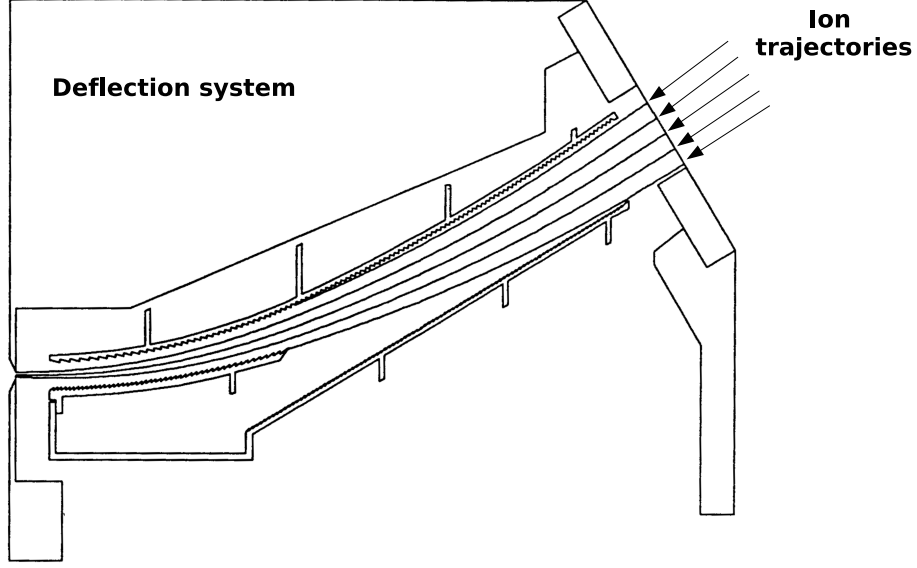
Figure 3.6.: Schematic side view of the deflection system. Five parallel ion beams pass the entrance slit at the right hand side. The ion beam is deflected, additionally the beam profile becomes smaller.

surface is indicated as δ. In this two-dimensional construct the velocity vector $\vec{v}$ while passing s_1 is indicated as $\vec{v}_1 = (\dot{x}_1, \dot{y}_1)$ and while passing s_2 as $\vec{v}_2 = (\dot{x}_2, \dot{y}_2)$. δ and δ' are then given by

$$\delta = \arctan\left(\frac{\dot{y}_1}{\dot{x}_1}\right), \tag{3.13}$$

$$\delta' = \arctan\left(\frac{\dot{y}_2}{\dot{x}_2}\right). \tag{3.14}$$

The energy ΔE transferred to an ion with charge q while passing a potential difference U_{acc} is given by

$$\Delta E = q \cdot U_{acc}. \tag{3.15}$$

The applied voltage only causes an acceleration in the x-direction. Thus, we obtain

$$\ddot{x} = \frac{q \cdot U_{acc}}{m \cdot d}, \tag{3.16}$$

$$\ddot{y} = 0. \tag{3.17}$$

In equation 3.16 m is the mass of the ion and d is the acceleration distance as indicated in Figure 3.7. By integration we obtain the velocity components which are then given by

$$\dot{x} = \dot{x}_1 + \frac{q \cdot U_{acc}}{m \cdot d} \cdot t, \tag{3.18}$$

$$\dot{y} = \dot{y}_1. \tag{3.19}$$
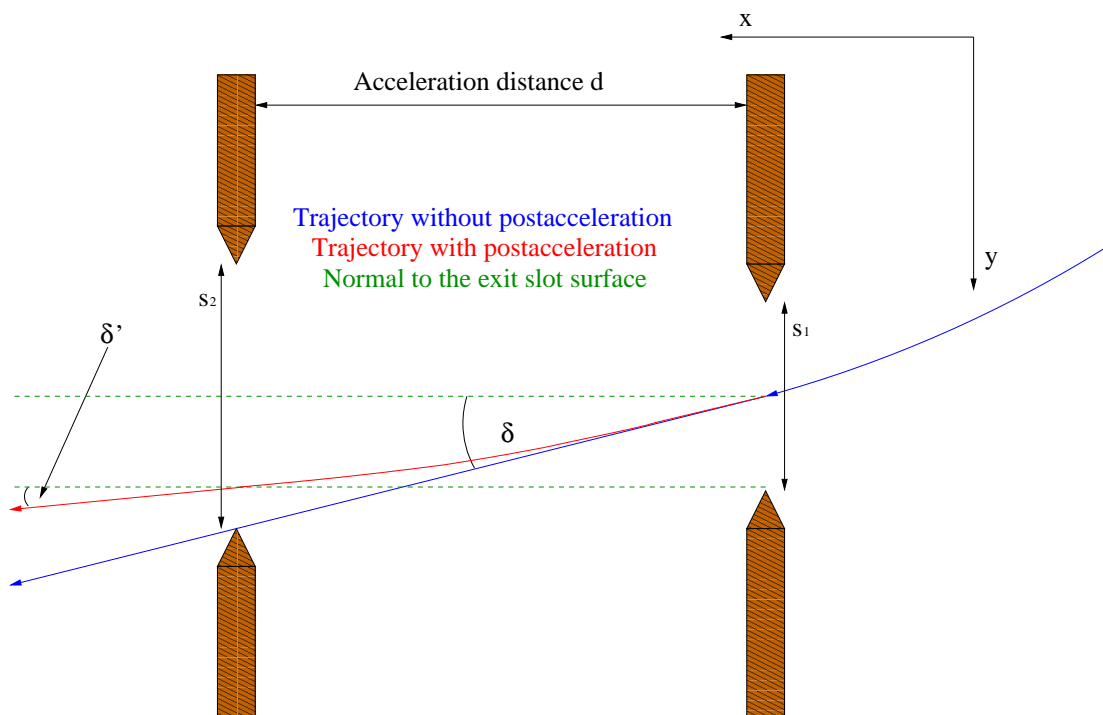
Figure 3.7.: Sketch of the post acceleration section. A perturbed trajectory of an ion centrally passes the exit slit s_1 of the deflection system. The angle between the normal of the exit slot surface and the trajectory is indicated as $\delta = \arctan\left(\frac{\dot{y}_1}{\dot{x}_1}\right)$. The post acceleration increases the x-component of the velocity. The ratio of the velocity components while passing s_2 is then given by $\delta' = \arctan\left(\frac{\dot{y}_2}{\dot{x}_2}\right)$.

A second integration delivers the time-dependent spatial function.

$$x = x_1 + \dot{x}_1 \cdot t + \frac{1}{2} \cdot \frac{q \cdot U_{acc}}{m \cdot d} \cdot t^2, \tag{3.20}$$

$$y = y_1 + \dot{y}_1 \cdot t. \tag{3.21}$$

Without loss of generality we can set $y_1 = x_1 = 0$. Using equation 3.20 with x=d and solving for t delivers

$$t = \frac{m}{q} \cdot \frac{-\dot{x}_1 \pm \sqrt{\dot{x}_1^2 + \frac{2qU_{acc}}{m}}}{U_{acc}} \cdot d. \tag{3.22}$$

The solution for the negative square root in the second fraction in equation 3.22 is not used in the further calculation, because t becomes negative in that case.

To describe the focussing effect of such an acceleration we use the equations 3.13 and 3.14, solve them for $\dot{y}_1$ and for $\dot{y}_2$ respectively and equate both, because the y-component of the velocity does not change. Thus we obtain

$$\delta' = \arctan\left(\tan(\delta) \cdot \frac{\dot{x}_1}{\dot{x}_2}\right). \tag{3.23}$$

Using the equations 3.18 and 3.22 we obtain

$$\dot{x}_2 = \dot{x}_1 + \frac{q \cdot U_{acc}}{m \cdot d} \cdot \frac{m}{q} \cdot \frac{-\dot{x}_1 \pm \sqrt{\dot{x}_1^2 + \frac{2qU_{acc}}{m}}}{U_{acc}} \cdot d = \sqrt{\dot{x}_1^2 + \frac{2qU_{acc}}{m}}. \tag{3.24}$$

Then δ' is given by

$$\delta' = \arctan\left(\tan(\delta) \cdot \frac{\dot{x}_1}{\sqrt{\dot{x}_1^2 + \frac{2qU_{acc}}{m}}}\right) = \arctan\left(\tan(\delta) \cdot \frac{\dot{x}_1}{\dot{x}_1 \cdot \sqrt{1 + \frac{2qU_{acc}}{m\dot{x}_1^2}}}\right). \tag{3.25}$$

Normally the δ angles that can occur in the SWICS instrument are smaller than five degrees, thus for the energy E before the post acceleration we can assume

$$E = \frac{1}{2}m|\vec{v}^2| \approx \frac{1}{2}m\dot{x}_1^2. \tag{3.26}$$

Therefore we obtain the following simple equation for δ' as a function of δ, energy per charge E/q, and U_{acc}.

$$\delta'(\delta, E/q, U_{acc}) = \arctan\left(\left(\tan(\delta) \cdot \frac{1}{\sqrt{1 + \frac{U_{acc}}{\frac{E}{q}}}}\right)\right) \tag{3.27}$$

3.3. Carbon foil

The passage of an ion through a thin carbon foil is accompanied by three important effects we have to consider.

- Energy loss ΔE

- Ejection of secondary electrons from the foil

- Angular scattering

As an example, Figure 3.8 shows the trajectories of 100 oxygen atoms with an initial energy of $100\,keV$ passing through a carbon foil with a thickness of $110\,\mathring{A}$. The plot is based on SRIM (*Ziegler et al.* [1985]) simulation data. All ions enter the carbon foil at the same point. The trajectories of the projectile atoms are randomly scattered due to collisions with the atoms of the target material. Furthermore, the kinetic energy of the particles decreases while passing through the foil as is shown in Figure 3.9.

3.3.1. Energy loss

The main contributions leading to the energy loss are Coulomb interactions with electrons and nuclear collisions between the projectile and the target nuclei. Additionally there is a small contribution due to the energy transferred to the crystal structure of the carbon atoms, e.g. phonon excitation. Compared to the main contributions the last effect can be neglected.

The absolute energy loss ΔE of particles passing through the carbon foil can be calculated by integrating the differential energy loss over the thickness d of the target material,

$$\Delta E = \int_0^d \Big(S_n(E) + S_e(E) + S_o(E) \Big) dx. \tag{3.28}$$

S_n and S_e indicate the nuclear and the electronic differential energy loss dE/dx. S_o includes all other effects causing an energy loss as mentioned above. Generally the differential energy loss is a function of the target materials nuclear charge and of energy, mass, and nuclear charge of the projectile. Theoretically the interactions between projectile and target material can be described with mathematical equations which can be very complicated. Another approach to that problem is to use experiments with ion beams passing the target material while the energy before the passage is adjusted and the energy afterwards is measured. Based on the results of several such measurements a semi-empirical model was developed by *Ipavich et al.* [1982] to calculate the differential energy losses dE/dx for projectile elements from hydrogen to krypton in the energy range from 1 keV/nuc up to 1 MeV/nuc.

A more sophisticated model is provided by the simulation program SRIM (Stopping and Range of Ions in Matter) based on measurements of *Ziegler et al.* [1985] but also including the results of many other stopping experiments. The simulation program as well as the citation references corresponding to the different stopping experiments are available on the internet site www.srim.org. The data SRIM is based on includes more measurements from the last 25 years as opposed to the Ipavich model which is based on data measured until 1982. It seems that those measurements created a different view on the differential energy loss, especially considering the electronic stopping, S_e. Consequently this leads to a different absolute energy loss. Figure 3.10 and 3.12 show the electronic and nuclear stopping respectively as a function of the particle
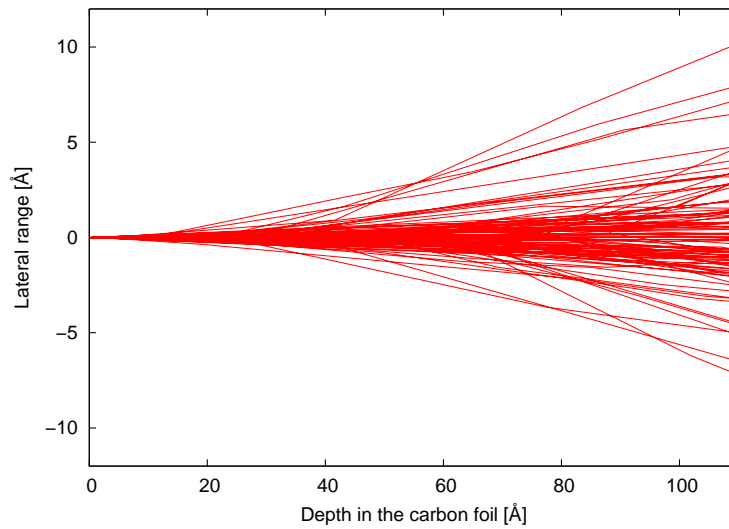
Figure 3.8.: Trajectories of 100 oxygen atoms passing through a thin carbon foil (initial energy: 100keV, foil thickness: $110\mathring{A}$) based on data from SRIM simulations. Single collisions with the atoms in the crystal structure of the target material slightly change the flight trajectory which results in an angular scattering. The mean number of interactions per projectile atom is 1.69.
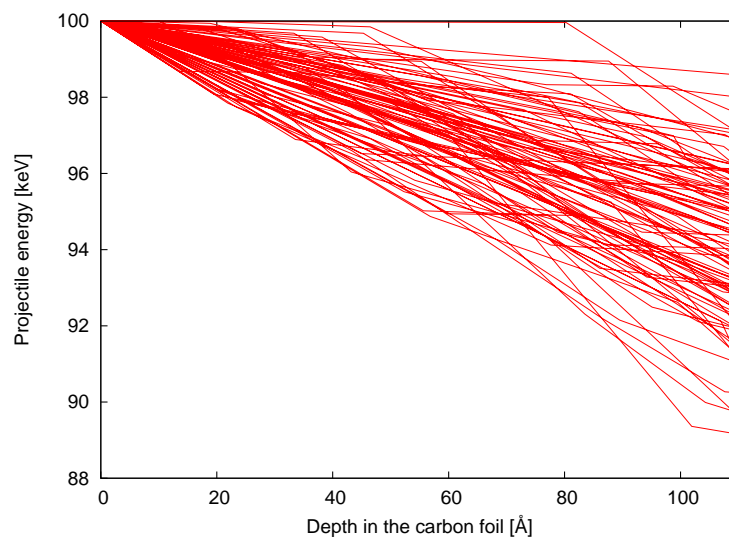
Figure 3.9.: Kinetic energy of 100 oxygen atoms while passing through a thin carbon foil (initial energy: 100keV, foil thickness: $110\mathring{A}$). Each collision causes an energy transfer from the projectile atom to the target material and, thus, decreases the mean energy of the particle beam.

energy for $^4_2$He, $^{12}_6$C, $^8_{16}$O, and $^{56}_{26}$Fe calculated with SRIM. Note that the y-axis of Figure 3.12 is logarithmic. According to these data Figure 3.14 shows the averaged absolute energy loss of particles passing through a carbon foil with a thickness of about $2.5\mu g/cm^2$. ΔE is calculated by an iterative discrete integration. The data SRIM provides are tables of the differential energy loss as a function of the initial projectile energy. Thus the analytical integration given in equation 3.28 is approximated by the following discrete summation,

$$\Delta E = \sum_{x=1\,\overset{\circ}{A}}^{d} \Big(S_n(E(x)) + S_e(E(x)) \Big) \Delta x. \tag{3.29}$$

To achieve the best accuracy for the absolute energy loss we have used differential energy losses in units of eV/Å.

Figures 3.11, 3.13, 3.15 show the relative deviation between the predictions of both models that can amount to almost 15 %. Taking into account the larger data set the Ziegler model is based on, the energy loss ΔE in the efficiency model for the SWICS instrument is calculated with SRIM.

3.3.2. Secondary electrons

The secondary-electron emission of ions passing through a carbon foil was analyzed by *Rothard et al.* [1989]. It was found that the average number of secondary electrons ejected from the foil, γ, is proportional to the electronic differential energy loss S_e.

$$\gamma_F = \Gamma_F S_e, \tag{3.30}$$

$$\gamma_B = \Gamma_B S_e, \tag{3.31}$$

γ_F indicates the number of electrons in forward direction, γ_B in backward direction respectively. The behaviour of this relation is not the same for all ion species. Thus, one has to introduce ion-specific quality factors, C_F and C_B

$$\Gamma_F = \Gamma_{FH} \cdot C_F, \tag{3.32}$$

$$\Gamma_B = \Gamma_{BH} \cdot C_B. \tag{3.33}$$

Rothard et al. [1989] found the following values valid for all ions,

$$\Gamma_{FH} = 0.22 \overset{\circ}{A}/eV, \tag{3.34}$$

$$\Gamma_{BH} = 0.14 \overset{\circ}{A}/eV. \tag{3.35}$$

For hydrogen
$$C_F = C_B = 1, \tag{3.36}$$

for helium
$$C_F = 0.68, \tag{3.37}$$

$$C_B = 0.6, \tag{3.38}$$

and for all heavy ions
$$C_F = 0.5, \tag{3.39}$$
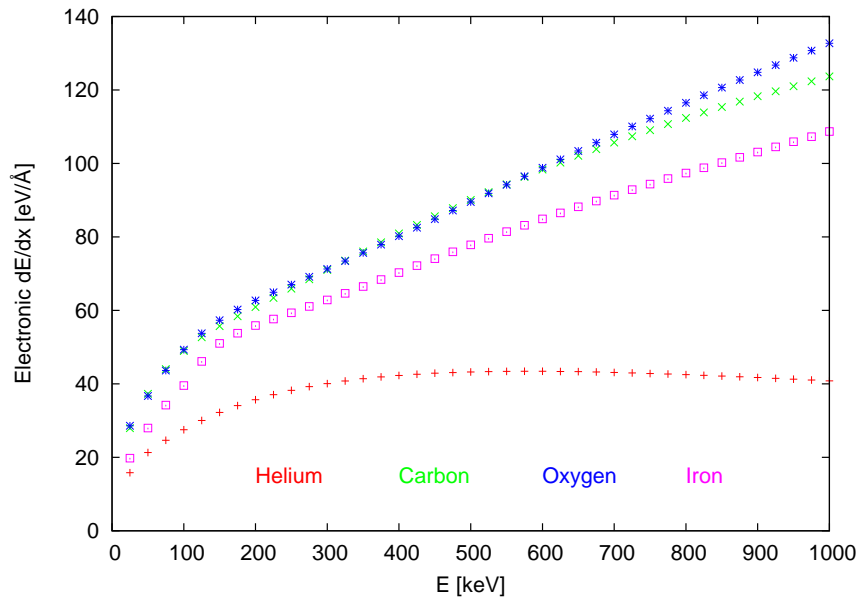
Figure 3.10.: Differential energy loss due to Coulomb interaction as a function of the particle energy calculated with SRIM for a sample of abundant solar wind ions in the energy range up to 1 MeV. The target material is carbon. The absolute electronic energy loss can be derived by integrating over the foil thickness.
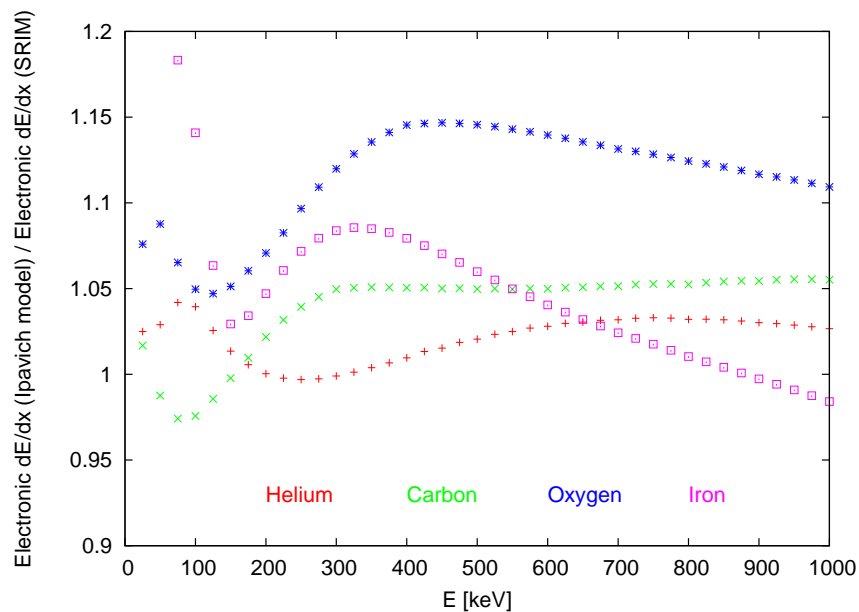
Figure 3.11.: Ratio of the electronic stopping between the Ipavich model and SRIM. The relative deviation is usually less than 15 %, also for other solar wind ions which are not shown here.
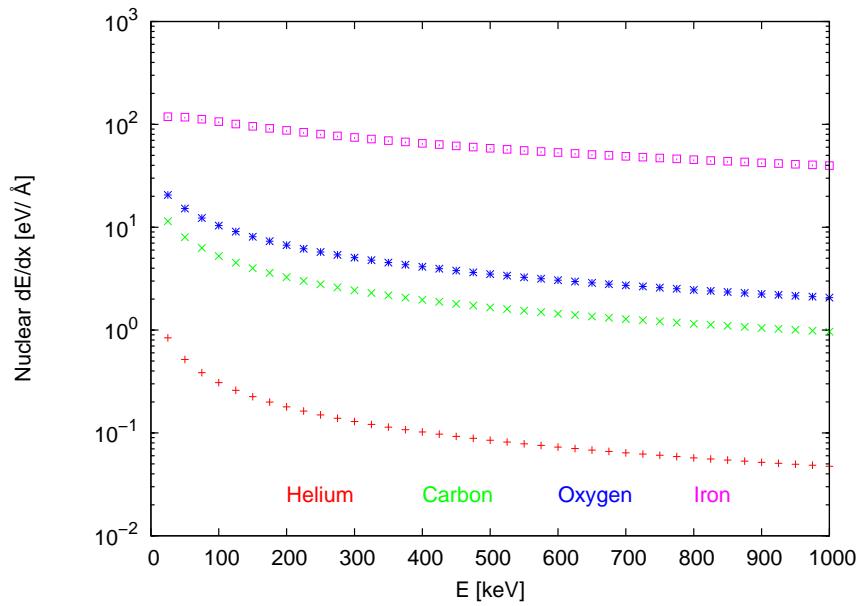
Figure 3.12.: Differential energy loss due to nuclear interaction as a function of the particle energy calculated with SRIM for a sample of abundant solar wind ions in the energy range up to 1 MeV. The target material is carbon. The absolute nuclear energy loss can be derived by integrating over the foil thickness.
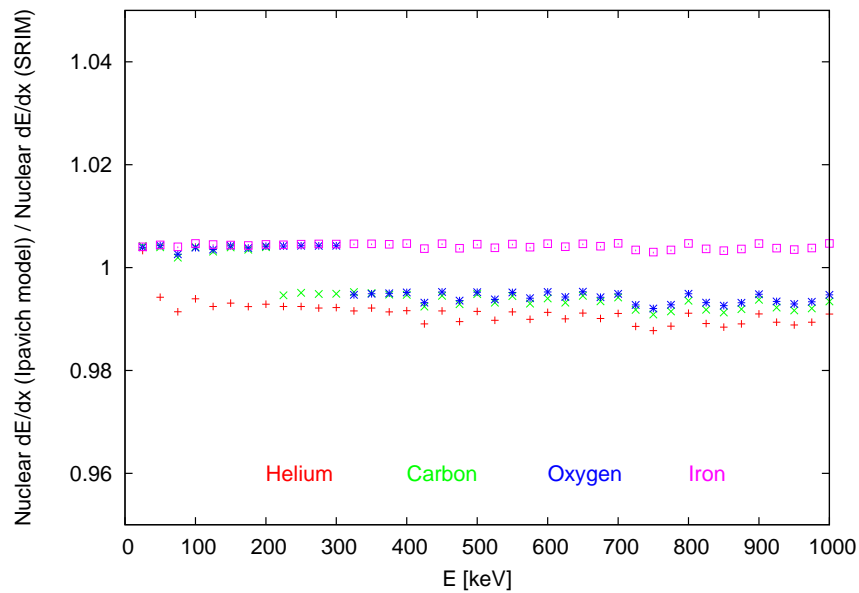
Figure 3.13.: Ratio of the nuclear stopping between the Ipavich model and SRIM. Astonishingly the relative deviation is on the order of about 1 % also for other solar wind ions which are not shown here.
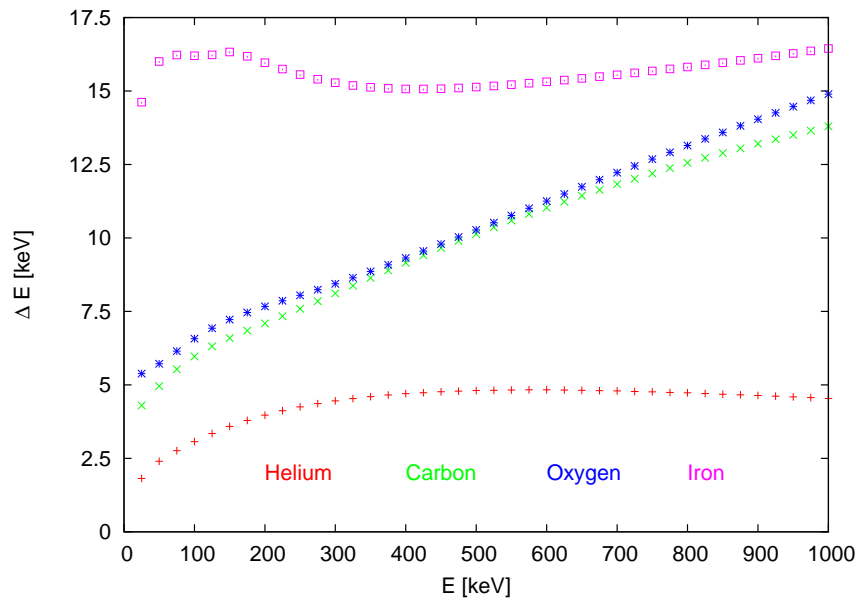
Figure 3.14.: Absolute energy loss of an ion passing a carbon foil with a thickness of $2.5\,\mu\text{g}/\text{cm}^2$) as a function of its initial energy. Shown are the results from SRIM calculation for a sample of abundant solar wind ions.
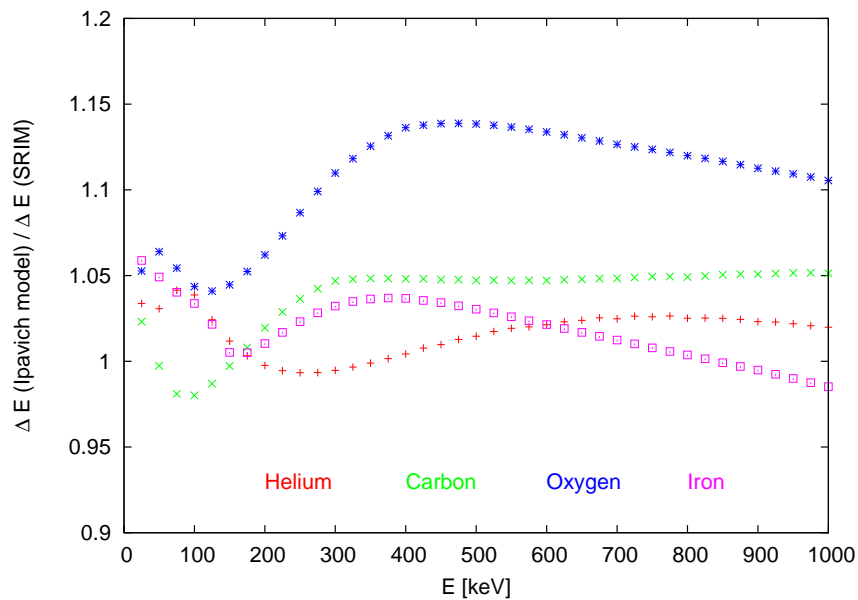
Figure 3.15.: Relative deviation of the absolute energy loss between the Ipavich model and SRIM. The large differences are mainly caused by different values of the differential energy loss due to Coulomb interactions.

$$C_B = 0.3. \tag{3.40}$$

Other references report somewhat different values. For example, *Wimmer* [p.c.] found during the calibration campaign of SWICS

$$\Gamma_{FH} = 0.17 \mathring{A}/\text{eV}, \tag{3.41}$$

$$\Gamma_{BH} = 0.14 \mathring{A}/\text{eV}, \tag{3.42}$$

which results in slightly different average numbers of secondary electrons in forward direction for the same electronic differential energy loss. In the efficiency model we used the values found by *Wimmer* [p.c.] because these are based on measurements with SWICS and thus, better reflect the properties of the carbon foil in the instrument.

3.3.3. Angular scattering

For the calculations of the angular scattering of ions passing through the thin carbon foil the results of *Högberg et al.* [1970] and *Gonin* [1995] are used. *Högberg et al.* [1970] measured the angular distribution in the energy range from 3 keV to 54 keV for H, He, Li, N, Ne, and Ar for foil thicknesses of 2.5, 3.5, 5.7, 7.8, 10.8, and 15.6 μg/cm^2. *Gonin* [1995] measured the angular scattering in the energy range from 0.5 to 5.0 keV/amu for Ca, N, Ni, O, and Ar for foil thicknesses of 1.1 to 5.0 μg/cm^2. For energies exceeding that range, the results of SRIM simulations are implemented in the efficiency model.

Gonin [1995] found that the differential angular distribution is well approximated by a special case of a $\mathcal{K}$-function,

$$\frac{dN}{d\Omega} = f(\varphi, \vartheta) = A \cdot \left(1 + \frac{\vartheta^2}{4\sigma^2}\right)^{-2}. \tag{3.43}$$

The scale factor A is given by

$$A = \frac{1}{4\pi\sigma^2}. \tag{3.44}$$

Because of the cylindrical symmetry around the norm trajectory the function does not depend on φ. Note that 3.43 describes a cut through the two-dimensional distribution function. Thus, to obtain the angular distribution, $N(\vartheta)$, one has to integrate over the solid angle $d\Omega = \sin\vartheta d\vartheta d\varphi$. Note also that σ is not the half width at half maximum $\vartheta_{1/2}$ which is given by

$$\vartheta_{1/2} = 2\sqrt{\sqrt{2} - 1} \cdot \sigma = 1.287\sigma. \tag{3.45}$$

Högberg et al. [1970] found that the following simple empirical expression approximates the results of the measurements very well

$$\vartheta_{1/2} = 12 \cdot \frac{Z^{0.75} \cdot t}{\bar{E}}, \tag{3.46}$$

where t indicates the thickness of the carbon foil in units of μg/cm^2. Z is the nuclear charge and $\bar{E}$ is the average energy [keV] of the particle while passing through the foil

$$\bar{E} = E - \frac{\Delta E}{2}. \tag{3.47}$$
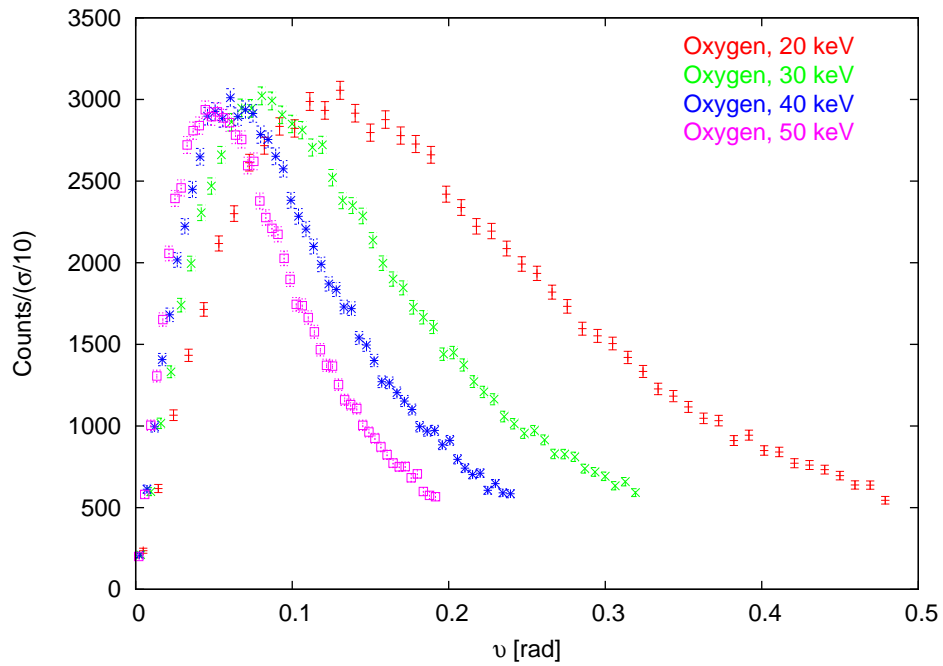
Figure 3.16.: Angular distribution of 100000 oxygen atoms scattered at a carbon foil with a thickness of $110\mathring{A}$ based on SRIM simulation data. The angular bin width is $0.1 \cdot \sigma$ of the differential angular distribution $\frac{dN}{d\Omega}$ given in equation 3.43.
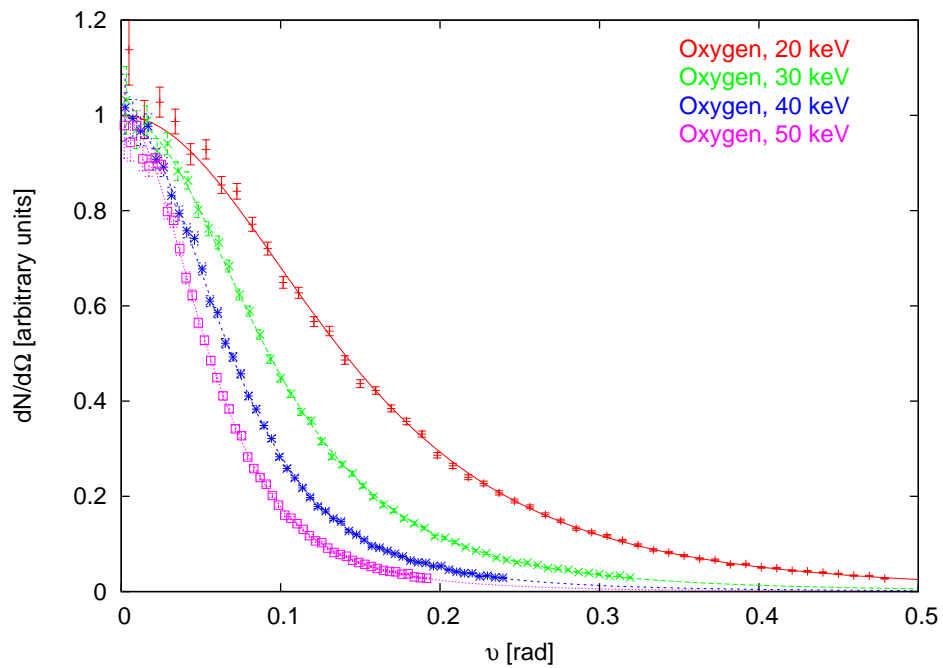
Figure 3.17.: Differential angular distribution $\frac{dN}{d\Omega}$ corresponding to SRIM simulation data shown in Figure 3.16. The continuous lines show the fit function as given in equation 3.43.
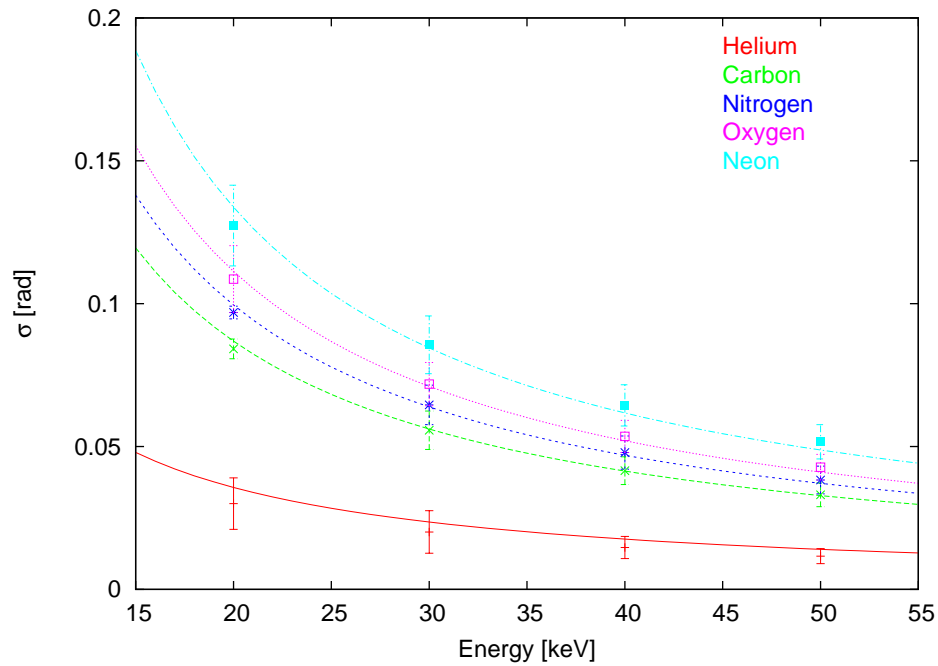
Figure 3.18.: Comparison between the model of *Högberg et al.* [1970] (continuous lines) and the results from the SRIM simulation at energies of 20, 30, 40, and 50 keV for a sample of abundant solar wind ions.
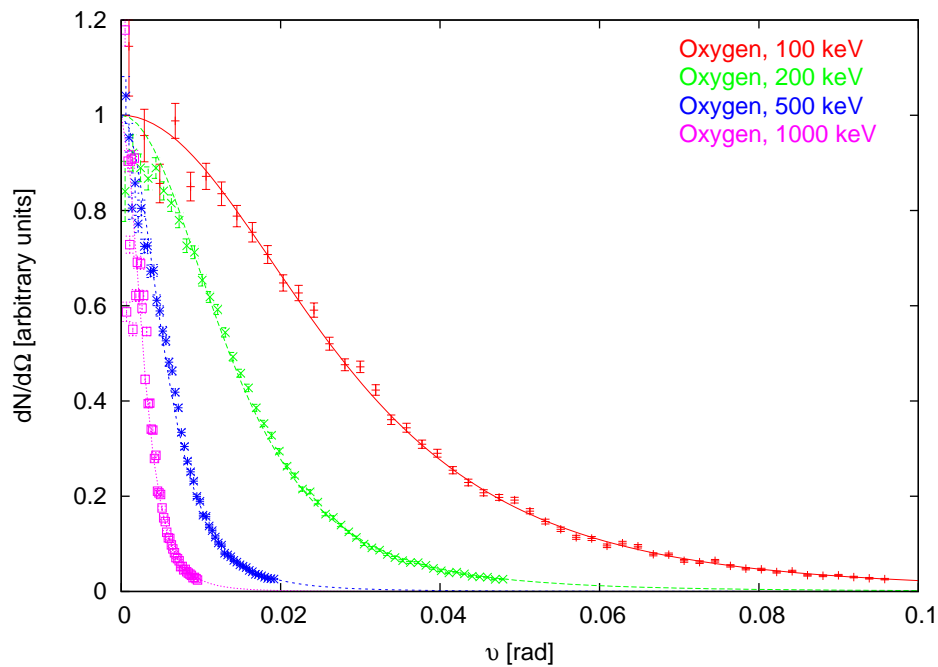
Figure 3.19.: Differential angular distribution $\frac{dN}{d\Omega}$ of oxygen for several selected energies up to 1 MeV. The continuous lines describe the fit function as given in equation 3.43.
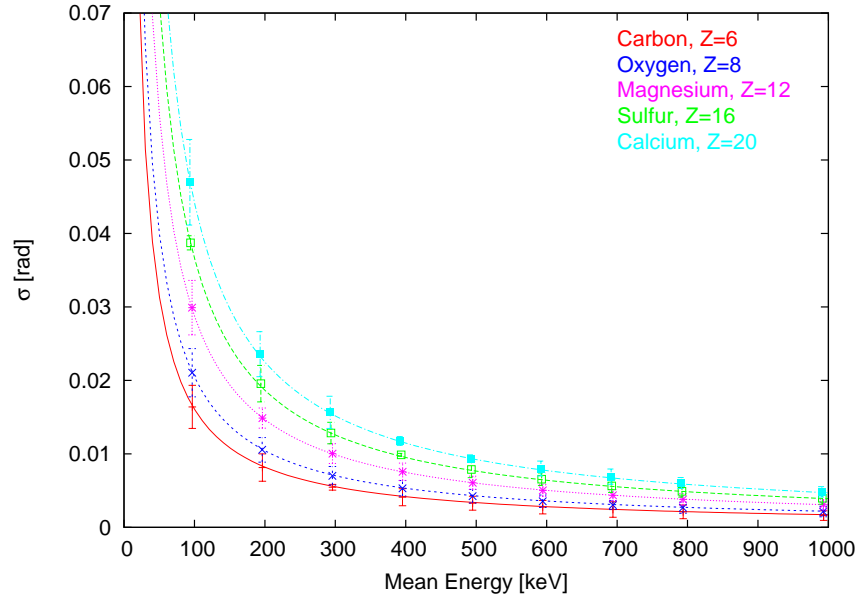
Figure 3.20.: σ-values of the differential angular distribution functions for a sample of abundant solar wind ions in the energy range from 100 keV to 1 MeV based on SRIM simulation data. The continuous lines describe the σ-distribution function as given in equation 3.48.
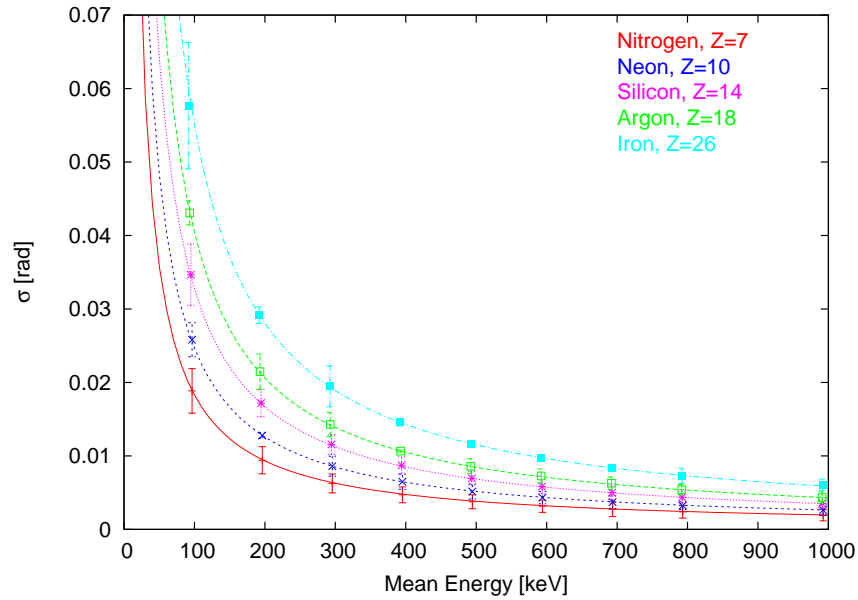
Figure 3.21.: σ-values of the differential angular distribution functions for a sample of abundant solar wind ions in the energy range from 100 keV to 1 MeV based on SRIM simulation data. The continuous lines describe the σ-distribution function as given in equation 3.48.

To check for consistency, SRIM simulations were performed for helium, carbon, nitrogen, oxygen, and neon. The simulations were accomplished with the initial energies 20, 30, 40, and 50 keV which cover mainly the energy range measured by *Högberg et al.* [1970]. The data includes scattering information of 100000 particles passing a carbon foil with a thickness of 110 $\mathring{A}$. As an example, Figure 3.16 shows $N(\vartheta)$ for oxygen with different initial energies.

Corresponding to these data, Figure 3.17 qualitatively shows the differential angular distribution $\frac{dN}{d\Omega}$, or in other words a cut through the two-dimensional peak. It is clearly visible that equation 3.43 fits very well in the energy range up to 50 keV. The fitted σ-values and the prediction of *Högberg et al.* [1970] (equation 3.46) for helium, carbon, nitrogen, oxygen and neon are shown in Figure 3.18.

We also performed SRIM simulations in the energy range up to 1 MeV and checked whether the function found by *Gonin* [1995] fits the differential angular distribution. As an example Figure 3.19 shows the results for oxygen.

The σ-values from these fits for a sample of abundant heavy solar wind ions were used to find a general expression for σ as a function of nuclear charge, foil thickness, and the particle energy. For that we used the function as has been used by *Gonin* [1995] in the energy range up to $5keV/nuc$,

$$\sigma = a \cdot Z^b \cdot t^c \cdot \bar{E}^d. \tag{3.48}$$

In the range the foil thickness can vary from about $2\mu g/cm^2$ to $3\mu g/cm^2$ we found that c can be set to -1. The parameters a,b, and d were fitted to the σ-values in the energy range from $100\,keV$ up to $1\,MeV$. We found $a = 1.26$, $b = 0.84$, and $d = -0.97$ whereas *Gonin* [1995] found $a = 13.342$, $b = 0.7455$, $c = 0.6748$, and $d = 0.1356$ in the energy range of 0.5keV/amu to 5keV/amu. Note that equation 3.46 gives the $\vartheta_{1/2}$ in units of *degree* whereas equation 3.48 gives σ in units of *radian* with $a = 1.26$ and in units of *degree* with $a = 13.342$. For the sake of lucidity the results are split into two plots and are shown in Figure 3.20 and Figure 3.21.

3.4. Time-of-Flight measurement

The Time-of-Flight measurement trigger efficiency is given by the product of several single probabilities. The probability for a single ion to trigger a start signal depends mainly on the number of secondary electrons which are ejected from the carbon foil in forward direction by the ion's passage through. According to equation 3.33 the amount of secondary electrons again depends on the differential energy loss (dE/dx). *Wimmer* [*p.c.*] found the following simple equation that describes the start-signal trigger probability P_1 very well as a function of the number of secondary electrons ejected in forward direction γ_1.

$$P_1 = \left(1 - (1 + \gamma_1) \cdot e^{-\gamma_1}\right) \cdot \left(1 - pf_1^{\gamma_1}\right) \tag{3.49}$$

The only parameter in this equation is pf_1 which can be interpreted as the probability for each secondary electron not to trigger a start signal. Different measurements during the calibration campaign revealed that $pf_1 = 0.784 \pm 4.5\%$. Figure 3.22 shows the start-signal trigger probability for a sample of abundant solar wind ions as a function of the energy-per-charge value in the deflection system.
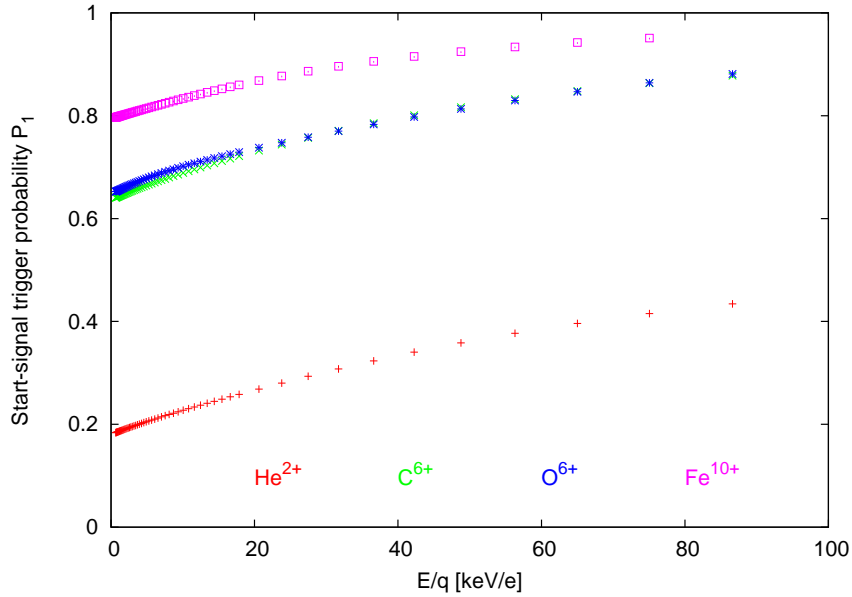
Figure 3.22.: Start-signal trigger probability as a function of energy per charge calculated for a sample of abundant solar wind ions.

The stop-signal trigger probability P_2 can be calculated analogously as a function of the number of ejected secondary electrons in backward direction pf_2 by the ion's impact on the SSD surface

$$P_2 = \left(1 - (1 + \gamma_2) \cdot e^{-\gamma_2}\right) \cdot \left(1 - pf_2^{\gamma_2}\right). \tag{3.50}$$

Because of the symmetry of the positioning of the carbon foil, the SSDs and the MCPs (see Figure 3.4) we can assume that pf_2 has the same numerical value as pf_1.

Additionally, in that case one has to consider the probability P_{SSD} that the ion hits the SSD surface at all. This is accomplished by integrating the two-dimensional angular distribution of

the ion beam after the foil over the angular limits which are given by the borders of the SSD,

$$P_{\text{SSD}} = \iint\limits_{SSD} \frac{1}{4\pi\sigma^2} \cdot \left(1 + \frac{\vartheta^2}{4\sigma^2}\right)^{-2} \sin\vartheta \mathrm{d}\vartheta \mathrm{d}\varphi. \qquad (3.51)$$

Figure 3.23 shows the stop-signal trigger probability for a sample of abundant solar wind ions as a function of the energy-per-charge value in the deflection system. The effective efficiency to
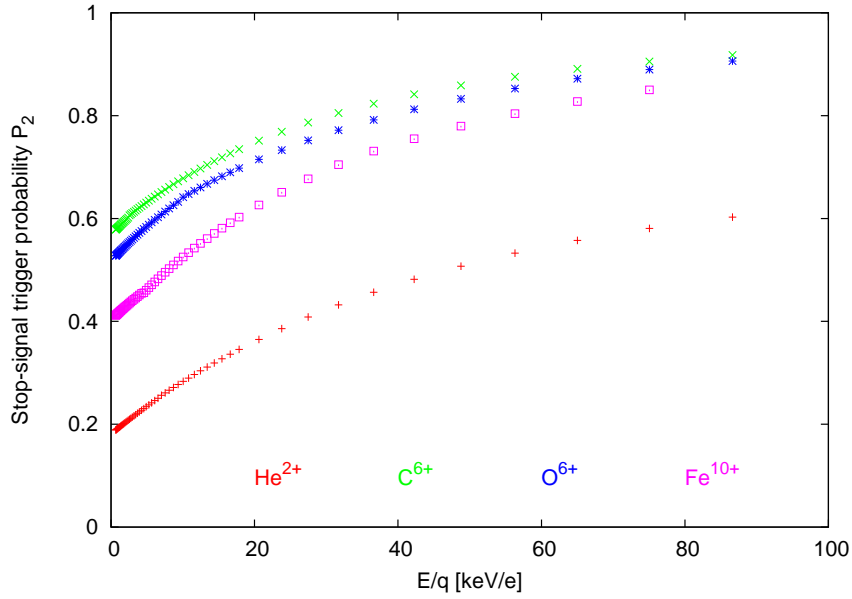
Figure 3.23.: Stop-signal trigger probability as a function of energy per charge calculated for a sample of abundant solar wind ions.

trigger a time-of-flight measurement is then given by

$$P_{\text{ToF}} = P_1 \cdot P_2 \cdot P_{\text{SSD}}. \qquad (3.52)$$

3.5. Energy measurement

The energy measurement in SWICS is performed by three Solid-State Detectors (SSDs). Two of them are PIPS (Passivated Ion Implanted Planar) detectors while the third one is a gold coated surface barrier detector. The SWICS instrument on ACE is the flight spare of Ulysses/SWICS. Originally there were three surface barrier detectors, but for the ACE mission two of them were replaced by PIPS detectors. The different detector types show slightly different Pulse Height Defect (PHD) properties. The PHD η depends on the ion species and its energy E_{ion} and indicates the fraction of the particle energy which is measured,

$$E_{\mathrm{meas}} = \eta \cdot E_{\mathrm{ion}}. \tag{3.53}$$

The PHD value is always less than 100 % because there is always an energy loss, e.g. due to the detector dead layer, phonon excitation in the atomic structure of the detector, and electron-hole-pair recombination. The results of the PHD calibration in the relevant energy range, in which SWICS is able to measure, are shown in Table 3.1 for the surface barrier detector and in Table 3.2 for the PIPSes. The PHD values for elements and energies for which no measurements are available are calculated by an appropriate interpolation method. The PHD as a function of energy E or energy per mass E/amu for a single element species locally shows a characteristic which can be described satisfyingly as a proportionality $\eta \propto \ln(\mathrm{E})$ or $\eta \propto \ln(\mathrm{E/amu})$. Thus, η for an energy E where no calibration data are available is calculated with

$$\eta(E) = \frac{\ln(\mathrm{E}) - \ln(\mathrm{E_0})}{\ln(\mathrm{E_1}) - \ln(\mathrm{E_0})} \cdot (\eta(E_1) - \eta(E_0)) + \eta(E_0). \tag{3.54}$$

E_0 and E_1 indicate the next lower or higher energy respectively where η is available. As an example Figure 3.24 shows the η-values of the PIPS detectors as a function of E/amu for oxygen including the interpolated values. The PHD as a function of nuclear charge for a specific energy per mass does generally seem to be a kind of exponential function, although there are significant irregularities comparing one calibration point with the neighbouring points towards lower and higher Z-values respectively. Therefore, in this case we used a linear interpolation. Thus, η for an element with nuclear charge Z for which no calibration data are available is calculated with

$$\eta(Z) = \frac{Z - Z_0}{Z_1 - Z_0} \cdot (\eta(Z_1) - \eta(Z_0)) + \eta(Z_0). \tag{3.55}$$

Z_0 and Z_1 indicate the elements with the next lower or higher nuclear charge respectively for which η is available. As an example Figure 3.25 shows the η-values of the PIPS detectors as a function of nuclear charge Z for a defined energy-per-mass value of 2.5 keV/amu including the interpolated values.

An energy measurement can only be triggered when the energy of the detected particle is above the energy threshold E_{thresh} of the detectors. The energy measurement trigger probability P_3 is then given by the product of the integral of the energy distribution function $f(E)$ over the limits E_{thresh} and $+\infty$, P_{T}, and the probability that the ion hits the active regions of the SSDs $P_{\mathrm{AR\,SSD}}$. Unfortunately $P_{\mathrm{AR\,SSD}}$ is not the same as P_{SSD} (compare equation 3.51) because there are small stripes at the borders of the SSD which cannot make an energy measurement but eject secondary electrons,

$$P_3 = \int_{E_{\mathrm{thresh}}}^{+\infty} f(E)\,\mathrm{dE} \cdot \iint\limits_{\mathrm{AR\,SSD}} \frac{1}{4\pi\sigma^2} \cdot \left(1 + \frac{\vartheta^2}{4\sigma^2}\right)^{-2} \sin\vartheta\,\mathrm{d}\vartheta\,\mathrm{d}\varphi. \tag{3.56}$$
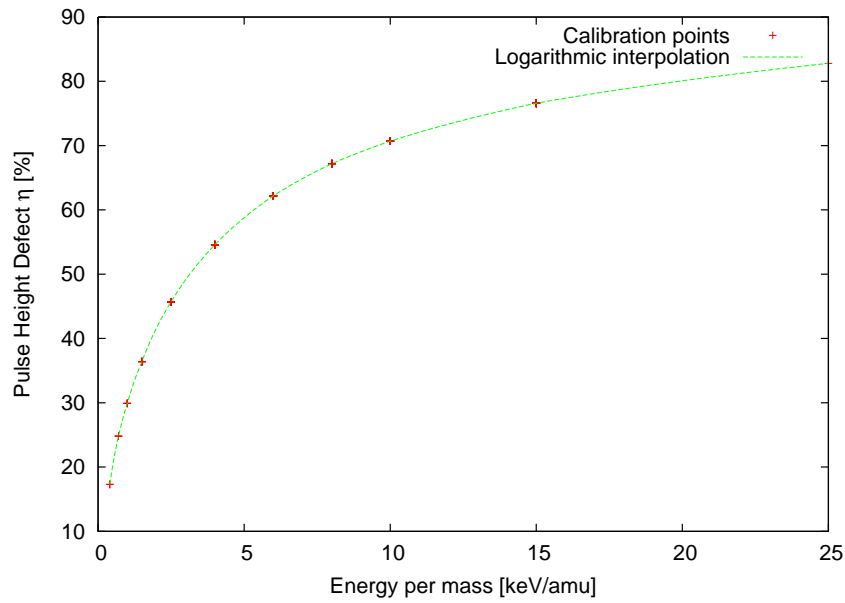
Figure 3.24.: Pulse height defect calibration data of the PIPS detectors for oxygen as a function of energy per charge. The red crosses indicate energy-per-charge values where measurements were accomplished. The green curve indicates the logarithmic interpolation in-between.
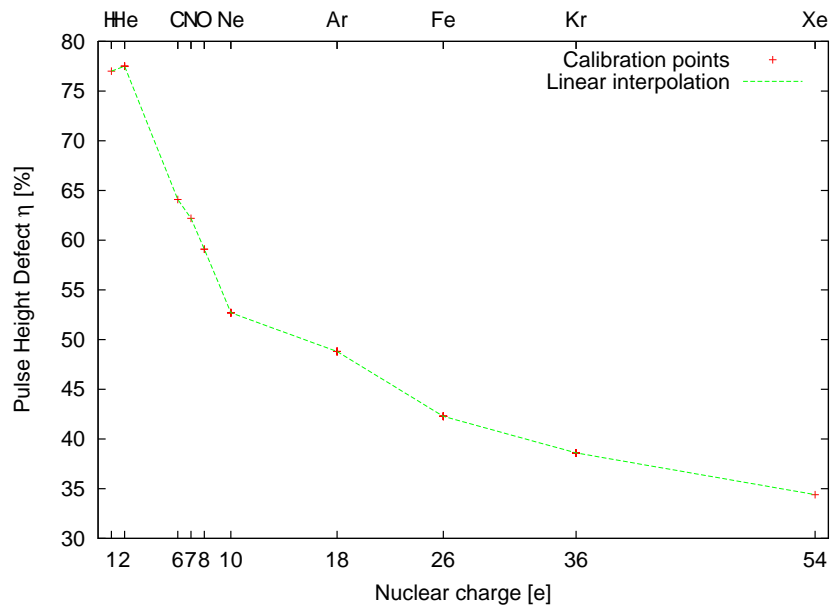
Figure 3.25.: Pulse height defect calibration data of the PIPS detectors for an energy-per-charge value of 2.5keV/nuc as a function of nuclear charge Z. The red crosses indicate Z values where measurements were accomplished. The green curve indicates the linear interpolation in-between.

The energy distribution $f(E)$ can be described as the convolution of the energy distributions resulting from the uncertainty of the energy-per-charge analyzer, the scattering in the carbon foil, and the energy resolution of the detector system. As a example, Figure 3.26 shows $P_{\mathrm{AR\,SSD}}$, P_{T}, and P_3 as a function of the measured energy E_{meas} for oxygen and an aspect angle of about 25 degrees which means that the ion beam hits the middle SSD almost centrally. Above energies of 70keV P_3 only depends on the ion beam profile after the foil because in this energy range P_{T} is practically 1.
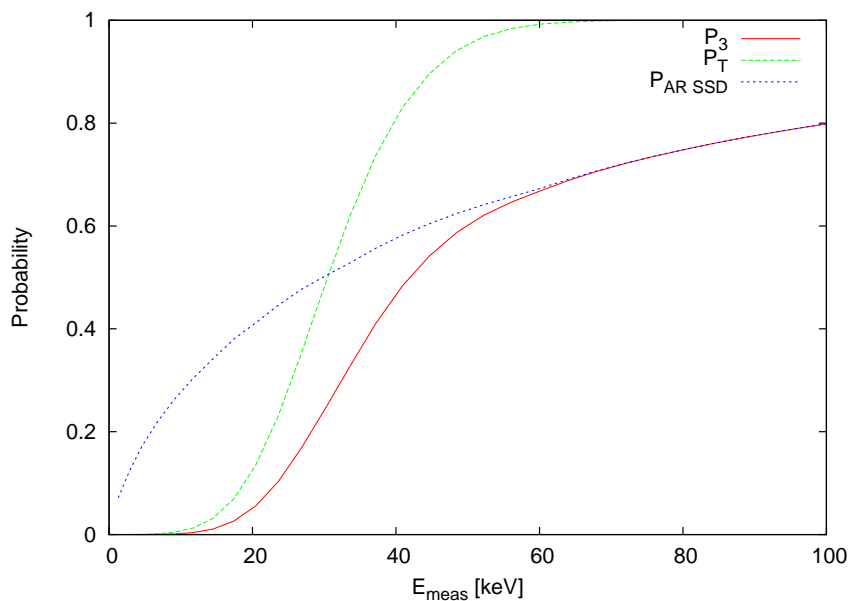
Figure 3.26.: SSD trigger probability as a function of the measured energy E_{meas} for oxygen entering the instrument with an aspect angle of 25 degrees. The blue curve indicates the probability that the ion hits the active area of the SSD surface whereas the green curve indicates the probability that an ion which hits the active area of the SSD triggers an energy measurement. The red curve is the product of both probabilities.

keV	H	He	C	N	O	Ne	Ar	Fe	Kr	Xe
0.4	32.9	28.7	16.3	15.1	15.0	14.9	14.0	13.1	12.8	12.7
0.7	42.9	39.3	24.3	22.6	21.0	20.3	19.3	17.4	16.2	16.2
1.0	49.3	45.9	29.7	27.7	24.9	23.6	22.7	21.0	20.0	19.1
1.5	55.8	53.1	36.4	34.2	28.2	28.0	27.0	24.8	24.0	22.2
2.5	63.1	61.4	45.4	43.5	37.7	34.9	33.8	29.6	28.6	25.9
4.0	69.2	68.2	54.3	52.4	45.8	42.9	40.9	34.2	33.0	29.7
6.0	74.4	73.4	62.2	60.0	54.5	50.5	47.6	38.9	37.4	33.2
8.0	77.9	76.6	67.2	65.0	60.6	55.9	52.2	42.3	41.0	35.7
10.0	80.3	79.0	70.6	68.5	64.8	60.0	55.8	45.2	43.9	37.8
15.0	83.8	82.9	76.3	74.4	71.7	67.3	62.1	51.4	49.2	42.4
25.0	87.6	86.8	82.3	80.6	78.6	75.4	70.0	60.6	57.0	48.8
40.0	90.2	89.3	86.4	85.2	83.6	80.5	76.0	69.5	64.8	56.5
60.0	92.0	91.1	89.4	88.5	86.5	84.2	80.7	76.1	71.2	62.9
80.0	93.0	91.9	91.2	90.4	88.2	86.4	83.4	79.8	75.3	67.0
100.0	93.8	92.5	92.1	91.5	89.3	87.8	85.4	81.9	77.7	69.4
150.0	94.9	93.4	93.8	93.1	91.4	89.8	88.7	85.2	81.7	73.3
250.0	95.9	94.3	95.3	94.8	93.5	92.1	91.9	88.9	86.6	77.1
400.0	96.6	94.9	96.3	95.8	94.9	93.6	93.7	91.5	90.1	79.6
600.0	96.9	95.3	96.8	96.4	95.7	94.6	94.9	93.2	92.1	81.5
800.0	97.0	95.4	97.1	96.7	96.2	95.2	95.4	94.0	93.2	82.6
1000.0	97.1	95.5	97.3	96.9	96.5	95.5	95.8	94.5	93.9	82.9

Table 3.1.: Pulse height defect data for the gold coated surface barrier detector (percentage of total energy).

keV/amu	H	He	C	N	O	Ne	Ar	Fe	Kr	Xe
0.40	35.50	32.80	18.20	17.30	17.20	17.10	15.20	11.72	14.00	13.90
0.70	45.50	43.40	26.20	24.80	23.20	22.50	20.50	15.89	17.40	17.40
1.00	51.90	50.00	31.60	29.90	27.10	25.80	23.90	19.13	21.20	20.30
1.50	58.40	57.20	38.30	36.40	32.90	30.20	28.20	23.40	25.20	23.40
2.50	65.70	65.50	47.30	45.70	41.50	37.10	35.00	29.66	29.80	27.10
4.00	71.80	72.30	56.20	54.60	50.40	45.10	42.10	36.19	34.20	30.90
6.00	77.00	77.50	64.10	62.20	59.10	52.70	48.80	42.28	38.60	34.40
8.00	80.50	80.70	69.10	67.20	64.60	58.10	53.40	46.76	42.20	36.90
10.00	82.90	83.10	72.50	70.70	68.40	62.20	57.00	50.27	45.10	39.00
15.00	86.40	87.00	78.20	76.60	74.50	69.50	63.30	56.63	50.40	43.60
25.00	90.20	90.90	84.20	82.80	80.80	77.60	71.20	64.31	58.20	50.00

Table 3.2.: Pulse height defect data for the PIPS detectors (percentage of total energy).

4. CALIBRATION

There are two data sources which were used for the calibration of the instrument. The PFC (Pre-Flight-Calibration) data were taken before launch and include measurements while SWICS was exposed to an ion beam. The IFC (In-Flight-Calibration) data include measurements of the instrument in space.

4.1. Pre-Flight Calibration

The PFC of the instrument was accomplished by using ion sources to simulate solar wind flux conditions. Thus, the calibration data include count rates of the instrument while it was exposed to an ion beam with a defined particle mass m, charge q, and energy E. These data sets of different ion species with various energies were used to determine a set of instrument-specific parameters. The analysis of the calibration data is described in detail in the diploma thesis *Köten* [2005], but for the sake of completeness we will give a very short description of the adaption method. The measured count rates for each ion species at a defined particle energy are

- FSR : Number of ions which triggered a start signal

- DCR : Number of ions which triggered a ToF measurement

- TCR : Number of ions which triggered a ToF- and an energy measurement

According to the trigger probabilities as described in section 3.4 and section 3.5 ratios of these count rates can be written as

$$\frac{DCR}{FSR} = P_2 \cdot P_{\text{SSD}}, \tag{4.1}$$

$$\frac{TCR}{DCR} = \frac{P_{\text{AR\,SSD}}}{P_{SSD}} \cdot P_T, \tag{4.2}$$

$$\frac{TCR}{FSR} = P_2 \cdot P_{\text{AR\,SSD}} \cdot P_T. \tag{4.3}$$

We have developed an advanced efficiency model of the instrument and adapted the free parameters of the model to the calibration data. These parameters are itemized below.

- E_{thresh}: Energy threshold of the solid state detectors (SSDs)

- $FWHM$: Full width at half maximum of the SSD electronic noise

- C_1: Factor of proportionality between dE/dx(carbon) and the number of secondary electrons ejected from the foil

- pf_1: Probability that at least one of those secondary electrons triggers a start signal for the time-of-flight measurement

- C_2: Factor of proportionality between dE/dx(silicon) and the number of secondary electrons ejected from the SSD surface

- pf_2: Probability that at least one of those secondary electrons trigger a stop signal for the time-of-flight measurement

- $defl$: Angular spread of the ion beam in front of the carbon foil

- $thick$: Foil thickness

A detailed reevaluation of the calibration data revealed the following set of parameters. The Levenberg-Marquardt fit used for the adaption and the estimation of the confidence intervals were performed according to *Press et al.* [1992] for a fit in a multidimensional parameter space.

Parameter	Fit result	1-sigma error
E_{thresh}	30.46 keV	$\pm 6.0\,\%$
$FWHM$	15.43 keV	$\pm 13.0\,\%$
C_1	0.085 dx/dE	$\pm 11.5\,\%$
C_2	0.157 dx/dE	$\pm 13.0\,\%$
pf_1	0.784	$\pm 4.5\,\%$
pf_2	0.784	$\pm 4.5\,\%$
$defl$	0.0687 rad	$\pm 1.0\,\%$
$thick$	2.5 μg/cm^2	$\pm 11.5\,\%$

Table 4.1.: Set of parameters resulting from the fit to the calibration data including 1-σ error bars.

4.2. In-Flight Calibration

The data we get from the instrument in space are PHA (Pulse Height Analysis) words which include information about energy- and ToF-channel of each detected ion. These data are used to produce a two-dimensional histogram, the so-called ET-matrix. There is always one matrix for each step of the energy-per-charge analyzer. Each solar-wind ion got its specific position in these matrices depending on the energy-per-charge setting of the deflection system which is stepped logarithmically from 86 keV/e to 0.66 keV/e every 12 seconds. All in all there are 60 steps. Thus, it takes 12 minutes to step over the whole energy-per-charge range. That also means that the highest time resolution we can achieve is exactly 12 minutes. Figure 4.1 shows an example of an ET-matrix of long-term data (2001,2002,2004,2006, and 2007) in the E/q step 30 which corresponds to an energy-per-charge value of about 4.9keV/e.

The aim of the IFC was to determine the exact positions of all solar wind ion in the ET-matrices. That means that we have to know in which of the 1024 Time-of-Flight (ToF) channels and in which of the 256 Energy channels an ion with a specific charge state and energy triggers a signal. This is crucial for the whole data analysis especially with regard to the objective to analyse overlapping peaks with a resolution of 1 %. This is necessary to distinguish the relatively small peak of the carbon isotope ^{13}C from the two orders of magnitude bigger ^{12}C peak.
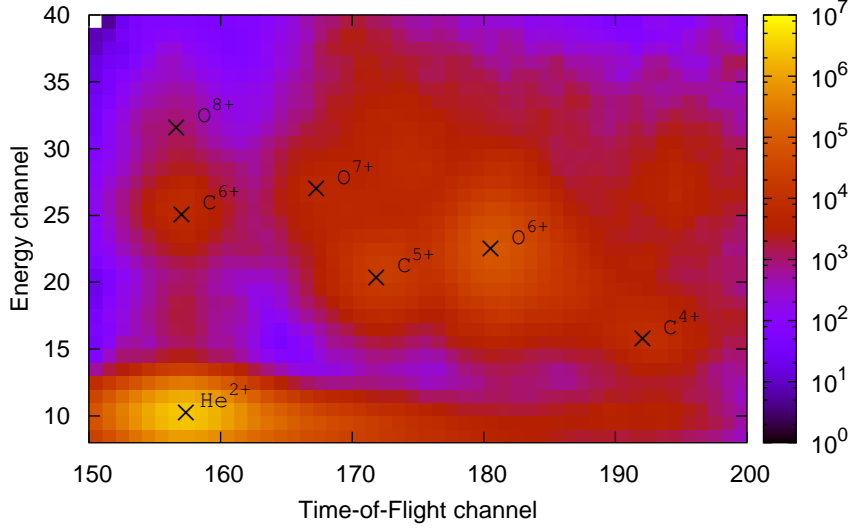
Figure 4.1.: ET (Energy, ToF) matrix of long-term data accumulated over 5 years (2001, 2002, 2004, 2006, and 2007) in the E/q-step 30 (4.9keV/e). Each solar wind ion got its specific position. The positions of parts of the charge state sequences of oxygen and carbon as well as the position of He^{2+} are indicated with crosses.

There are different functions given to calculate the ToF channel ($\hat{T}$) from the ToF τ and the Energy channel ($\hat{E}$) from the measured energy E_{meas}. The formulae described in the SWICS instrument paper *Gloeckler et al.* [1998] are given by

$$\hat{T} = \frac{\tau}{0.176\,\mathrm{ns/channel}} \tag{4.4}$$

$$\hat{E} = \frac{E_{\mathrm{meas}}}{2.34\,\mathrm{keV/channel}} \tag{4.5}$$

whereas the conversion functions *Dobler* [2000] are given by

$$\hat{T} = \tau \cdot \frac{1023\,\mathrm{channel}}{200\,\mathrm{ns}} \tag{4.6}$$

$$\hat{E} = E_{\mathrm{meas}} \cdot \frac{256\,\mathrm{channel}}{610.78\,\mathrm{keV}} \tag{4.7}$$

These formulae are idealized transformations and are just rough approximations. To find the real instrumental response functions we used long-term data (2001-2004) and fitted two-dimensional Gaussians to the peaks in the ET-matrices using a new improved analysis technique developed by *Berger* [2008]. The positions of He^{2+}, and a sample of abundant heavy solar wind ions O^{6+}, and C^{6+}, were used to find the transformation of ToF to $\hat{T}$ and E_{meas} to $\hat{E}$ respectively. For technical reasons we had to bin two channels in $\hat{T}$ and $\hat{E}$ direction (*Berger* [2008]) so that

we had 512 x 128 channels. In the $\hat{E}$ and $\hat{T}$ ranges relevant for the search for the ^{13}C isotope in the solar wind we found:

$$\hat{T} = (\tau \cdot 2.43 \, \text{channel} \, / \, \text{ns} + 6.41 \, \text{channel}) \pm 0.26 \, \text{channel}, \tag{4.8}$$

$$\hat{E} = (E_{\text{meas}} \cdot 0.189 \, \text{channel} \, / \, \text{keV} + 0.448 \, \text{channel}) \pm 0.39 \, \text{channel}. \tag{4.9}$$

These formulae are the result of the following procedure. There has to be a unique transformation between the ToF and the $\hat{T}$ for all elements. According to equation 3.7 for a given ion species and a given initial energy, τ only depends on the post acceleration voltage (PAPS=Post Acceleration Power Supply) and on the energy loss due to the passage through the carbon foil. The efficiency model allows to calculate τ for any solar wind ion. We compared these ToF values with the fitted $\hat{T}$ positions. Ideally that curve has to be a straight line and be valid for all ion species. Using the PAPS value given from the instrument housekeeping data (≈ -24.9kV) and the foil thickness given by the manufacturer (2.5μg/cm^2) we accomplished this consistency check and found that there is no straight line. Even considering differential nonlinearities of the ADC (Analog Digital Converter) the transformation has to be unique and independent of the ion species. Using the PAPS value and the foil thickness as mentioned above the data of different ion species do not coincide in the overlapping regions as one can see in Figure 4.2.

We get the most reliable positions in the ET-matrices from the most abundant solar wind ion except for H$^+$, He^{2+}, because these peaks are always well isolated and there is only little contamination due to other peaks. The He^{2+} positions were used to fit a straight line $g(\tau)$ to the $\hat{T}$ versus τ data. This fit was accomplished for different combinations of PAPS and carbon foil thickness. The idea was to find the most probable combination of these two parameters (PAPS and foil thickness) by looking for the least deviation between the straight line fitted to the He^{2+} data and the corresponding data $\hat{T}(\tau)$ of other abundant solar wind ions or in other words by minimizing

$$\chi^2 = \sum_{i=1}^{N} \sum_{j=2}^{59} \left(g(\tau_{i,j}) - \hat{T}_{i,j}(\tau_{i,j}) \right)^2. \tag{4.10}$$

N indicates the number of ions used for the IFC. The index j covers the range of the energy-per-charge steps used here. Although there are all in all 60 steps, the first and the last step are not used for technical reasons. Figure 4.4 shows the χ^2-value as a function of PAPS and foil thickness.

The minimum of that distribution is at a foil thickness of about 2.5μg/cm^2 and a PAPS value of about -23.9 kV. That means that the absolute value of the post acceleration voltage is probably 1kV less than expected, whereas the specification of the manufacturer about the foil thickness is reliable. The mapping of τ versus $\hat{T}$ with PAPS = -23.9 kV is well approximated by a single straight line g(τ) as one can see in Figure 4.3.

The energy calibration was accomplished by the following procedure. Using the efficiency model we calculated the measured energy E_{meas} corresponding to the PHDs (Pulse Height Defects) given in Table 3.2. For that the PAPS value and the foil thickness obtained from the $\hat{T}$ calibration were used. Ideally the mapping of these data versus the fitted $\hat{E}$ positions is again a single straight line and valid for all ion species. Figure 4.5 shows the result of the $\hat{E}$ calibration including data from He^{2+} and the two most abundant heavy solar wind ions O^{6+} and C^{6+}.
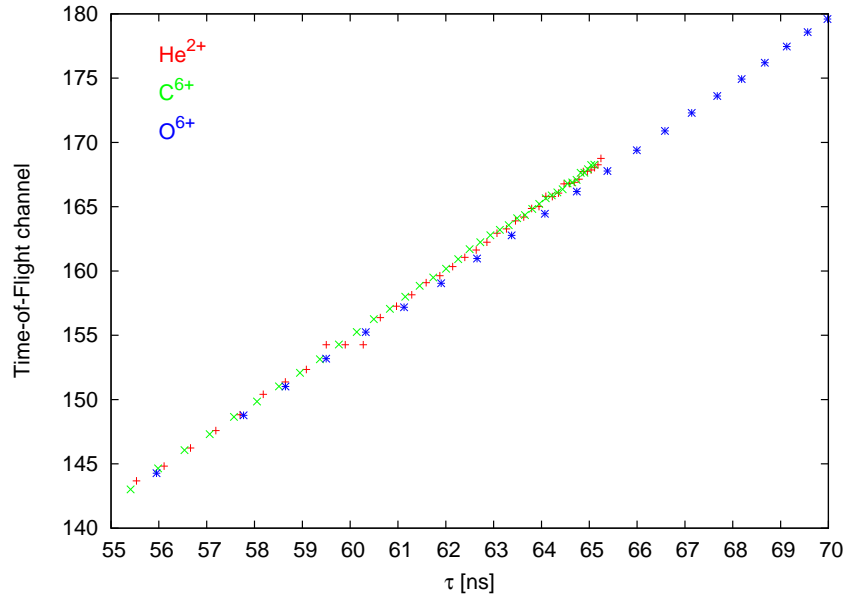
Figure 4.2.: ToF-position in the ET-matrices from two-dimensional fits to long-term data versus the ToF calculated with the efficiency model with a foil thickness of $110\mathring{A}$ and a post acceleration voltage of about -24.9 kV as stated in the housekeeping data of the instrument.
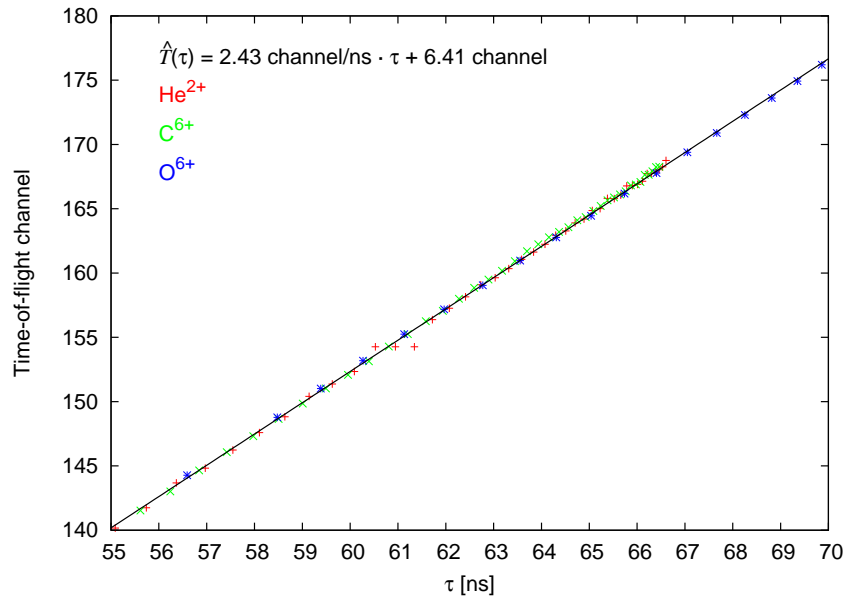
Figure 4.3.: ToF-positions in the ET-matrices from two-dimensional fits to long-term data versus the ToF calculated with the efficiency model with a foil thickness of $110\mathring{A}$ and a post acceleration voltage of about -23.9 kV. $\hat{T}(\tau)$ is a linear function fitted to these data.
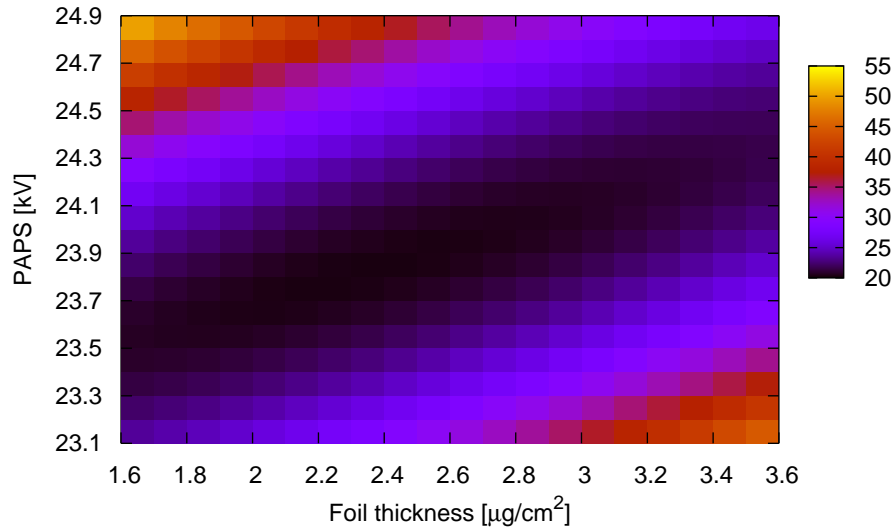
Figure 4.4.: Colour-coded plot of χ^2 as given in equation 4.10 as a function of foil thickness and post acceleration voltage. The minimum of this distribution gives the most probable combination of these quantities which is at $2.5\mu g/cm^2$ and 23.9 kV respectively.
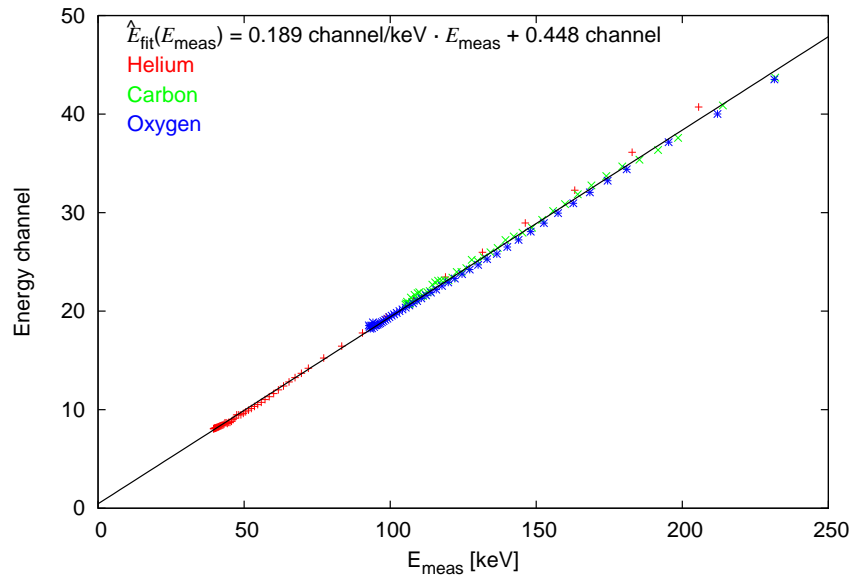
Figure 4.5.: Energy-positions in the ET-matrices from two-dimensional fits to long-term data versus the measured energy calculated with the efficiency model with a foil thickness of $110\mathring{A}$ and a post acceleration voltage of about -23.9 kV. $\hat{E}(E_{meas})$ is a linear function fitted to these data.

5. DATA PRODUCTS

The efficiency model provides mainly two data products. First it can be used to calculate the detection efficiencies depending on ion species, i.e., mass m and charge q, and the flight trajectory. The knowledge of the efficiencies of all solar wind ions is a fundamental component of a comprehensive data analysis. Physical quantities like ion densities, temperatures and absolute fluxes of the solar wind plasma can only be derived accurately from the count rates of the instrument in space accounting for the different efficiencies of the different ions. A description of the whole ACE/SWICS data analysis is given in *Berger* [2008].

The ions detected from the instrument in space are those ions which trigger at least a so-called double coincidence (DC) viz. those which triggered a start- and a stop-signal for the Time-of-Flight measurement. In our data analysis we used mainly triple coincidence (TC) data viz. data of those ions which triggered additionally an SSD-signal for the energy measurement. The respective probabilities to trigger one of these events can be calculated with the efficiency model. The TC probability is then given by the product of these three single probabilities. For a detailed description see *Köten* [2005]. As an example Figure 5.1 shows the detection efficiencies of O^{6+} depending on the energy-per-charge value and the aspect angle which is the angle between the instrumental rotation axis and the ions flight trajectory.

The aspect-angle dependency of the efficiency results from the fact that there are three SSDs which are not adjacent but with a gap in-between. Additionally, the areas (vertical stripes) where the efficiency drops to zero is due to the frame of the carbon foil. Figure 5.2 shows schematically the dimension and the holder of the respective foil elements. According to Figure 5.1, in the further discussion we will use the following indexing: SSD1 at the right, SSD2 in the middle, SSD3 at the left.

The error estimation of the efficiencies was accomplished by using the individual errors of the parameters of the efficiency model. By putting a gaussian noise on the single parameters, Gaussians were fitted to the distribution around the nominal efficiency for any energy-per-charge step and any solar wind ion. In the energy range SWICS is able to measure, the error bars of the efficiencies are on the order of about $\pm$ 5 % to 8 % absolutely and $\pm$ 8 % to 20 % relative to the detection efficiency. As an example Figure 5.3 shows the distribution around the nominal efficiency of O^{6+} in step 30 which corresponds to an energy-per-charge value of about 4.9keV/e and an aspect angle of 35 degrees. In this example the efficiency including the $1 - \sigma$ error bar is 0.38 $\pm$ 0.077. The relative error bar is then given by $\pm 0.077/0.38 \approx 20\%$. The resulting TC efficiency of O^{6+} including error bars for all steps are shown in Figure 5.4. The efficiencies of all solar wind ions are given in appendix A.

The second contribution of this work for the ACE/SWICS data analysis is the prediction of the ECH and TCH position in the ET-matrices for any solar wind ion in any energy-per-charge step. Knowing the exact positions of a specific ion makes the further data analysis more precise because the number of free parameters of the two dimensional distribution function that describes the abundance of each ion in each matrix is reduced by two. That accelerates the fitting process and saves computing time. It is also essential for the evidence of the ^{13}C isotope
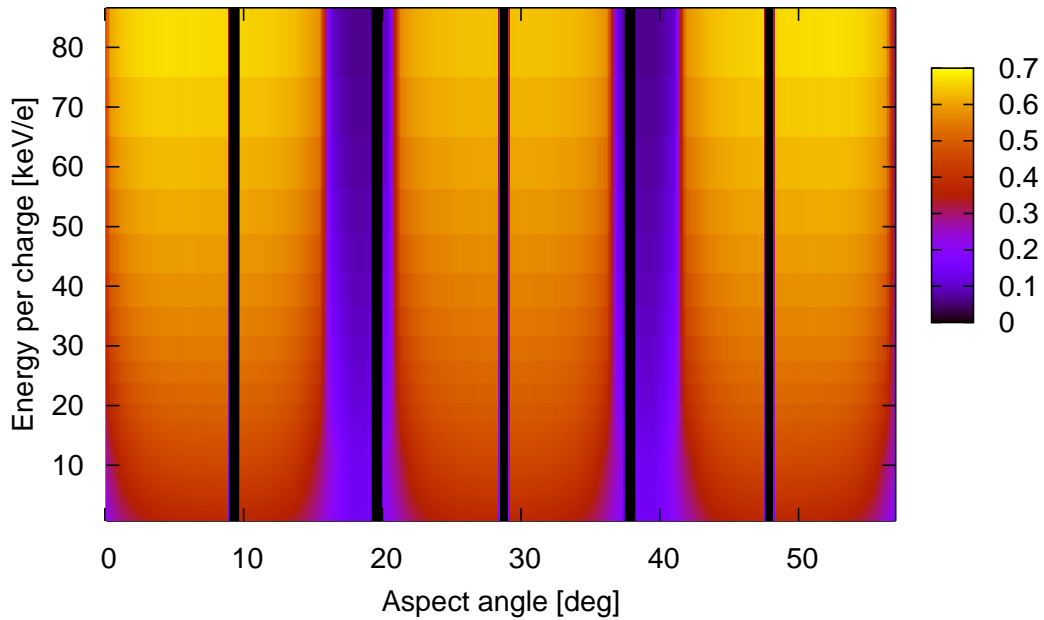
Figure 5.1.: Colour-coded plot of the detection efficiency of ACE/SWICS for O6+ as a function of energy-per-charge value and the aspect angle. The bright yellow and red areas between the vertical purple stripes indicate that there are three solid-state detectors. The purple stripes show the gaps between the SSDs. The thin black vertical stripes where the efficiency drops to zero are due to the frame of the carbon foil.
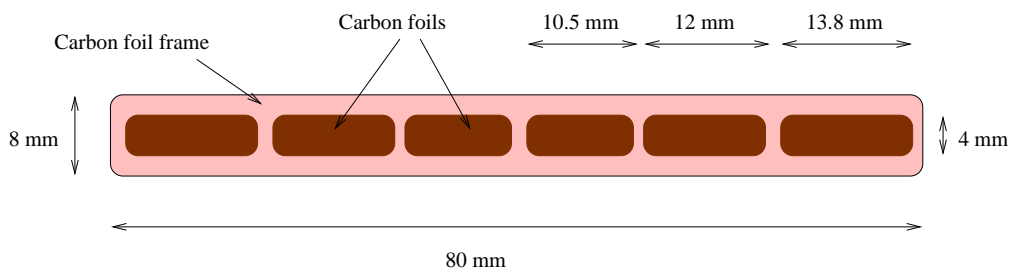
Figure 5.2.: Schematic view of the dimensions and the housing of the different carbon foil elements.
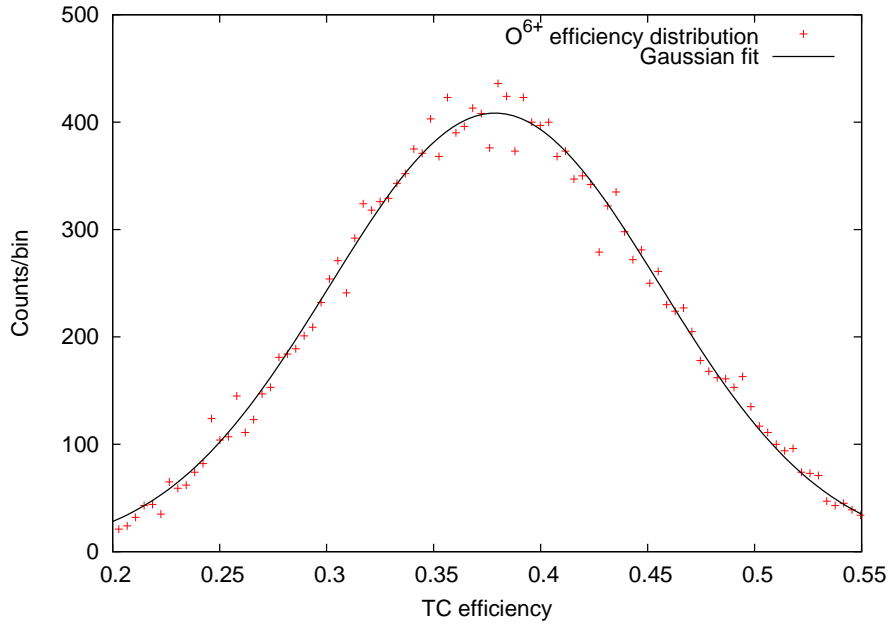
Figure 5.3.: Gaussian fitted to the distribution around the nominal efficiency of O^{6+} in step 30 which corresponds to an energy-per-charge value of about $4.9\,\mathrm{keV/e}$. The aspect angle is $35°$ which corresponds to a flight trajectory that hits the SSD2 according to Figure 5.1.
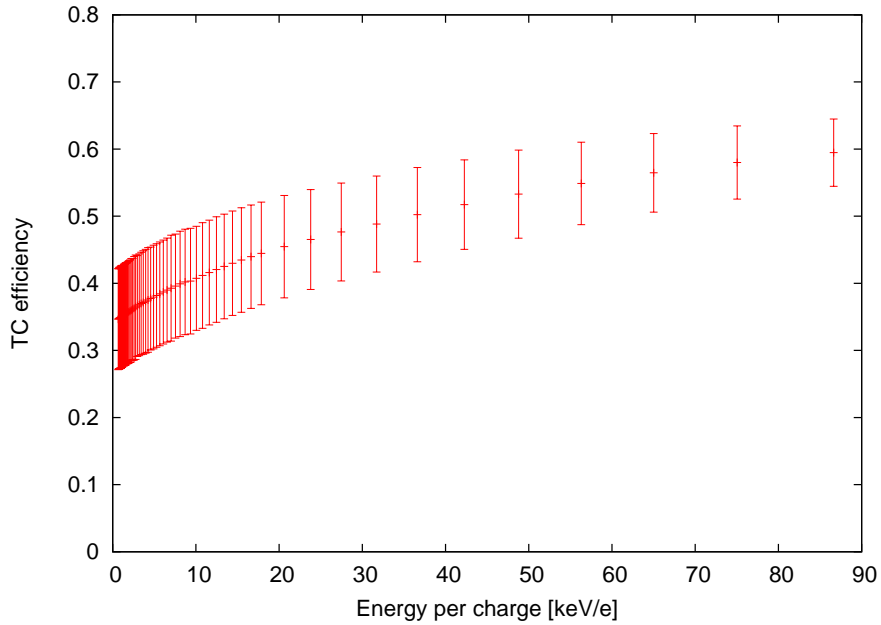
Figure 5.4.: Probability of O^{6+} to trigger a triple coincidence for all E/q-steps including $1-\sigma$ error bars. The efficiencies are calculated for an aspect angle of $35°$ which corresponds to a flight trajectory that hits the SSD2 according to Figure 5.1.

in the solar wind. The abundance of ^{12}C is estimated to be about two orders of magnitude higher than the abundance of ^{13}C. Thus, one of the preconditions to achieve a 1% resolution that is required here is information about the exact ion positions. As an example Figure 5.5 shows the sequence of positions in the ET-matrices for a sample of abundant solar wind ions. The accuracy of these predictions was estimated to be about ±0.26 channels for the Time-of-Flight and ±0.39 channels for the energy measurement. The sequences of the positions of all solar wind ions are available in appendix A.
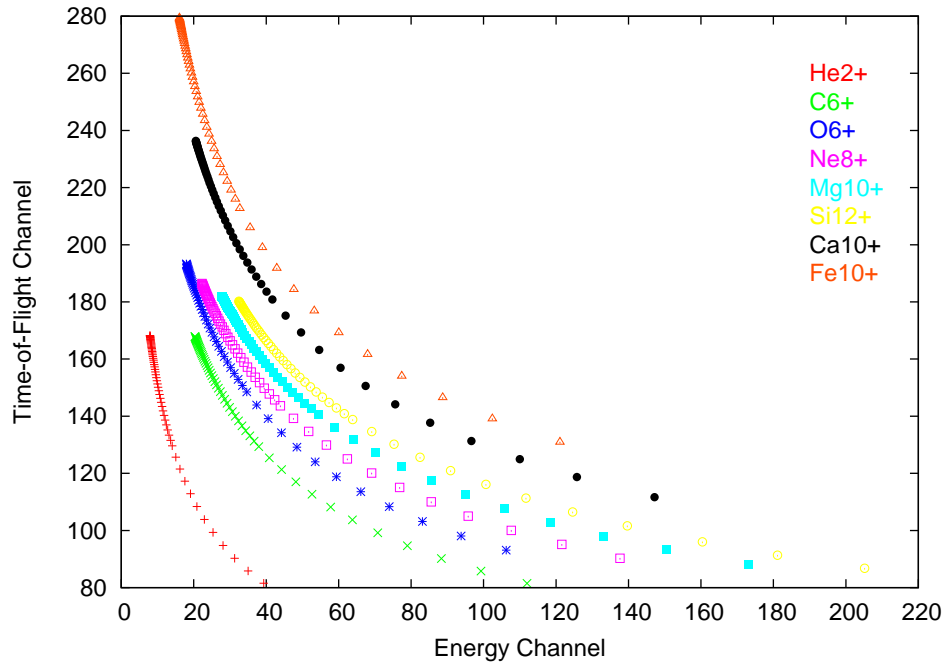
Figure 5.5.: Sequence of TCH- and ECH-positions in the 58 ET-matrices belonging to 58 different energy-per-charge steps calculated for a sample of abundant solar wind ions. Although there are all in all 60 steps, step 1 and step 60 are not used for technical reasons.

At the University of Michigan a similar ACE/SWICS data analysis is performed. For the prediction of the ion positions in the ET-matrices they used a model developed by Simon Hefti. Possibly there are considerable deviations between our predictions and those of Hefti. As an example, Figure 5.6 and Figure 5.7 show comparisons of both predictions of the energy channel and the ToF channel respectively for a sample of abundant solar wind ions.
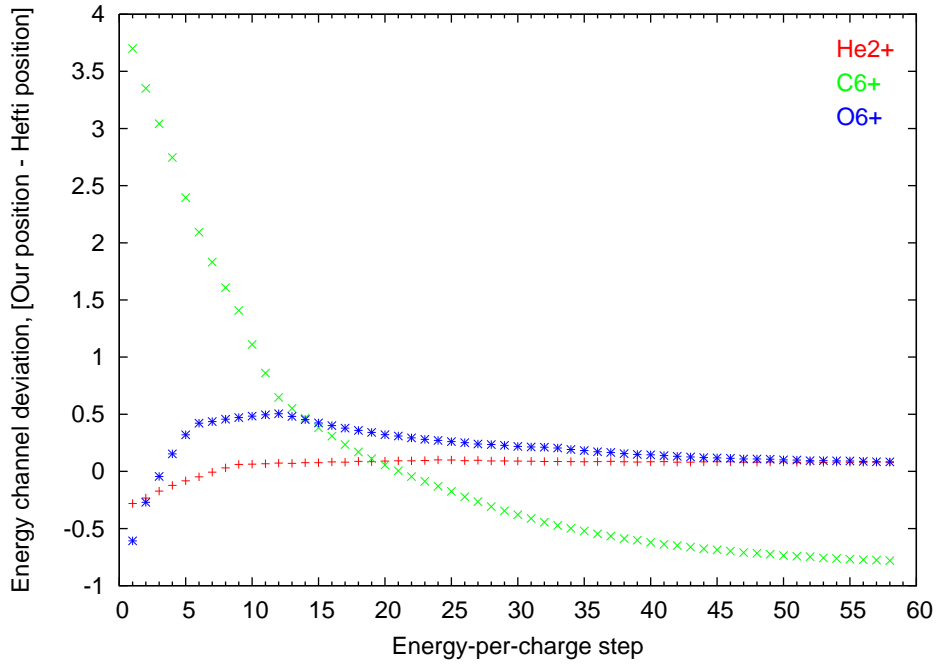
Figure 5.6.: Deviation of the energy-channel positions between our predictions and those result-ing from the Hefti model for He^{2+}, C^{6+}, and O^{6+} in the energy-per charge steps 2 to 59. The channels 1 and 60 are not used for technical reasons.
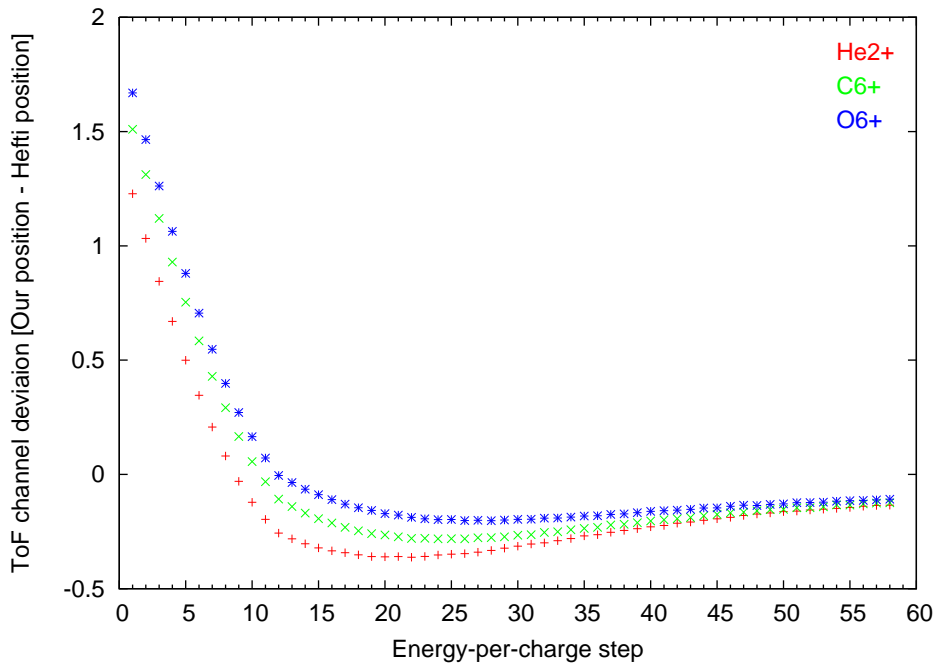
Figure 5.7.: Deviation of the ToF-channel positions between our predictions and those resulting from the Hefti model for He^{2+}, C^{6+}, and O^{6+} in the energy-per charge steps 2 to 59. The channels 1 and 60 are not used for technical reasons.

6. DETECTION OF ^{13}C IN THE ACE/SWICS DATA

Carbon is the fourth most abundant element in the solar wind after hydrogen, helium, and oxygen. Carbon is also a highly volatile element and therefore, the terrestrial abundance with respect to fractionary elements is lower than it is observed from the solar elemental composition. Nevertheless, it is assumed that the isotopic composition in the solar wind be similar to the terrestrial composition. Otherwise, a deviation between both compositions would be a sign of mass dependent fractionation processes in the solar atmosphere or in the interplanetary space. Carbon has only two stable isotopes, $^{12}_{6}$C and $^{13}_{6}$C. The mass range of the carbon isotopes extends from 8 to 22 but most of them are just intermediates of radioactive decays of heavier elements with half-life times not exceeding a few tens of minutes. An exception is the radioactive $^{14}_{6}$C-isotope with a half-life time of about 5730 years. This isotope is often used for age determination of fossils which are not older than a few ten thousand years. In opposite to the stable isotopes which are products of nuclear synthesis in stars, $^{14}_{6}$C originates in the Earth's upper atmosphere from the reaction of $^{14}_{7}$N and neutrons which again originate from the interaction between the Earth's atmosphere and highly-energetic galactic cosmic rays.

$$^{14}_{7}\text{N} + {}^{1}_{0}\text{n} \rightarrow {}^{14}_{6}\text{C}^* + {}^{1}_{1}\text{p}$$
$$^{14}_{6}\text{C}^* \rightarrow {}^{14}_{7}\text{N} + {}^{0}_{-1}\text{e}^- + \overline{\nu}$$
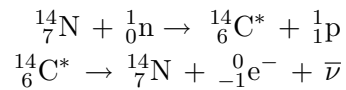
The relative abundance of $^{12}_{6}$C determined from measurements of terrestrial samples and samples of extraterrestrial regoliths is about 98.9 % and of $^{13}_{6}$C about 1.1 % resulting in a ratio of about 89:1 (*Woods and Willacy* [2009], *Woods* [2009], and *Clayton* [2003]).

As mentioned in Chapter 2 the nuclear synthesis processes in the core of the Sun cause an enrichment of $^{13}_{6}$C at the expense of $^{12}_{6}$C. During their lifetime these $^{13}_{6}$C isotopes do not reach the outer convection zone and remain in the core until they are destroyed and converted to nitrogen according to the CNO-cycle. Thus, it is assumed that the carbon isotopic composition revealed from measurements on Earth and from measurements of the solar wind, which both reflect mainly the carbon isotopic ratio in the presolar nebula, are the same. Deviations of the isotopic ratio would indicate that there are mass dependent fractionation processes in the origination or propagation of the solar wind.

Up to now, the determinations of the solar isotopic composition of carbon were accomplished from photospheric observations. The isotopic composition was obtained from the analysis of CO absorption lines, e.g. by *Harris et al.* [1987] ($^{12}_{6}$C/$^{13}_{6}$C = 84 ± 5). Therefore, in this work we present for the first time the carbon isotopic ratio in the solar wind determined by in-situ measurements. The results presented in this work are based on measurements of ACE/SWICS. As described in section 4.2 the preprocessed data are so-called ET-matrices. In each ET-matrix each solar wind ion has its maximum abundance at a certain point with a distribution around this point. Thus, each ion causes a 'hill' whose volume is correlated with the abundance of the respective ion in the considered ET-matrix. Therefore, besides the knowledge of the exact

positions in the ET-matrices we also have to know the shapes of the peaks to correctly distribute the counts to the respective ions. A detailed analysis of these shapes is given in the following section.

6.1. Instrumental Response Function

The identification and verification of $^{13}_{6}$C in the solar wind requires a $1\,\%$ resolution in the data analysis method. Therefore, it is necessary to understand the instrumental response function very well, viz. the positions of the peaks in the ET-matrices for all solar wind ions have to be known. The positions we use are the results of the In-Flight Calibration as described in section 4.2.

Especially when the peaks overlap it is of fundamental importance to know the shapes of the peaks to avoid mismatching of the counts to other ion abundances. The assumption that the peaks in the ET-matrices be two-dimensional Gaussians is an approximation that does not satisfy the requirement that we need a $1\,\%$ resolution to locate and identify the $^{13}_{6}$C-peak in the ET-matrices. Studying the peak characteristics in more detail shows that the peaks in fact are Gaussians in energy direction for a fixed ToF-channel but asymmetric Kappa-functions $\mathcal{K}(T)$ in ToF direction for a fixed energy channel. The $\mathcal{K}$-Function is a generalized distribution function and is given by

$$\mathcal{K}(x) = K_0 \cdot \left(1 + \frac{(x - x_0)^2}{\kappa\,\sigma_\kappa^2}\right)^{-\kappa}.$$

(6.1)

The κ-value is a parameter which can be used to variably weight the tail of the distribution. With $\kappa = 1$ the distribution corresponds to a Lorentzian. In the case that $\kappa = \infty$ the $\mathcal{K}$-distribution fits a Gaussian with $\sigma_\kappa = \sigma_{\text{Gauss}} \cdot \sqrt{2}$. Figure 6.1 shows the $\mathcal{K}$-distribution for different κ-values with $\sigma_\kappa = 1$ and $K_0 = 1$.

The special shape of the peak in the ET-matrices is just clearly visible looking at isolated peaks like He^{2+} as shown in the Figure 6.2. The iso-contour lines clarify this. According to Figure 6.2, Figure 6.3 shows the one-dimensional ToF-distributions for the energy channels 8 to 12 normalized to the number of counts which have occurred at the one-dimensional peak maximum. We have used the function

$$f(x) = \begin{cases} K_0 \cdot \left(1 + \frac{(x-x_0)^2}{\kappa_l\,\sigma_l^2}\right)^{-\kappa_l}, & x < x_0 \\ K_0 \cdot \left(1 + \frac{(x-x_0)^2}{\kappa_r\,\sigma_r^2}\right)^{-\kappa_r}, & x \geq x_0 \end{cases}$$

(6.2)

as an analytical expression for the ToF-distribution. For each energy channel we have accomplished a fit via the parameters K_0, x_0, κ_l, κ_r, σ_l, σ_r. The results of the one-dimensional fit for the energy channel 8 to 12 are shown in the Figures 6.4 and 6.5. In the considered example the shapes towards lower ToF channels seen from the peak maximum can be described by $\mathcal{K}$-functions with κ_l-values of 4 or higher, that means that the distribution to lower ToF channels is well approximated by a Gaussian. Towards higher ToF channels the shape depends on the energy channel.

Astonishingly the σ_l-values stay almost constant in all energy channels while the κ_r-values increase to higher energy channels. To verify these results obtained from the fits to the data from step 30 we have accomplished analogue fits for the neighbouring energy-per-charge steps (28 to 32) where the He^{2+} peak delivers a similar good statistic. The Figures 6.6, 6.7, 6.8, and 6.9 show the parameters resulting from these fits which confirm first results from step 30.
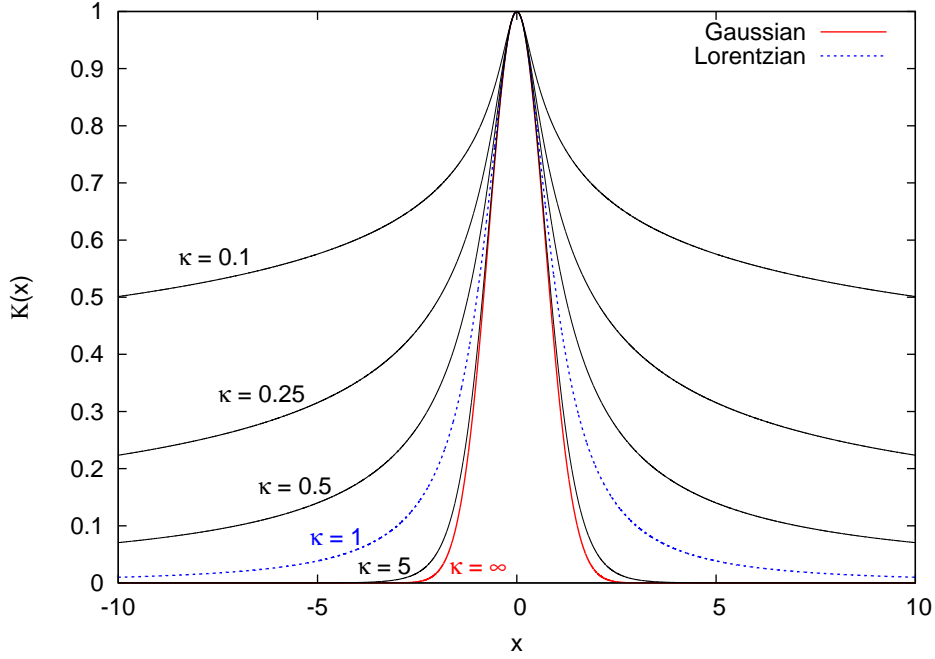
Figure 6.1.: Kappa functions $\mathcal{K}(\text{x})$ with $K_0 = 1$ and $\sigma_\kappa = 1$ but different κ-values. $\kappa = 1$ corresponds to a Lorentzian, $\kappa = \infty$ corresponds to a Gaussian with $\sigma_\kappa = \sigma_{\text{Gauss}} \cdot \sqrt{2}$.

Assuming that the ToF distribution can be approximated by an asymmetric $\mathcal{K}$-function with the additional assumption that there is always a linear relation between the κ_{r} and the energy channel while σ_{r} stays constant, we have accomplished two-dimensional fits to the He^{2+} peak in all steps which are relevant for the final evidence of ^{13}C. The focus of this work concentrates on the six times charged carbon (see section 6.3). Therefore, for all ions with mass-per-charge values of $m/q = 2$ e/amu (e.g. He^{2+} and ^{12}C^{6+}), the relevant steps in the typical solar wind speed range between 350 km/s and 800 km/s are mainly in the range from step 30 to step 50.

The two-dimensional analytical expression as a function of the energy channel E and the ToF channel T, $F(E,T)$ used as fit function is given by the product of the distribution in energy direction which is approximated by a symmetric Gaussian, and the distribution in ToF direction which is approximated by an asymmetric $\mathcal{K}$-function. Additionally, we have to consider that the κ_{r}-values of one-dimensional TOF-distributions increase to higher energy channels seen from the peak maximum and decrease to lower energy channels. For that, we introduce two new variables, $\kappa_{\text{r},1}$ and $\kappa_{\text{r},2}$, which describe the variability of κ_{r}.

$$\kappa_{\text{r}} = \kappa_{\text{r},1} \cdot (E - \hat{E}) + \kappa_{\text{r},2} \tag{6.3}$$

Finally, the fit function is then given by

$$F(E,T) = A \cdot e^{-\frac{(E-\hat{E})^2}{2\sigma_{\text{G}}^2}} \cdot \begin{cases} \left(1 + \frac{(T-\hat{T})^2}{\kappa_{\text{l}}\,\sigma_{\kappa,\text{l}}^2}\right)^{-\kappa_{\text{l}}}, & T < \hat{T} \\[2ex] \left(1 + \frac{(T-\hat{T})^2}{\left(\kappa_{\text{r},1}\cdot(E-\hat{E})+\kappa_{\text{r},2}\right)\sigma_{\kappa,\text{r}}^2}\right)^{-\left(\kappa_{\text{r},1}\cdot(E-\hat{E})+\kappa_{\text{r},2}\right)}, & T \geq \hat{T}. \end{cases} \tag{6.4}$$
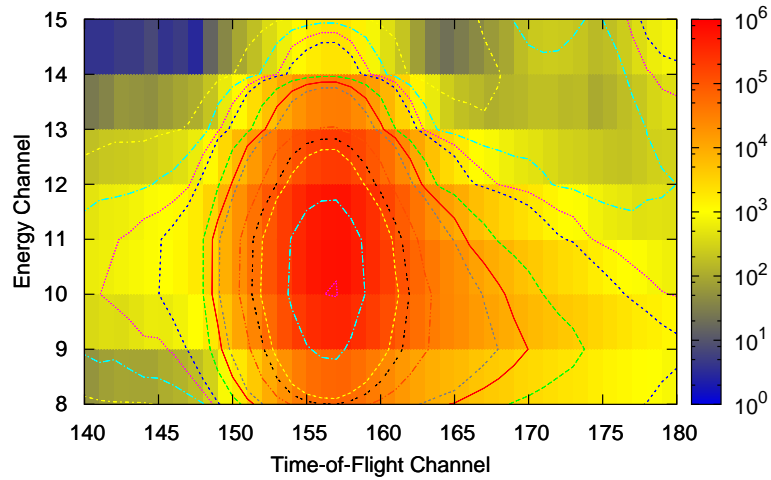
Figure 6.2.: Part of an ET-matrix showing the He^{2+} peak in the energy-per-charge step 30. The asymmetry of the peak is clearly visible. For a fixed ToF-channel the distribution as a function of the energy channel can be well approximated by a Gaussian. For a fixed energy channel, the distribution towards lower ToF-channels seen from the peak maximum can also be well approximated by a Gaussian. The shape of the peak towards higher ToF channels can be approximated by a $\mathcal{K}$-Function with increasing κ-values towards higher energy channels.
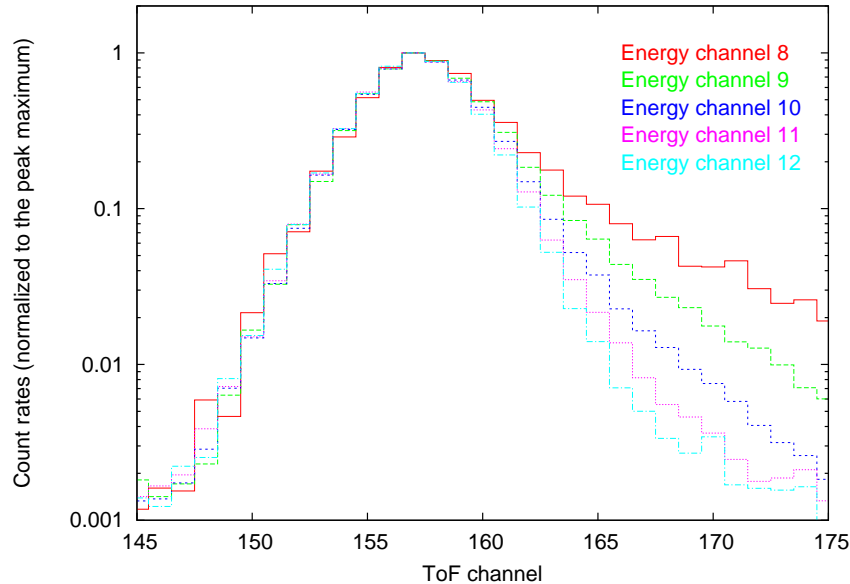
Figure 6.3.: One-dimensional distributions of the count rates for different energy channels normalized to the maximum value. The one-dimensional distribution towards lower ToF-channels is more or less independent from the energy channel, whereas towards higher ToF-channels the tail of the distribution is more weighted towards lower energy channels.

Figure 6.4.: σ-values resulting from one-dimensional fits of the function given in equation 6.2 to the ToF-distribution of the He^{2+} peak in the energy channels 8 to 12 based on long-term data of the energy-per-charge step 30. Left and Right indicate the shapes of the peak towards lower and higher ToF channels respectively.

Figure 6.5.: κ-values resulting from one-dimensional fits of the function given in equation 6.2 to the ToF-distribution of the He^{2+} peak in the energy channels 8 to 12 based on long-term data of the energy-per-charge step 30. Left and Right indicate the shapes of the peak towards lower and higher ToF channels respectively.

Figure 6.6.: σ_l-values resulting from one-dimensional fits of the function given in equation 6.2 to the ToF-distribution of the He^{2+} peak in the energy channels 8 to 12 for different energy-per-charge steps.

Figure 6.7.: σ_r-values resulting from one-dimensional fits of the function given in equation 6.2 to the ToF-distribution of the He^{2+} peak in the energy channels 8 to 12 for different energy-per-charge steps.

54

Figure 6.8.: κ_l-values resulting from one-dimensional fits of the function given in equation 6.2 to the ToF-distribution of the He^{2+} peak in the energy channels 8 to 12 for different energy-per-charge steps.

Figure 6.9.: κ_r-values resulting from one-dimensional fits of the function given in equation 6.2 to the ToF-distribution of the He^{2+} peak in the energy channels 8 to 12 for different energy-per-charge steps.

Figure 6.10.: Variability of κ_l and $\kappa_{r,2}$ as a function of the energy-per-charge step. The κ_l-value is again always higher than 4 as expected from the results of the one-dimensional fits. $\kappa_{r,2}$ indicates κ_r at the peak position.
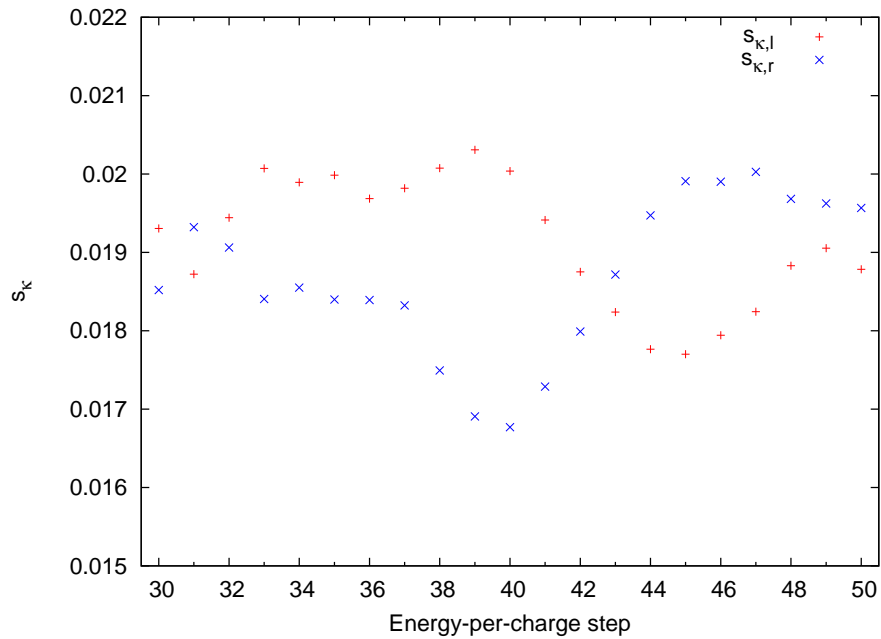
Figure 6.11.: Variability of $s_{\kappa,l}$ and $s_{\kappa,r}$ as a function of the energy-per-charge step. The ToF-distribution shapes towards higher and lower ToF channels are weighted differently depending on the considered step. Clearly visible is an anti-correlation between both s_κ-values.
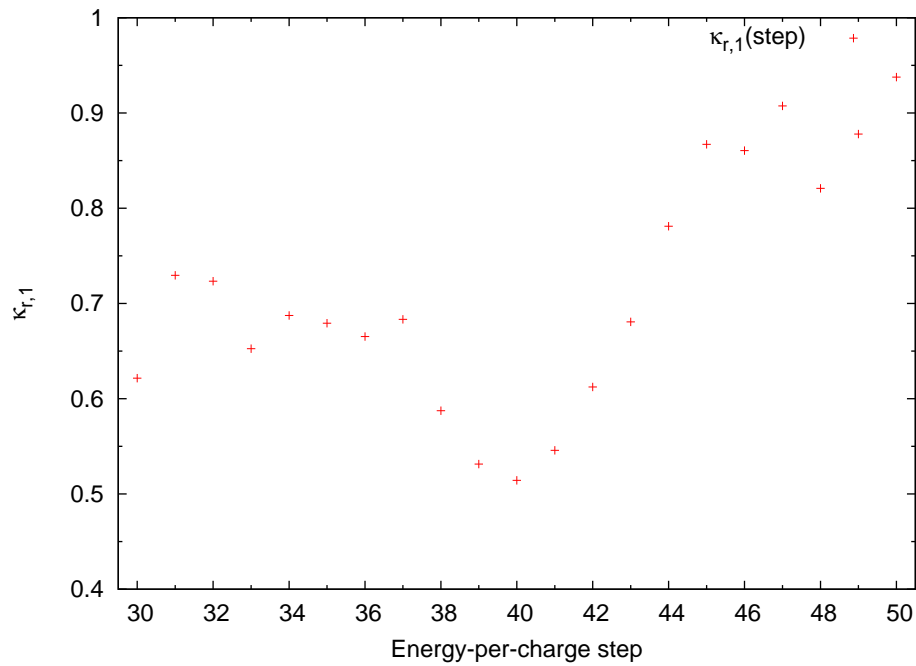
Figure 6.12.: Variability of $\kappa_{r,1}$ as a function of the energy-per-charge step which shows a similar behaviour like $\kappa_{r,2}$.
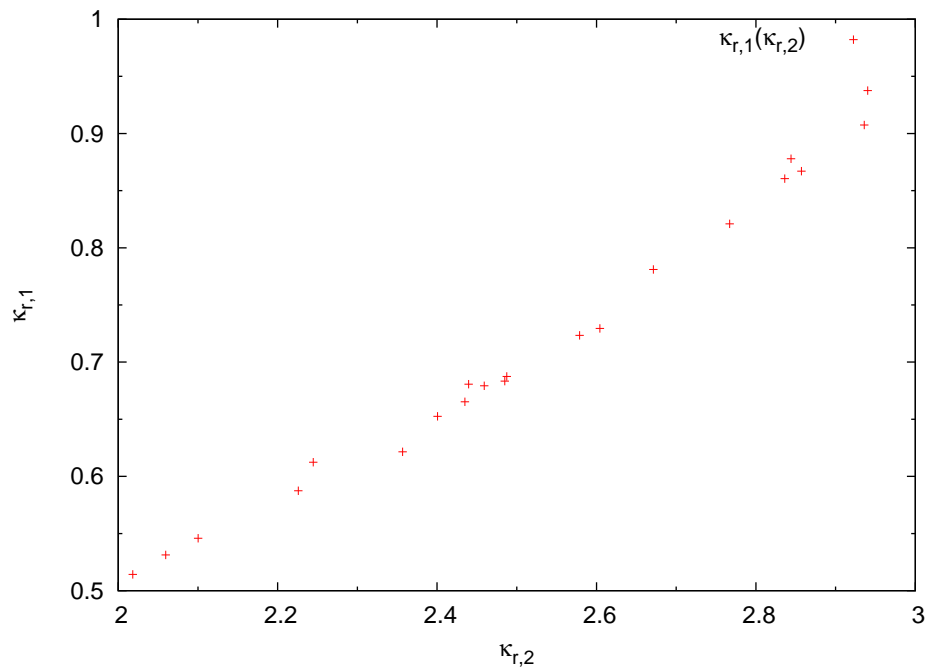
Figure 6.13.: $\kappa_{r,1}$ versus $\kappa_{r,2}$ obtained from the two-dimensional fits in in the step-range 30 to 50 indicating a linear relation between both parameters.

57
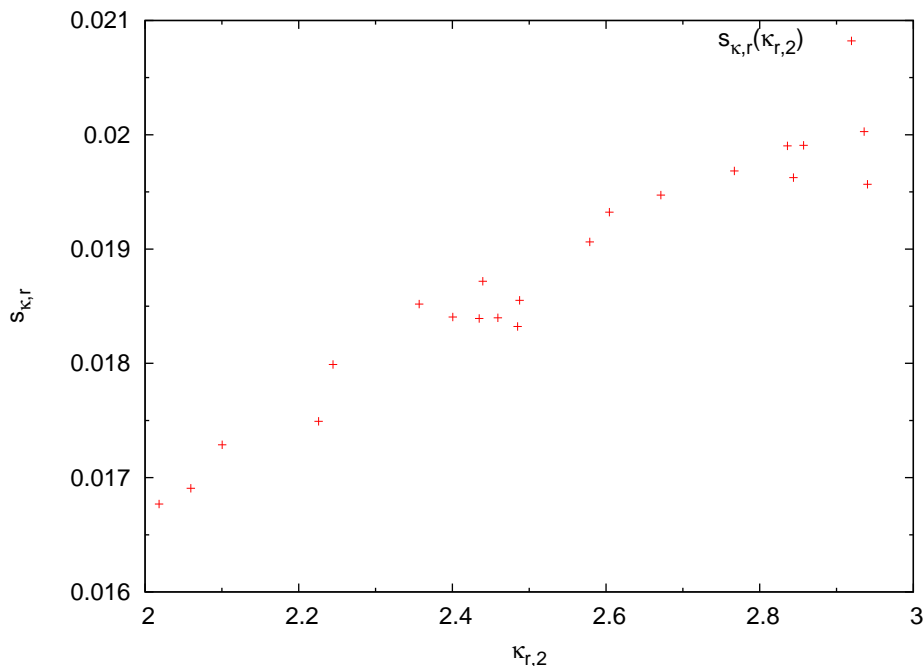
Figure 6.14.: $s_{\kappa,\mathrm{r}}$ versus $\kappa_{\mathrm{r},2}$ obtained from the two-dimensional fits in in the step-range 30 to 50 indicating a linear relation between both parameters.

The fit was accomplished via the parameters, A, $\hat{E}$, $\hat{T}$, σ_{G}, $\sigma_{\kappa,\mathrm{l}}$, $\sigma_{\kappa,\mathrm{r}}$, κ_{l}, $\kappa_{\mathrm{r},1}$, and $\kappa_{\mathrm{r},2}$. The σ-values resulting from these fits are not offhand comparable to the widths of the peaks of other solar wind ions. Nevertheless, a realistic assumption is to claim that the σ-value of the Gaussian is proportional to the measured energy E_{meas}, and the σ-values of the asymmetric $\mathcal{K}$-function are proportional to the Time of Flight τ. With regard to the offset in the formula for the calculation of $\hat{E}$ from E_{meas} and $\hat{T}$ from τ respectively, the following variables are introduced which can then be easily used to estimate the peak widths, σ_{G}, $\sigma_{\kappa,\mathrm{l}}$, and $\sigma_{\kappa,\mathrm{r}}$, for all solar wind ions in each considered energy-per-charge step from the known peak positions.

$$s_{\mathrm{G}} = \sigma_{\mathrm{G}}/(\hat{E} - \Delta\hat{E}), \tag{6.5}$$

$$s_{\kappa,\mathrm{l}} = \sigma_{\kappa,\mathrm{l}}/(\hat{T} - \Delta\hat{T}), \tag{6.6}$$

$$s_{\kappa,\mathrm{r}} = \sigma_{\kappa,\mathrm{r}}/(\hat{T} - \Delta\hat{T}). \tag{6.7}$$

According to the equations 4.8 and 4.9 the offset values are given by $\Delta\hat{E} = 0.448$ channels and $\Delta\hat{T} = 6.41$ channels. The parameters resulting from the two-dimensional fits show that the peak characteristics are not the same for all steps. An exception is the parameter s_{G} which can be set to 0.11 in all considered steps.

Especially the weighting of the asymmetric shapes of the ToF distribution depends extremely on the considered step as can be seen in Figure 6.10 and Figure 6.11 which show κ_{l} and $\kappa_{\mathrm{r},2}$, and $s_{\kappa,\mathrm{l}}$ and $s_{\kappa,\mathrm{r}}$ respectively as a function of the step number. Figure 6.12 shows analogously the variability of $\kappa_{\mathrm{r},1}$. Astonishingly there are linear relations between $\kappa_{\mathrm{r},1}$ and $\kappa_{\mathrm{r},2}$ as shown in Figure 6.13, and between $s_{\kappa,\mathrm{r}}$ and $\kappa_{\mathrm{r},2}$ in Figure 6.14. Presumably these characteristics are

attributed to variable properties of the energy-per-charge analyzer in the different steps. These effects cannot be explained satisfyingly but have to be considered in the further data analysis.

Summarizing, the two-dimensional distribution function of each peak can then be calculated with equation 6.4. The energy- and the ToF-position of each ion in each step are available in the tables in Appendix A. The κ-values can be obtained from the Figures 6.10 and 6.12. The σ-values can be calculated with the equations 6.5, 6.6, and 6.7 by using the s-values from Figure 6.11 for the ToF-distribution and $s_G = 0.11$ for the energy-distribution.

6.2. Data selection

The data analysis to detect ^{13}C in the solar wind and therefore to achieve a 1 % resolution requires two preconditions. First, to guarantee a good statistic, long-term data are accumulated. We used data from the the years 2001, 2002, 2004, 2006, and 2007. When preparing the results of this work the data from these years were available in a format which could be used for further analysis. The disadvantage of using long-term data is that we cannot conclude anything about spatial and time-dependent variabilities of the ratio ^{13}C/^{12}C. The second precondition is to use solar-wind-speed filters generally to minimize the effect that the tails of faster or slower solar wind might contaminate the analyzed peaks. The importance of the speed filters will be demonstrated with the following example. Assuming that there is a solar wind beam with a bulk velocity of 400 km/s and a $\overline{v} = 10$ km/s, the velocity distribution function is given by a Maxwellian as shown in Figure 6.15.

We will now have a look at two different solar wind ions ($^{12}_{6}$C^{6+} and $^{16}_{8}$O^{7+}) with different mass-per-charge (m/q) values (2 and 2.29 amu/e respectively) but the same speed, and in which energy-per-charge step they will be detected most likely. For that, we have to know the energy-per-charge values belonging to the different steps. The correlation between the step number and the nominal E/q-value is shown in Figure 6.16. As mentioned in Chapter 5 step 1 and step 60 are not used for technical reasons.

Assuming that both ions have the same speed the energy-per-charge value of $^{16}_{8}$O^{7+} is $\frac{8}{7}$-times higher than it is for $^{12}_{6}$C^{6+}, because

$$(E/q)_{O^{7+}} : (E/q)_{C^{6+}} = (m/q)_{O^{7+}} : (m/q)_{C^{6+}} = \frac{16}{7} : \frac{12}{6} = 8 : 7. \qquad (6.8)$$

That means that different ions with the same speed occur in different E/q-steps depending on their m/q-value. Figure 6.17 shows the speed as a function of the step number for different mass-per-charge values. This m/q-dependent projection of the same speed onto different E/q-steps results in a shift between the two Maxwellians of $^{12}_{6}$C^{6+} and $^{16}_{8}$O^{7+} as shown in Figure 6.18. Thus, $^{12}_{6}$C^{6+} with a speed of 400 km/s will occur most likely in step 46 whereas $^{16}_{8}$O^{7+} will occur most likely in step 44.

In the example shown here, without a speed filter $^{16}_{8}$O^{7+} ions with a lower velocity would occur in the same E/q-steps where the distribution of the $^{12}_{6}$C^{6+} ions got its maximum abundance. This would make the search for the $^{13}_{6}$C^{6+} isotope which is, looking at the ET-matrices, in the triangle spanned by $^{12}_{6}$C^{6+}, $^{16}_{8}$O^{7+}, and $^{14}_{7}$O^{6+} more complicated. Thus, minimizing the abundances of the other solar wind ions in the ET-matrices means minimizing the error sources for the determination of the ratio $^{13}_{6}$C^{6+}/$^{12}_{6}$C^{6+}. The Figures 6.19 and 6.20 show parts of ET-matrices without speed filter and with a speed filter of $\Delta v = 10$km/s (400 km/s - 410 km/s) respectively. The data correspond to long-term data in the E/q-step 44 where $^{12}_{6}$C^{6+} with a
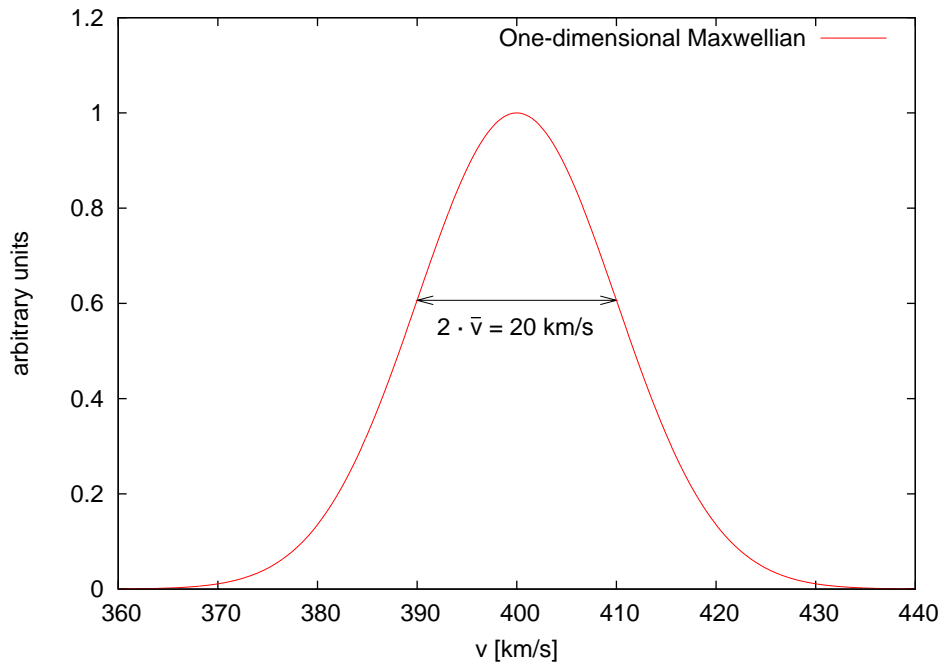
Figure 6.15.: One-dimensional velocity distribution function given by a Maxwellian with a bulk speed of 400 km/s and $\bar{v} = 10$ km/s.
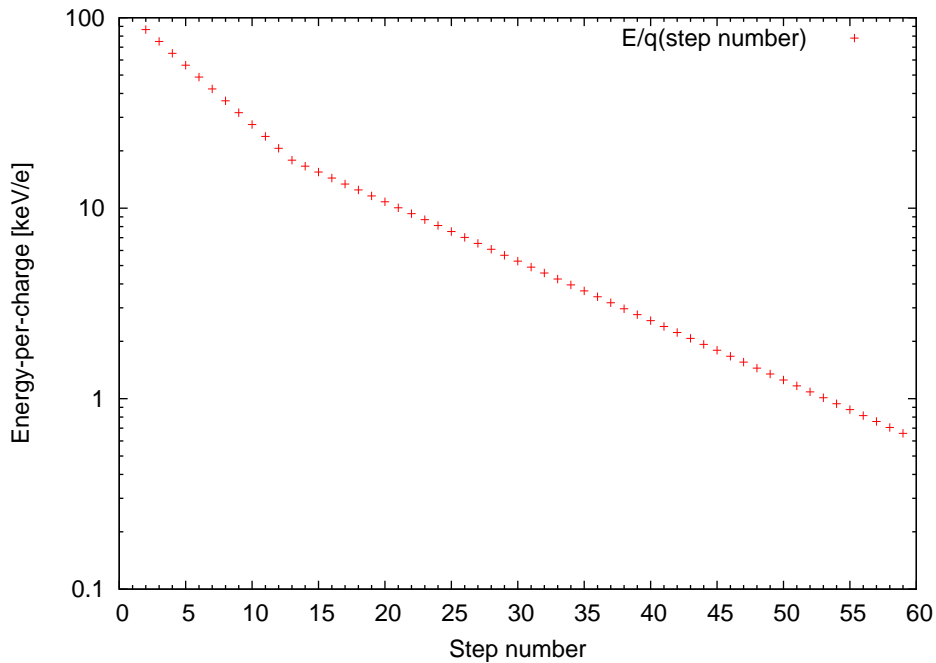
Figure 6.16.: Correlation between the E/q-step and the corresponding nominal energy-per-charge value.
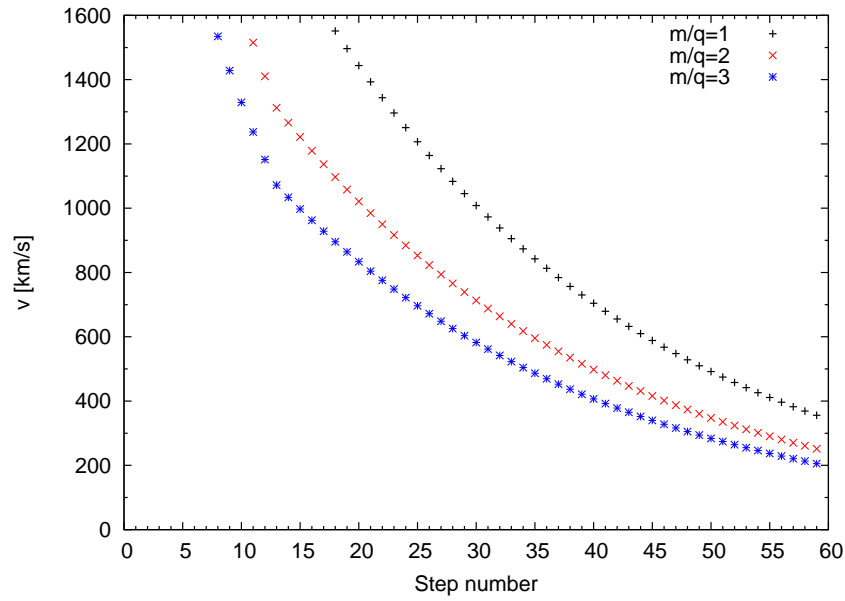
Figure 6.17.: Solar wind speed v as a function of the E/q-step number for different m/q values.
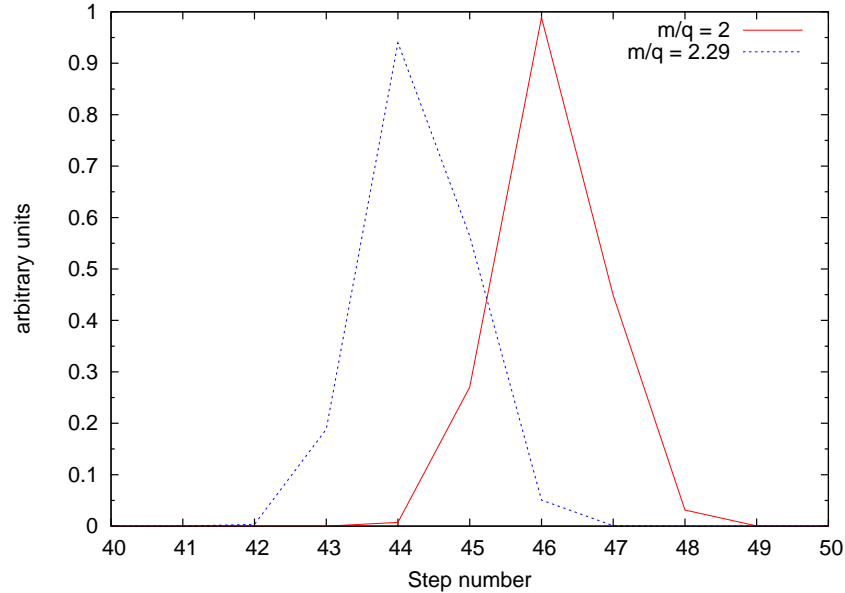
Figure 6.18.: Projection of two Maxwellians with the same bulk speed $= 400$ km/s and the same $\overline{v} = 10$ km/s but different m/q-values ($^{12}_{6}\mathrm{C}^{6+} \rightarrow 2\,\mathrm{amu/e}$, $^{16}_{8}\mathrm{O}^{7+} \rightarrow 2.29\,\mathrm{amu/e}$) onto the E/q-steps. The same initial speed but different m/q-values cause a shift between both distributions.
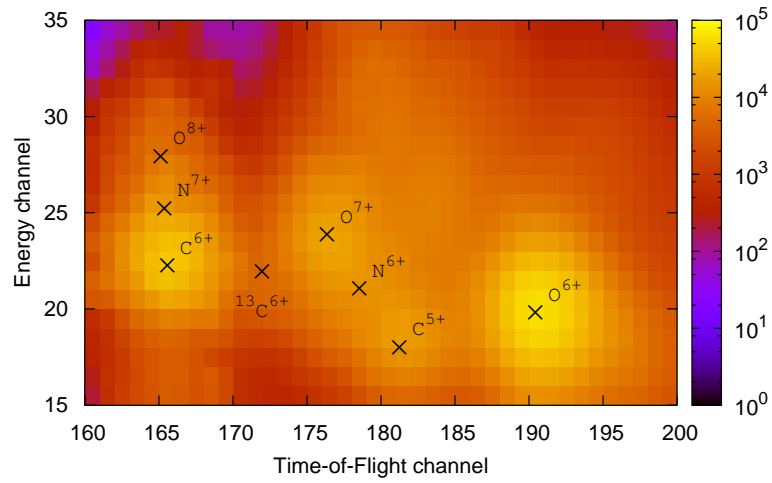
Figure 6.19.: Colour coded plot of an ET-matrix of long-term data accumulated over five years (2001, 2002, 2004, 2006, and 2007) in the E/q-step 44 (1.67 keV/e) without speed filter. The left shape (towards lower ToF-channels) of the $^{16}_{8}$O^{7+} peak overlaps with the $^{13}_{6}$C^{6+} peak and makes the detection of the latter more complicated.
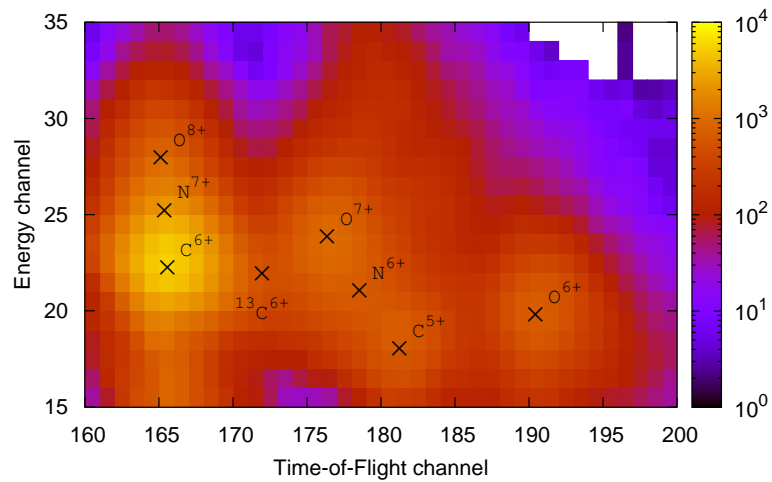
Figure 6.20.: Colour coded plot of an ET-matrix corresponding to Figure 6.19 with a speed filter of Δv = 10km/s (400 km/s - 410 km/s). Generally the count rates decreased compared to Figure 6.19, but the higher the m/q-value of the ions the stronger the decrease of the count rates.

velocity of 400 km/s got its maximum abundance according to Figure 6.18. The higher the m/q-value of the ions the more the count rates in the ET-matrix with speed filter decrease compared to the ET-matrix without speed filter.

As a compromise between these two preconditions we have chosen speed filters of $\Delta v = 40$km/s. This reduces the influence of the tails of other ions appropriately with respect to the analysis of the carbon peaks but also delivers relatively high count rates and thus a good statistic.

6.3. Charge state selection

There are mainly three abundant charge states of carbon in the solar wind, ($_6^{12}C^{4+}$, $_6^{12}C^{5+}$, and $_6^{12}C^{6+}$). Measurements with Ulysses/SWICS from *von Steiger et al.* [2000] revealed that the most abundant charge state of carbon in the slow and fast solar wind is $_6^{12}C^{6+}$ and $_6^{12}C^{5+}$ respectively. The data we are looking at to detect the carbon isotope $_6^{13}C$ are long-term data accumulated
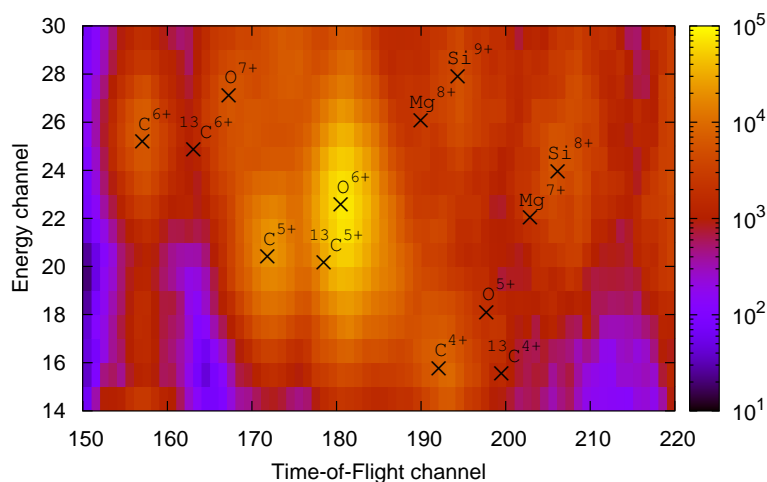
Figure 6.21.: Colour coded plot of an ET-matrix of long-term data accumulated over five years (2001, 2002, 2004, 2006, and 2007) in the E/q-step 30. $_6^{13}C^{4+}$ and $_6^{13}C^{5+}$ are at the tail of $_8^{16}O^{5+}$, and $_8^{16}O^{6+}$ respectively and thus, difficult to detect. The advantage of $_6^{13}C^{6+}$ is that its position is relatively well separated from the $_8^{16}O^{7+}$ peak.

over five years from ACE/SWICS at L1. Thus, the data correspond to a mixture of different types of solar wind. Except for Coronal Mass Ejections (CMEs) which occur irregularly, the data contains mainly measurements of slow solar wind with bulk velocities of about 400 km/s originating from the solar corona with temperatures on the order of about a few million Kelvin, and fast solar wind with bulk velocities of about 800 km/s originating from coronal holes. Thus, all three above-mentioned charge states of carbon are present in the long-term data. However, to determine the isotopic ratio $_6^{13}C/_6^{12}C$, in this work we have concentrated on the six times charged carbon. The reason becomes clear looking at the positions of the different charge states of the carbon isotopes in the ET-matrices. As an example, Figure 6.21 shows an ET-matrix of long-term data in the E/q-step 30. $_6^{13}C^{5+}$ is very difficult to detect because it is always at the tail of the most abundant heavy solar wind ion, $_8^{16}O^{6+}$. This would require an analysis technique which delivers a resolution of a few per mill in opposite to the method we used which delivers

a resolution of about 1 %.

A similar problem exists in trying to detect $^{13}_{6}C^{4+}$ which is at the tail of $^{16}_{8}O^{5+}$. Additionally, in the latter case much more ions have to be considered and need to be included in the final fit to determine the respective abundances. These ions are mainly low charged particles with nuclear charge Z=10 or higher. Although these ions are relatively far away from the $^{13}_{6}C^{4+}$ position, the large number of ions which have to be considered and influence each other holds error sources which can falsify any conclusion about the abundance of $^{13}_{6}C^{4+}$. In the case of $^{13}_{6}C^{6+}$, this problem can be largely avoided using appropriate speed filters which cause a decrease of the count rates depending on the m/q-value. Thus, many ions which have to be included to detect $^{13}_{6}C^{4+}$ can be neglected in the final fit to detect $^{13}_{6}C^{6+}$.

6.4. Final fit

The final fits to detect $^{13}_{6}C^{6+}$ were accomplished for different solar wind speed intervals. The speed filter as mentioned above is set to $\Delta v = 40$km/s starting at 340 km/s. For each speed filter the fits were performed in those E/q-steps where ions with an $m/q = 2$ ($^{12}_{6}C^{6+}$) or $m/q = 2.17$ ($^{13}_{6}C^{6+}$) reach their maximum abundance plus three steps up and three steps down. The nearest E/q-step corresponding to the mean speed of each speed filter is shown in Table 6.1.

The fit algorithm used here is a two-dimensional least-squares Levenberg-Marquard fit (*Press et al.* [1992]) including all ions in the ET-matrices which can possibly influence the abundances of $^{13}_{6}C^{6+}$ and $^{12}_{6}C^{6+}$. The fit parameters are just the peak heights of all included ions whereas all other parameters which characterize the different peaks are held fixed. The peak positions result from the In-Flight calibration as described in section 4.2, and the s- and the κ-values result from the analysis of the helium-peak as described in section 6.1.

Solar wind speed filter	360 ± 20	400 ± 20	440 ± 20	480 ± 20
E/q-step $^{12}_{6}C^{6+}$	49	46	43	41
E/q-step $^{13}_{6}C^{6+}$	48	45	42	40

Table 6.1.: Solar wind speed filters [km/s] and the corresponding E/q-steps of the mean speed.

7. RESULTS

Unfortunately the fit described above does not always deliver accurate results, especially in those steps where the dimension of the peak heights of $^{16}_{8}O^{7+}$ and $^{12}_{6}C^{6+}$ are comparable or the former one exceeds the latter one. The reason becomes clear bringing to mind that the shape of the ToF-distribution towards lower ToF-channels is approximated by just a single $\mathcal{K}$-distribution with different σ-values for the respective peaks. However, the results from the fits of asymmetric $\mathcal{K}$-functions to the one-dimensional ToF-distribution for each energy channel revealed that the corresponding κ-values of the left shape show a relatively big variance compared to the other parameters (see Figures 6.3 - 6.6).

This uncertainty about the shape of the peaks reflects in a big variance of the height of the $^{13}_{6}C^{6+}$ peak resulting from the final fit, and can undo any conclusion about the ratio of $^{13}_{6}C^{6+}$ and $^{12}_{6}C^{6+}$. Thus, reliable results can only be obtained using those E/q-steps where the variability due to the uncertainty of the shape towards lower ToF-channels can be neglected. As an example, Figure 7.1 shows the count rates at the peak positions of $^{12}_{6}C^{6+}$ and $^{16}_{8}O^{7+}$ as a function of the E/q-step. These count rates can be approximately used as a tracer for the respective ion abundance in the ET-matrices. The data correspond to long-term data obtained with a solar wind speed filter of 360 km/s $\pm$ 20 km/s. Thus, we used only those E/q-steps where $^{13}_{6}C^{6+}$ could be resolved with appropriate error bars. For the respective speed intervals the steps with accurate results are listed in Table 7.1.

Solar wind speed filter	360 ± 20	400 ± 20	440 ± 20	480 ± 20
Used E/q-steps	46-52	44-49	41-46	37-44

Table 7.1.: Solar wind speed filters [km/s] and the corresponding E/q-steps where the ratio of $^{13}_{6}C^{6+}$ and $^{12}_{6}C^{6+}$ could be resolved. The count rates in the steps higher or lower than these are not high enough to resolve the $^{13}_{6}C^{6+}$ peak.

For the respective speed intervals the peak heights of $^{12}_{6}C^{6+}$ and $^{13}_{6}C^{6+}$ as a function of the E/q-step resulting from the final fit are shown in Figure 7.2, 7.3, 7.4, and 7.5 respectively including an error estimation. The error bars include both, the error resulting from the fit and from the uncertainties of the efficiency model. To calculate the ratio of both carbon isotopes from these peak heights we have to consider some instrument specific properties. The count rates in the ET-matrices correspond to those ions which trigger a Tripe-Coincidence (TC), that means a start- and a stop signal for the Time-of-Flight measurement, and an energy measurement. The detection efficiencies of the considered carbon isotopes are not the same for the respective E/q-steps. In each step $^{12}_{6}C^{6+}$ has a slightly higher probability to be detected than $^{13}_{6}C^{6+}$. This mainly results from the slightly lower electronic differential energy loss S_e of $^{13}_{6}C^{6+}$ at the SSD surface.

According to equation 3.31 the number of secondary electrons ejected from the SSD surface by the impact of the ion is proportional to S_e. According to equation 3.50 the stop-signal trigger
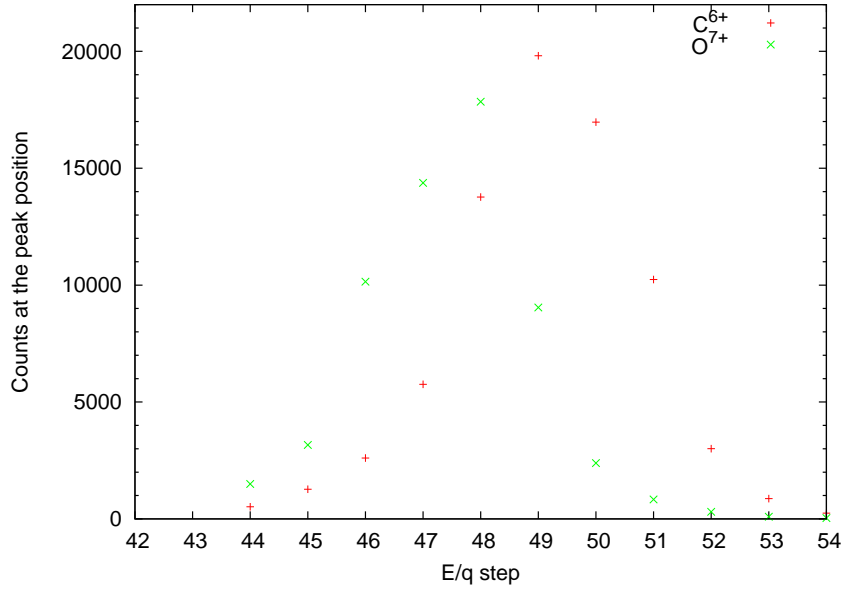
Figure 7.1.: Count rates at the peak positions of $^{12}_{6}\text{C}^{6+}$ and $^{16}_{8}\text{O}^{7+}$ (speed filter: 360 km/s $\pm$ 20 km/s) as a function of the step number. The counts at the theoretical peak positions can be approximately used as a tracer for the abundance of the respective ions. The relatively high counts at the position of $^{16}_{8}\text{O}^{7+}$ compared to the counts at the position of $^{16}_{8}\text{O}^{7+}$ plus the uncertainty of the shape of the peak in each ET-matrix towards lower ToF-channels results in a large uncertainty of the $^{13}_{6}\text{C}^{6+}$-abundance in the steps up to step 48.

probability again depends on the number of secondary electrons. The resulting TC efficiency of the considered carbon isotopes $^{12}_{6}\text{C}^{6+}$ and $^{13}_{6}\text{C}^{6+}$ as a function of the E/q-step is shown in Figure 7.6. These efficiencies are mean values averaged over all aspect angles. The relative deviation between the efficiencies of both isotopes is shown in Figure 7.7. The error bars of the efficiencies result from the uncertainties of the parameters of the efficiency model corresponding to Table 4.1. Considering ratios of the efficiencies most of these uncertainties cancel out because deviations of the properties of the instrument do have similar consequences for both ions. Generally, this results in much smaller error bars for ratios of efficiencies.

A second property of the instrument which has to be considered is associated to the energy-per-charge acceptance of the E/q-steps. According to equation 3.5, in each step the ions are selected by their energy-per charge and only those ions can pass the entrance system whose energy-per-charge value is in the interval $E/q \pm \Delta E$, where E/q is the nominal value belonging to the considered step. This is caused by the geometry of the deflection system.

The same energy-per-charge interval reflects in different speed intervals depending on the mass-per-charge value of the considered ion as shown in the example below.

$$\Delta \frac{E}{q} = \frac{1}{2} \cdot \frac{m_1}{q} \cdot \Delta v_1^2 = \frac{1}{2} \cdot \frac{m_2}{q} \cdot \Delta v_2^2 \tag{7.1}$$

$$\frac{\Delta v_1}{\Delta v_2} = \sqrt{\frac{m_1/q_1}{m_2/q_2}} \tag{7.2}$$
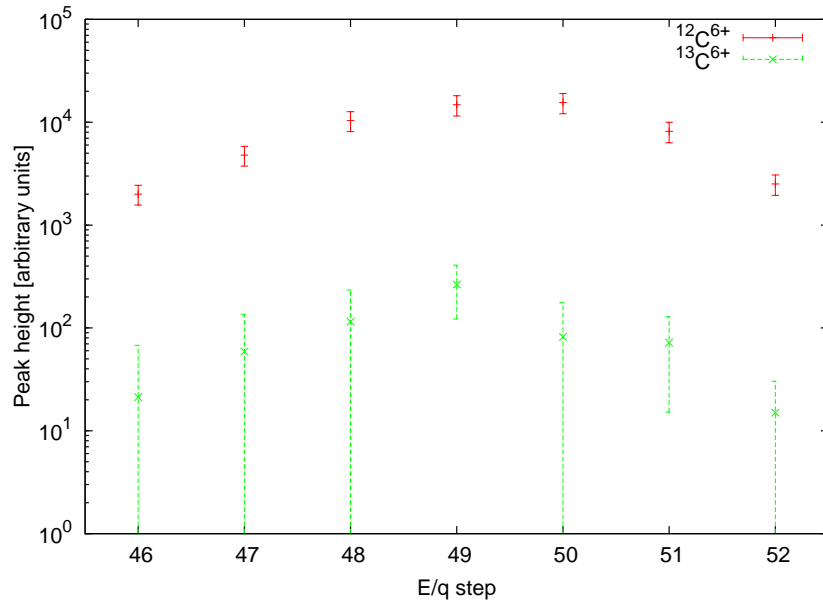
Figure 7.2.: Peak heights of $^{12}_6C^{6+}$ and $^{13}_6C^{6+}$ resulting from the two-dimensional fit in the solar wind speed interval 360 ± 20 km/s including 1-σ-error bars.
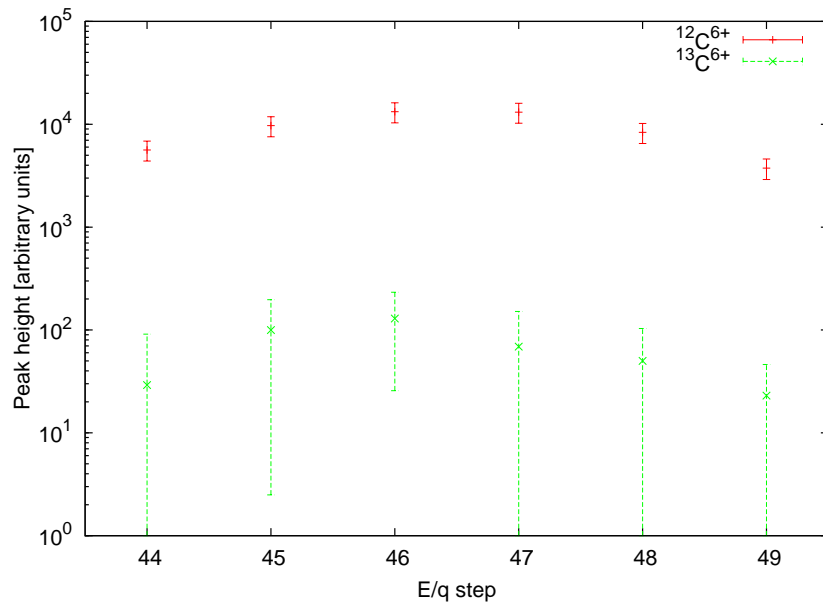
Figure 7.3.: Peak heights of $^{12}_6C^{6+}$ and $^{13}_6C^{6+}$ resulting from the two-dimensional fit in the solar wind speed interval 400 ± 20 km/s including 1-σ-error bars.
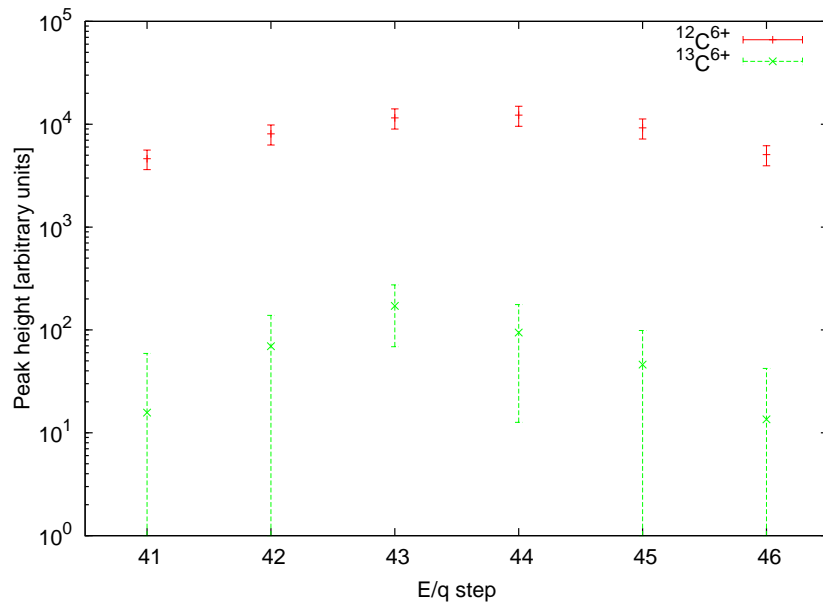
Figure 7.4.: Peak heights of $^{12}_{6}C^{6+}$ and $^{13}_{6}C^{6+}$ resulting from the two-dimensional fit in the solar wind speed interval 440 ± 20 km/s including 1-σ-error bars.
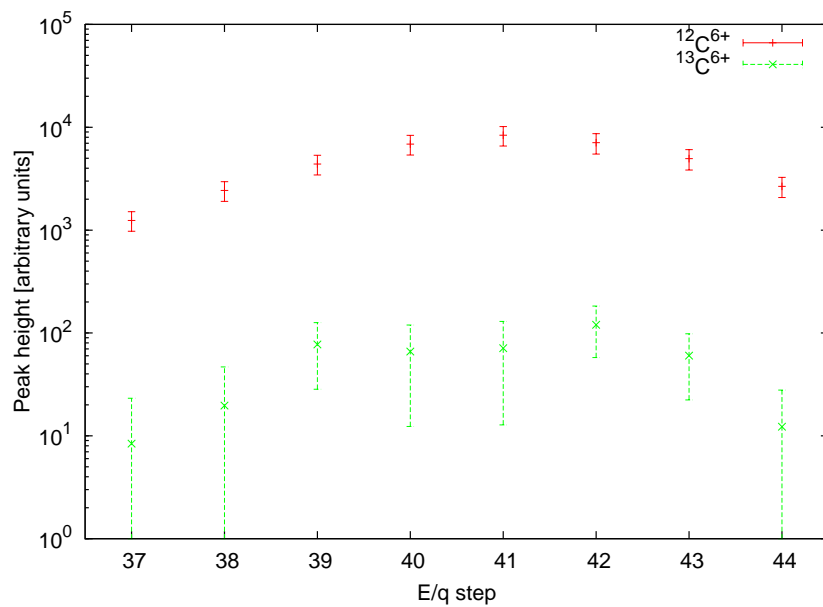
Figure 7.5.: Peak heights of $^{12}_{6}C^{6+}$ and $^{13}_{6}C^{6+}$ resulting from the two-dimensional fit in the solar wind speed interval 480 ± 20 km/s including 1-σ-error bars.
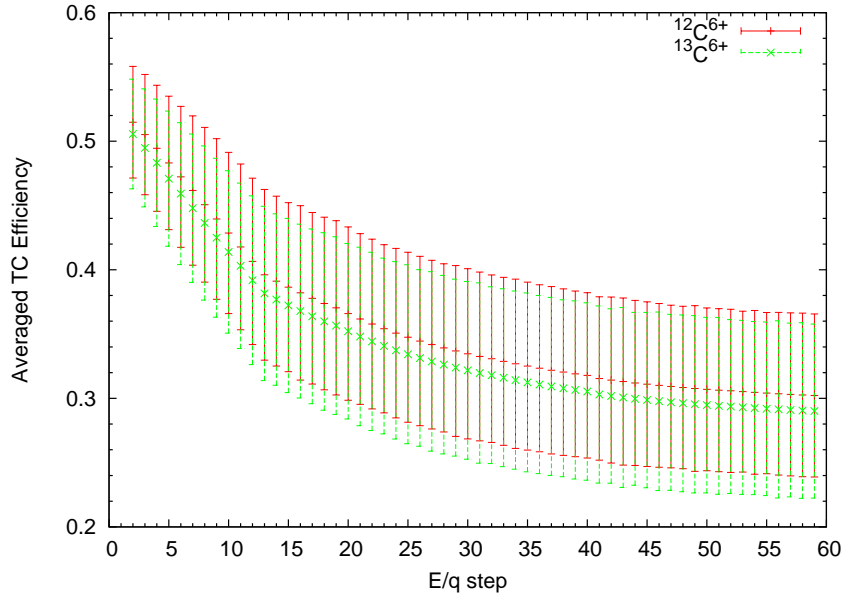
Figure 7.6.: Tripe Coincidence efficiency of the carbon isotopes $^{12}_{6}C^{6+}$ and $^{13}_{6}C^{6+}$ as a function of the E/q-step (averaged over all aspect angles) including an error estimation.
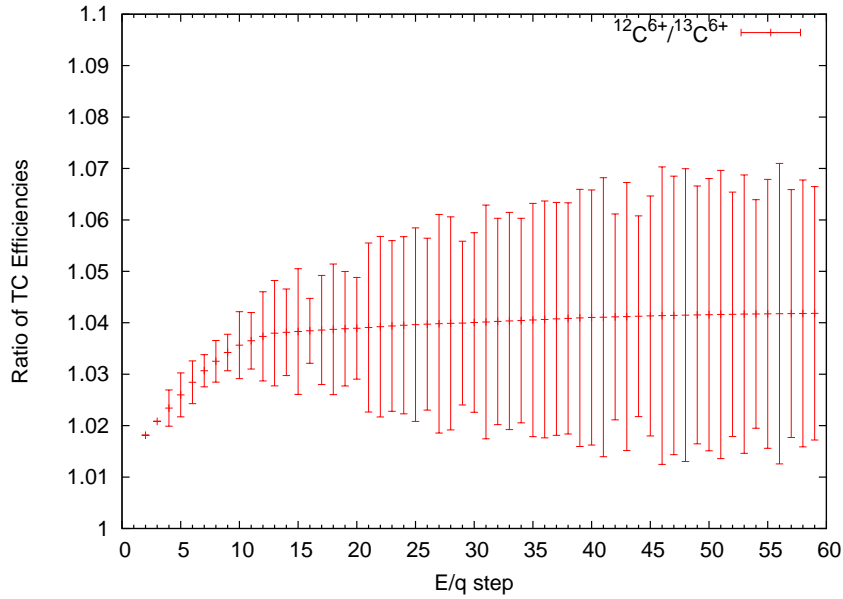
Figure 7.7.: Relative deviation between the Triple Coincidence efficiencies of $^{12}_{6}C^{6+}$ and $^{13}_{6}C^{6+}$ as a function of the E/q-step (averaged over all aspect angles). The error bars of the ratio of the efficiencies are much smaller than the errors of the efficiencies for a single ion (see Table 4.1). The reason is that the error bars are mainly caused by uncertainties of the parameters of the efficiency model. These mostly cancel out when considering ratios of efficiencies for different ions.

7. RESULTS

For the considered carbon isotopes ${}^{12}_{6}C^{6+}$ and ${}^{13}_{6}C^{6+}$ this means that the respective peak height of the former isotope always corresponds to a larger speed interval than the peak height of the latter isotope. Thus, to get a realistic comparison between the abundances of both isotopes in each step the peak height belonging to the distribution of ${}^{13}_{6}C^{6+}$ has to be weighted $\sqrt{\frac{m_1/q_1}{m_2/q_2}} = \sqrt{\frac{m_1}{m_2}}$-times higher than the peak height belonging to ${}^{12}_{6}C^{6+}$.

Finally, for the conversion of the peak heights into isotopic ratios we have to consider the slightly different width of the distributions function in the ET-matrices. According to equation 6.4 the two-dimensional distribution of each ion is given by the product of the respective one-dimensional distribution in energy direction which is approximated by a Gaussian and in ToF direction which is approximated by an asymmetric $\mathcal{K}$-function. The scale factor of a one-dimensional Gaussian is given by $1/(\sqrt{2\pi}\sigma_G)$. Thus, for a normalized Gaussian σ_G is anti-proportional to the peak height. That means for a given peak height the integral is proportional to σ_G.

In the case of the $\mathcal{K}$-function there is not a simple scale factor which is valid for all κ- and σ_κ-values. Therefore, we have integrated one-dimensional $\mathcal{K}$-functions for different κ- and σ_κ-values over the limits $-\infty$ and $+\infty$.

$$\mathcal{K}_{I(\kappa,\sigma_\kappa)} = \int_{-\infty}^{+\infty} \mathcal{K}(x,\kappa,\sigma_\kappa)dx \tag{7.3}$$

The integral $\mathcal{K}_{I(\kappa,\sigma_\kappa)}$ for a sample of κ-values as a function of σ_κ is shown in Figure 7.8. In the range of the parameter space we have typically used we can assume that there is a linear relation between the integral and σ_κ.
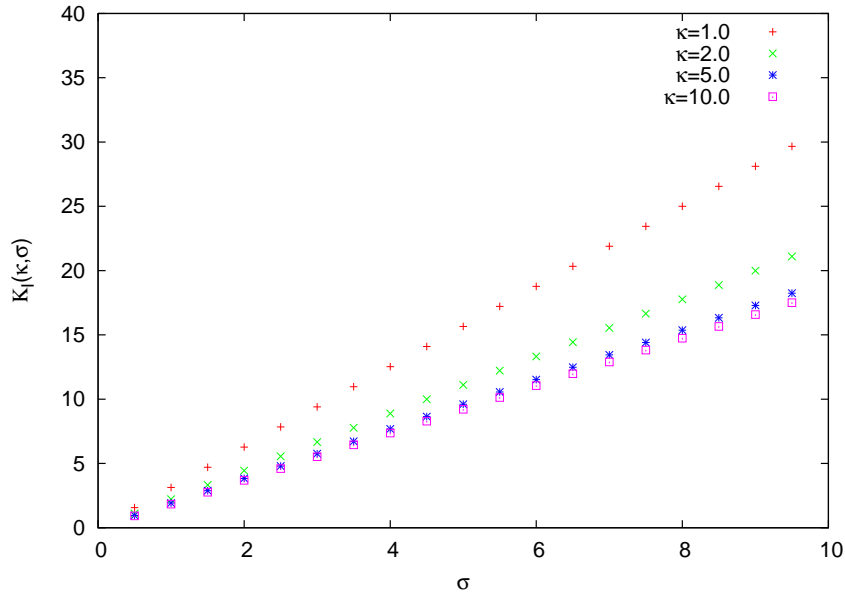
Figure 7.8.: Integral of the $\mathcal{K}$-function over the limits $-\infty$ and $+\infty$ for a sample of κ-values as a function of σ_κ. The relation between $\mathcal{K}_I$ can be approximated to be linear.

For the determination of the isotopic ratio ${}^{13}_{6}C^{6+}/{}^{12}_{6}C^{6+}$, other instrument specific properties which are important for the determination of absolute ion fluxes like the geometry factor and

the duty cycle (*von Steiger et al.* [2000]) of the instrument do not need to be considered because variations of these properties do have the same consequences for both isotopes.

The resulting isotopic ratio in the solar wind for the above mentioned speed intervals are shown in Figure **??** There is no significant speed-dependent trend for the enrichment or the depletion of the $_6^{13}C^{6+}$ abundances related to those of $_6^{12}C^{6+}$. Therefore we assumed that the ratio of both isotopes in the considered speed ranges can be approximated by a single constant.

The average value resulting from all speed intervals weighted with the respective abundances in each speed interval comes up to 0.01024 $\pm$ 0.00107 which corresponds to a ratio of $_6^{13}C^{6+}/_6^{12}C^{6+} = 1 : 97.7^{+10.3}_{-9.3}$.

The average value and the error estimation were obtained by using the ratios resulting from the fits in the respective speed filters as a function of the energy-per charge step. For those steps which were relevant for more than one speed interval the average ratio from all corresponding speed intervals was used. The mean value $m = \frac{13}{6}C^{6+}/\frac{12}{6}C^{6+}$ and the error of the mean value σ_m are calculated by

$$m = \frac{\sum_{\text{step}=37}^{\text{step}=52} \frac{(_6^{13}C^{6+}/_6^{12}C^{6+})_{\text{step}}}{\sigma_{\text{step}}}}{\sum_{\text{step}=37}^{\text{step}=52} \frac{1}{\sigma_{\text{step}}}}, \tag{7.4}$$

$$\sigma_m = \sqrt{\frac{N}{\left(\sum_{\text{step}=37}^{\text{step}=52} \frac{1}{\sigma_{\text{step}}}\right)^2}}. \tag{7.5}$$

$N = 16$ is the total number of steps which are used. For the considered sample of data points σ_m comes up to 0.00107.

The ratios corresponding to the respective energy-per-charge steps, the mean value m, and the $1 - \sigma$ error of the mean value σ_m are listed in Table 7.2 and shown in Figure 7.10. At the first sight the terrestrial ratio of 1:89 is somewhat lower than our value but within the error bars of $\pm 10.5\%$.

E/q-step	$_6^{13}C^{6+}/_6^{12}C^{6+}$	E/q-step	$_6^{13}C^{6+}/_6^{12}C^{6+}$
37	0.00752 ± 0.00888	45	0.00858 ± 0.00398
38	0.00900 ± 0.00799	46	0.00898 ± 0.00389
39	0.01956 ± 0.00647	47	0.00794 ± 0.00450
40	0.01069 ± 0.00498	48	0.00982 ± 0.00477
41	0.00743 ± 0.00394	49	0.01727 ± 0.00415
42	0.01394 ± 0.00381	50	0.00585 ± 0.00419
43	0.01563 ± 0.00381	51	0.00980 ± 0.00435
44	0.00735 ± 0.00351	52	0.00666 ± 0.00408

Table 7.2.: Carbon isotopic ratios resulting from the fits in the respective E/q-steps. In the case that one step is relevant for more than one speed filter the average values are given. The error bars indicate 1-σ deviations. The mean value from all considered steps comes up to **0.01024 $\pm$ 0.00107**.
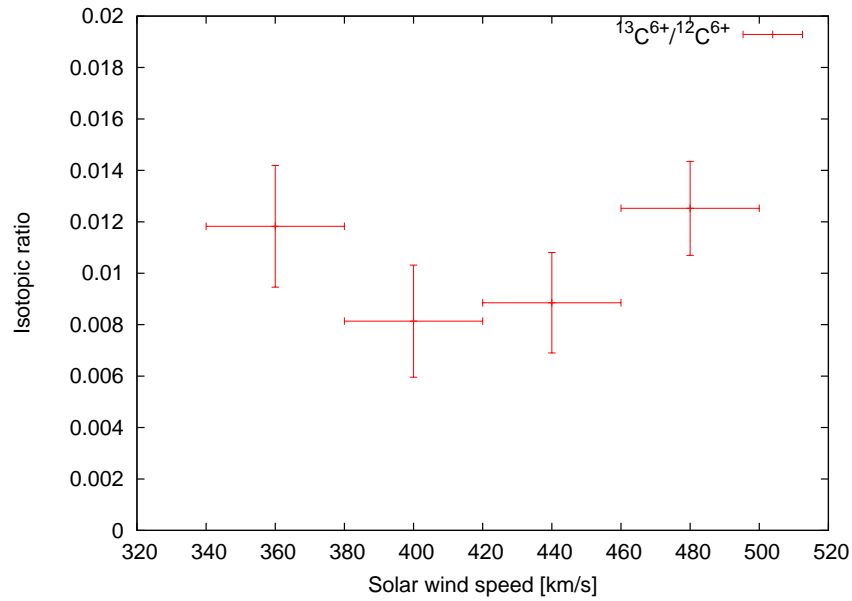
Figure 7.9.: Isotopic ratio of the carbon isotopes $^{13}_{6}\text{C}^{6+}$ and $^{12}_{6}\text{C}^{6+}$ in the solar wind calculated for the solar wind speed intervals 360 ± 20 km/s, 400 ± 20 km/s, 440 ± 20 km/s, and 480 ± 20 km/s.
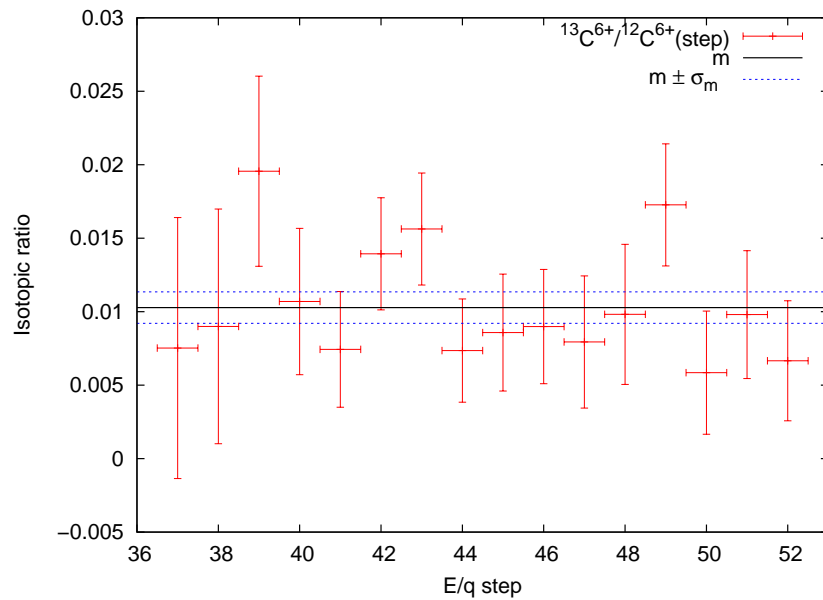
Figure 7.10.: $^{13}_{6}\text{C}^{6+}/\,^{12}_{6}\text{C}^{6+}$ ratios in all E/q-steps which are relevant for the above mentioned speed intervals. Additionally the mean value m and the error of mean value σ_m are shown.

8. SUMMARY AND CONCLUSIONS

The efficiency model of ACE/SWICS presented in this work is based on that presented in *Köten* [2005]. The model can be used for two different but connected purposes.

- Calculation of the detection efficiency for all solar wind ions subject to mass, charge, and velocity.

- Prediction of the position of all solar wind ions in the ET-Matrices of all E/q-steps.

For the purpose of a more detailed data analysis the [2005]-model needed to be modified and improved. The previous model as well as the current model provide accurate efficiencies for the analysis of abundant solar wind ions with appropriate error bars. For the detection of rare ions the exact position of the ions in the ET-matrices have to be known. Using peak positions which show marginal deviations from the correct peak positions can falsify any conclusion about the abundance or the absence of rare solar wind ions. Therefore, the current model includes, apart from the results of the Pre-Flight calibration, the results from a detailed In-Flight calibration for the calculation of the exact peak positions. This is one of the preconditions to achieve a 1% resolution for the detection of the carbon isotope $^{13}_{6}$C in the solar wind because in the solar system $^{13}_{6}$C is about two orders of magnitude rarer than the most abundant carbon isotope $^{12}_{6}$C. In this context it is worth mentioning that we found during the In-Flight calibration that the absolute value of the post acceleration voltage inside the instrument is about 1 kV lower than it is stated in the housekeeping data (-23.9 kV instead of -24.86 kV).

The second precondition is the knowledge about the shapes of the respective peaks in the ET-matrices. These were determined by a detailed analysis of the isolated He^{2+} peak using long-term data accumulated over 5 years. We found that the two-dimensional distribution of each peak can be well approximated by the product of a one-dimensional distribution in energy direction which can be approximated by a Gaussian and a one-dimensional distribution in ToF-direction which can be approximated by an asymmetric $\mathcal{K}$-function where the σ-values are assumed to be proportional to the measured energy and the Time-of-Flight respectively. In each E/q-step the κ-value of the ToF-distribution towards lower Time-of-Flight channels seen from the peak position is at least 4 or higher, viz. this shape can be well approximated by a Gaussian. Towards higher ToF-channels the κ-value shows a variable behaviour depending on the distance from the peak position in energy direction. We found that the parameters which quantify the described general peak characteristics, e.g., the κ-values of the ToF-distribution, also show a variability depending on the considered E/q-step. These instrument-specific properties (IRFs=Instrumental response functions) have to included for a detailed data analysis. For the detection of rare elements or isotopes especially when the peaks in the ET-matrices overlap it is essential to consider the IRFs distributing the counts in the ET-matrices correctly to the appropriate solar wind ions.

From long-term data of ACE/SWICS and using the above mentioned instrument specific properties we have determined in this work for the first time the carbon isotopic ratio in the solar wind. The analysis was accomplished mainly for the slow solar wind in the speed range from 340 km/s up to 500 km/s in the time period 2001-2007 without 2003 and 2005. We found

an average isotopic ratio of $^{13}_{6}C^{6+}/^{12}_{6}C^{6+} = 1 : 97.7^{+10,3}_{-9,3}$. We have only investigated the isotopic ratio of the six times charged carbon due to instrumental restrictions. Nevertheless, this ratio can be assumed to represent the total isotopic ratio $^{13}_{6}C/^{12}_{6}C$ in the solar wind because there are no significant deviations between the energies required for the different stages of thermal excitation and ionization comparing both carbon isotopes.

The average carbon isotopic ratio $^{13}_{6}C/^{12}_{6}C$ determined from different terrestrial samples is about 1:89 (*Woods and Willacy* [2009], *Woods* [2009], and *Clayton* [2003]) which is about ten percent lower than the value we have determined. This could indicate mass dependent fractionation processes in the solar wind evolution and propagation. Previous measurements concerning the carbon isotopic ratio of the Sun by spectroscopic observations of the solar photosphere found somewhat lower ratios (for an overview see *Woods and Willacy* [2009], *Woods* [2009], and *Harris et al.* [1987]), e. g., *Harris et al.* [1987] found $1 : 84 \pm 5$. The ratio of *Harris et al.* [1987], as well as the ratio we have found, overlap with the terrestrial ratio within $1 - \sigma$ error bars. Thus, our current measurements with ACE/SWICS are not yet precise enough to conclude directly that there is a mass dependent fractionation in the solar wind which enriches the abundance of $^{12}_{6}C$ compared to that of $^{13}_{6}C$. Presumably, the accumulation of data over a longer period of time, viz. additionally using the data of the years 2003,2005, and 2008, would result in smaller statistical error bars and possibly allow conclusions about possible fractionation processes. The error bars are mainly caused by the uncertainties resulting from the determination of the shapes of the helium peaks during the IFC. These uncertainties are a mixture of statistical and systematical uncertainties. Thus, an estimation to which extent the amount of the resulting error bar of the mean value of the carbon isotopic ratio can be reduced by using data from a longer period of time cannot be easily made.

Except for gravitational settling in the OCZ, which would deplete the heavy isotope by 0.43-0.61% (*Turcotte and Wimmer-Schweingruber* [2003]), for the interstream wind we have looked at, two processes can lead to fractionation in the solar wind which enriches lighter isotopes compared to the heavier ones. In coronal hole associated high speed streams there are fractionation processes due to wave particle interaction. *Kohl et al.* [1997] showed that these effects can be neglected in the slow solar wind. We will give a short explanation of the relevant theories which come into consideration. For that, first we introduce the factor $f_{i,j}$ which describes the enrichment or the depletion of an ion i with respect to a second ion j in the solar wind compared to the ratio of the respective abundances of both ions in the outer convection zone (OCZ) of the Sun,

$$f_{i,j} := \frac{([i]/[j])}{([i]/[j])_o},\tag{8.1}$$

where $([i]/[j])$ and $([i]/[j])_o$ denote the ratio in the solar wind and the photospheric ratio respectively.

The elemental abundances in the solar wind depends on the first ionization potential (FIP) of the respective elements. Elements with FIP-values below about 10 eV are enriched in the solar wind compared to elements with higher FIP-values (*Aschwanden* [2004], *von Steiger et al.* [2000]). This theory describes mainly the elemental fractionation. According to *Bodmer and Bochsler* [1998] the FIP fractionation factor $f_{i,j}$ for isotopes is given by

$$f_{i,j} \approx \frac{r_{jH}}{r_{iH}} \sqrt{\frac{\tau_j}{\tau_i}} \left(\frac{m_i + 1}{m_i} \frac{m_j}{m_j + 1} \right)^{1/4}.\tag{8.2}$$

The r-values indicate the respective collisional radii with neutral hydrogen whereas the τ-values indicate the respective mean first ionization time. m_i and m_j denote the masses of the elements in units of amu. Assuming that r and τ are the same for both considered carbon isotopes the mass dependent term contributes to the fractionation factor with the fourth root power resulting in a fractionation of about 0.15 %. This is a very small effect and it is very unlikely to resolve this deviation of the isotopic abundances even if accumulating ACE/SWICS data over a much longer time.

A second theory which describes mass dependent fractionation in the solar wind is the so-called Coulomb-drag effect. The Coulomb-drag model assumes that the solar wind acceleration of heavy ions is due to multiple collisions with hot protons. Light isotopes are accelerated more efficiently whereas the heavier ones are left behind which finally results in a depletion of the heavier isotopes in the solar wind. This effect can be quantified by introducing Γ which is given by

$$\Gamma := \frac{2m - q - 1}{q^2} \sqrt{\frac{m+1}{m}} \tag{8.3}$$

where m is the mass and q is the charge state if the solar wind ion. The reciprocal value Γ^{-1} is called Coulomb-drag factor and can be assumed to be a measure for the efficiency of the Coulomb-drag effect. Ions with low Γ^{-1}-values are depleted in the solar wind relative to ions with high Coulomb-drag factors compared to their relative abundances in the OCZ. In this model the fractionation factor $f_{i,j}$ is given by

$$f_{i,j} = \frac{[1 - \frac{C_p^* \Gamma_i}{\Phi_p}]}{[1 - \frac{C_p^* \Gamma_j}{\Phi_p}]} \tag{8.4}$$

where Φ_p indicates the proton flux in the source region and C_p^* denotes a numerical factor which relates electrostatic interaction of the ion species with the surrounding protons and the solar gravitational attraction. Applying this model to both considered carbon isotopes results in a fractionation of about 2.2 %, i.e., a depletion of the heavy isotope by 2.2 %. While our value of $^{12}_{6}\mathrm{C}/^{12}_{6}\mathrm{C} = 97.7^{+10,3}_{-9,3}$ is isotopically light compared to the terrestrial value, the ratio of the solar wind value to the terrestrial value exceeds the probable fractionation by inefficient Coulomb drag.

The Coulomb drag model also predicts that the fractionation of the isotopes of heavy ions are correlated with the ratio $^4\mathrm{He}^{2+}/\mathrm{H}^+$. According to equation 8.3, $^4\mathrm{He}^{2+}$ has the highest Γ-value of all solar wind ions except for H^+ for which Γ is not defined. Thus, the enrichment or the depletion of $^4\mathrm{He}$ compared to H^+ is the best tracer for the efficiency of possible fractionation due to Coulomb drag. A decrease of the ratio $^4\mathrm{He}^{2+}/\mathrm{H}^+$ caused by Coulomb drag, correlated with the ratio of the isotopic abundances of an heavy element would indicate that the depletion of the heavy isotope is due to the Coulomb drag effect.

From measurements with SOHO/CELIAS/MTOF *Kallenbach et al.* [1997b] found that there is in fact a correlation between the isotopic ratio of magnesium $^{24}\mathrm{Mg}/^{26}\mathrm{Mg}$ and the ratio of $^4\mathrm{He}^{2+}$ and H^+. It was observed that this isotopic ratio also correlates with the solar wind speed. The depletion of the heavier isotope is strongest in the slow solar wind and for low ratios $^4\mathrm{He}^{2+}/\mathrm{H}^+$ ($\approx 0.02 - 0.03$). The isotopic ratio $^{24}\mathrm{Mg}/^{26}\mathrm{Mg}$ decreases towards higher solar wind speeds and higher ratios of $^4\mathrm{He}^{2+}$ and H^+. The verification of these correlations for the carbon isotopic ratio is still in progress and thus not presented in this thesis. In the speed range we

have investigated from 340 km/s to 500 km/s, we did not see any systematic dependence of the ratio $^{12}\text{C}/^{13}\text{C}$ on the solar wind velocity. As shown in Figure 7.10, in the above mentioned speed range we found an average ratio $^{13}_{6}\text{C}^{6+}/^{12}_{6}\text{C}^{6+} = 1 : 97.7^{+10,3}_{-9,3}$.

A. POSITIONS IN THE ET-MATRICES AND DETECTION EFFICIENCIES

Table A.1 shows the E/q-step numbers and the corresponding energy-per-charge values. The tables from the next page forward show the positions in the ET-matrices, and the efficiencies in each E/q-step, of all elements which are included in the ACE/SWICS data analysis. There is one table for each possible charge state of each element. We will give a short description of the columns of each table.

- Step: Energy-per-charge step.

- $\hat{T}$: Time-of-Flight channel position.

- $\hat{E}$: Energy channel position.

- P_1: Start-signal trigger probability.

- P_2: Stop-signal trigger probability.

- P_T: Probabiliy to trigger an energy measurement assumed that the ion hits the active region of the SSD.

- P_S: Probability to hit the sensitive area of the SSD for the ejection of secondary electrons averaged over all aspect angles. (In section 3.4 this probability is called P_{SSD}.)

- P_{AS}: Probability to hit the sensitive area of the SSD for an energy measurement averaged over all aspect angles. (In section 3.5 this probability is called P_{ARSSD}.)

Table A.1.: E/q-step number and the corresponding energy-per-charge value.

Step	E/q [keV/e]	Step	E/q [keV/e]	Step	E/q [keV/e]	Step	E/q [keV/e]
1	not used	16	14.396	31	4.904	46	1.671
2	86.636	17	13.399	32	4.565	47	1.555
3	75.049	18	12.471	33	4.248	48	1.447
4	65.011	19	11.607	34	3.954	49	1.347
5	56.316	20	10.803	35	3.680	50	1.254
6	48.784	21	10.055	36	3.425	51	1.167
7	42.259	22	9.358	37	3.188	52	1.086
8	36.607	23	8.710	38	2.967	53	1.011
9	31.711	24	8.106	39	2.762	54	0.941
10	27.470	25	7.545	40	2.570	55	0.876
11	23.796	26	7.022	41	2.392	56	0.815
12	20.613	27	6.536	42	2.227	57	0.758
13	17.856	28	6.083	43	2.072	58	0.706
14	16.619	29	5.662	44	1.929	59	0.657
15	15.468	30	5.269	45	1.795	60	not used

Table A.2.: $1H^{1+}$

Step	$\hat{E}$	$\hat{T}$	P_1	P_2	P_T	P_S	P_{AS}	Step	$\hat{E}$	$\hat{T}$	P_1	P_2	P_T	P_S	P_{AS}
2	20.37	59.51	50.82	18.35	100.0	73.92	60.92	31	5.13	112.45	41.78	18.43	23.07	77.94	64.0
3	18.18	62.59	51.67	19.31	100.0	74.38	61.29	32	5.07	113.11	41.57	18.3	21.84	77.9	63.95
4	16.27	65.75	52.12	20.14	100.0	74.85	61.68	33	5.01	113.73	41.37	18.17	20.72	77.75	63.82
5	14.64	68.96	52.24	20.82	100.0	75.34	62.08	34	4.96	114.32	41.19	18.06	19.71	77.62	63.7
6	13.23	72.2	52.1	21.35	99.99	75.97	62.6	35	4.91	114.87	41.02	17.95	18.8	77.49	63.59
7	12.01	75.45	51.7	21.72	99.99	76.65	63.15	36	4.87	115.4	40.86	17.85	17.98	77.37	63.48
8	10.96	78.69	51.12	21.94	99.92	77.28	63.67	37	4.82	115.89	40.71	17.76	17.24	77.26	63.38
9	10.05	81.89	50.44	22.03	99.49	77.85	64.14	38	4.78	116.36	40.57	17.67	16.57	77.16	63.29
10	9.26	85.04	49.68	22.0	97.96	78.35	64.55	39	4.75	116.8	40.44	17.59	15.95	77.06	63.2
11	8.58	88.1	48.88	21.86	94.42	78.75	64.87	40	4.71	117.22	40.32	17.51	15.4	76.97	63.12
12	8.0	91.06	48.06	21.62	88.46	78.91	65.0	41	4.68	117.61	40.2	17.43	14.88	76.89	63.04
13	7.49	93.9	47.3	21.38	80.47	79.04	65.1	42	4.65	117.97	40.08	17.35	14.41	76.81	62.97
14	7.26	95.27	46.89	21.22	75.95	79.09	65.14	43	4.62	118.32	39.98	17.28	13.99	76.74	62.91
15	7.05	96.6	46.51	21.06	71.29	79.14	65.17	44	4.6	118.64	39.88	17.21	13.6	76.68	62.85
16	6.85	97.9	46.12	20.88	66.61	79.17	65.2	45	4.57	118.94	39.78	17.15	13.24	76.62	62.8
17	6.67	99.15	45.74	20.71	62.01	79.2	65.22	46	4.55	119.23	39.7	17.09	12.92	76.56	62.74
18	6.5	100.37	45.39	20.54	57.58	79.22	65.24	47	4.53	119.49	39.62	17.04	12.62	76.51	62.7
19	6.34	101.55	45.03	20.35	53.37	79.3	65.3	48	4.51	119.74	39.54	16.99	12.35	76.46	62.66
20	6.2	102.68	44.7	20.17	49.43	79.2	65.21	49	4.49	119.98	39.47	16.94	12.1	76.42	62.62
21	6.06	103.78	44.39	20.0	45.76	79.11	65.14	50	4.47	120.2	39.41	16.9	11.87	76.39	62.58
22	5.93	104.83	44.06	19.81	42.39	78.89	64.91	51	4.46	120.4	39.35	16.86	11.66	76.35	62.55
23	5.82	105.84	43.75	19.64	39.3	78.76	64.79	52	4.44	120.59	39.29	16.82	11.46	76.34	62.54
24	5.71	106.81	43.46	19.48	36.49	78.64	64.67	53	4.43	120.77	39.24	16.78	11.29	76.29	62.49
25	5.61	107.73	43.19	19.32	33.94	78.52	64.56	54	4.42	120.94	39.19	16.75	11.12	76.24	62.45
26	5.51	108.62	42.92	19.14	31.63	78.41	64.46	55	4.41	121.1	39.14	16.72	10.97	76.2	62.41
27	5.42	109.46	42.66	18.98	29.54	78.31	64.35	56	4.4	121.25	39.1	16.69	10.83	76.16	62.37
28	5.34	110.27	42.42	18.84	27.67	78.21	64.26	57	4.39	121.38	39.06	16.67	10.7	76.12	62.34
29	5.27	111.03	42.2	18.7	25.97	78.11	64.17	58	4.38	121.51	39.03	16.64	10.59	76.09	62.3
30	5.2	111.76	42.0	18.57	24.45	78.02	64.08	59	4.37	121.63	38.99	16.62	10.48	76.06	62.27

Table A.3.: $3He^{1+}$

Step	$\hat{E}$	$\hat{T}$	P_1	P_2	P_T	P_S	P_{AS}	Step	$\hat{E}$	$\hat{T}$	P_1	P_2	P_T	P_S	P_{AS}
2	19.27	99.13	64.81	54.55	100.0	71.86	59.2	31	4.58	192.21	37.56	18.02	13.56	62.87	50.93
3	17.15	104.52	62.68	51.75	100.0	72.05	59.35	32	4.52	193.37	37.29	17.76	12.73	62.66	50.75
4	15.32	110.04	60.54	48.89	100.0	72.23	59.49	33	4.47	194.47	37.04	17.52	11.99	62.4	50.54
5	13.75	115.64	58.43	46.02	99.99	72.39	59.61	34	4.42	195.51	36.81	17.3	11.33	62.16	50.33
6	12.38	121.31	56.41	43.22	99.99	72.54	59.72	35	4.37	196.49	36.59	17.09	10.74	61.93	50.13
7	11.19	127.0	54.49	40.46	99.95	72.6	59.77	36	4.33	197.42	36.38	16.9	10.21	61.71	49.95
8	10.17	132.68	52.7	37.83	99.55	72.34	59.5	37	4.29	198.3	36.19	16.72	9.74	61.5	49.77
9	9.29	138.3	51.02	35.34	97.92	71.93	59.1	38	4.25	199.13	36.0	16.55	9.31	61.3	49.61
10	8.53	143.82	49.47	33.03	93.81	71.44	58.63	39	4.21	199.9	35.81	16.39	8.92	61.12	49.45
11	7.88	149.21	48.04	30.91	86.62	70.87	58.09	40	4.18	200.64	35.64	16.24	8.58	60.94	49.3
12	7.31	154.43	46.69	28.94	76.73	70.14	57.42	41	4.15	201.33	35.49	16.1	8.27	60.78	49.17
13	6.82	159.44	45.45	27.19	65.69	69.37	56.71	42	4.12	201.98	35.34	15.97	7.98	60.63	49.04
14	6.61	161.85	44.85	26.38	60.19	68.98	56.35	43	4.1	202.59	35.2	15.85	7.73	60.48	48.91
15	6.4	164.21	44.27	25.61	54.91	68.58	55.98	44	4.07	203.16	35.07	15.74	7.49	60.35	48.8
16	6.22	166.49	43.7	24.88	49.92	68.17	55.61	45	4.05	203.7	34.95	15.64	7.28	60.22	48.69
17	6.04	168.71	43.17	24.2	45.29	67.76	55.24	46	4.03	204.2	34.84	15.55	7.08	60.1	48.59
18	5.88	170.86	42.64	23.55	41.05	67.35	54.87	47	4.01	204.67	34.74	15.46	6.91	60.0	48.5
19	5.73	172.94	42.14	22.94	37.2	66.98	54.53	48	3.99	205.11	34.64	15.37	6.75	59.89	48.41
20	5.59	174.95	41.67	22.37	33.73	66.51	54.1	49	3.98	205.53	34.55	15.3	6.6	59.8	48.33
21	5.46	176.88	41.19	21.83	30.64	66.04	53.69	50	3.96	205.92	34.47	15.23	6.47	59.71	48.26
22	5.34	178.74	40.75	21.32	27.88	65.59	53.29	51	3.95	206.28	34.39	15.16	6.34	59.63	48.19
23	5.23	180.52	40.33	20.86	25.43	65.15	52.9	52	3.93	206.62	34.32	15.1	6.23	59.56	48.13
24	5.13	182.23	39.92	20.41	23.25	64.73	52.51	53	3.92	206.94	34.25	15.04	6.12	59.47	48.06
25	5.03	183.87	39.52	19.99	21.31	64.32	52.15	54	3.91	207.23	34.19	14.99	6.03	59.39	47.99
26	4.94	185.43	39.15	19.61	19.59	64.16	52.04	55	3.9	207.51	34.13	14.94	5.94	59.32	47.92
27	4.86	186.92	38.8	19.24	18.08	63.88	51.8	56	3.89	207.77	34.07	14.89	5.86	59.25	47.86
28	4.78	188.35	38.47	18.91	16.73	63.61	51.57	57	3.88	208.01	34.02	14.85	5.79	59.18	47.81
29	4.71	189.7	38.16	18.6	15.55	63.35	51.35	58	3.87	208.24	33.98	14.81	5.72	59.12	47.75
30	4.64	190.99	37.85	18.3	14.49	63.1	51.13	59	3.86	208.45	33.93	14.77	5.65	59.06	47.7

Table A.4.: 3He^{2+}

Step	$\hat{E}$	$\hat{T}$	P_1	P_2	P_T	P_S	P_{AS}	Step	$\hat{E}$	$\hat{T}$	P_1	P_2	P_T	P_S	P_{AS}
2	39.76	71.56	74.96	66.97	100.0	74.14	61.1	31	9.65	135.92	51.73	36.39	98.85	79.72	65.56
3	35.47	75.33	73.77	65.64	100.0	74.63	61.51	32	9.52	136.71	51.49	36.04	98.58	79.71	65.53
4	31.74	79.18	72.47	64.12	100.0	75.14	61.92	33	9.41	137.47	51.26	35.7	98.29	79.58	65.42
5	28.49	83.1	71.06	62.43	100.0	75.66	62.35	34	9.31	138.18	51.06	35.39	97.98	79.47	65.32
6	25.69	87.04	69.58	60.62	100.0	76.34	62.91	35	9.21	138.85	50.86	35.1	97.64	79.36	65.22
7	23.28	91.0	68.04	58.67	100.0	77.09	63.52	36	9.12	139.49	50.68	34.83	97.29	79.26	65.13
8	21.2	94.94	66.48	56.69	100.0	77.8	64.1	37	9.03	140.09	50.51	34.58	96.92	79.17	65.05
9	19.39	98.83	64.93	54.7	100.0	78.46	64.64	38	8.95	140.66	50.35	34.34	96.54	79.08	64.97
10	17.84	102.65	63.42	52.75	100.0	79.06	65.13	39	8.88	141.19	50.2	34.12	96.15	79.0	64.9
11	16.5	106.37	61.96	50.8	100.0	79.55	65.54	40	8.81	141.7	50.06	33.92	95.76	78.93	64.83
12	15.34	109.97	60.56	48.92	100.0	79.8	65.74	41	8.75	142.17	49.93	33.73	95.37	78.86	64.77
13	14.34	113.41	59.27	47.19	100.0	80.01	65.91	42	8.69	142.62	49.81	33.54	94.98	78.8	64.71
14	13.9	115.07	58.64	46.31	99.99	80.11	65.99	43	8.64	143.03	49.69	33.36	94.59	78.74	64.65
15	13.48	116.69	58.04	45.48	99.99	80.2	66.06	44	8.58	143.43	49.58	33.2	94.21	78.68	64.61
16	13.09	118.26	57.47	44.69	99.99	80.28	66.12	45	8.54	143.8	49.48	33.04	93.84	78.64	64.56
17	12.73	119.79	56.94	43.95	99.99	80.35	66.18	46	8.49	144.14	49.38	32.9	93.47	78.59	64.52
18	12.39	121.26	56.43	43.25	99.99	80.42	66.24	47	8.45	144.47	49.29	32.77	93.12	78.55	64.48
19	12.07	122.69	55.93	42.54	99.99	80.56	66.35	48	8.41	144.77	49.21	32.64	92.78	78.52	64.45
20	11.78	124.07	55.47	41.87	99.98	80.47	66.27	49	8.38	145.05	49.13	32.53	92.45	78.48	64.42
21	11.51	125.39	55.03	41.24	99.97	80.39	66.2	50	8.35	145.32	49.06	32.42	92.13	78.45	64.39
22	11.25	126.67	54.6	40.62	99.95	80.32	66.15	51	8.32	145.57	48.99	32.32	91.83	78.43	64.37
23	11.02	127.89	54.2	40.04	99.92	80.27	66.1	52	8.29	145.8	48.93	32.23	91.54	78.42	64.36
24	10.8	129.07	53.83	39.49	99.87	80.23	66.07	53	8.26	146.02	48.87	32.14	91.27	78.38	64.32
25	10.6	130.19	53.48	38.98	99.81	80.2	66.04	54	8.24	146.22	48.82	32.06	91.0	78.34	64.28
26	10.41	131.26	53.14	38.48	99.72	80.18	66.02	55	8.21	146.41	48.77	31.99	90.75	78.3	64.25
27	10.23	132.29	52.82	38.0	99.61	79.97	65.81	56	8.19	146.59	48.72	31.92	90.51	78.27	64.21
28	10.07	133.26	52.52	37.56	99.46	79.9	65.74	57	8.17	146.76	48.67	31.85	90.29	78.23	64.18
29	9.92	134.19	52.24	37.15	99.29	79.83	65.67	58	8.15	146.91	48.63	31.79	90.08	78.2	64.16
30	9.78	135.08	51.97	36.76	99.08	79.77	65.61	59	8.13	147.06	48.59	31.73	89.87	78.18	64.13

Table A.5.: He^{1+}

Step	$\hat{E}$	$\hat{T}$	P_1	P_2	P_T	P_S	P_{AS}	Step	$\hat{E}$	$\hat{T}$	P_1	P_2	P_T	P_S	P_{AS}
2	19.02	113.29	59.3	47.21	100.0	71.87	59.21	31	4.46	220.03	31.45	12.84	12.36	62.98	51.03
3	16.91	119.49	57.03	44.07	100.0	72.06	59.36	32	4.4	221.36	31.17	12.64	11.62	62.78	50.85
4	15.08	125.83	54.85	40.98	100.0	72.24	59.49	33	4.35	222.61	30.92	12.46	10.96	62.52	50.64
5	13.5	132.29	52.79	37.97	99.99	72.4	59.62	34	4.3	223.8	30.68	12.29	10.37	62.28	50.43
6	12.14	138.81	50.86	35.12	99.99	72.56	59.74	35	4.25	224.92	30.45	12.13	9.85	62.05	50.24
7	10.97	145.35	49.05	32.4	99.89	72.62	59.79	36	4.21	225.98	30.24	11.98	9.37	61.83	50.06
8	9.97	151.88	47.33	29.87	99.23	72.37	59.53	37	4.17	226.98	30.05	11.84	8.95	61.63	49.88
9	9.09	158.34	45.69	27.54	96.87	71.96	59.13	38	4.14	227.92	29.87	11.72	8.57	61.44	49.72
10	8.34	164.69	44.12	25.43	91.56	71.48	58.67	39	4.1	228.81	29.69	11.59	8.23	61.25	49.56
11	7.69	170.87	42.63	23.52	83.1	70.92	58.13	40	4.07	229.65	29.53	11.48	7.92	61.08	49.42
12	7.14	176.85	41.15	21.81	72.51	70.2	57.46	41	4.04	230.44	29.37	11.38	7.64	60.92	49.28
13	6.66	182.58	39.82	20.31	61.31	69.44	56.77	42	4.02	231.18	29.23	11.28	7.38	60.77	49.15
14	6.44	185.35	39.17	19.62	55.85	69.04	56.41	43	3.99	231.87	29.1	11.19	7.15	60.62	49.03
15	6.24	188.04	38.54	18.97	50.68	68.65	56.05	44	3.97	232.53	28.97	11.11	6.94	60.49	48.92
16	6.06	190.66	37.92	18.36	45.87	68.25	55.68	45	3.95	233.14	28.86	11.03	6.75	60.37	48.81
17	5.89	193.19	37.33	17.79	41.47	67.84	55.31	46	3.92	233.71	28.75	10.96	6.57	60.25	48.71
18	5.73	195.65	36.76	17.26	37.47	67.44	54.95	47	3.91	234.25	28.65	10.89	6.41	60.14	48.62
19	5.58	198.03	36.22	16.76	33.87	67.07	54.61	48	3.89	234.76	28.55	10.83	6.27	60.04	48.54
20	5.45	200.32	35.71	16.3	30.66	66.6	54.19	49	3.87	235.23	28.47	10.77	6.13	59.95	48.46
21	5.32	202.52	35.21	15.86	27.8	66.14	53.78	50	3.86	235.67	28.39	10.72	6.01	59.86	48.38
22	5.2	204.65	34.73	15.45	25.27	65.7	53.38	51	3.84	236.09	28.31	10.67	5.9	59.78	48.31
23	5.09	206.68	34.28	15.08	23.02	65.26	52.99	52	3.83	236.48	28.24	10.62	5.79	59.71	48.26
24	4.99	208.64	33.87	14.73	21.04	64.84	52.61	53	3.82	236.84	28.18	10.58	5.7	59.63	48.19
25	4.9	210.5	33.45	14.39	19.3	64.43	52.25	54	3.8	237.18	28.11	10.54	5.61	59.55	48.12
26	4.81	212.29	33.07	14.08	17.76	64.26	52.12	55	3.79	237.49	28.06	10.5	5.53	59.47	48.05
27	4.73	214.0	32.71	13.8	16.4	63.98	51.88	56	3.78	237.79	28.01	10.46	5.46	59.4	47.99
28	4.65	215.62	32.37	13.53	15.2	63.72	51.65	57	3.77	238.07	27.96	10.43	5.39	59.34	47.94
29	4.58	217.17	32.06	13.29	14.14	63.46	51.44	58	3.77	238.33	27.91	10.4	5.33	59.28	47.88
30	4.52	218.64	31.75	13.06	13.2	63.21	51.23	59	3.76	238.57	27.87	10.37	5.27	59.22	47.84

Table A.6.: He^{2+}

Step	$\hat{E}$	$\hat{T}$	P_1	P_2	P_T	P_S	P_{AS}	Step	$\hat{E}$	$\hat{T}$	P_1	P_2	P_T	P_S	P_{AS}
2	39.43	81.58	71.58	63.06	100.0	74.14	61.11	31	9.45	155.61	46.39	28.52	98.17	79.76	65.59
3	35.11	85.92	69.97	61.09	100.0	74.63	61.51	32	9.32	156.52	46.15	28.19	97.79	79.75	65.57
4	31.39	90.35	68.28	59.0	100.0	75.14	61.92	33	9.21	157.39	45.93	27.88	97.38	79.62	65.46
5	28.17	94.85	66.5	56.74	100.0	75.66	62.35	34	9.11	158.21	45.72	27.59	96.94	79.51	65.36
6	25.39	99.39	64.71	54.4	100.0	76.35	62.91	35	9.01	158.98	45.53	27.32	96.48	79.4	65.26
7	22.99	103.94	62.9	52.05	100.0	77.1	63.53	36	8.92	159.71	45.34	27.07	96.01	79.3	65.17
8	20.93	108.47	61.14	49.69	100.0	77.81	64.11	37	8.83	160.41	45.17	26.84	95.52	79.21	65.09
9	19.15	112.95	59.43	47.39	100.0	78.47	64.65	38	8.76	161.06	45.02	26.62	95.02	79.13	65.01
10	17.61	117.34	57.82	45.17	100.0	79.07	65.14	39	8.68	161.67	44.87	26.42	94.51	79.05	64.94
11	16.26	121.62	56.29	43.03	100.0	79.56	65.55	40	8.61	162.25	44.73	26.23	94.01	78.97	64.87
12	15.1	125.75	54.88	41.01	100.0	79.82	65.75	41	8.55	162.79	44.6	26.05	93.51	78.9	64.81
13	14.09	129.72	53.6	39.17	99.99	80.03	65.93	42	8.49	163.3	44.48	25.89	93.02	78.84	64.75
14	13.64	131.63	53.0	38.28	99.99	80.13	66.0	43	8.44	163.78	44.35	25.73	92.53	78.78	64.7
15	13.23	133.49	52.42	37.42	99.99	80.22	66.08	44	8.39	164.23	44.24	25.58	92.06	78.73	64.65
16	12.84	135.3	51.87	36.61	99.99	80.3	66.14	45	8.34	164.66	44.13	25.44	91.6	78.68	64.6
17	12.48	137.05	51.36	35.86	99.99	80.38	66.2	46	8.3	165.05	44.03	25.31	91.15	78.64	64.56
18	12.15	138.75	50.88	35.15	99.99	80.45	66.26	47	8.26	165.43	43.94	25.19	90.72	78.6	64.52
19	11.84	140.39	50.41	34.44	99.98	80.58	66.37	48	8.22	165.77	43.85	25.08	90.3	78.56	64.49
20	11.55	141.98	49.96	33.78	99.97	80.49	66.29	49	8.18	166.1	43.77	24.97	89.91	78.53	64.46
21	11.29	143.5	49.55	33.16	99.94	80.42	66.23	50	8.15	166.41	43.69	24.88	89.53	78.5	64.43
22	11.04	144.97	49.15	32.55	99.9	80.35	66.17	51	8.12	166.69	43.62	24.79	89.16	78.48	64.41
23	10.81	146.38	48.77	31.99	99.84	80.3	66.13	52	8.09	166.96	43.56	24.7	88.82	78.47	64.4
24	10.59	147.73	48.42	31.46	99.76	80.26	66.09	53	8.06	167.21	43.5	24.63	88.49	78.43	64.36
25	10.39	149.02	48.09	30.96	99.65	80.23	66.06	54	8.04	167.44	43.44	24.55	88.17	78.39	64.32
26	10.21	150.26	47.76	30.49	99.5	80.21	66.05	55	8.02	167.66	43.39	24.49	87.88	78.35	64.29
27	10.03	151.43	47.45	30.04	99.32	80.0	65.84	56	7.99	167.87	43.34	24.42	87.6	78.32	64.26
28	9.87	152.56	47.16	29.62	99.09	79.94	65.77	57	7.97	168.06	43.29	24.36	87.33	78.28	64.23
29	9.72	153.63	46.88	29.22	98.82	79.87	65.7	58	7.96	168.24	43.25	24.31	87.08	78.26	64.2
30	9.58	154.64	46.63	28.86	98.52	79.81	65.64	59	7.94	168.4	43.21	24.26	86.85	78.23	64.17

Table A.7.: C^{1+}

Step	$\hat{E}$	$\hat{T}$	P_1	P_2	P_T	P_S	P_{AS}	Step	$\hat{E}$	$\hat{T}$	P_1	P_2	P_T	P_S	P_{AS}
2	15.18	194.58	59.2	65.05	99.99	62.95	51.47	31	3.95	397.15	29.56	30.26	0.75	31.74	25.27
3	13.44	205.88	57.14	62.94	99.9	61.49	50.15	32	3.92	399.84	29.29	29.82	0.69	31.37	24.97
4	11.94	217.47	55.02	60.96	99.18	59.82	48.64	33	3.88	402.4	29.04	29.4	0.64	31.0	24.67
5	10.67	229.31	52.86	59.01	96.11	58.06	47.07	34	3.85	404.82	28.81	29.02	0.6	30.65	24.38
6	9.58	241.31	50.74	57.15	88.26	56.34	45.61	35	3.82	407.12	28.59	28.66	0.56	30.45	24.22
7	8.65	253.41	48.61	55.36	75.04	54.43	43.98	36	3.79	409.29	28.39	28.33	0.53	30.2	24.03
8	7.87	265.53	46.53	53.59	59.0	52.34	42.21	37	3.77	411.34	28.2	28.02	0.5	29.97	23.84
9	7.21	277.57	44.5	51.84	43.19	50.09	40.31	38	3.75	413.28	28.02	27.73	0.47	29.75	23.66
10	6.65	289.46	42.55	50.1	30.03	48.27	38.79	39	3.73	415.11	27.83	27.53	0.45	29.54	23.49
11	6.18	301.11	40.72	48.37	20.27	46.4	37.25	40	3.71	416.83	27.64	27.34	0.43	29.35	23.34
12	5.78	312.44	39.05	46.71	13.52	44.43	35.62	41	3.69	418.45	27.47	27.17	0.41	29.16	23.19
13	5.44	323.38	37.51	44.98	9.06	42.42	33.96	42	3.67	419.97	27.31	27.01	0.4	28.99	23.05
14	5.29	328.69	36.79	44.09	7.45	41.64	33.32	43	3.65	421.41	27.16	26.86	0.38	28.82	22.91
15	5.15	333.87	36.12	43.22	6.16	40.89	32.7	44	3.64	422.75	27.02	26.72	0.37	28.66	22.79
16	5.02	338.92	35.47	42.3	5.12	40.15	32.1	45	3.63	424.02	26.89	26.6	0.36	28.52	22.67
17	4.9	343.84	34.86	41.44	4.28	39.41	31.49	46	3.61	425.2	26.77	26.48	0.35	28.38	22.56
18	4.8	348.62	34.3	40.51	3.6	38.67	30.89	47	3.6	426.32	26.66	26.36	0.34	28.25	22.45
19	4.7	353.25	33.77	39.6	3.06	37.96	30.31	48	3.59	427.36	26.56	26.26	0.33	28.13	22.36
20	4.6	357.74	33.27	38.74	2.61	37.23	29.71	49	3.58	428.34	26.46	26.16	0.32	28.01	22.27
21	4.52	362.08	32.81	37.82	2.25	36.51	29.13	50	3.57	429.25	26.37	26.07	0.31	27.91	22.18
22	4.44	366.27	32.39	36.91	1.96	35.81	28.56	51	3.56	430.11	26.29	25.99	0.31	27.81	22.1
23	4.37	370.31	31.99	36.06	1.71	35.34	28.17	52	3.55	430.91	26.21	25.91	0.3	27.72	22.02
24	4.3	374.19	31.61	35.26	1.51	34.83	27.77	53	3.55	431.66	26.14	25.84	0.3	27.63	21.95
25	4.24	377.92	31.27	34.37	1.34	34.35	27.37	54	3.54	432.36	26.07	25.77	0.29	27.54	21.88
26	4.18	381.5	30.96	33.52	1.2	33.87	26.99	55	3.53	433.02	26.01	25.71	0.29	27.46	21.82
27	4.13	384.92	30.66	32.73	1.08	33.41	26.62	56	3.53	433.63	25.95	25.65	0.28	27.39	21.76
28	4.08	388.2	30.39	31.99	0.97	32.97	26.26	57	3.52	434.2	25.89	25.6	0.28	27.32	21.71
29	4.03	391.33	30.13	31.29	0.89	32.55	25.92	58	3.52	434.74	25.84	25.55	0.27	27.25	21.65
30	3.99	394.31	29.85	30.73	0.81	32.14	25.58	59	3.51	435.24	25.79	25.5	0.27	27.19	21.6

Step	$\hat{E}$	$\hat{T}$	P_1	P_2	P_T	P_S	P_{AS}	Step	$\hat{E}$	$\hat{T}$	P_1	P_2	P_T	P_S	P_{AS}
2	32.69	137.5	70.06	79.35	100.0	70.56	58.11	31	7.48	272.46	45.34	52.57	49.7	54.66	44.04
3	28.94	145.24	68.36	77.02	100.0	70.58	58.12	32	7.39	274.17	45.05	52.32	47.49	54.32	43.75
4	25.71	153.16	66.77	74.75	100.0	70.57	58.1	33	7.3	275.79	44.79	52.09	45.42	53.95	43.44
5	22.92	161.24	65.25	72.58	100.0	70.52	58.04	34	7.22	277.32	44.54	51.88	43.51	53.6	43.14
6	20.54	169.42	63.77	70.51	100.0	69.83	57.38	35	7.15	278.77	44.3	51.68	41.74	53.26	42.86
7	18.51	177.63	62.28	68.59	100.0	69.17	56.76	36	7.08	280.14	44.07	51.47	40.1	52.94	42.59
8	16.77	185.84	60.79	66.81	99.99	68.41	56.05	37	7.02	281.43	43.86	51.27	38.58	52.83	42.5
9	15.28	193.97	59.31	65.17	99.99	67.54	55.25	38	6.96	282.65	43.65	51.09	37.19	52.62	42.33
10	14.01	201.96	57.85	63.65	99.96	66.58	54.36	39	6.91	283.8	43.46	50.92	35.9	52.43	42.17
11	12.9	209.77	56.45	62.26	99.79	65.51	53.39	40	6.85	284.88	43.28	50.76	34.72	52.25	42.02
12	11.96	217.33	55.04	60.98	99.2	64.28	52.28	41	6.81	285.9	43.12	50.61	33.63	52.07	41.88
13	11.15	224.59	53.72	59.79	97.76	63.0	51.13	42	6.77	286.86	42.96	50.47	32.64	51.91	41.74
14	10.79	228.1	53.08	59.21	96.59	62.35	50.55	43	6.72	287.76	42.82	50.34	31.72	51.76	41.62
15	10.46	231.52	52.46	58.66	95.09	61.99	50.26	44	6.69	288.61	42.69	50.22	30.87	51.61	41.5
16	10.15	234.85	51.89	58.15	93.2	61.51	49.85	45	6.65	289.4	42.56	50.1	30.09	51.48	41.39
17	9.86	238.08	51.32	57.65	90.94	61.02	49.44	46	6.62	290.15	42.44	50.0	29.37	51.35	41.28
18	9.59	241.21	50.75	57.16	88.35	60.54	49.03	47	6.59	290.85	42.34	49.9	28.71	51.23	41.18
19	9.34	244.24	50.22	56.71	85.49	60.09	48.64	48	6.56	291.5	42.23	49.81	28.1	51.12	41.09
20	9.11	247.17	49.7	56.27	82.43	59.57	48.2	49	6.54	292.11	42.14	49.72	27.54	51.02	41.01
21	8.9	249.99	49.2	55.85	79.22	59.06	47.77	50	6.51	292.69	42.05	49.64	27.02	50.93	40.93
22	8.7	252.7	48.73	55.46	75.93	58.56	47.34	51	6.49	293.23	41.97	49.57	26.54	50.84	40.85
23	8.52	255.31	48.29	55.09	72.62	58.07	46.93	52	6.47	293.73	41.89	49.5	26.09	50.76	40.79
24	8.35	257.81	47.84	54.71	69.38	57.59	46.53	53	6.45	294.2	41.82	49.43	25.69	50.67	40.72
25	8.2	260.21	47.42	54.36	66.2	57.13	46.13	54	6.43	294.64	41.75	49.36	25.31	50.59	40.65
26	8.05	262.5	47.03	54.02	63.11	56.68	45.75	55	6.42	295.05	41.68	49.29	24.96	50.51	40.58
27	7.92	264.69	46.67	53.71	60.13	56.25	45.39	56	6.4	295.44	41.62	49.23	24.64	50.44	40.52
28	7.8	266.78	46.31	53.41	57.3	55.83	45.03	57	6.39	295.8	41.56	49.18	24.34	50.37	40.47
29	7.68	268.77	45.97	53.11	54.61	55.43	44.69	58	6.37	296.14	41.51	49.12	24.06	50.31	40.41
30	7.58	270.66	45.64	52.83	52.08	55.04	44.36	59	6.36	296.45	41.46	49.08	23.81	50.25	40.36

Step	$\hat{E}$	$\hat{T}$	P_1	P_2	P_T	P_S	P_{AS}	Step	$\hat{E}$	$\hat{T}$	P_1	P_2	P_T	P_S	P_{AS}
2	51.04	112.77	76.89	87.19	100.0	72.51	59.74	31	11.57	220.68	54.45	60.44	98.67	67.11	54.54
3	45.26	119.0	74.96	85.21	100.0	72.78	59.96	32	11.42	222.03	54.21	60.22	98.4	66.89	54.34
4	40.21	125.38	73.13	83.17	100.0	73.05	60.18	33	11.28	223.31	53.97	60.0	98.1	66.62	54.1
5	35.89	131.87	71.42	81.1	100.0	73.32	60.38	34	11.16	224.52	53.74	59.8	97.78	66.36	53.87
6	32.19	138.43	69.85	79.06	100.0	73.62	60.63	35	11.04	225.67	53.52	59.61	97.44	66.11	53.65
7	29.04	145.03	68.41	77.08	100.0	73.88	60.84	36	10.93	226.75	53.32	59.43	97.08	65.88	53.44
8	26.31	151.6	67.08	75.19	100.0	74.04	60.96	37	10.82	227.78	53.13	59.26	96.72	65.66	53.25
9	23.94	158.12	65.84	73.4	100.0	74.09	61.0	38	10.73	228.74	52.96	59.11	96.34	65.63	53.24
10	21.91	164.52	64.65	71.73	100.0	73.84	60.74	39	10.64	229.65	52.8	58.96	95.96	65.48	53.11
11	20.18	170.77	63.52	70.18	100.0	73.51	60.41	40	10.56	230.5	52.64	58.82	95.58	65.34	53.0
12	18.7	176.81	62.43	68.77	100.0	73.03	59.94	41	10.48	231.31	52.5	58.7	95.19	65.22	52.89
13	17.43	182.62	61.39	67.5	99.99	72.5	59.45	42	10.41	232.06	52.37	58.58	94.81	65.1	52.79
14	16.86	185.42	60.87	66.9	99.99	72.23	59.2	43	10.34	232.77	52.24	58.46	94.43	64.99	52.69
15	16.33	188.14	60.38	66.33	99.99	71.96	58.94	44	10.28	233.44	52.13	58.36	94.06	64.88	52.6
16	15.84	190.8	59.9	65.79	99.99	71.68	58.68	45	10.22	234.07	52.02	58.26	93.69	64.78	52.52
17	15.38	193.37	59.42	65.28	99.99	71.39	58.42	46	10.17	234.66	51.92	58.17	93.32	64.69	52.45
18	14.96	195.87	58.97	64.8	99.99	71.11	58.15	47	10.12	235.21	51.82	58.09	92.97	64.61	52.37
19	14.57	198.28	58.55	64.34	99.98	70.86	57.92	48	10.07	235.73	51.74	58.01	92.63	64.53	52.31
20	14.21	200.61	58.11	63.9	99.97	70.49	57.59	49	10.02	236.21	51.66	57.94	92.3	64.46	52.25
21	13.88	202.85	57.69	63.49	99.95	70.13	57.27	50	9.98	236.66	51.58	57.87	91.98	64.39	52.19
22	13.56	205.01	57.3	63.1	99.92	69.78	56.95	51	9.95	237.09	51.5	57.8	91.67	64.33	52.14
23	13.27	207.08	56.93	62.73	99.88	69.44	56.64	52	9.91	237.49	51.43	57.74	91.38	64.29	52.1
24	13.0	209.07	56.58	62.38	99.81	69.11	56.34	53	9.88	237.86	51.36	57.68	91.1	64.22	52.04
25	12.74	210.97	56.22	62.05	99.73	68.79	56.06	54	9.85	238.2	51.29	57.63	90.84	64.15	51.98
26	12.51	212.79	55.87	61.74	99.63	68.48	55.78	55	9.82	238.53	51.23	57.58	90.59	64.09	51.93
27	12.29	214.53	55.55	61.44	99.49	68.18	55.51	56	9.79	238.83	51.18	57.53	90.35	64.03	51.88
28	12.09	216.18	55.25	61.17	99.33	67.9	55.25	57	9.77	239.12	51.13	57.48	90.12	63.98	51.83
29	11.9	217.76	54.97	60.91	99.14	67.62	55.0	58	9.75	239.38	51.08	57.44	89.91	63.93	51.79
30	11.73	219.26	54.7	60.67	98.92	67.36	54.76	59	9.72	239.63	51.04	57.4	89.7	63.88	51.75

Table A.10.: C^{4+}

Step	$\hat{E}$	$\hat{T}$	P_1	P_2	P_T	P_S	P_{AS}	Step	$\hat{E}$	$\hat{T}$	P_1	P_2	P_T	P_S	P_{AS}
2	69.58	98.15	81.8	91.53	100.0	73.48	60.55	31	15.89	190.52	59.95	65.85	99.99	74.67	61.15
3	61.74	103.52	79.96	90.01	100.0	73.88	60.88	32	15.68	191.67	59.74	65.62	99.99	74.58	61.05
4	55.02	109.01	78.11	88.35	100.0	74.3	61.22	33	15.49	192.76	59.53	65.4	99.99	74.39	60.89
5	49.26	114.58	76.32	86.61	100.0	74.72	61.56	34	15.31	193.8	59.35	65.2	99.99	74.22	60.74
6	44.23	120.22	74.6	84.82	100.0	75.25	61.99	35	15.14	194.77	59.17	65.01	99.99	74.06	60.59
7	39.86	125.87	72.99	83.02	100.0	75.8	62.45	36	14.99	195.69	59.0	64.83	99.99	73.91	60.45
8	36.11	131.5	71.51	81.22	100.0	76.29	62.84	37	14.85	196.56	58.85	64.67	99.99	73.76	60.33
9	32.91	137.08	70.16	79.48	100.0	76.71	63.18	38	14.72	197.38	58.7	64.51	99.98	73.63	60.21
10	30.16	142.56	68.93	77.81	100.0	77.04	63.45	39	14.59	198.16	58.57	64.36	99.98	73.5	60.09
11	27.8	147.9	67.82	76.24	100.0	77.26	63.63	40	14.48	198.89	58.44	64.23	99.98	73.39	59.99
12	25.75	153.07	66.79	74.78	100.0	77.27	63.63	41	14.37	199.57	58.31	64.1	99.98	73.28	59.89
13	23.97	158.03	65.85	73.43	100.0	77.24	63.6	42	14.27	200.22	58.18	63.98	99.97	73.18	59.8
14	23.18	160.42	65.41	72.79	100.0	77.21	63.57	43	14.18	200.82	58.07	63.86	99.97	73.08	59.71
15	22.45	162.75	64.98	72.18	100.0	77.08	63.42	44	14.1	201.39	57.96	63.76	99.96	72.99	59.63
16	21.77	165.02	64.56	71.6	100.0	76.98	63.33	45	14.02	201.92	57.86	63.66	99.96	72.91	59.56
17	21.14	167.22	64.16	71.05	100.0	76.89	63.23	46	13.94	202.42	57.77	63.57	99.96	72.84	59.49
18	20.56	169.35	63.78	70.53	100.0	76.79	63.13	47	13.87	202.89	57.68	63.48	99.95	72.77	59.43
19	20.02	171.41	63.4	70.03	100.0	76.75	63.07	48	13.81	203.33	57.6	63.4	99.95	72.71	59.37
20	19.51	173.4	63.05	69.56	100.0	76.54	62.88	49	13.75	203.74	57.53	63.32	99.94	72.65	59.32
21	19.05	175.31	62.71	69.11	100.0	76.34	62.69	50	13.69	204.13	57.46	63.25	99.94	72.6	59.27
22	18.62	177.15	62.37	68.7	100.0	76.14	62.51	51	13.64	204.49	57.39	63.19	99.93	72.55	59.23
23	18.22	178.92	62.05	68.3	99.99	75.95	62.33	52	13.59	204.83	57.33	63.13	99.92	72.52	59.2
24	17.85	180.62	61.75	67.93	99.99	75.76	62.16	53	13.54	205.14	57.27	63.07	99.92	72.46	59.14
25	17.51	182.24	61.46	67.58	99.99	75.59	61.99	54	13.5	205.44	57.22	63.02	99.91	72.4	59.09
26	17.18	183.79	61.17	67.25	99.99	75.41	61.84	55	13.46	205.71	57.17	62.97	99.91	72.35	59.04
27	16.88	185.27	60.9	66.93	99.99	75.25	61.68	56	13.42	205.97	57.12	62.92	99.9	72.3	59.0
28	16.61	186.69	60.64	66.64	99.99	75.09	61.54	57	13.39	206.21	57.08	62.88	99.9	72.25	58.95
29	16.35	188.03	60.4	66.36	99.99	74.95	61.4	58	13.36	206.44	57.04	62.84	99.89	72.21	58.92
30	16.11	189.31	60.18	66.1	99.99	74.8	61.27	59	13.33	206.65	57.0	62.8	99.89	72.17	58.88

Table A.11.: C^{5+}

Step	$\hat{E}$	$\hat{T}$	P_1	P_2	P_T	P_S	P_{AS}	Step	$\hat{E}$	$\hat{T}$	P_1	P_2	P_T	P_S	P_{AS}
2	88.43	88.21	85.26	94.06	100.0	74.07	61.04	31	20.33	170.21	63.62	70.32	100.0	79.2	65.1
3	78.57	93.0	83.59	92.9	100.0	74.55	61.44	32	20.06	171.23	63.44	70.07	100.0	79.18	65.07
4	69.99	97.89	81.89	91.6	100.0	75.05	61.85	33	19.81	172.19	63.26	69.84	100.0	79.05	64.96
5	62.63	102.86	80.18	90.2	100.0	75.56	62.26	34	19.59	173.11	63.1	69.62	100.0	78.93	64.85
6	56.32	107.87	78.49	88.7	100.0	76.23	62.82	35	19.37	173.97	62.95	69.42	100.0	78.82	64.75
7	50.9	112.9	76.85	87.15	100.0	76.96	63.41	36	19.18	174.79	62.8	69.23	100.0	78.71	64.65
8	46.22	117.91	75.29	85.56	100.0	77.64	63.97	37	18.99	175.56	62.66	69.06	100.0	78.61	64.56
9	42.1	122.86	73.83	83.97	100.0	78.28	64.49	38	18.82	176.28	62.53	68.89	100.0	78.52	64.48
10	38.56	127.72	72.49	82.43	100.0	78.85	64.96	39	18.66	176.97	62.4	68.74	100.0	78.43	64.4
11	35.53	132.46	71.27	80.92	100.0	79.32	65.34	40	18.52	177.61	62.28	68.59	100.0	78.35	64.33
12	32.93	137.04	70.17	79.49	100.0	79.54	65.52	41	18.38	178.22	62.17	68.46	99.99	78.28	64.26
13	30.69	141.44	69.18	78.15	100.0	79.73	65.68	42	18.25	178.79	62.07	68.33	99.99	78.21	64.2
14	29.7	143.56	68.72	77.52	100.0	79.81	65.74	43	18.13	179.32	61.98	68.22	99.99	78.15	64.14
15	28.77	145.62	68.28	76.91	100.0	79.89	65.8	44	18.02	179.83	61.89	68.11	99.99	78.1	64.09
16	27.92	147.63	67.87	76.32	100.0	79.96	65.85	45	17.92	180.3	61.8	68.0	99.99	78.04	64.04
17	27.12	149.58	67.48	75.76	100.0	80.02	65.9	46	17.82	180.74	61.73	67.91	99.99	78.0	64.0
18	26.36	151.46	67.11	75.23	100.0	80.07	65.95	47	17.74	181.15	61.65	67.82	99.99	77.95	63.96
19	25.66	153.29	66.75	74.72	100.0	80.19	66.04	48	17.65	181.54	61.59	67.74	99.99	77.91	63.92
20	25.01	155.05	66.41	74.23	100.0	80.1	65.96	49	17.58	181.91	61.52	67.66	99.99	77.88	63.89
21	24.41	156.74	66.09	73.77	100.0	80.02	65.89	50	17.5	182.25	61.46	67.58	99.99	77.85	63.86
22	23.85	158.38	65.79	73.33	100.0	79.95	65.84	51	17.44	182.57	61.4	67.51	99.99	77.82	63.83
23	23.33	159.94	65.49	72.92	100.0	79.9	65.79	52	17.37	182.87	61.34	67.45	99.99	77.81	63.83
24	22.85	161.44	65.22	72.52	100.0	79.85	65.75	53	17.32	183.15	61.29	67.39	99.99	77.77	63.78
25	22.41	162.88	64.96	72.15	100.0	79.66	65.55	54	17.26	183.41	61.24	67.33	99.99	77.72	63.74
26	21.99	164.25	64.7	71.8	100.0	79.57	65.47	55	17.21	183.65	61.2	67.28	99.99	77.68	63.71
27	21.61	165.57	64.46	71.47	100.0	79.48	65.38	56	17.17	183.88	61.15	67.23	99.99	77.65	63.67
28	21.25	166.81	64.24	71.15	100.0	79.41	65.31	57	17.12	184.09	61.11	67.19	99.99	77.61	63.64
29	20.92	168.0	64.02	70.86	100.0	79.33	65.23	58	17.08	184.29	61.08	67.14	99.99	77.58	63.61
30	20.61	169.14	63.82	70.58	100.0	79.26	65.16	59	17.04	184.48	61.04	67.1	99.99	77.56	63.59

Table A.12.: C^{6+}

Step	$\hat{E}$	$\hat{T}$	P_1	P_2	P_T	P_S	P_{AS}	Step	$\hat{E}$	$\hat{T}$	P_1	P_2	P_T	P_S	P_{AS}
2	107.48	80.89	87.73	95.59	100.0	74.46	61.37	31	24.9	155.36	66.35	74.15	100.0	82.06	67.58
3	95.47	85.26	86.27	94.71	100.0	74.99	61.81	32	24.57	156.28	66.18	73.9	100.0	82.13	67.64
4	85.15	89.71	84.73	93.7	100.0	75.55	62.27	33	24.27	157.15	66.01	73.66	100.0	82.08	67.6
5	76.27	94.24	83.16	92.58	100.0	76.12	62.74	34	23.99	157.98	65.86	73.44	100.0	82.04	67.57
6	68.56	98.8	81.57	91.35	100.0	76.89	63.36	35	23.72	158.76	65.71	73.23	100.0	82.01	67.54
7	61.94	103.37	80.01	90.05	100.0	77.73	64.06	36	23.48	159.5	65.58	73.03	100.0	81.98	67.51
8	56.26	107.93	78.47	88.69	100.0	78.55	64.73	37	23.25	160.2	65.45	72.85	100.0	81.96	67.49
9	51.38	112.43	77.0	87.3	100.0	79.33	65.37	38	23.04	160.85	65.33	72.68	100.0	81.94	67.47
10	47.18	116.84	75.62	85.9	100.0	80.06	65.97	39	22.84	161.47	65.21	72.52	100.0	81.92	67.46
11	43.46	121.15	74.33	84.52	100.0	80.69	66.49	40	22.66	162.06	65.11	72.36	100.0	81.91	67.45
12	40.26	125.3	73.15	83.2	100.0	81.06	66.79	41	22.49	162.61	65.01	72.22	100.0	81.61	67.17
13	37.52	129.29	72.08	81.93	100.0	81.39	67.06	42	22.33	163.12	64.91	72.09	100.0	81.57	67.13
14	36.29	131.21	71.59	81.31	100.0	81.55	67.19	43	22.19	163.61	64.82	71.96	100.0	81.53	67.09
15	35.16	133.08	71.12	80.72	100.0	81.7	67.31	44	22.05	164.06	64.74	71.85	100.0	81.49	67.06
16	34.11	134.9	70.67	80.15	100.0	81.85	67.43	45	21.92	164.49	64.66	71.74	100.0	81.46	67.03
17	33.13	136.67	70.26	79.6	100.0	81.98	67.54	46	21.8	164.89	64.59	71.64	100.0	81.43	67.0
18	32.22	138.38	69.86	79.08	100.0	82.11	67.65	47	21.69	165.26	64.52	71.54	100.0	81.4	66.98
19	31.38	140.03	69.49	78.57	100.0	82.34	67.83	48	21.59	165.62	64.45	71.45	100.0	81.38	66.95
20	30.6	141.63	69.14	78.09	100.0	82.26	67.76	49	21.5	165.95	64.39	71.37	100.0	81.36	66.93
21	29.88	143.16	68.8	77.63	100.0	82.19	67.71	50	21.41	166.26	64.34	71.29	100.0	81.34	66.92
22	29.21	144.64	68.49	77.2	100.0	82.14	67.66	51	21.33	166.54	64.29	71.22	100.0	81.33	66.9
23	28.58	146.06	68.19	76.78	100.0	82.09	67.62	52	21.25	166.81	64.24	71.15	100.0	81.33	66.9
24	28.0	147.42	67.91	76.38	100.0	82.06	67.59	53	21.18	167.07	64.19	71.09	100.0	81.3	66.87
25	27.47	148.72	67.65	76.01	100.0	82.03	67.57	54	21.11	167.3	64.15	71.03	100.0	81.27	66.84
26	26.96	149.96	67.4	75.65	100.0	82.02	67.56	55	21.05	167.52	64.11	70.98	100.0	81.24	66.81
27	26.49	151.15	67.17	75.32	100.0	82.01	67.55	56	21.0	167.73	64.07	70.93	100.0	81.21	66.79
28	26.05	152.28	66.95	75.0	100.0	82.01	67.55	57	20.94	167.92	64.04	70.88	100.0	81.18	66.76
29	25.64	153.36	66.74	74.7	100.0	82.02	67.55	58	20.89	168.1	64.01	70.83	100.0	81.16	66.74
30	25.26	154.38	66.54	74.42	100.0	82.04	67.57	59	20.85	168.27	63.98	70.79	100.0	81.14	66.72

Table A.13.: $13C^{1+}$

Step	$\hat{E}$	$\hat{T}$	P_1	P_2	P_T	P_S	P_{AS}	Step	$\hat{E}$	$\hat{T}$	P_1	P_2	P_T	P_S	P_{AS}
2	14.97	202.21	57.81	63.63	99.98	62.96	51.48	31	3.89	412.98	28.04	27.75	0.66	31.76	25.28
3	13.22	213.96	55.66	61.56	99.83	61.5	50.16	32	3.86	415.78	27.74	27.45	0.61	31.39	24.98
4	11.75	226.0	53.47	59.56	98.77	59.84	48.65	33	3.82	418.43	27.46	27.17	0.57	31.02	24.68
5	10.49	238.3	51.24	57.61	94.85	58.07	47.09	34	3.79	420.94	27.2	26.91	0.53	30.67	24.4
6	9.41	250.78	49.07	55.74	85.8	56.36	45.62	35	3.77	423.32	26.96	26.67	0.5	30.46	24.23
7	8.5	263.35	46.89	53.88	71.93	54.45	44.0	36	3.74	425.57	26.73	26.45	0.47	30.22	24.04
8	7.73	275.94	44.77	52.04	55.67	52.36	42.23	37	3.72	427.69	26.52	26.24	0.45	29.99	23.85
9	7.08	288.46	42.72	50.25	40.19	50.11	40.33	38	3.69	429.7	26.33	26.04	0.42	29.77	23.67
10	6.54	300.82	40.78	48.43	27.64	48.29	38.81	39	3.67	431.59	26.14	25.86	0.4	29.56	23.51
11	6.07	312.93	38.97	46.58	18.47	46.43	37.27	40	3.65	433.37	25.96	25.68	0.39	29.36	23.35
12	5.68	324.71	37.33	44.77	12.23	44.46	35.64	41	3.64	435.05	25.8	25.51	0.37	29.18	23.2
13	5.35	336.1	35.84	42.83	8.13	42.45	33.98	42	3.62	436.63	25.64	25.36	0.35	29.0	23.06
14	5.2	341.62	35.14	41.83	6.67	41.66	33.33	43	3.6	438.11	25.5	25.22	0.34	28.84	22.93
15	5.06	347.01	34.5	40.84	5.5	40.91	32.72	44	3.59	439.51	25.37	25.09	0.33	28.68	22.8
16	4.94	352.27	33.88	39.8	4.56	40.17	32.11	45	3.58	440.82	25.24	24.96	0.32	28.54	22.68
17	4.82	357.4	33.31	38.81	3.81	39.43	31.51	46	3.56	442.04	25.13	24.85	0.31	28.4	22.57
18	4.72	362.38	32.78	37.76	3.21	38.7	30.91	47	3.55	443.2	25.02	24.74	0.3	28.27	22.47
19	4.62	367.21	32.29	36.72	2.73	37.98	30.33	48	3.54	444.28	24.92	24.64	0.29	28.15	22.37
20	4.53	371.9	31.82	35.75	2.33	37.25	29.73	49	3.53	445.29	24.83	24.55	0.29	28.03	22.28
21	4.45	376.42	31.4	34.71	2.01	36.53	29.14	50	3.52	446.24	24.74	24.46	0.28	27.93	22.19
22	4.37	380.79	31.01	33.7	1.75	35.83	28.57	51	3.51	447.13	24.66	24.38	0.28	27.83	22.11
23	4.3	385.01	30.65	32.74	1.53	35.35	28.19	52	3.51	447.96	24.59	24.31	0.27	27.74	22.04
24	4.23	389.06	30.31	31.85	1.34	34.85	27.78	53	3.5	448.74	24.52	24.24	0.26	27.65	21.97
25	4.17	392.96	29.94	31.07	1.19	34.36	27.38	54	3.49	449.47	24.45	24.17	0.26	27.56	21.9
26	4.12	396.69	29.59	30.36	1.06	33.88	27.0	55	3.48	450.15	24.39	24.11	0.26	27.48	21.84
27	4.06	400.26	29.26	29.7	0.96	33.43	26.63	56	3.48	450.78	24.34	24.06	0.25	27.41	21.78
28	4.02	403.67	28.96	29.08	0.87	32.98	26.27	57	3.47	451.38	24.28	24.01	0.25	27.34	21.72
29	3.97	406.93	28.68	28.5	0.79	32.56	25.93	58	3.47	451.93	24.23	23.96	0.25	27.28	21.67
30	3.93	410.03	28.37	28.07	0.72	32.15	25.59	59	3.46	452.45	24.19	23.91	0.24	27.22	21.62

Table A.14.: 13C^{2+}

Step	$\hat{E}$	$\hat{T}$	P_1	P_2	P_T	P_S	P_{AS}	Step	$\hat{E}$	$\hat{T}$	P_1	P_2	P_T	P_S	P_{AS}
2	32.35	142.85	68.86	77.72	100.0	70.57	58.12	31	7.34	283.14	43.57	50.99	46.49	54.69	44.07
3	28.63	150.91	67.21	75.38	100.0	70.58	58.12	32	7.25	284.92	43.28	50.74	44.33	54.35	43.78
4	25.39	159.16	65.64	73.12	100.0	70.57	58.1	33	7.17	286.6	43.02	50.51	42.33	53.98	43.47
5	22.63	167.56	64.1	70.98	100.0	70.52	58.04	34	7.09	288.19	42.77	50.29	40.49	53.63	43.17
6	20.28	176.06	62.57	68.96	100.0	69.83	57.38	35	7.02	289.7	42.53	50.08	38.79	53.29	42.88
7	18.27	184.6	61.02	67.08	99.99	69.18	56.76	36	6.96	291.12	42.3	49.87	37.22	52.97	42.62
8	16.54	193.13	59.47	65.35	99.99	68.42	56.06	37	6.9	292.46	42.08	49.66	35.78	52.85	42.52
9	15.07	201.58	57.93	63.74	99.99	67.55	55.26	38	6.84	293.73	41.88	49.47	34.45	52.65	42.35
10	13.79	209.89	56.41	62.26	99.92	66.59	54.37	39	6.79	294.93	41.69	49.29	33.22	52.45	42.19
11	12.7	218.0	54.94	60.89	99.64	65.52	53.4	40	6.74	296.05	41.51	49.12	32.1	52.27	42.04
12	11.76	225.85	53.49	59.59	98.79	64.3	52.3	41	6.69	297.11	41.35	48.97	31.07	52.1	41.9
13	10.97	233.41	52.14	58.38	96.93	63.02	51.15	42	6.65	298.11	41.19	48.82	30.12	51.94	41.76
14	10.61	237.05	51.47	57.8	95.45	62.37	50.56	43	6.61	299.05	41.05	48.69	29.24	51.78	41.64
15	10.27	240.6	50.84	57.26	93.59	62.01	50.28	44	6.57	299.93	40.91	48.56	28.44	51.64	41.52
16	9.97	244.06	50.24	56.74	91.36	61.52	49.86	45	6.54	300.75	40.79	48.44	27.7	51.5	41.41
17	9.68	247.42	49.66	56.24	88.78	61.04	49.45	46	6.51	301.53	40.67	48.33	27.02	51.38	41.3
18	9.42	250.67	49.08	55.76	85.9	60.56	49.04	47	6.48	302.25	40.56	48.23	26.39	51.26	41.21
19	9.17	253.82	48.54	55.3	82.78	60.11	48.65	48	6.45	302.93	40.46	48.13	25.82	51.15	41.11
20	8.95	256.86	48.01	54.85	79.54	59.59	48.22	49	6.42	303.57	40.36	48.04	25.29	51.05	41.03
21	8.74	259.79	47.49	54.4	76.22	59.08	47.78	50	6.4	304.17	40.28	47.96	24.8	50.95	40.95
22	8.55	262.61	47.01	53.99	72.84	58.58	47.36	51	6.38	304.73	40.19	47.88	24.34	50.86	40.88
23	8.37	265.32	46.56	53.59	69.47	58.09	46.95	52	6.36	305.25	40.12	47.81	23.93	50.79	40.82
24	8.2	267.92	46.11	53.2	66.14	57.62	46.55	53	6.34	305.74	40.05	47.73	23.54	50.7	40.74
25	8.05	270.41	45.68	52.83	62.9	57.16	46.15	54	6.32	306.2	39.97	47.66	23.19	50.62	40.67
26	7.91	272.79	45.28	52.49	59.78	56.71	45.77	55	6.31	306.63	39.91	47.59	22.86	50.54	40.61
27	7.78	275.07	44.91	52.16	56.8	56.27	45.41	56	6.29	307.03	39.85	47.52	22.56	50.46	40.55
28	7.66	277.24	44.56	51.85	53.97	55.86	45.05	57	6.28	307.4	39.79	47.46	22.28	50.4	40.49
29	7.54	279.31	44.21	51.55	51.31	55.45	44.71	58	6.26	307.75	39.74	47.4	22.02	50.33	40.44
30	7.44	281.28	43.88	51.26	48.82	55.07	44.38	59	6.25	308.08	39.69	47.35	21.78	50.28	40.39

Table A.15.: 13C^{3+}

Step	$\hat{E}$	$\hat{T}$	P_1	P_2	P_T	P_S	P_{AS}	Step	$\hat{E}$	$\hat{T}$	P_1	P_2	P_T	P_S	P_{AS}
2	50.67	117.12	75.53	85.81	100.0	72.51	59.74	31	11.39	229.34	52.89	59.04	98.1	67.13	54.55
3	44.81	123.61	73.62	83.73	100.0	72.78	59.96	32	11.24	230.74	52.64	58.82	97.74	66.91	54.36
4	39.8	130.25	71.83	81.62	100.0	73.05	60.18	33	11.1	232.07	52.39	58.6	97.36	66.64	54.12
5	35.53	137.0	70.17	79.5	100.0	73.32	60.39	34	10.98	233.33	52.15	58.4	96.95	66.38	53.88
6	31.87	143.83	68.65	77.43	100.0	73.62	60.63	35	10.86	234.52	51.93	58.2	96.52	66.13	53.67
7	28.72	150.69	67.25	75.44	100.0	73.88	60.84	36	10.74	235.65	51.72	58.03	96.07	65.9	53.46
8	25.98	157.53	65.94	73.55	100.0	74.04	60.96	37	10.64	236.71	51.53	57.86	95.61	65.68	53.27
9	23.64	164.31	64.7	71.79	100.0	74.09	61.0	38	10.54	237.71	51.35	57.7	95.14	65.64	53.25
10	21.63	170.97	63.48	70.15	100.0	73.85	60.74	39	10.46	238.66	51.18	57.56	94.67	65.5	53.13
11	19.92	177.46	62.31	68.64	100.0	73.52	60.41	40	10.37	239.54	51.02	57.42	94.19	65.36	53.01
12	18.45	183.75	61.18	67.26	99.99	73.03	59.95	41	10.29	240.38	50.88	57.29	93.72	65.23	52.9
13	17.19	189.78	60.09	66.01	99.99	72.51	59.46	42	10.22	241.17	50.74	57.17	93.26	65.12	52.8
14	16.62	192.69	59.55	65.43	99.99	72.24	59.21	43	10.16	241.91	50.61	57.06	92.8	65.0	52.71
15	16.1	195.53	59.04	64.88	99.99	71.97	58.95	44	10.09	242.6	50.49	56.96	92.35	64.9	52.62
16	15.62	198.28	58.54	64.36	99.99	71.69	58.69	45	10.04	243.25	50.38	56.86	91.92	64.8	52.54
17	15.17	200.96	58.04	63.86	99.99	71.4	58.43	46	9.98	243.86	50.28	56.77	91.5	64.71	52.46
18	14.75	203.55	57.57	63.38	99.98	71.12	58.16	47	9.93	244.44	50.18	56.69	91.09	64.63	52.39
19	14.36	206.06	57.13	62.93	99.97	70.87	57.93	48	9.89	244.97	50.09	56.61	90.7	64.55	52.32
20	13.99	208.48	56.67	62.5	99.94	70.51	57.6	49	9.84	245.48	50.01	56.53	90.32	64.48	52.26
21	13.66	210.81	56.24	62.1	99.91	70.15	57.28	50	9.8	245.95	49.93	56.47	89.96	64.41	52.21
22	13.35	213.05	55.83	61.71	99.85	69.8	56.96	51	9.77	246.39	49.85	56.4	89.61	64.35	52.15
23	13.06	215.2	55.44	61.35	99.78	69.46	56.66	52	9.73	246.8	49.77	56.34	89.28	64.31	52.12
24	12.79	217.27	55.08	61.01	99.68	69.13	56.36	53	9.7	247.19	49.7	56.28	88.97	64.24	52.06
25	12.54	219.25	54.7	60.68	99.56	68.81	56.07	54	9.67	247.55	49.64	56.22	88.67	64.17	52.0
26	12.31	221.14	54.35	60.36	99.4	68.5	55.79	55	9.64	247.88	49.58	56.17	88.38	64.11	51.95
27	12.1	222.94	54.02	60.06	99.21	68.2	55.52	56	9.62	248.2	49.52	56.13	88.12	64.05	51.9
28	11.9	224.66	53.71	59.78	98.98	67.91	55.26	57	9.59	248.49	49.47	56.08	87.86	64.0	51.85
29	11.71	226.3	53.42	59.52	98.72	67.64	55.02	58	9.57	248.77	49.42	56.04	87.62	63.95	51.81
30	11.54	227.86	53.14	59.27	98.42	67.38	54.78	59	9.55	249.03	49.37	56.0	87.4	63.9	51.77

Table A.16.: 13C^{4+}

Step	$\hat{E}$	$\hat{T}$	P_1	P_2	P_T	P_S	P_{AS}	Step	$\hat{E}$	$\hat{T}$	P_1	P_2	P_T	P_S	P_{AS}
2	69.1	101.91	80.5	90.47	100.0	73.48	60.55	31	15.67	198.0	58.6	64.41	99.99	74.68	61.15
3	61.31	107.5	78.61	88.82	100.0	73.89	60.88	32	15.46	199.19	58.37	64.19	99.99	74.59	61.06
4	54.64	113.21	76.75	87.06	100.0	74.3	61.22	33	15.27	200.33	58.16	63.98	99.99	74.41	60.9
5	48.85	119.01	74.96	85.21	100.0	74.72	61.56	34	15.1	201.4	57.96	63.78	99.99	74.23	60.75
6	43.79	124.87	73.27	83.33	100.0	75.25	62.0	35	14.93	202.41	57.77	63.59	99.98	74.07	60.6
7	39.46	130.75	71.7	81.46	100.0	75.8	62.45	36	14.78	203.37	57.6	63.42	99.98	73.92	60.46
8	35.75	136.61	70.26	79.62	100.0	76.29	62.85	37	14.64	204.28	57.44	63.25	99.98	73.78	60.34
9	32.57	142.42	68.96	77.85	100.0	76.71	63.18	38	14.5	205.13	57.29	63.1	99.97	73.64	60.22
10	29.85	148.12	67.77	76.18	100.0	77.04	63.45	39	14.38	205.93	57.15	62.96	99.97	73.52	60.1
11	27.47	153.68	66.67	74.6	100.0	77.26	63.63	40	14.26	206.69	57.01	62.82	99.96	73.4	60.0
12	25.42	159.05	65.66	73.14	100.0	77.27	63.63	41	14.15	207.4	56.88	62.7	99.95	73.29	59.9
13	23.67	164.21	64.71	71.81	100.0	77.24	63.6	42	14.05	208.07	56.75	62.58	99.95	73.19	59.81
14	22.89	166.7	64.25	71.19	100.0	77.21	63.57	43	13.96	208.7	56.63	62.47	99.94	73.1	59.72
15	22.16	169.13	63.82	70.59	100.0	77.08	63.43	44	13.88	209.29	56.52	62.36	99.93	73.01	59.65
16	21.49	171.49	63.39	70.03	100.0	76.99	63.33	45	13.79	209.85	56.41	62.26	99.92	72.93	59.57
17	20.87	173.77	62.98	69.49	100.0	76.9	63.23	46	13.72	210.37	56.32	62.17	99.91	72.85	59.51
18	20.29	175.99	62.58	68.98	100.0	76.8	63.13	47	13.65	210.85	56.23	62.09	99.91	72.79	59.44
19	19.76	178.13	62.19	68.49	100.0	76.75	63.07	48	13.59	211.31	56.14	62.01	99.9	72.72	59.39
20	19.27	180.2	61.82	68.03	100.0	76.55	62.88	49	13.53	211.74	56.06	61.94	99.89	72.67	59.33
21	18.81	182.19	61.47	67.6	99.99	76.35	62.7	50	13.47	212.14	55.99	61.87	99.88	72.61	59.28
22	18.38	184.1	61.11	67.19	99.99	76.15	62.51	51	13.42	212.51	55.92	61.81	99.87	72.56	59.24
23	17.98	185.94	60.78	66.8	99.99	75.96	62.34	52	13.37	212.86	55.86	61.75	99.86	72.54	59.21
24	17.61	187.7	60.47	66.43	99.99	75.77	62.17	53	13.33	213.19	55.8	61.69	99.85	72.47	59.16
25	17.26	189.39	60.17	66.09	99.99	75.6	62.0	54	13.28	213.5	55.74	61.64	99.84	72.42	59.1
26	16.94	191.0	59.86	65.77	99.99	75.42	61.84	55	13.25	213.79	55.69	61.59	99.83	72.36	59.06
27	16.65	192.54	59.58	65.46	99.99	75.26	61.69	56	13.21	214.05	55.64	61.55	99.82	72.31	59.01
28	16.38	194.01	59.31	65.18	99.99	75.1	61.55	57	13.18	214.3	55.6	61.5	99.82	72.27	58.97
29	16.12	195.41	59.06	64.91	99.99	74.96	61.41	58	13.14	214.54	55.56	61.46	99.81	72.22	58.93
30	15.88	196.74	58.83	64.65	99.99	74.82	61.28	59	13.12	214.76	55.52	61.43	99.8	72.18	58.89

Table A.17.: 13C^{5+}

Step	$\hat{E}$	$\hat{T}$	P_1	P_2	P_T	P_S	P_{AS}	Step	$\hat{E}$	$\hat{T}$	P_1	P_2	P_T	P_S	P_{AS}
2	87.92	91.58	84.09	93.26	100.0	74.07	61.05	31	20.07	176.88	62.42	68.77	100.0	79.21	65.11
3	78.03	96.56	82.35	91.97	100.0	74.55	61.44	32	19.81	177.94	62.23	68.53	100.0	79.19	65.08
4	69.51	101.65	80.59	90.55	100.0	75.05	61.85	33	19.56	178.95	62.04	68.31	100.0	79.06	64.96
5	62.2	106.81	78.84	89.03	100.0	75.56	62.27	34	19.34	179.9	61.88	68.1	100.0	78.94	64.85
6	55.93	112.03	77.13	87.43	100.0	76.23	62.82	35	19.13	180.79	61.72	67.9	100.0	78.82	64.75
7	50.53	117.26	75.49	85.77	100.0	76.96	63.41	36	18.93	181.64	61.57	67.71	99.99	78.72	64.66
8	45.76	122.47	73.95	84.1	100.0	77.65	63.98	37	18.75	182.44	61.42	67.54	99.99	78.62	64.57
9	41.68	127.62	72.52	82.46	100.0	78.28	64.49	38	18.58	183.2	61.28	67.38	99.99	78.53	64.49
10	38.18	132.68	71.21	80.85	100.0	78.85	64.96	39	18.42	183.91	61.15	67.23	99.99	78.44	64.41
11	35.17	137.61	70.03	79.31	100.0	79.32	65.35	40	18.27	184.58	61.03	67.09	99.99	78.36	64.34
12	32.59	142.38	68.96	77.87	100.0	79.54	65.53	41	18.13	185.21	60.91	66.95	99.99	78.29	64.27
13	30.38	146.95	68.0	76.51	100.0	79.73	65.68	42	18.01	185.8	60.81	66.83	99.99	78.22	64.21
14	29.39	149.16	67.56	75.88	100.0	79.82	65.74	43	17.89	186.36	60.71	66.71	99.99	78.16	64.15
15	28.46	151.31	67.13	75.26	100.0	79.89	65.8	44	17.78	186.88	60.61	66.6	99.99	78.1	64.1
16	27.59	153.4	66.72	74.68	100.0	79.96	65.86	45	17.68	187.37	60.53	66.5	99.99	78.05	64.05
17	26.78	155.42	66.34	74.12	100.0	80.02	65.91	46	17.58	187.83	60.44	66.41	99.99	78.01	64.01
18	26.03	157.39	65.97	73.59	100.0	80.08	65.95	47	17.49	188.26	60.37	66.32	99.99	77.96	63.97
19	25.34	159.29	65.62	73.08	100.0	80.2	66.05	48	17.41	188.67	60.3	66.24	99.99	77.92	63.93
20	24.7	161.12	65.28	72.61	100.0	80.1	65.97	49	17.33	189.04	60.23	66.16	99.99	77.89	63.9
21	24.1	162.88	64.95	72.15	100.0	80.02	65.9	50	17.26	189.4	60.17	66.09	99.99	77.86	63.87
22	23.55	164.58	64.65	71.72	100.0	79.95	65.84	51	17.2	189.73	60.1	66.02	99.99	77.83	63.84
23	23.04	166.21	64.35	71.31	100.0	79.9	65.79	52	17.13	190.04	60.04	65.96	99.99	77.82	63.83
24	22.56	167.77	64.06	70.92	100.0	79.86	65.76	53	17.08	190.33	59.99	65.9	99.99	77.78	63.79
25	22.12	169.26	63.79	70.56	100.0	79.66	65.56	54	17.02	190.6	59.94	65.85	99.99	77.73	63.75
26	21.71	170.69	63.53	70.22	100.0	79.57	65.47	55	16.97	190.86	59.89	65.8	99.99	77.69	63.71
27	21.33	172.05	63.29	69.89	100.0	79.49	65.39	56	16.93	191.09	59.85	65.75	99.99	77.66	63.68
28	20.98	173.35	63.05	69.59	100.0	79.41	65.31	57	16.88	191.31	59.81	65.7	99.99	77.62	63.65
29	20.65	174.59	62.83	69.3	100.0	79.34	65.24	58	16.84	191.52	59.77	65.66	99.99	77.59	63.62
30	20.35	175.77	62.63	69.03	100.0	79.27	65.17	59	16.81	191.71	59.73	65.63	99.99	77.57	63.59

Table A.18.: 13C^{6+}

Step	$\hat{E}$	$\hat{T}$	P_1	P_2	P_T	P_S	P_{AS}	Step	$\hat{E}$	$\hat{T}$	P_1	P_2	P_T	P_S	P_{AS}
2	106.87	83.97	86.71	94.99	100.0	74.46	61.37	31	24.59	161.44	65.22	72.52	100.0	82.06	67.59
3	94.92	88.51	85.15	93.99	100.0	75.0	61.81	32	24.26	162.4	65.04	72.27	100.0	82.13	67.64
4	84.66	93.14	83.54	92.86	100.0	75.55	62.27	33	23.96	163.3	64.88	72.04	100.0	82.09	67.6
5	75.74	97.84	81.91	91.62	100.0	76.12	62.74	34	23.68	164.17	64.72	71.82	100.0	82.05	67.57
6	68.08	102.59	80.27	90.27	100.0	76.89	63.36	35	23.42	164.98	64.57	71.62	100.0	82.01	67.54
7	61.51	107.35	78.66	88.86	100.0	77.73	64.06	36	23.18	165.75	64.43	71.43	100.0	81.98	67.52
8	55.86	112.09	77.11	87.41	100.0	78.55	64.73	37	22.96	166.47	64.3	71.24	100.0	81.96	67.5
9	51.01	116.77	75.64	85.93	100.0	79.33	65.37	38	22.75	167.16	64.17	71.08	100.0	81.94	67.48
10	46.72	121.36	74.27	84.45	100.0	80.06	65.97	39	22.55	167.8	64.06	70.92	100.0	81.92	67.46
11	43.03	125.84	73.0	83.02	100.0	80.69	66.49	40	22.37	168.41	63.95	70.77	100.0	81.91	67.45
12	39.86	130.16	71.85	81.65	100.0	81.06	66.79	41	22.21	168.98	63.84	70.63	100.0	81.62	67.18
13	37.14	134.31	70.81	80.34	100.0	81.4	67.06	42	22.05	169.51	63.75	70.5	100.0	81.58	67.14
14	35.93	136.31	70.33	79.72	100.0	81.55	67.19	43	21.9	170.02	63.66	70.38	100.0	81.54	67.1
15	34.8	138.26	69.88	79.11	100.0	81.71	67.31	44	21.77	170.49	63.57	70.26	100.0	81.5	67.07
16	33.76	140.16	69.45	78.54	100.0	81.85	67.43	45	21.64	170.93	63.49	70.16	100.0	81.47	67.03
17	32.79	141.99	69.05	77.98	100.0	81.99	67.54	46	21.53	171.35	63.41	70.06	100.0	81.44	67.01
18	31.89	143.77	68.67	77.45	100.0	82.12	67.65	47	21.42	171.74	63.34	69.96	100.0	81.41	66.98
19	31.06	145.49	68.3	76.94	100.0	82.34	67.83	48	21.32	172.11	63.28	69.88	100.0	81.39	66.96
20	30.29	147.15	67.96	76.46	100.0	82.26	67.77	49	21.23	172.45	63.21	69.8	100.0	81.37	66.94
21	29.57	148.75	67.64	75.99	100.0	82.2	67.71	50	21.14	172.77	63.16	69.72	100.0	81.35	66.92
22	28.9	150.29	67.33	75.55	100.0	82.14	67.66	51	21.06	173.07	63.1	69.65	100.0	81.34	66.91
23	28.26	151.76	67.04	75.14	100.0	82.1	67.62	52	20.98	173.35	63.05	69.59	100.0	81.34	66.91
24	27.68	153.18	66.77	74.74	100.0	82.06	67.59	53	20.91	173.62	63.01	69.52	100.0	81.31	66.88
25	27.13	154.53	66.51	74.36	100.0	82.04	67.57	54	20.85	173.86	62.96	69.47	100.0	81.27	66.85
26	26.62	155.83	66.27	74.01	100.0	82.02	67.56	55	20.79	174.09	62.92	69.41	100.0	81.24	66.82
27	26.16	157.06	66.03	73.68	100.0	82.01	67.55	56	20.73	174.31	62.88	69.36	100.0	81.22	66.79
28	25.72	158.24	65.81	73.36	100.0	82.01	67.55	57	20.68	174.51	62.85	69.32	100.0	81.19	66.77
29	25.31	159.36	65.61	73.06	100.0	82.02	67.56	58	20.63	174.69	62.82	69.27	100.0	81.17	66.75
30	24.94	160.42	65.41	72.79	100.0	82.04	67.57	59	20.58	174.87	62.79	69.23	100.0	81.15	66.73

Table A.19.: N^{1+}

Step	$\hat{E}$	$\hat{T}$	P_1	P_2	P_T	P_S	P_{AS}	Step	$\hat{E}$	$\hat{T}$	P_1	P_2	P_T	P_S	P_{AS}
2	13.41	209.76	62.47	67.97	99.94	60.53	49.34	31	2.17	432.45	32.51	32.18	0.42	27.69	22.0
3	11.62	222.01	60.79	66.5	99.45	58.72	47.71	32	2.14	435.44	32.18	31.85	0.39	27.35	21.73
4	10.11	234.6	59.01	65.02	97.11	56.91	46.12	33	2.1	438.28	31.88	31.55	0.36	27.01	21.46
5	8.82	247.47	57.1	63.47	90.46	55.05	44.54	34	2.07	440.97	31.6	31.27	0.34	26.69	21.2
6	7.73	260.54	55.15	61.89	78.44	52.95	42.75	35	2.05	443.52	31.33	31.0	0.32	26.43	20.99
7	6.81	273.73	53.08	60.23	62.57	50.61	40.77	36	2.02	445.92	31.07	30.74	0.3	26.2	20.81
8	6.04	286.95	50.94	58.43	45.97	48.4	38.92	37	2.0	448.2	30.83	30.5	0.28	25.98	20.63
9	5.38	300.1	48.8	56.53	31.59	46.37	37.23	38	1.97	450.35	30.6	30.28	0.27	25.78	20.47
10	4.83	313.1	46.69	54.47	20.79	44.22	35.45	39	1.95	452.38	30.39	30.07	0.26	25.58	20.31
11	4.37	325.84	44.69	52.2	13.39	41.96	33.58	40	1.93	454.3	30.19	29.88	0.24	25.4	20.17
12	3.97	338.26	42.86	49.91	8.6	40.18	32.13	41	1.92	456.1	30.01	29.7	0.23	25.22	20.03
13	3.64	350.28	41.22	47.44	5.59	38.39	30.66	42	1.9	457.8	29.84	29.53	0.22	25.06	19.89
14	3.49	356.12	40.47	46.21	4.54	37.49	29.93	43	1.88	459.4	29.68	29.37	0.22	24.9	19.77
15	3.35	361.84	39.79	44.9	3.72	36.59	29.19	44	1.87	460.9	29.53	29.22	0.21	24.76	19.65
16	3.23	367.43	39.16	43.63	3.07	35.69	28.46	45	1.86	462.32	29.39	29.09	0.2	24.62	19.54
17	3.11	372.88	38.6	42.34	2.55	35.01	27.92	46	1.85	463.64	29.27	28.96	0.2	24.49	19.44
18	3.01	378.19	38.1	41.06	2.13	34.35	27.38	47	1.83	464.89	29.15	28.84	0.19	24.37	19.34
19	2.91	383.35	37.63	39.83	1.8	33.69	26.85	48	1.82	466.06	29.04	28.73	0.19	24.25	19.25
20	2.82	388.36	37.2	38.68	1.53	33.03	26.31	49	1.82	467.15	28.93	28.63	0.18	24.14	19.16
21	2.73	393.22	36.8	37.59	1.31	32.38	25.78	50	1.81	468.18	28.84	28.53	0.18	24.04	19.08
22	2.65	397.92	36.43	36.57	1.13	31.74	25.27	51	1.8	469.14	28.75	28.45	0.18	23.95	19.01
23	2.58	402.46	36.03	35.68	0.99	31.12	24.76	52	1.79	470.04	28.66	28.36	0.17	23.86	18.94
24	2.52	406.82	35.48	35.14	0.86	30.51	24.27	53	1.78	470.89	28.58	28.28	0.17	23.78	18.87
25	2.45	411.0	34.97	34.64	0.76	30.09	23.93	54	1.78	471.67	28.5	28.2	0.17	23.7	18.81
26	2.4	415.01	34.5	34.16	0.68	29.65	23.58	55	1.77	472.41	28.43	28.13	0.16	23.62	18.75
27	2.34	418.84	34.05	33.72	0.61	29.23	23.24	56	1.77	473.1	28.37	28.07	0.16	23.56	18.69
28	2.3	422.49	33.63	33.3	0.55	28.82	22.91	57	1.76	473.75	28.3	28.01	0.16	23.49	18.64
29	2.25	425.98	33.23	32.9	0.5	28.43	22.6	58	1.75	474.35	28.25	27.95	0.16	23.43	18.59
30	2.21	429.29	32.86	32.53	0.46	28.05	22.29	59	1.75	474.91	28.19	27.9	0.16	23.37	18.55

Table A.20.: N^{2+}

Step	$\dot{E}$	$\dot{T}$	P_1	P_2	P_T	P_S	P_{AS}	Step	$\dot{E}$	$\dot{T}$	P_1	P_2	P_T	P_S	P_{AS}
2	31.51	148.23	71.58	79.37	100.0	69.74	57.43	31	5.65	294.52	49.69	57.33	37.31	50.27	40.4
3	27.58	156.55	70.07	77.24	100.0	69.65	57.34	32	5.56	296.38	49.39	57.06	35.33	49.97	40.15
4	24.23	165.07	68.7	75.26	100.0	69.26	56.96	33	5.47	298.15	49.12	56.82	33.52	49.65	39.88
5	21.37	173.76	67.41	73.49	100.0	68.62	56.35	34	5.4	299.82	48.85	56.58	31.87	49.34	39.63
6	18.93	182.57	66.18	71.9	99.99	67.85	55.63	35	5.32	301.41	48.58	56.32	30.35	49.05	39.39
7	16.84	191.44	64.96	70.5	99.99	66.94	54.79	36	5.26	302.9	48.33	56.07	28.97	48.77	39.16
8	15.06	200.3	63.76	69.22	99.99	65.9	53.85	37	5.2	304.31	48.1	55.84	27.71	48.5	38.94
9	13.52	209.1	62.56	68.06	99.95	64.75	52.79	38	5.14	305.65	47.88	55.63	26.55	48.25	38.73
10	12.2	217.76	61.38	67.0	99.73	63.47	51.64	39	5.08	306.9	47.67	55.43	25.5	48.02	38.54
11	11.08	226.23	60.21	66.01	98.98	62.08	50.38	40	5.03	308.09	47.48	55.24	24.54	47.79	38.35
12	10.13	234.44	59.03	65.04	97.16	60.86	49.34	41	4.99	309.2	47.3	55.07	23.66	47.58	38.18
13	9.3	242.34	57.87	64.09	93.75	59.66	48.32	42	4.95	310.25	47.14	54.91	22.86	47.38	38.01
14	8.94	246.16	57.3	63.63	91.38	59.05	47.8	43	4.91	311.23	46.98	54.75	22.13	47.2	37.86
15	8.6	249.88	56.76	63.19	88.61	58.44	47.28	44	4.87	312.16	46.84	54.61	21.45	47.02	37.71
16	8.29	253.5	56.25	62.77	85.47	57.83	46.76	45	4.83	313.03	46.7	54.48	20.84	46.85	37.58
17	8.0	257.02	55.7	62.33	82.12	57.22	46.24	46	4.8	313.84	46.58	54.36	20.28	46.7	37.45
18	7.74	260.43	55.17	61.91	78.56	56.61	45.72	47	4.77	314.61	46.46	54.24	19.76	46.55	37.33
19	7.49	263.74	54.66	61.5	74.85	56.02	45.22	48	4.75	315.32	46.35	54.13	19.28	46.42	37.21
20	7.26	266.92	54.14	61.09	71.07	55.39	44.68	49	4.72	316.0	46.24	54.0	18.85	46.29	37.11
21	7.05	270.0	53.66	60.69	67.29	54.76	44.15	50	4.7	316.62	46.14	53.88	18.45	46.17	37.01
22	6.86	272.96	53.2	60.33	63.56	54.15	43.64	51	4.67	317.21	46.04	53.77	18.08	46.06	36.92
23	6.68	275.8	52.73	59.94	59.93	53.55	43.13	52	4.65	317.76	45.95	53.67	17.74	45.96	36.84
24	6.51	278.53	52.29	59.57	56.45	52.96	42.63	53	4.63	318.28	45.87	53.57	17.43	45.85	36.75
25	6.36	281.15	51.87	59.21	53.13	52.39	42.15	54	4.62	318.76	45.79	53.49	17.15	45.75	36.67
26	6.22	283.65	51.47	58.88	50.0	52.05	41.87	55	4.6	319.21	45.72	53.4	16.88	45.66	36.59
27	6.09	286.04	51.1	58.56	47.07	51.66	41.55	56	4.58	319.63	45.65	53.32	16.64	45.57	36.52
28	5.96	288.32	50.71	58.22	44.33	51.29	41.25	57	4.57	320.03	45.59	53.25	16.41	45.49	36.45
29	5.85	290.49	50.35	57.91	41.8	50.94	40.95	58	4.56	320.39	45.53	53.18	16.2	45.42	36.38
30	5.75	292.56	50.01	57.61	39.46	50.6	40.67	59	4.54	320.74	45.48	53.12	16.01	45.35	36.33

Table A.21.: N^{3+}

Step	$\dot{E}$	$\dot{T}$	P_1	P_2	P_T	P_S	P_{AS}	Step	$\dot{E}$	$\dot{T}$	P_1	P_2	P_T	P_S	P_{AS}
2	50.52	121.72	78.13	87.29	100.0	71.95	59.28	31	9.73	238.09	58.53	64.63	95.82	63.37	51.36
3	44.44	128.4	76.19	85.21	100.0	72.16	59.44	32	9.58	239.55	58.3	64.44	95.17	63.17	51.18
4	39.24	135.24	74.41	83.11	100.0	72.35	59.59	33	9.44	240.95	58.09	64.26	94.49	62.92	50.97
5	34.81	142.2	72.81	81.05	100.0	72.52	59.72	34	9.31	242.27	57.88	64.1	93.79	62.68	50.77
6	31.01	149.24	71.39	79.1	100.0	72.7	59.86	35	9.19	243.51	57.69	63.95	93.07	62.45	50.57
7	27.68	156.32	70.11	77.29	100.0	72.79	59.93	36	9.08	244.69	57.52	63.8	92.35	62.23	50.39
8	24.84	163.39	68.96	75.64	100.0	72.77	59.9	37	8.97	245.8	57.35	63.67	91.62	62.03	50.22
9	22.42	170.4	67.9	74.14	100.0	72.24	59.38	38	8.87	246.85	57.19	63.54	90.9	61.84	50.06
10	20.34	177.3	66.91	72.83	100.0	71.79	58.94	39	8.78	247.84	57.05	63.43	90.18	61.66	49.9
11	18.57	184.03	65.97	71.66	99.99	71.25	58.42	40	8.7	248.77	56.92	63.32	89.48	61.48	49.76
12	17.03	190.55	65.08	70.63	99.99	70.55	57.78	41	8.62	249.65	56.79	63.21	88.79	61.32	49.62
13	15.72	196.82	64.24	69.71	99.99	69.81	57.1	42	8.55	250.47	56.67	63.12	88.12	61.17	49.49
14	15.14	199.85	63.82	69.28	99.99	69.43	56.75	43	8.48	251.24	56.56	63.03	87.47	61.03	49.37
15	14.6	202.79	63.43	68.88	99.99	69.05	56.4	44	8.42	251.97	56.46	62.95	86.84	60.9	49.26
16	14.09	205.67	63.03	68.5	99.97	68.66	56.04	45	8.36	252.65	56.36	62.87	86.24	60.77	49.15
17	13.62	208.45	62.65	68.14	99.95	68.26	55.68	46	8.31	253.29	56.27	62.8	85.66	60.66	49.06
18	13.19	211.15	62.29	67.8	99.92	67.87	55.32	47	8.26	253.9	56.19	62.73	85.1	60.55	48.97
19	12.78	213.76	61.95	67.48	99.87	67.51	54.99	48	8.21	254.46	56.1	62.66	84.58	60.45	48.88
20	12.41	216.29	61.58	67.17	99.79	67.05	54.58	49	8.17	254.99	56.02	62.59	84.09	60.36	48.8
21	12.07	218.72	61.24	66.88	99.68	66.6	54.17	50	8.13	255.48	55.94	62.53	83.62	60.27	48.73
22	11.75	221.06	60.92	66.61	99.53	66.15	53.78	51	8.09	255.94	55.87	62.47	83.18	60.19	48.66
23	11.45	223.31	60.62	66.36	99.33	65.73	53.39	52	8.05	256.38	55.8	62.41	82.76	60.13	48.6
24	11.18	225.47	60.32	66.11	99.08	65.31	53.02	53	8.02	256.78	55.73	62.36	82.36	60.04	48.53
25	10.92	227.53	60.02	65.85	98.78	64.9	52.66	54	7.99	257.16	55.68	62.31	81.98	59.96	48.46
26	10.69	229.51	59.73	65.61	98.42	64.51	52.31	55	7.96	257.51	55.62	62.27	81.63	59.88	48.4
27	10.47	231.39	59.46	65.39	98.01	64.36	52.2	56	7.94	257.84	55.57	62.23	81.29	59.81	48.34
28	10.27	233.19	59.2	65.18	97.54	64.1	51.98	57	7.91	258.15	55.52	62.19	80.98	59.75	48.28
29	10.08	234.91	58.97	64.98	97.01	63.85	51.76	58	7.89	258.44	55.47	62.15	80.68	59.69	48.23
30	9.9	236.54	58.74	64.8	96.44	63.6	51.55	59	7.87	258.71	55.43	62.12	80.4	59.63	48.18

Table A.22.: N^{4+}

Step	$\hat{E}$	$\hat{T}$	P_1	P_2	P_T	P_S	P_{AS}	Step	$\hat{E}$	$\hat{T}$	P_1	P_2	P_T	P_S	P_{AS}
2	69.97	106.08	83.26	92.0	100.0	73.07	60.21	31	14.14	205.37	63.08	68.54	99.98	71.45	58.33
3	61.79	111.82	81.31	90.34	100.0	73.41	60.49	32	13.93	206.61	62.9	68.37	99.97	71.31	58.2
4	54.77	117.7	79.39	88.55	100.0	73.77	60.78	33	13.73	207.79	62.74	68.22	99.96	71.08	58.0
5	48.63	123.67	77.55	86.68	100.0	74.12	61.06	34	13.55	208.91	62.59	68.08	99.95	70.87	57.81
6	43.38	129.7	75.84	84.8	100.0	74.56	61.41	35	13.38	209.97	62.45	67.95	99.94	70.68	57.63
7	38.89	135.76	74.28	82.95	100.0	74.99	61.76	36	13.22	210.97	62.31	67.82	99.92	70.49	57.47
8	35.04	141.8	72.9	81.17	100.0	75.34	62.04	37	13.07	211.91	62.19	67.71	99.91	70.31	57.31
9	31.74	147.78	71.67	79.49	100.0	75.6	62.25	38	12.93	212.8	62.07	67.6	99.89	70.15	57.16
10	28.87	153.67	70.57	77.94	100.0	75.76	62.38	39	12.8	213.64	61.96	67.5	99.87	69.99	57.02
11	26.39	159.41	69.6	76.55	100.0	75.8	62.41	40	12.69	214.43	61.85	67.4	99.85	69.85	56.89
12	24.27	164.97	68.72	75.28	100.0	75.54	62.15	41	12.58	215.17	61.74	67.31	99.83	69.71	56.77
13	22.45	170.3	67.92	74.16	100.0	75.23	61.85	42	12.47	215.87	61.64	67.22	99.8	69.59	56.66
14	21.64	172.88	67.54	73.66	100.0	75.07	61.69	43	12.38	216.52	61.55	67.14	99.78	69.47	56.55
15	20.89	175.39	67.18	73.18	100.0	74.91	61.52	44	12.29	217.14	61.46	67.07	99.75	69.36	56.46
16	20.19	177.83	66.83	72.73	100.0	74.73	61.36	45	12.21	217.72	61.38	67.0	99.73	69.26	56.36
17	19.55	180.2	66.5	72.31	100.0	74.56	61.19	46	12.13	218.26	61.31	66.94	99.7	69.16	56.28
18	18.95	182.5	66.19	71.91	99.99	74.38	61.02	47	12.06	218.77	61.24	66.88	99.67	69.08	56.2
19	18.39	184.72	65.88	71.55	99.99	74.25	60.88	48	11.99	219.24	61.17	66.82	99.65	69.0	56.13
20	17.88	186.86	65.58	71.2	99.99	73.97	60.63	49	11.93	219.69	61.11	66.77	99.62	68.92	56.06
21	17.4	188.93	65.3	70.88	99.99	73.7	60.39	50	11.88	220.11	61.05	66.72	99.59	68.85	56.0
22	16.95	190.92	65.03	70.58	99.99	73.44	60.15	51	11.82	220.5	61.0	66.68	99.57	68.79	55.94
23	16.54	192.83	64.77	70.29	99.99	73.19	59.91	52	11.77	220.87	60.95	66.63	99.54	68.75	55.9
24	16.16	194.66	64.53	70.02	99.99	72.94	59.69	53	11.73	221.21	60.9	66.59	99.51	68.67	55.84
25	15.8	196.41	64.29	69.76	99.99	72.7	59.47	54	11.68	221.53	60.86	66.56	99.49	68.6	55.77
26	15.47	198.09	64.06	69.53	99.99	72.47	59.26	55	11.65	221.83	60.82	66.52	99.46	68.54	55.71
27	15.17	199.69	63.84	69.3	99.99	72.25	59.06	56	11.61	222.11	60.78	66.49	99.44	68.48	55.66
28	14.89	201.22	63.64	69.09	99.99	72.03	58.86	57	11.57	222.37	60.75	66.46	99.42	68.42	55.61
29	14.62	202.67	63.44	68.89	99.99	71.83	58.68	58	11.54	222.61	60.71	66.43	99.4	68.37	55.56
30	14.37	204.05	63.26	68.71	99.98	71.64	58.5	59	11.51	222.84	60.68	66.41	99.37	68.33	55.52

Table A.23.: N^{5+}

Step	$\hat{E}$	$\hat{T}$	P_1	P_2	P_T	P_S	P_{AS}	Step	$\hat{E}$	$\hat{T}$	P_1	P_2	P_T	P_S	P_{AS}
2	89.82	95.45	86.92	94.74	100.0	73.73	60.77	31	18.72	183.43	66.05	71.76	99.99	76.64	62.86
3	79.36	100.57	85.15	93.49	100.0	74.17	61.12	32	18.44	184.53	65.9	71.58	99.99	76.57	62.8
4	70.4	105.8	83.35	92.08	100.0	74.62	61.49	33	18.19	185.57	65.76	71.41	99.99	76.41	62.66
5	62.72	111.12	81.55	90.55	100.0	75.08	61.86	34	17.95	186.55	65.63	71.25	99.99	76.26	62.52
6	56.14	116.48	79.78	88.92	100.0	75.67	62.35	35	17.73	187.48	65.5	71.11	99.99	76.12	62.39
7	50.38	121.86	78.09	87.24	100.0	76.3	62.86	36	17.53	188.36	65.38	70.97	99.99	75.99	62.27
8	45.43	127.23	76.52	85.57	100.0	76.88	63.33	37	17.34	189.19	65.27	70.84	99.99	75.87	62.16
9	41.19	132.53	75.09	83.93	100.0	77.39	63.75	38	17.16	189.98	65.16	70.72	99.99	75.75	62.06
10	37.56	137.75	73.8	82.35	100.0	77.83	64.11	39	17.0	190.72	65.06	70.61	99.99	75.64	61.96
11	34.44	142.83	72.68	80.87	100.0	78.15	64.37	40	16.84	191.41	64.96	70.5	99.99	75.54	61.87
12	31.76	147.74	71.68	79.51	100.0	78.26	64.45	41	16.7	192.07	64.87	70.4	99.99	75.45	61.78
13	29.43	152.47	70.79	78.25	100.0	78.32	64.5	42	16.57	192.68	64.79	70.31	99.99	75.36	61.71
14	28.38	154.74	70.38	77.68	100.0	78.34	64.51	43	16.45	193.26	64.72	70.22	99.99	75.28	61.63
15	27.41	156.96	70.0	77.14	100.0	78.35	64.52	44	16.33	193.8	64.64	70.14	99.99	75.21	61.57
16	26.51	159.12	69.64	76.62	100.0	78.36	64.52	45	16.23	194.31	64.58	70.07	99.99	75.14	61.5
17	25.67	161.21	69.31	76.13	100.0	78.35	64.52	46	16.13	194.79	64.51	70.0	99.99	75.07	61.45
18	24.9	163.24	68.98	75.67	100.0	78.34	64.51	47	16.04	195.24	64.46	69.93	99.99	75.02	61.39
19	24.18	165.2	68.68	75.23	100.0	78.28	64.41	48	15.95	195.66	64.4	69.87	99.99	74.96	61.34
20	23.51	167.1	68.39	74.83	100.0	78.12	64.25	49	15.88	196.05	64.34	69.82	99.99	74.92	61.3
21	22.9	168.92	68.12	74.44	100.0	77.95	64.1	50	15.8	196.42	64.29	69.76	99.99	74.87	61.26
22	22.33	170.68	67.86	74.08	100.0	77.8	63.95	51	15.73	196.77	64.24	69.71	99.99	74.83	61.22
23	21.8	172.36	67.61	73.76	100.0	77.64	63.81	52	15.67	197.09	64.2	69.67	99.99	74.81	61.2
24	21.3	173.98	67.38	73.45	100.0	77.5	63.67	53	15.61	197.39	64.16	69.62	99.99	74.76	61.15
25	20.85	175.53	67.16	73.16	100.0	77.35	63.54	54	15.56	197.67	64.12	69.58	99.99	74.71	61.11
26	20.43	177.01	66.95	72.88	100.0	77.22	63.41	55	15.5	197.94	64.08	69.55	99.99	74.66	61.06
27	20.03	178.42	66.75	72.63	100.0	77.09	63.29	56	15.46	198.18	64.05	69.51	99.99	74.61	61.02
28	19.67	179.77	66.56	72.38	100.0	76.97	63.18	57	15.41	198.41	64.02	69.48	99.99	74.57	60.98
29	19.33	181.05	66.39	72.16	100.0	76.85	63.06	58	15.37	198.63	63.99	69.45	99.99	74.54	60.95
30	19.01	182.27	66.22	71.95	99.99	76.74	62.96	59	15.33	198.83	63.96	69.42	99.99	74.5	60.92

Table A.24.: N^{6+}

Step	$\hat{E}$	$\hat{T}$	P_1	P_2	P_T	P_S	P_{AS}	Step	$\hat{E}$	$\hat{T}$	P_1	P_2	P_T	P_S	P_{AS}
2	109.81	87.62	89.49	96.35	100.0	74.18	61.14	31	23.4	167.43	68.34	74.76	100.0	80.08	65.87
3	97.24	92.29	87.97	95.43	100.0	74.68	61.55	32	23.07	168.42	68.19	74.55	100.0	80.08	65.86
4	86.34	97.05	86.36	94.36	100.0	75.19	61.97	33	22.75	169.36	68.05	74.35	100.0	79.96	65.75
5	76.95	101.89	84.7	93.14	100.0	75.72	62.4	34	22.46	170.25	67.92	74.17	100.0	79.85	65.65
6	68.9	106.77	83.02	91.8	100.0	76.42	62.97	35	22.19	171.09	67.8	74.0	100.0	79.74	65.56
7	61.99	111.67	81.36	90.38	100.0	77.18	63.6	36	21.94	171.89	67.68	73.85	100.0	79.65	65.47
8	56.07	116.54	79.76	88.91	100.0	77.91	64.19	37	21.71	172.64	67.57	73.7	100.0	79.56	65.39
9	50.88	121.36	78.24	87.4	100.0	78.58	64.75	38	21.5	173.35	67.47	73.57	100.0	79.47	65.31
10	46.42	126.09	76.84	85.93	100.0	79.2	65.26	39	21.29	174.01	67.37	73.44	100.0	79.4	65.24
11	42.59	130.7	75.57	84.49	100.0	79.72	65.68	40	21.11	174.64	67.28	73.32	100.0	79.32	65.18
12	39.3	135.15	74.43	83.13	100.0	79.98	65.89	41	20.93	175.23	67.2	73.21	100.0	79.26	65.12
13	36.48	139.43	73.42	81.86	100.0	80.22	66.08	42	20.77	175.79	67.12	73.11	100.0	79.2	65.06
14	35.22	141.49	72.97	81.26	100.0	80.32	66.17	43	20.62	176.31	67.05	73.01	100.0	79.14	65.01
15	34.06	143.5	72.53	80.68	100.0	80.42	66.24	44	20.48	176.8	66.98	72.92	100.0	79.09	64.96
16	32.97	145.45	72.13	80.13	100.0	80.51	66.32	45	20.35	177.26	66.91	72.84	100.0	79.04	64.92
17	31.97	147.35	71.75	79.61	100.0	80.59	66.38	46	20.23	177.69	66.85	72.76	100.0	79.0	64.88
18	31.04	149.18	71.4	79.12	100.0	80.67	66.44	47	20.12	178.1	66.79	72.68	100.0	78.96	64.84
19	30.16	150.96	71.07	78.65	100.0	80.82	66.57	48	20.02	178.48	66.74	72.62	100.0	78.93	64.81
20	29.33	152.67	70.75	78.19	100.0	80.73	66.49	49	19.92	178.83	66.69	72.55	100.0	78.9	64.78
21	28.57	154.32	70.46	77.78	100.0	80.66	66.43	50	19.83	179.16	66.65	72.49	100.0	78.87	64.76
22	27.86	155.91	70.18	77.39	100.0	80.59	66.37	51	19.75	179.47	66.6	72.44	100.0	78.85	64.73
23	27.21	157.43	69.93	77.02	100.0	80.54	66.33	52	19.67	179.77	66.56	72.38	100.0	78.84	64.73
24	26.6	158.89	69.68	76.67	100.0	80.5	66.29	53	19.6	180.04	66.53	72.33	100.0	78.8	64.69
25	26.03	160.29	69.45	76.34	100.0	80.47	66.27	54	19.53	180.29	66.49	72.29	100.0	78.76	64.65
26	25.51	161.63	69.24	76.03	100.0	80.45	66.25	55	19.47	180.53	66.46	72.25	100.0	78.72	64.62
27	25.02	162.9	69.04	75.74	100.0	80.44	66.24	56	19.41	180.75	66.43	72.21	100.0	78.69	64.58
28	24.57	164.12	68.85	75.47	100.0	80.25	66.04	57	19.35	180.96	66.4	72.17	100.0	78.66	64.55
29	24.15	165.28	68.67	75.21	100.0	80.19	65.98	58	19.3	181.16	66.37	72.14	100.0	78.63	64.53
30	23.76	166.38	68.5	74.98	100.0	80.13	65.93	59	19.25	181.34	66.35	72.1	100.0	78.61	64.5

Table A.25.: N^{7+}

Step	$\hat{E}$	$\hat{T}$	P_1	P_2	P_T	P_S	P_{AS}	Step	$\hat{E}$	$\hat{T}$	P_1	P_2	P_T	P_S	P_{AS}
2	0.0	81.54	91.32	97.32	100.0	74.5	61.41	31	28.22	155.11	70.32	77.59	100.0	82.3	67.78
3	115.17	85.86	90.03	96.66	100.0	75.04	61.85	32	27.81	156.02	70.16	77.36	100.0	82.36	67.84
4	102.41	90.26	88.64	95.85	100.0	75.6	62.31	33	27.44	156.88	70.02	77.16	100.0	82.32	67.8
5	91.43	94.74	87.16	94.9	100.0	76.18	62.79	34	27.09	157.7	69.88	76.96	100.0	82.28	67.77
6	81.88	99.25	85.61	93.83	100.0	76.95	63.42	35	26.77	158.47	69.75	76.77	100.0	82.25	67.74
7	73.7	103.77	84.06	92.65	100.0	77.81	64.13	36	26.47	159.2	69.63	76.6	100.0	82.22	67.72
8	66.68	108.27	82.51	91.38	100.0	78.64	64.81	37	26.19	159.89	69.52	76.44	100.0	82.2	67.7
9	60.65	112.71	81.01	90.07	100.0	79.44	65.46	38	25.93	160.54	69.41	76.28	100.0	82.18	67.68
10	55.47	117.08	79.58	88.74	100.0	80.19	66.08	39	25.69	161.16	69.32	76.14	100.0	82.16	67.66
11	50.92	121.32	78.25	87.41	100.0	80.84	66.61	40	25.47	161.73	69.22	76.01	100.0	82.15	67.65
12	47.01	125.43	77.03	86.14	100.0	81.22	66.92	41	25.26	162.27	69.14	75.89	100.0	82.14	67.65
13	43.65	129.36	75.93	84.91	100.0	81.57	67.21	42	25.07	162.78	69.06	75.77	100.0	82.14	67.64
14	42.15	131.26	75.41	84.31	100.0	81.74	67.35	43	24.89	163.26	68.98	75.66	100.0	82.13	67.64
15	40.76	133.11	74.94	83.75	100.0	81.9	67.47	44	24.72	163.71	68.91	75.56	100.0	82.13	67.64
16	39.47	134.91	74.49	83.21	100.0	82.05	67.6	45	24.57	164.14	68.85	75.47	100.0	81.83	67.35
17	38.28	136.65	74.06	82.68	100.0	82.2	67.72	46	24.42	164.53	68.79	75.38	100.0	81.8	67.33
18	37.17	138.34	73.67	82.18	100.0	82.34	67.83	47	24.29	164.9	68.73	75.3	100.0	81.78	67.3
19	36.14	139.97	73.3	81.7	100.0	82.57	68.02	48	24.16	165.25	68.68	75.22	100.0	81.76	67.28
20	35.19	141.55	72.95	81.24	100.0	82.49	67.96	49	24.05	165.58	68.62	75.15	100.0	81.74	67.26
21	34.3	143.06	72.63	80.8	100.0	82.43	67.9	50	23.94	165.88	68.58	75.09	100.0	81.72	67.25
22	33.48	144.52	72.32	80.39	100.0	82.37	67.86	51	23.84	166.17	68.53	75.02	100.0	81.71	67.23
23	32.72	145.92	72.03	80.0	100.0	82.33	67.82	52	23.74	166.44	68.49	74.97	100.0	81.72	67.24
24	32.01	147.26	71.77	79.64	100.0	82.3	67.79	53	23.66	166.69	68.45	74.91	100.0	81.68	67.21
25	31.35	148.55	71.52	79.29	100.0	82.27	67.77	54	23.58	166.92	68.42	74.86	100.0	81.65	67.18
26	30.74	149.78	71.29	78.96	100.0	82.26	67.76	55	23.5	167.14	68.39	74.82	100.0	81.62	67.15
27	30.16	150.95	71.07	78.65	100.0	82.25	67.75	56	23.43	167.34	68.36	74.77	100.0	81.6	67.12
28	29.62	152.07	70.86	78.35	100.0	82.25	67.75	57	23.37	167.53	68.33	74.73	100.0	81.57	67.1
29	29.11	153.14	70.67	78.07	100.0	82.26	67.76	58	23.3	167.71	68.3	74.7	100.0	81.55	67.08
30	28.65	154.15	70.49	77.82	100.0	82.28	67.77	59	23.25	167.88	68.27	74.66	100.0	81.53	67.06

A. POSITIONS IN THE ET-MATRICES AND DETECTION EFFICIENCIES

Table A.26.: O^{1+}

Step	$\hat{E}$	$\hat{T}$	P_1	P_2	P_T	P_S	P_{AS}	Step	$\hat{E}$	$\hat{T}$	P_1	P_2	P_T	P_S	P_{AS}
2	12.92	223.97	59.59	65.39	99.56	58.21	47.29	31	3.06	466.64	29.54	29.23	0.23	24.57	19.51
3	11.3	237.08	57.16	63.3	97.6	56.34	45.66	32	3.03	469.94	29.22	28.92	0.21	24.26	19.26
4	9.92	250.55	54.68	61.2	91.56	54.4	44.01	33	3.01	473.08	28.93	28.63	0.2	23.95	19.01
5	8.76	264.32	52.2	59.14	80.07	52.22	42.15	34	2.98	476.06	28.65	28.35	0.19	23.66	18.78
6	7.79	278.33	49.8	57.12	63.88	49.77	40.07	35	2.96	478.88	28.38	28.08	0.18	23.39	18.56
7	6.99	292.49	47.48	55.13	46.64	47.54	38.21	36	2.94	481.55	28.13	27.83	0.17	23.12	18.35
8	6.32	306.73	45.33	53.09	31.63	45.33	36.38	37	2.92	484.08	27.9	27.6	0.16	22.93	18.2
9	5.76	320.95	43.37	51.05	20.26	42.97	34.42	38	2.9	486.47	27.68	27.38	0.15	22.74	18.04
10	5.29	335.07	41.66	48.87	12.56	40.74	32.59	39	2.89	488.73	27.48	27.18	0.15	22.56	17.9
11	4.88	349.01	40.22	46.51	7.69	38.78	30.99	40	2.87	490.85	27.29	27.0	0.14	22.39	17.76
12	4.55	362.67	39.01	44.13	4.77	36.73	29.31	41	2.86	492.86	27.11	26.82	0.13	22.23	17.63
13	4.27	375.97	38.11	41.55	3.04	34.83	27.77	42	2.85	494.75	26.95	26.66	0.13	22.07	17.51
14	4.15	382.46	37.73	40.27	2.45	34.03	27.12	43	2.83	496.53	26.8	26.51	0.12	21.93	17.4
15	4.03	388.84	37.45	38.89	1.99	33.23	26.48	44	2.82	498.21	26.66	26.37	0.12	21.79	17.29
16	3.93	395.09	37.19	37.58	1.63	32.44	25.83	45	2.81	499.78	26.53	26.24	0.12	21.67	17.19
17	3.83	401.2	36.59	36.63	1.35	31.64	25.19	46	2.8	501.26	26.4	26.11	0.11	21.55	17.09
18	3.74	407.13	35.96	35.79	1.12	30.86	24.56	47	2.79	502.64	26.29	26.0	0.11	21.43	17.0
19	3.66	412.88	35.36	35.02	0.95	30.19	24.01	48	2.79	503.95	26.18	25.89	0.11	21.33	16.92
20	3.58	418.43	34.7	34.36	0.8	29.59	23.53	49	2.78	505.17	26.08	25.79	0.11	21.23	16.84
21	3.51	423.78	34.08	33.74	0.69	29.01	23.07	50	2.77	506.31	25.98	25.69	0.1	21.13	16.76
22	3.45	428.93	33.5	33.17	0.6	28.44	22.61	51	2.76	507.38	25.89	25.6	0.1	21.05	16.69
23	3.39	433.87	32.95	32.62	0.52	27.89	22.17	52	2.76	508.39	25.8	25.52	0.1	20.96	16.63
24	3.34	438.61	32.42	32.1	0.46	27.35	21.73	53	2.75	509.33	25.72	25.44	0.1	20.89	16.56
25	3.29	443.17	31.93	31.61	0.41	26.83	21.31	54	2.75	510.21	25.65	25.36	0.1	20.81	16.51
26	3.24	447.54	31.48	31.16	0.36	26.33	20.91	55	2.74	511.03	25.58	25.3	0.1	20.74	16.45
27	3.2	451.72	31.05	30.73	0.33	25.97	20.62	56	2.74	511.8	25.52	25.23	0.09	20.68	16.4
28	3.16	455.72	30.63	30.32	0.3	25.6	20.33	57	2.73	0.0	25.46	25.17	0.09	20.62	16.35
29	3.12	459.53	30.24	29.93	0.27	25.24	20.04	58	2.73	0.0	25.41	25.12	0.09	20.56	16.31
30	3.09	463.18	29.88	29.57	0.25	24.9	19.77	59	2.73	0.0	25.35	25.07	0.09	20.51	16.27

Table A.27.: O^{2+}

Step	$\hat{E}$	$\hat{T}$	P_1	P_2	P_T	P_S	P_{AS}	Step	$\hat{E}$	$\hat{T}$	P_1	P_2	P_T	P_S	P_{AS}
2	29.33	157.9	71.18	78.05	100.0	68.94	56.76	31	5.99	314.9	44.17	51.9	24.62	46.56	37.34
3	25.77	166.85	69.67	75.99	100.0	68.47	56.31	32	5.91	316.92	43.9	51.62	23.09	46.2	37.04
4	22.75	176.03	68.16	74.03	100.0	67.75	55.64	33	5.84	318.83	43.64	51.35	21.71	45.82	36.73
5	20.16	185.37	66.56	72.15	99.99	66.92	54.85	34	5.77	320.64	43.41	51.1	20.47	45.46	36.43
6	17.93	194.83	64.91	70.37	99.99	65.93	53.94	35	5.71	322.36	43.19	50.82	19.34	45.12	36.15
7	16.04	204.34	63.2	68.68	99.99	64.78	52.9	36	5.65	323.98	42.98	50.56	18.33	44.8	35.89
8	14.4	213.84	61.46	67.05	99.92	63.5	51.73	37	5.6	325.52	42.79	50.32	17.41	44.49	35.63
9	13.01	223.26	59.72	65.5	99.61	62.07	50.44	38	5.55	326.96	42.62	50.09	16.58	44.2	35.39
10	11.83	232.54	58.0	64.02	98.6	60.66	49.19	39	5.5	328.33	42.45	49.88	15.83	43.92	35.16
11	10.81	241.6	56.33	62.6	96.14	59.39	48.11	40	5.46	329.62	42.3	49.69	15.15	43.66	34.95
12	9.94	250.38	54.71	61.23	91.67	58.0	46.93	41	5.42	330.83	42.15	49.5	14.54	43.42	34.74
13	9.2	258.83	53.18	59.95	85.26	56.56	45.71	42	5.38	331.97	42.02	49.33	13.98	43.35	34.7
14	8.87	262.92	52.44	59.34	81.47	55.84	45.1	43	5.35	333.04	41.89	49.17	13.47	43.2	34.57
15	8.57	266.9	51.75	58.77	77.35	55.11	44.48	44	5.32	334.05	41.77	49.02	13.01	43.05	34.45
16	8.29	270.78	51.09	58.22	73.0	54.38	43.86	45	5.29	335.0	41.66	48.88	12.59	42.91	34.33
17	8.03	274.55	50.44	57.67	68.53	53.66	43.24	46	5.26	335.89	41.56	48.75	12.21	42.77	34.22
18	7.8	278.21	49.82	57.13	64.02	52.93	42.63	47	5.24	336.72	41.47	48.63	11.86	42.65	34.12
19	7.58	281.75	49.23	56.63	59.58	52.23	42.04	48	5.21	337.5	41.38	48.51	11.54	42.54	34.03
20	7.38	285.18	48.66	56.14	55.34	51.64	41.54	49	5.19	338.23	41.3	48.38	11.25	42.43	33.94
21	7.2	288.48	48.12	55.68	51.36	51.11	41.1	50	5.17	338.92	41.23	48.25	10.98	42.33	33.86
22	7.03	291.66	47.61	55.24	47.61	50.59	40.68	51	5.15	339.56	41.16	48.14	10.74	42.23	33.78
23	6.88	294.72	47.13	54.81	44.09	50.08	40.26	52	5.13	340.16	41.1	48.03	10.51	42.15	33.71
24	6.73	297.65	46.67	54.38	40.83	49.59	39.85	53	5.12	340.73	41.04	47.93	10.31	42.06	33.64
25	6.6	300.47	46.25	53.97	37.82	49.11	39.45	54	5.1	341.25	40.99	47.84	10.12	41.97	33.57
26	6.48	303.17	45.85	53.59	35.07	48.65	39.07	55	5.09	341.75	40.94	47.75	9.95	41.89	33.51
27	6.36	305.74	45.47	53.24	32.55	48.2	38.69	56	5.07	342.21	40.89	47.67	9.79	41.82	33.44
28	6.26	308.2	45.11	52.87	30.27	47.76	38.33	57	5.06	342.64	40.85	47.6	9.64	41.75	33.39
29	6.16	310.55	44.78	52.52	28.19	47.34	37.99	58	5.05	343.04	40.81	47.53	9.5	41.69	33.34
30	6.07	312.78	44.47	52.2	26.32	46.94	37.66	59	5.04	343.42	40.77	47.46	9.38	41.63	33.29

Table A.28.: O^{3+}

Step	$\dot{E}$	$\dot{T}$	P_1	P_2	P_T	P_S	P_{AS}	Step	$\dot{E}$	$\dot{T}$	P_1	P_2	P_T	P_S	P_{AS}
2	46.67	129.32	76.83	85.57	100.0	71.42	58.83	31	9.58	254.28	54.03	60.65	88.92	60.1	48.61
3	41.15	136.52	75.2	83.56	100.0	71.55	58.93	32	9.45	255.85	53.73	60.41	87.73	59.85	48.39
4	36.45	143.89	73.7	81.57	100.0	71.67	59.01	33	9.32	257.34	53.45	60.18	86.53	59.55	48.14
5	32.39	151.39	72.31	79.64	100.0	71.75	59.08	34	9.2	258.75	53.19	59.96	85.33	59.27	47.9
6	28.87	158.98	70.99	77.79	100.0	71.8	59.11	35	9.09	260.09	52.95	59.76	84.15	59.0	47.68
7	25.86	166.61	69.72	76.05	100.0	71.49	58.8	36	8.99	261.35	52.72	59.57	82.99	58.74	47.46
8	23.3	174.22	68.46	74.41	100.0	71.01	58.34	37	8.9	262.54	52.51	59.4	81.85	58.5	47.26
9	21.12	181.76	67.19	72.87	100.0	70.45	57.8	38	8.81	263.66	52.31	59.23	80.73	58.28	47.07
10	19.22	189.17	65.91	71.42	99.99	69.8	57.19	39	8.73	264.72	52.13	59.08	79.66	58.06	46.88
11	17.6	196.4	64.63	70.09	99.99	69.06	56.5	40	8.66	265.72	51.95	58.94	78.62	57.86	46.71
12	16.22	203.39	63.37	68.85	99.99	68.16	55.68	41	8.59	266.65	51.79	58.8	77.62	57.67	46.55
13	15.01	210.11	62.15	67.69	99.96	67.22	54.83	42	8.52	267.54	51.64	58.68	76.66	57.49	46.4
14	14.48	213.36	61.55	67.13	99.93	66.74	54.39	43	8.46	268.37	51.5	58.56	75.75	57.32	46.26
15	13.98	216.52	60.98	66.6	99.87	66.25	53.95	44	8.41	269.15	51.37	58.45	74.88	57.16	46.12
16	13.53	219.59	60.41	66.09	99.78	65.76	53.51	45	8.35	269.88	51.24	58.35	74.05	57.01	46.0
17	13.11	222.57	59.85	65.61	99.65	65.27	53.06	46	8.3	270.56	51.13	58.25	73.26	56.88	45.88
18	12.72	225.46	59.32	65.15	99.45	64.77	52.61	47	8.26	271.21	51.02	58.16	72.51	56.75	45.77
19	12.36	228.26	58.82	64.72	99.19	64.3	52.19	48	8.22	271.81	50.92	58.08	71.81	56.62	45.67
20	12.02	230.96	58.3	64.27	98.85	63.76	51.7	49	8.18	272.37	50.82	57.99	71.14	56.51	45.57
21	11.71	233.56	57.81	63.85	98.41	63.47	51.47	50	8.14	272.9	50.73	57.91	70.51	56.41	45.48
22	11.42	236.07	57.34	63.46	97.86	63.08	51.14	51	8.11	273.4	50.64	57.84	69.92	56.31	45.4
23	11.15	238.47	56.91	63.09	97.2	62.71	50.82	52	8.08	273.86	50.56	57.77	69.36	56.23	45.33
24	10.89	240.78	56.49	62.73	96.44	62.34	50.51	53	8.05	274.3	50.48	57.71	68.84	56.13	45.25
25	10.66	242.99	56.07	62.37	95.58	61.98	50.21	54	8.02	274.7	50.42	57.65	68.35	56.03	45.17
26	10.45	245.1	55.67	62.04	94.63	61.64	49.92	55	8.0	275.08	50.35	57.59	67.89	55.95	45.09
27	10.25	247.12	55.3	61.73	93.6	61.31	49.63	56	7.97	275.43	50.29	57.54	67.46	55.86	45.02
28	10.06	249.05	54.95	61.43	92.5	60.99	49.36	57	7.95	275.76	50.23	57.49	67.05	55.79	44.96
29	9.89	250.88	54.62	61.15	91.34	60.68	49.1	58	7.93	276.07	50.18	57.44	66.67	55.72	44.9
30	9.73	252.62	54.31	60.89	90.15	60.38	48.85	59	7.91	276.36	50.13	57.4	66.32	55.65	44.84

Table A.29.: O^{4+}

Step	$\dot{E}$	$\dot{T}$	P_1	P_2	P_T	P_S	P_{AS}	Step	$\dot{E}$	$\dot{T}$	P_1	P_2	P_T	P_S	P_{AS}
2	64.59	112.48	81.48	90.37	100.0	72.66	59.87	31	13.57	219.27	60.47	66.15	99.79	68.37	55.64
3	57.05	118.66	79.64	88.61	100.0	72.96	60.11	32	13.38	220.6	60.22	65.93	99.74	68.17	55.46
4	50.53	124.99	77.92	86.8	100.0	73.25	60.35	33	13.2	221.87	59.98	65.72	99.68	67.91	55.23
5	44.96	131.42	76.34	84.98	100.0	73.54	60.57	34	13.04	223.06	59.76	65.53	99.62	67.67	55.01
6	40.19	137.92	74.9	83.17	100.0	73.88	60.85	35	12.88	224.2	59.55	65.35	99.55	67.44	54.81
7	36.12	144.45	73.59	81.42	100.0	74.19	61.1	36	12.74	225.27	59.36	65.18	99.47	67.22	54.61
8	32.61	150.96	72.39	79.75	100.0	74.41	61.27	37	12.61	226.27	59.18	65.03	99.39	67.01	54.43
9	29.55	157.41	71.26	78.16	100.0	74.52	61.35	38	12.49	227.23	59.01	64.88	99.3	66.82	54.26
10	26.93	163.75	70.2	76.68	100.0	74.52	61.35	39	12.37	228.12	58.85	64.74	99.2	66.64	54.09
11	24.7	169.93	69.17	75.32	100.0	74.17	60.98	40	12.27	228.97	58.68	64.6	99.11	66.47	53.94
12	22.78	175.91	68.18	74.06	100.0	73.74	60.57	41	12.17	229.76	58.53	64.47	99.01	66.31	53.8
13	21.15	181.65	67.21	72.89	100.0	73.28	60.14	42	12.08	230.51	58.38	64.35	98.91	66.16	53.67
14	20.41	184.42	66.73	72.34	99.99	73.04	59.91	43	11.99	231.21	58.25	64.23	98.81	66.02	53.54
15	19.72	187.12	66.27	71.81	99.99	72.8	59.68	44	11.91	231.87	58.13	64.12	98.71	65.89	53.43
16	19.08	189.74	65.8	71.31	99.99	72.55	59.45	45	11.84	232.49	58.01	64.03	98.6	65.95	53.5
17	18.5	192.29	65.36	70.83	99.99	72.3	59.21	46	11.77	233.07	57.9	63.93	98.5	65.86	53.43
18	17.95	194.75	64.93	70.38	99.99	72.05	58.97	47	11.71	233.62	57.8	63.85	98.4	65.79	53.36
19	17.45	197.14	64.5	69.96	99.99	71.83	58.77	48	11.64	234.13	57.7	63.76	98.29	65.72	53.3
20	16.98	199.44	64.09	69.55	99.99	71.49	58.46	49	11.59	234.6	57.61	63.69	98.19	65.65	53.25
21	16.55	201.65	63.7	69.16	99.99	71.16	58.16	50	11.54	235.05	57.53	63.62	98.09	65.59	53.19
22	16.14	203.79	63.3	68.78	99.99	70.84	57.87	51	11.49	235.47	57.45	63.55	98.0	65.53	53.15
23	15.76	205.83	62.93	68.43	99.98	70.52	57.59	52	11.44	235.86	57.38	63.49	97.91	65.5	53.12
24	15.41	207.8	62.58	68.09	99.97	70.21	57.31	53	11.4	236.23	57.32	63.43	97.82	65.43	53.06
25	15.09	209.68	62.24	67.77	99.96	69.92	57.04	54	11.36	236.57	57.25	63.38	97.73	65.37	53.0
26	14.78	211.47	61.9	67.45	99.95	69.63	56.78	55	11.32	236.89	57.19	63.33	97.65	65.31	52.95
27	14.5	213.19	61.58	67.16	99.93	69.36	56.53	56	11.29	237.19	57.14	63.28	97.57	65.26	52.91
28	14.24	214.82	61.29	66.88	99.9	69.09	56.29	57	11.26	237.47	57.09	63.24	97.49	65.21	52.86
29	14.0	216.38	61.01	66.62	99.87	68.84	56.06	58	11.23	237.73	57.04	63.2	97.42	65.16	52.82
30	13.78	217.86	60.75	66.38	99.84	68.6	55.85	59	11.2	237.97	57.0	63.16	97.35	65.12	52.79

Table A.30.: O^{5+}

Step	$\hat{E}$	$\hat{T}$	P_1	P_2	P_T	P_S	P_{AS}	Step	$\hat{E}$	$\hat{T}$	P_1	P_2	P_T	P_S	P_{AS}
2	82.82	101.06	85.19	93.46	100.0	73.41	60.49	31	17.74	195.75	64.75	70.2	99.99	74.16	60.7
3	73.21	106.56	83.36	92.01	100.0	73.81	60.82	32	17.49	196.93	64.53	69.99	99.99	74.06	60.6
4	64.98	112.19	81.57	90.46	100.0	74.21	61.14	33	17.26	198.05	64.34	69.79	99.99	73.87	60.43
5	57.92	117.91	79.86	88.83	100.0	74.62	61.48	34	17.05	199.1	64.15	69.61	99.99	73.69	60.27
6	51.78	123.68	78.26	87.17	100.0	75.13	61.9	35	16.85	200.1	63.98	69.44	99.99	73.52	60.12
7	46.54	129.48	76.8	85.52	100.0	75.67	62.33	36	16.67	201.05	63.81	69.27	99.99	73.36	59.98
8	42.05	135.25	75.47	83.91	100.0	76.13	62.71	37	16.5	201.94	63.64	69.11	99.99	73.22	59.85
9	38.21	140.97	74.27	82.34	100.0	76.52	63.03	38	16.33	202.78	63.49	68.96	99.99	73.08	59.72
10	34.92	146.59	73.18	80.87	100.0	76.83	63.28	39	16.18	203.57	63.34	68.82	99.99	72.95	59.61
11	32.05	152.07	72.19	79.47	100.0	77.02	63.43	40	16.04	204.32	63.2	68.69	99.99	72.83	59.5
12	29.57	157.37	71.27	78.17	100.0	77.01	63.41	41	15.91	205.02	63.08	68.57	99.98	72.71	59.4
13	27.44	162.45	70.42	76.98	100.0	76.95	63.36	42	15.79	205.68	62.96	68.45	99.98	72.61	59.3
14	26.49	164.91	70.0	76.42	100.0	76.91	63.32	43	15.68	206.3	62.85	68.35	99.98	72.51	59.21
15	25.61	167.3	69.6	75.89	100.0	76.72	63.11	44	15.57	206.88	62.74	68.25	99.98	72.42	59.13
16	24.8	169.62	69.22	75.39	100.0	76.62	63.01	45	15.48	207.43	62.64	68.15	99.98	72.34	59.06
17	24.05	171.87	68.85	74.91	100.0	76.51	62.9	46	15.39	207.94	62.55	68.07	99.97	72.26	58.99
18	23.35	174.06	68.49	74.44	100.0	76.4	62.78	47	15.3	208.42	62.47	67.98	99.97	72.19	58.92
19	22.71	176.17	68.14	74.0	100.0	76.34	62.71	48	15.22	208.87	62.39	67.91	99.97	72.12	58.86
20	22.11	178.21	67.79	73.59	100.0	76.12	62.51	49	15.15	209.29	62.31	67.83	99.97	72.06	58.81
21	21.56	180.17	67.45	73.19	100.0	75.91	62.32	50	15.08	209.69	62.23	67.76	99.96	72.01	58.76
22	21.04	182.05	67.14	72.81	100.0	75.71	62.13	51	15.02	210.06	62.16	67.7	99.96	71.96	58.71
23	20.55	183.87	66.82	72.45	99.99	75.5	61.94	52	14.96	210.4	62.1	67.64	99.96	71.93	58.68
24	20.1	185.6	66.52	72.11	99.99	75.31	61.76	53	14.91	210.72	62.04	67.58	99.96	71.86	58.62
25	19.68	187.27	66.25	71.78	99.99	75.12	61.59	54	14.86	211.03	61.98	67.53	99.95	71.8	58.57
26	19.29	188.86	65.96	71.48	99.99	74.94	61.42	55	14.81	211.31	61.93	67.48	99.95	71.75	58.52
27	18.94	190.37	65.69	71.19	99.99	74.77	61.26	56	14.77	211.57	61.88	67.44	99.95	71.7	58.47
28	18.6	191.82	65.44	70.92	99.99	74.6	61.11	57	14.73	211.82	61.84	67.39	99.95	71.65	58.43
29	18.29	193.2	65.21	70.67	99.99	74.45	60.97	58	14.69	212.05	61.79	67.35	99.94	71.6	58.39
30	18.0	194.51	64.97	70.43	99.99	74.3	60.83	59	14.65	212.26	61.75	67.32	99.94	71.56	58.35

Table A.31.: O^{6+}

Step	$\hat{E}$	$\hat{T}$	P_1	P_2	P_T	P_S	P_{AS}	Step	$\hat{E}$	$\hat{T}$	P_1	P_2	P_T	P_S	P_{AS}
2	101.41	92.65	88.06	95.45	100.0	73.91	60.91	31	22.01	178.56	67.73	73.51	100.0	78.01	64.07
3	89.7	97.66	86.34	94.3	100.0	74.37	61.29	32	21.71	179.63	67.54	73.3	100.0	77.97	64.02
4	79.62	102.78	84.61	93.02	100.0	74.85	61.68	33	21.43	180.64	67.38	73.1	100.0	77.83	63.89
5	71.0	107.98	82.9	91.63	100.0	75.33	62.08	34	21.17	181.6	67.22	72.91	100.0	77.7	63.77
6	63.61	113.23	81.25	90.16	100.0	75.97	62.6	35	20.92	182.5	67.06	72.72	99.99	77.57	63.66
7	57.24	118.5	79.69	88.66	100.0	76.65	63.16	36	20.69	183.36	66.91	72.55	99.99	77.45	63.55
8	51.72	123.74	78.25	87.16	100.0	77.28	63.67	37	20.47	184.16	66.77	72.39	99.99	77.34	63.45
9	47.0	128.93	76.93	85.68	100.0	77.86	64.15	38	20.28	184.92	66.64	72.24	99.99	77.24	63.36
10	42.95	134.03	75.74	84.25	100.0	78.37	64.56	39	20.09	185.64	66.52	72.1	99.99	77.14	63.27
11	39.48	138.99	74.67	82.88	100.0	78.77	64.89	40	19.92	186.32	66.41	71.97	99.99	77.06	63.19
12	36.5	143.8	73.71	81.6	100.0	78.94	65.02	41	19.76	186.95	66.3	71.84	99.99	76.97	63.12
13	33.95	148.4	72.85	80.4	100.0	79.07	65.13	42	19.61	187.55	66.2	71.73	99.99	76.9	63.05
14	32.78	150.63	72.44	79.83	100.0	79.13	65.17	43	19.48	188.11	66.09	71.62	99.99	76.83	62.99
15	31.7	152.79	72.06	79.29	100.0	79.17	65.2	44	19.35	188.63	66.0	71.52	99.99	76.76	62.93
16	30.69	154.9	71.7	78.77	100.0	79.21	65.23	45	19.23	189.13	65.91	71.43	99.99	76.7	62.87
17	29.76	156.94	71.34	78.28	100.0	79.24	65.26	46	19.12	189.59	65.83	71.34	99.99	76.65	62.82
18	28.89	158.92	71.0	77.81	100.0	79.27	65.28	47	19.02	190.03	65.75	71.26	99.99	76.6	62.78
19	28.09	160.83	70.69	77.36	100.0	79.35	65.34	48	18.92	190.43	65.68	71.18	99.99	76.55	62.73
20	27.35	162.67	70.39	76.93	100.0	79.25	65.25	49	18.83	190.82	65.62	71.11	99.99	76.51	62.7
21	26.66	164.45	70.08	76.53	100.0	79.16	65.18	50	18.75	191.17	65.55	71.04	99.99	76.48	62.66
22	26.02	166.16	69.79	76.15	100.0	78.95	64.96	51	18.67	191.51	65.5	70.98	99.99	76.44	62.63
23	25.43	167.8	69.52	75.78	100.0	78.82	64.84	52	18.6	191.82	65.44	70.92	99.99	76.43	62.62
24	24.89	169.37	69.26	75.44	100.0	78.7	64.73	53	18.54	192.11	65.39	70.87	99.99	76.38	62.57
25	24.38	170.88	69.02	75.12	100.0	78.59	64.62	54	18.47	192.39	65.35	70.82	99.99	76.33	62.53
26	23.9	172.32	68.78	74.81	100.0	78.48	64.51	55	18.42	192.64	65.3	70.77	99.99	76.29	62.49
27	23.47	173.69	68.55	74.52	100.0	78.37	64.41	56	18.36	192.88	65.26	70.72	99.99	76.25	62.45
28	23.06	175.0	68.33	74.25	100.0	78.28	64.32	57	18.31	193.1	65.22	70.68	99.99	76.21	62.42
29	22.68	176.25	68.12	73.99	100.0	78.18	64.23	58	18.27	193.31	65.19	70.65	99.99	76.18	62.39
30	22.33	177.44	67.92	73.74	100.0	78.09	64.14	59	18.22	193.51	65.15	70.61	99.99	76.15	62.36

Table A.32.: O^{7+}

Step	$\hat{E}$	$\hat{T}$	P_1	P_2	P_T	P_S	P_{AS}	Step	$\hat{E}$	$\hat{T}$	P_1	P_2	P_T	P_S	P_{AS}
2	119.68	86.13	90.25	96.74	100.0	74.27	61.21	31	26.34	165.3	69.94	76.34	100.0	80.77	66.47
3	106.25	90.76	88.71	95.85	100.0	74.78	61.63	32	25.98	166.28	69.77	76.12	100.0	80.77	66.46
4	94.54	95.49	87.08	94.81	100.0	75.31	62.06	33	25.64	167.21	69.61	75.91	100.0	80.66	66.36
5	84.3	100.29	85.45	93.66	100.0	75.85	62.51	34	25.33	168.09	69.47	75.72	100.0	80.56	66.27
6	75.53	105.14	83.83	92.4	100.0	76.57	63.1	35	25.04	168.92	69.33	75.54	100.0	80.46	66.18
7	68.01	110.0	82.26	91.07	100.0	77.36	63.74	36	24.77	169.71	69.21	75.37	100.0	80.37	66.1
8	61.57	114.84	80.77	89.7	100.0	78.11	64.36	37	24.52	170.45	69.09	75.21	100.0	80.29	66.03
9	55.99	119.62	79.37	88.34	100.0	78.82	64.94	38	24.29	171.15	68.97	75.06	100.0	80.21	65.96
10	51.17	124.32	78.1	86.99	100.0	79.47	65.48	39	24.07	171.81	68.86	74.92	100.0	80.14	65.89
11	47.03	128.89	76.94	85.69	100.0	80.03	65.93	40	23.87	172.43	68.76	74.79	100.0	80.08	65.83
12	43.48	133.32	75.9	84.44	100.0	80.32	66.18	41	23.68	173.02	68.66	74.66	100.0	80.01	65.78
13	40.44	137.56	74.97	83.27	100.0	80.59	66.39	42	23.51	173.57	68.57	74.55	100.0	79.96	65.73
14	39.08	139.6	74.55	82.71	100.0	80.71	66.49	43	23.35	174.08	68.48	74.44	100.0	79.91	65.68
15	37.82	141.6	74.15	82.18	100.0	80.83	66.58	44	23.2	174.57	68.4	74.34	100.0	79.86	65.64
16	36.66	143.53	73.77	81.66	100.0	80.94	66.67	45	23.06	175.02	68.33	74.24	100.0	79.82	65.6
17	35.57	145.41	73.41	81.17	100.0	81.04	66.75	46	22.93	175.45	68.26	74.15	100.0	79.78	65.56
18	34.57	147.23	73.06	80.7	100.0	81.13	66.83	47	22.8	175.85	68.19	74.07	100.0	79.75	65.53
19	33.64	148.99	72.74	80.25	100.0	81.3	66.97	48	22.69	176.22	68.13	73.99	100.0	79.72	65.5
20	32.75	150.69	72.43	79.82	100.0	81.22	66.9	49	22.59	176.57	68.07	73.92	100.0	79.69	65.47
21	31.93	152.32	72.15	79.41	100.0	81.15	66.83	50	22.49	176.9	68.01	73.85	100.0	79.67	65.45
22	31.16	153.89	71.87	79.02	100.0	81.08	66.78	51	22.4	177.21	67.96	73.79	100.0	79.65	65.43
23	30.45	155.4	71.61	78.65	100.0	81.04	66.74	52	22.32	177.49	67.91	73.73	100.0	79.64	65.43
24	29.8	156.85	71.35	78.3	100.0	81.0	66.71	53	22.24	177.76	67.86	73.68	100.0	79.6	65.39
25	29.19	158.24	71.12	77.97	100.0	80.97	66.68	54	22.17	178.01	67.82	73.63	100.0	79.57	65.35
26	28.62	159.56	70.9	77.65	100.0	80.95	66.67	55	22.1	178.25	67.78	73.58	100.0	79.53	65.32
27	28.09	160.82	70.69	77.36	100.0	80.94	66.66	56	22.03	178.47	67.74	73.53	100.0	79.5	65.29
28	27.61	162.03	70.49	77.08	100.0	80.95	66.66	57	21.98	178.67	67.71	73.49	100.0	79.47	65.27
29	27.15	163.18	70.3	76.81	100.0	80.96	66.66	58	21.92	178.87	67.67	73.45	100.0	79.45	65.24
30	26.73	164.27	70.11	76.57	100.0	80.97	66.68	59	21.87	179.04	67.64	73.42	100.0	79.42	65.22

Table A.33.: O^{8+}

Step	$\hat{E}$	$\hat{T}$	P_1	P_2	P_T	P_S	P_{AS}	Step	$\hat{E}$	$\hat{T}$	P_1	P_2	P_T	P_S	P_{AS}
2	0.0	80.87	91.96	97.61	100.0	74.54	61.44	31	30.79	154.68	71.73	78.82	100.0	82.51	67.96
3	122.64	85.2	90.56	96.91	100.0	75.08	61.89	32	30.37	155.59	71.57	78.6	100.0	82.57	68.01
4	109.33	89.62	89.1	96.08	100.0	75.65	62.35	33	29.97	156.46	71.42	78.39	100.0	82.53	67.98
5	97.82	94.11	87.56	95.13	100.0	76.23	62.83	34	29.61	157.27	71.28	78.2	100.0	82.49	67.95
6	87.65	98.64	86.01	94.06	100.0	77.02	63.47	35	29.27	158.05	71.15	78.01	100.0	82.46	67.92
7	78.93	103.17	84.48	92.91	100.0	77.89	64.19	36	28.95	158.78	71.03	77.84	100.0	82.43	67.89
8	71.45	107.69	83.0	91.71	100.0	78.73	64.88	37	28.66	159.47	70.91	77.67	100.0	82.41	67.87
9	65.04	112.15	81.59	90.47	100.0	79.54	65.54	38	28.38	160.12	70.8	77.52	100.0	82.39	67.86
10	59.53	116.53	80.26	89.22	100.0	80.3	66.17	39	28.13	160.73	70.7	77.38	100.0	82.38	67.84
11	54.73	120.79	79.05	88.01	100.0	80.97	66.72	40	27.9	161.31	70.61	77.24	100.0	82.36	67.83
12	50.6	124.91	77.94	86.82	100.0	81.36	67.04	41	27.68	161.85	70.52	77.12	100.0	82.36	67.83
13	47.06	128.86	76.94	85.7	100.0	81.73	67.34	42	27.47	162.36	70.44	77.0	100.0	82.35	67.82
14	45.48	130.76	76.49	85.16	100.0	81.9	67.48	43	27.28	162.84	70.36	76.89	100.0	82.35	67.82
15	44.01	132.62	76.06	84.64	100.0	82.07	67.62	44	27.11	163.29	70.28	76.79	100.0	82.35	67.82
16	42.66	134.42	75.65	84.14	100.0	82.23	67.75	45	26.94	163.72	70.21	76.69	100.0	82.35	67.82
17	41.4	136.17	75.27	83.65	100.0	82.38	67.87	46	26.79	164.11	70.14	76.6	100.0	82.35	67.82
18	40.23	137.86	74.91	83.19	100.0	82.53	67.99	47	26.65	164.49	70.08	76.52	100.0	82.36	67.82
19	39.15	139.5	74.57	82.74	100.0	82.77	68.19	48	26.52	164.83	70.02	76.44	100.0	82.37	67.83
20	38.14	141.08	74.25	82.32	100.0	82.7	68.13	49	26.39	165.16	69.96	76.37	100.0	82.07	67.56
21	37.21	142.6	73.95	81.91	100.0	82.63	68.07	50	26.28	165.47	69.91	76.3	100.0	82.06	67.54
22	36.34	144.07	73.66	81.52	100.0	82.58	68.03	51	26.18	165.75	69.86	76.24	100.0	82.05	67.53
23	35.54	145.47	73.39	81.16	100.0	82.54	67.99	52	26.08	166.02	69.81	76.18	100.0	82.05	67.53
24	34.79	146.82	73.14	80.81	100.0	82.51	67.97	53	25.98	166.27	69.77	76.12	100.0	82.02	67.5
25	34.1	148.11	72.9	80.47	100.0	82.48	67.95	54	25.9	166.5	69.73	76.07	100.0	81.99	67.47
26	33.46	149.34	72.68	80.16	100.0	82.47	67.93	55	25.82	166.72	69.7	76.02	100.0	81.96	67.45
27	32.84	150.51	72.47	79.86	100.0	82.46	67.93	56	25.75	166.92	69.66	75.98	100.0	81.94	67.42
28	32.27	151.63	72.27	79.58	100.0	82.46	67.93	57	25.68	167.12	69.63	75.93	100.0	81.91	67.4
29	31.74	152.7	72.08	79.31	100.0	82.47	67.93	58	25.61	167.29	69.6	75.9	100.0	81.89	67.38
30	31.25	153.71	71.91	79.06	100.0	82.49	67.94	59	25.55	167.46	69.57	75.86	100.0	81.87	67.36

Table A.34.: Ne^{1+}

Step	$\hat{E}$	$\hat{T}$	P_1	P_2	P_T	P_S	P_{AS}	Step	$\hat{E}$	$\hat{T}$	P_1	P_2	P_T	P_S	P_{AS}
2	10.25	249.74	55.06	61.56	96.38	54.23	43.89	31	1.63	0.0	17.96	17.74	0.12	19.92	15.8
3	8.77	264.5	52.94	59.89	88.71	51.97	41.97	32	1.61	0.0	17.72	17.5	0.11	19.66	15.59
4	7.54	279.72	50.74	58.07	74.57	49.43	39.81	33	1.58	0.0	17.5	17.28	0.1	19.41	15.39
5	6.52	295.31	48.37	56.02	56.36	47.01	37.79	34	1.56	0.0	17.28	17.06	0.1	19.17	15.2
6	5.68	311.18	45.93	53.71	38.39	44.61	35.8	35	1.54	0.0	17.08	16.86	0.09	18.94	15.02
7	4.97	327.23	43.23	50.75	24.01	41.98	33.62	36	1.53	0.0	16.89	16.68	0.09	18.72	14.84
8	4.38	343.33	40.31	47.01	14.2	39.62	31.68	37	1.51	0.0	16.72	16.51	0.08	18.51	14.68
9	3.89	359.34	37.21	42.5	8.23	37.35	29.82	38	1.49	0.0	16.56	16.35	0.08	18.32	14.52
10	3.5	375.14	33.96	37.3	4.91	34.96	27.88	39	1.48	0.0	16.41	16.2	0.08	18.13	14.37
11	3.17	390.56	30.32	31.18	2.99	33.1	26.38	40	1.47	0.0	16.27	16.06	0.07	17.99	14.26
12	2.89	405.53	27.84	27.55	1.88	31.16	24.8	41	1.45	0.0	16.14	15.93	0.07	17.85	14.15
13	2.66	420.22	26.29	26.0	1.21	29.41	23.39	42	1.44	0.0	16.02	15.81	0.07	17.72	14.05
14	2.55	427.44	25.57	25.29	0.99	28.63	22.76	43	1.43	0.0	15.91	15.7	0.07	17.59	13.95
15	2.45	434.56	24.88	24.6	0.81	27.86	22.14	44	1.42	0.0	15.81	15.6	0.06	17.48	13.86
16	2.36	441.54	24.24	23.96	0.67	27.09	21.52	45	1.41	0.0	15.71	15.5	0.06	17.37	13.77
17	2.28	448.34	23.61	23.34	0.56	26.32	20.91	46	1.4	0.0	15.61	15.4	0.06	17.26	13.69
18	2.2	454.97	23.03	22.77	0.47	25.71	20.42	47	1.4	0.0	15.52	15.32	0.06	17.17	13.61
19	2.13	461.42	22.48	22.22	0.41	25.12	19.95	48	1.39	0.0	15.44	15.24	0.05	17.08	13.54
20	2.07	467.68	21.96	21.7	0.35	24.54	19.48	49	1.38	0.0	15.36	15.16	0.05	16.99	13.47
21	2.01	473.75	21.47	21.22	0.31	23.96	19.02	50	1.38	0.0	15.29	15.09	0.05	16.91	13.41
22	1.96	479.62	21.02	20.77	0.27	23.4	18.57	51	1.37	0.0	15.23	15.03	0.05	16.83	13.35
23	1.91	485.28	20.58	20.33	0.24	22.89	18.16	52	1.37	0.0	15.16	14.97	0.05	16.76	13.29
24	1.87	490.74	20.18	19.93	0.22	22.46	17.82	53	1.36	0.0	15.11	14.91	0.05	16.7	13.24
25	1.82	496.0	19.8	19.56	0.19	22.04	17.48	54	1.36	0.0	15.05	14.86	0.05	16.64	13.19
26	1.79	501.05	19.45	19.21	0.18	21.64	17.16	55	1.35	0.0	15.0	14.81	0.05	16.58	13.14
27	1.75	505.89	19.11	18.87	0.16	21.25	16.85	56	1.35	0.0	14.96	14.76	0.05	16.52	13.1
28	1.72	510.53	18.79	18.56	0.15	20.87	16.55	57	1.34	0.0	14.92	14.72	0.05	16.47	13.06
29	1.69	0.0	18.49	18.26	0.14	20.51	16.26	58	1.34	0.0	14.88	14.68	0.05	16.42	13.02
30	1.66	0.0	18.22	17.99	0.13	20.2	16.02	59	1.34	0.0	14.84	14.65	0.05	16.38	12.99

Table A.35.: Ne^{2+}

Step	$\hat{E}$	$\hat{T}$	P_1	P_2	P_T	P_S	P_{AS}	Step	$\hat{E}$	$\hat{T}$	P_1	P_2	P_T	P_S	P_{AS}
2	26.05	175.99	68.12	74.02	100.0	66.81	54.89	31	4.08	352.54	38.55	44.51	10.36	40.18	32.11
3	22.55	185.94	65.95	71.57	99.99	65.89	54.04	32	4.01	354.81	38.13	43.91	9.58	39.84	31.83
4	19.58	196.13	63.87	69.37	99.99	64.84	53.06	33	3.95	356.97	37.72	43.31	8.89	39.49	31.55
5	17.07	206.53	61.91	67.45	99.99	63.62	51.95	34	3.9	359.0	37.28	42.62	8.32	39.16	31.28
6	14.94	217.08	60.08	65.77	99.95	62.21	50.67	35	3.84	360.93	36.87	41.97	7.81	38.84	31.02
7	13.14	227.71	58.35	64.26	99.73	60.6	49.21	36	3.8	362.75	36.48	41.35	7.36	38.54	30.77
8	11.62	238.36	56.73	62.9	98.9	59.05	47.87	37	3.75	364.47	36.12	40.78	6.96	38.25	30.54
9	10.34	248.94	55.18	61.65	96.64	57.54	46.58	38	3.71	366.09	35.78	40.24	6.6	37.98	30.32
10	9.25	259.38	53.67	60.47	92.04	55.91	45.2	39	3.67	367.61	35.47	39.74	6.28	37.73	30.11
11	8.33	269.6	52.21	59.29	84.64	54.18	43.73	40	3.64	369.05	35.17	39.27	5.99	37.48	29.91
12	7.55	279.53	50.76	58.09	74.78	52.32	42.15	41	3.61	370.41	34.9	38.82	5.73	37.25	29.73
13	6.9	289.09	49.32	56.85	63.77	50.58	40.69	42	3.58	371.68	34.64	38.41	5.49	37.04	29.55
14	6.62	293.72	48.61	56.23	58.26	49.88	40.11	43	3.55	372.88	34.41	38.03	5.28	36.83	29.38
15	6.36	298.23	47.94	55.64	52.89	49.18	39.52	44	3.52	374.0	34.18	37.67	5.09	36.64	29.23
16	6.11	302.63	47.31	55.08	47.76	48.47	38.94	45	3.5	375.06	33.98	37.33	4.92	36.46	29.08
17	5.89	306.9	46.61	54.39	42.96	47.77	38.36	46	3.48	376.05	33.76	36.97	4.76	36.29	28.94
18	5.69	311.05	45.95	53.73	38.52	47.08	37.79	47	3.45	376.97	33.53	36.59	4.62	36.25	28.91
19	5.5	315.07	45.29	53.05	34.49	46.41	37.23	48	3.44	377.84	33.31	36.23	4.49	36.14	28.82
20	5.32	318.94	44.63	52.32	30.85	45.7	36.65	49	3.42	378.66	33.12	35.9	4.38	36.04	28.74
21	5.16	322.68	44.0	51.63	27.61	45.01	36.08	50	3.4	379.42	32.93	35.59	4.27	35.94	28.66
22	5.01	326.29	43.41	50.96	24.72	44.34	35.52	51	3.39	380.13	32.76	35.3	4.17	35.85	28.59
23	4.87	329.75	42.77	50.18	22.17	43.68	34.97	52	3.37	380.8	32.6	35.03	4.08	35.77	28.52
24	4.74	333.07	42.17	49.43	19.93	43.03	34.44	53	3.36	381.42	32.45	34.78	4.0	35.68	28.45
25	4.63	336.26	41.61	48.73	17.97	42.6	34.09	54	3.34	382.01	32.31	34.54	3.93	35.61	28.39
26	4.52	339.31	41.08	48.07	16.25	42.16	33.73	55	3.33	382.55	32.18	34.32	3.86	35.53	28.33
27	4.42	342.22	40.53	47.32	14.74	41.73	33.38	56	3.32	383.06	32.06	34.12	3.8	35.46	28.27
28	4.32	344.99	39.98	46.55	13.42	41.32	33.05	57	3.31	383.54	31.94	33.93	3.74	35.4	28.22
29	4.24	347.64	39.47	45.83	12.26	40.93	32.72	58	3.3	383.98	31.84	33.75	3.69	35.34	28.17
30	4.16	350.15	38.99	45.15	11.25	40.54	32.41	59	3.29	384.4	31.74	33.59	3.64	35.28	28.13

Table A.36.: Ne^{3+}

Step	$\hat{E}$	$\hat{T}$	P_1	P_2	P_T	P_S	P_{AS}	Step	$\hat{E}$	$\hat{T}$	P_1	P_2	P_T	P_S	P_{AS}
2	43.67	144.26	76.12	83.52	100.0	70.38	57.96	31	7.24	283.94	50.14	57.56	69.77	53.6	43.15
3	38.04	152.25	73.93	80.94	100.0	70.37	57.94	32	7.12	285.72	49.85	57.31	67.73	53.24	42.85
4	33.19	160.44	71.82	78.39	100.0	70.33	57.9	33	7.01	287.4	49.58	57.08	65.76	52.86	42.52
5	29.08	168.77	69.79	75.97	100.0	69.99	57.56	34	6.91	289.0	49.33	56.86	63.88	52.68	42.38
6	25.59	177.2	67.85	73.71	100.0	69.4	57.0	35	6.81	290.51	49.1	56.66	62.09	52.43	42.18
7	22.64	185.67	66.0	71.63	99.99	68.7	56.34	36	6.72	291.94	48.88	56.47	60.39	52.19	41.98
8	20.12	194.12	64.27	69.78	99.99	67.89	55.59	37	6.64	293.29	48.68	56.29	58.78	51.96	41.79
9	17.99	202.51	62.65	68.17	99.99	66.97	54.74	38	6.57	294.56	48.48	56.12	57.26	51.75	41.61
10	16.17	210.76	61.16	66.75	99.98	65.95	53.81	39	6.5	295.76	48.31	55.96	55.83	51.55	41.44
11	14.62	218.83	59.79	65.51	99.93	64.81	52.78	40	6.43	296.89	48.14	55.82	54.48	51.35	41.28
12	13.31	226.65	58.52	64.4	99.77	63.52	51.62	41	6.37	297.95	47.98	55.68	53.22	51.17	41.14
13	12.19	234.17	57.36	63.43	99.34	62.18	50.41	42	6.32	298.95	47.84	55.55	52.04	51.0	40.99
14	11.7	237.81	56.81	62.97	98.97	61.79	50.1	43	6.26	299.89	47.7	55.43	50.94	50.84	40.86
15	11.24	241.36	56.29	62.53	98.45	61.28	49.67	44	6.21	300.77	47.58	55.32	49.91	50.69	40.74
16	10.82	244.81	55.78	62.13	97.76	60.77	49.23	45	6.17	301.6	47.46	55.22	48.95	50.55	40.62
17	10.43	248.16	55.29	61.74	96.88	60.26	48.8	46	6.13	302.38	47.35	55.12	48.05	50.42	40.51
18	10.07	251.42	54.82	61.38	95.79	59.76	48.37	47	6.09	303.11	47.23	55.0	47.21	50.3	40.41
19	9.73	254.56	54.38	61.03	94.5	59.28	47.96	48	6.05	303.79	47.12	54.89	46.43	50.18	40.31
20	9.42	257.6	53.93	60.67	93.02	58.74	47.5	49	6.02	304.43	47.01	54.79	45.71	50.07	40.22
21	9.14	260.54	53.5	60.33	91.36	58.2	47.05	50	5.99	305.03	46.91	54.69	45.03	49.97	40.14
22	8.88	263.36	53.1	60.01	89.52	57.68	46.6	51	5.96	305.59	46.82	54.6	44.41	49.88	40.06
23	8.63	266.07	52.73	59.72	87.53	57.17	46.17	52	5.93	306.12	46.73	54.51	43.82	49.8	40.0
24	8.41	268.68	52.35	59.41	85.43	56.67	45.75	53	5.91	306.61	46.65	54.43	43.28	49.7	39.92
25	8.2	271.17	51.97	59.1	83.24	56.19	45.34	54	5.88	307.07	46.58	54.36	42.77	49.62	39.85
26	8.01	273.56	51.62	58.8	80.99	55.72	44.94	55	5.86	307.5	46.51	54.29	42.31	49.54	39.78
27	7.83	275.84	51.29	58.53	78.7	55.26	44.56	56	5.84	307.9	46.45	54.23	41.87	49.46	39.72
28	7.66	278.02	50.97	58.27	76.42	54.82	44.19	57	5.82	308.28	46.39	54.17	41.46	49.39	39.66
29	7.51	280.09	50.68	58.02	74.15	54.4	43.83	58	5.8	308.63	46.33	54.11	41.09	49.32	39.6
30	7.37	282.06	50.41	57.8	71.92	53.99	43.48	59	5.79	308.95	46.28	54.06	40.74	49.26	39.55

Table A.37.: Ne^{4+}

Step	$\hat{E}$	$\hat{T}$	P_1	P_2	P_T	P_S	P_{AS}	Step	$\hat{E}$	$\hat{T}$	P_1	P_2	P_T	P_S	P_{AS}
2	62.12	125.54	81.74	89.56	100.0	71.88	59.21	31	10.86	244.45	55.83	62.17	97.84	63.03	51.06
3	54.27	132.41	79.6	87.39	100.0	72.07	59.36	32	10.68	245.95	55.61	61.99	97.49	62.82	50.89
4	47.6	139.44	77.5	85.1	100.0	72.25	59.5	33	10.52	247.37	55.4	61.83	97.11	62.56	50.67
5	41.93	146.59	75.47	82.76	100.0	72.41	59.63	34	10.36	248.72	55.21	61.68	96.71	62.32	50.47
6	37.04	153.81	73.52	80.44	100.0	72.57	59.75	35	10.22	249.99	55.03	61.54	96.3	62.09	50.27
7	32.85	161.06	71.67	78.21	100.0	72.65	59.81	36	10.09	251.19	54.85	61.4	95.87	61.87	50.08
8	29.29	168.29	69.91	76.11	100.0	72.41	59.57	37	9.97	252.33	54.7	61.28	95.44	61.66	49.91
9	26.26	175.46	68.24	74.16	100.0	72.01	59.17	38	9.85	253.4	54.55	61.16	95.0	61.47	49.74
10	23.69	182.49	66.69	72.37	100.0	71.54	58.71	39	9.75	254.41	54.4	61.05	94.57	61.28	49.59
11	21.49	189.36	65.23	70.8	99.99	70.98	58.18	40	9.65	255.36	54.26	60.94	94.13	61.11	49.44
12	19.61	196.01	63.9	69.39	99.99	70.26	57.52	41	9.56	256.25	54.13	60.83	93.71	60.94	49.3
13	18.02	202.39	62.68	68.19	99.99	69.51	56.83	42	9.48	257.09	54.0	60.73	93.29	60.79	49.17
14	17.3	205.48	62.1	67.64	99.99	69.12	56.47	43	9.4	257.89	53.89	60.64	92.87	60.65	49.05
15	16.65	208.48	61.56	67.11	99.99	68.72	56.11	44	9.32	258.63	53.78	60.55	92.47	60.51	48.94
16	16.04	211.41	61.05	66.64	99.98	68.32	55.75	45	9.26	259.33	53.68	60.47	92.07	60.39	48.83
17	15.48	214.24	60.56	66.2	99.97	67.92	55.38	46	9.19	259.98	53.58	60.4	91.69	60.27	48.73
18	14.96	216.99	60.1	65.78	99.95	67.52	55.01	47	9.13	260.59	53.49	60.33	91.32	60.16	48.64
19	14.48	219.66	59.65	65.38	99.92	67.15	54.67	48	9.08	261.17	53.41	60.26	90.96	60.05	48.55
20	14.03	222.23	59.23	65.01	99.88	66.68	54.26	49	9.03	261.71	53.34	60.2	90.62	59.96	48.47
21	13.62	224.71	58.83	64.67	99.83	66.22	53.85	50	8.98	262.21	53.26	60.14	90.29	59.87	48.39
22	13.24	227.09	58.45	64.34	99.75	65.77	53.45	51	8.94	262.68	53.2	60.09	89.98	59.79	48.32
23	12.89	229.38	58.09	64.04	99.66	65.34	53.06	52	8.9	263.13	53.14	60.04	89.68	59.72	48.27
24	12.56	231.58	57.76	63.76	99.53	64.91	52.68	53	8.86	263.54	53.08	60.0	89.39	59.64	48.19
25	12.26	233.69	57.43	63.49	99.38	64.5	52.31	54	8.83	263.93	53.02	59.95	89.12	59.55	48.12
26	11.98	235.7	57.13	63.23	99.2	64.31	52.16	55	8.79	264.29	52.97	59.91	88.86	59.48	48.06
27	11.72	237.63	56.84	62.99	98.99	64.04	51.93	56	8.76	264.62	52.93	59.88	88.62	59.41	48.0
28	11.48	239.46	56.57	62.76	98.75	63.77	51.7	57	8.73	264.94	52.88	59.84	88.39	59.34	47.94
29	11.26	241.21	56.31	62.55	98.48	63.51	51.48	58	8.71	265.23	52.84	59.81	88.17	59.28	47.89
30	11.05	242.87	56.07	62.35	98.17	63.26	51.27	59	8.68	265.51	52.81	59.78	87.96	59.22	47.84

Table A.38.: Ne^{5+}

Step	$\hat{E}$	$\hat{T}$	P_1	P_2	P_T	P_S	P_{AS}	Step	$\hat{E}$	$\hat{T}$	P_1	P_2	P_T	P_S	P_{AS}
2	80.99	112.83	85.82	93.22	100.0	72.78	59.97	31	14.75	218.11	59.91	65.61	99.94	69.35	56.5
3	71.2	118.95	83.85	91.53	100.0	73.09	60.22	32	14.52	219.43	59.69	65.42	99.93	69.17	56.33
4	62.53	125.21	81.84	89.66	100.0	73.4	60.47	33	14.3	220.67	59.49	65.24	99.91	68.92	56.11
5	55.16	131.57	79.86	87.66	100.0	73.71	60.72	34	14.1	221.85	59.29	65.07	99.89	68.69	55.9
6	48.88	137.99	77.92	85.57	100.0	74.08	61.02	35	13.91	222.97	59.11	64.91	99.87	68.47	55.71
7	43.54	144.43	76.07	83.46	100.0	74.43	61.29	36	13.73	224.03	58.94	64.76	99.84	68.26	55.52
8	38.97	150.85	74.31	81.38	100.0	74.68	61.5	37	13.57	225.02	58.78	64.62	99.82	68.07	55.35
9	35.0	157.2	72.64	79.38	100.0	74.84	61.62	38	13.42	225.96	58.63	64.5	99.79	67.88	55.18
10	31.62	163.44	71.08	77.49	100.0	74.89	61.66	39	13.28	226.85	58.49	64.38	99.76	67.71	55.03
11	28.74	169.53	69.62	75.76	100.0	74.67	61.42	40	13.15	227.68	58.36	64.27	99.73	67.55	54.89
12	26.28	175.41	68.25	74.17	100.0	74.29	61.06	41	13.03	228.47	58.24	64.16	99.7	67.4	54.75
13	24.19	181.05	67.0	72.72	100.0	73.89	60.66	42	12.91	229.21	58.12	64.07	99.67	67.26	54.62
14	23.25	183.78	66.41	72.07	100.0	73.67	60.46	43	12.81	229.9	58.01	63.98	99.63	67.12	54.51
15	22.39	186.43	65.84	71.46	99.99	73.45	60.25	44	12.71	230.55	57.91	63.89	99.6	67.0	54.4
16	21.59	189.01	65.3	70.88	99.99	73.23	60.04	45	12.62	231.17	57.82	63.81	99.56	66.89	54.29
17	20.85	191.52	64.79	70.32	99.99	73.0	59.83	46	12.54	231.74	57.73	63.74	99.52	66.78	54.2
18	20.17	193.95	64.3	69.82	99.99	72.78	59.61	47	12.46	232.28	57.65	63.67	99.49	66.68	54.11
19	19.54	196.29	63.84	69.34	99.99	72.59	59.43	48	12.39	232.78	57.57	63.61	99.45	66.59	54.03
20	18.95	198.56	63.4	68.9	99.99	72.27	59.15	49	12.32	233.25	57.5	63.55	99.42	66.51	53.95
21	18.41	200.74	62.99	68.5	99.99	71.96	58.86	50	12.26	233.7	57.43	63.49	99.38	66.43	53.88
22	17.91	202.84	62.59	68.11	99.99	71.66	58.59	51	12.2	234.11	57.37	63.44	99.35	66.36	53.82
23	17.44	204.86	62.22	67.75	99.99	71.36	58.32	52	12.15	234.5	57.31	63.39	99.32	66.31	53.77
24	17.01	206.79	61.87	67.41	99.99	71.08	58.06	53	12.09	234.86	57.25	63.34	99.28	66.38	53.85
25	16.61	208.65	61.53	67.09	99.99	70.8	57.81	54	12.05	235.2	57.2	63.3	99.25	66.32	53.8
26	16.24	210.42	61.22	66.8	99.98	70.53	57.57	55	12.0	235.52	57.15	63.26	99.22	66.26	53.75
27	15.9	212.11	60.93	66.53	99.98	70.27	57.33	56	11.96	235.81	57.11	63.22	99.19	66.21	53.71
28	15.58	213.72	60.65	66.28	99.97	70.03	57.11	57	11.93	236.09	57.07	63.18	99.17	66.16	53.66
29	15.28	215.26	60.39	66.04	99.96	69.79	56.9	58	11.89	236.35	57.03	63.15	99.14	66.12	53.63
30	15.01	216.72	60.14	65.82	99.95	69.56	56.69	59	11.86	236.59	56.99	63.12	99.11	66.08	53.59

Table A.39.: Ne^{6+}

Step	$\hat{E}$	$\hat{T}$	P_1	P_2	P_T	P_S	P_{AS}	Step	$\hat{E}$	$\hat{T}$	P_1	P_2	P_T	P_S	P_{AS}
2	99.74	103.47	88.78	95.45	100.0	73.38	60.47	31	18.85	198.95	63.33	68.83	99.99	74.0	60.56
3	87.9	109.05	87.02	94.18	100.0	73.77	60.79	32	18.56	200.14	63.1	68.61	99.99	73.9	60.46
4	77.78	114.75	85.2	92.7	100.0	74.17	61.11	33	18.29	201.27	62.89	68.4	99.99	73.71	60.29
5	68.86	120.53	83.34	91.07	100.0	74.58	61.44	34	18.03	202.33	62.69	68.21	99.99	73.53	60.13
6	61.09	126.37	81.48	89.3	100.0	75.09	61.86	35	17.79	203.34	62.5	68.02	99.99	73.36	59.98
7	54.46	132.22	79.66	87.45	100.0	75.61	62.29	36	17.57	204.29	62.32	67.85	99.99	73.2	59.84
8	48.82	138.06	77.9	85.55	100.0	76.07	62.66	37	17.37	205.19	62.16	67.69	99.99	73.05	59.71
9	44.01	143.82	76.24	83.66	100.0	76.45	62.97	38	17.18	206.04	62.0	67.54	99.99	72.91	59.58
10	39.9	149.49	74.68	81.82	100.0	76.75	63.21	39	17.0	206.83	61.86	67.4	99.99	72.78	59.46
11	36.31	155.0	73.21	80.06	100.0	76.93	63.36	40	16.84	207.59	61.72	67.27	99.99	72.66	59.35
12	33.24	160.34	71.85	78.43	100.0	76.91	63.33	41	16.69	208.29	61.6	67.15	99.99	72.55	59.25
13	30.62	165.46	70.59	76.91	100.0	76.85	63.28	42	16.55	208.96	61.48	67.04	99.99	72.44	59.16
14	29.46	167.92	69.99	76.21	100.0	76.71	63.12	43	16.41	209.58	61.37	66.93	99.98	72.34	59.07
15	28.38	170.33	69.43	75.53	100.0	76.6	63.01	44	16.29	210.17	61.26	66.84	99.98	72.25	58.98
16	27.39	172.66	68.88	74.9	100.0	76.5	62.9	45	16.18	210.72	61.17	66.75	99.98	72.17	58.91
17	26.47	174.93	68.36	74.3	100.0	76.39	62.79	46	16.07	211.24	61.08	66.67	99.98	72.09	58.84
18	25.62	177.13	67.86	73.72	100.0	76.28	62.67	47	15.97	211.72	60.99	66.59	99.98	72.02	58.77
19	24.83	179.25	67.39	73.18	100.0	76.21	62.6	48	15.88	212.18	60.91	66.52	99.98	71.95	58.71
20	24.1	181.3	66.95	72.66	100.0	75.99	62.4	49	15.8	212.6	60.84	66.45	99.98	71.89	58.66
21	23.42	183.27	66.52	72.19	100.0	75.78	62.2	50	15.72	213.0	60.77	66.39	99.97	71.84	58.61
22	22.8	185.17	66.11	71.75	99.99	75.57	62.01	51	15.65	213.37	60.71	66.33	99.97	71.78	58.56
23	22.21	186.99	65.72	71.33	99.99	75.37	61.82	52	15.58	213.72	60.65	66.28	99.97	71.75	58.53
24	21.68	188.74	65.36	70.94	99.99	75.17	61.64	53	15.51	214.05	60.59	66.23	99.97	71.69	58.47
25	21.18	190.41	65.02	70.56	99.99	74.98	61.46	54	15.46	214.35	60.54	66.18	99.97	71.63	58.42
26	20.71	192.01	64.69	70.22	99.99	74.8	61.3	55	15.4	214.64	60.49	66.14	99.97	71.57	58.37
27	20.28	193.54	64.38	69.9	99.99	74.62	61.14	56	15.35	214.91	60.45	66.1	99.96	71.52	58.32
28	19.88	195.0	64.1	69.6	99.99	74.46	60.98	57	15.3	215.15	60.41	66.06	99.96	71.47	58.28
29	19.52	196.38	63.82	69.32	99.99	74.3	60.83	58	15.26	215.39	60.37	66.02	99.96	71.43	58.23
30	19.17	197.7	63.57	69.07	99.99	74.15	60.7	59	15.22	215.6	60.33	65.99	99.96	71.39	58.2

Table A.40.: Ne^{7+}

Step	$\hat{E}$	$\hat{T}$	P_1	P_2	P_T	P_S	P_{AS}	Step	$\hat{E}$	$\hat{T}$	P_1	P_2	P_T	P_S	P_{AS}
2	118.87	96.21	90.92	96.83	100.0	73.81	60.83	31	23.11	184.22	66.31	71.97	99.99	77.32	63.46
3	104.79	101.37	89.41	95.88	100.0	74.26	61.2	32	22.75	185.31	66.08	71.72	99.99	77.27	63.41
4	92.76	106.63	87.78	94.75	100.0	74.72	61.58	33	22.42	186.34	65.86	71.48	99.99	77.12	63.27
5	82.48	111.98	86.1	93.45	100.0	75.2	61.96	34	22.11	187.32	65.66	71.26	99.99	76.98	63.15
6	73.66	117.37	84.36	91.98	100.0	75.81	62.46	35	21.83	188.24	65.46	71.05	99.99	76.85	63.03
7	65.72	122.78	82.62	90.4	100.0	76.46	63.0	36	21.56	189.12	65.28	70.85	99.99	76.72	62.92
8	58.95	128.16	80.92	88.74	100.0	77.07	63.49	37	21.32	189.94	65.11	70.67	99.99	76.61	62.81
9	53.18	133.48	79.27	87.05	100.0	77.61	63.93	38	21.09	190.72	64.96	70.5	99.99	76.5	62.71
10	48.25	138.7	77.71	85.34	100.0	78.08	64.32	39	20.87	191.45	64.81	70.34	99.99	76.4	62.62
11	44.04	143.78	76.25	83.67	100.0	78.44	64.62	40	20.68	192.14	64.67	70.19	99.99	76.3	62.54
12	40.44	148.7	74.89	82.07	100.0	78.58	64.72	41	20.49	192.79	64.54	70.06	99.99	76.22	62.46
13	37.3	153.41	73.63	80.57	100.0	78.68	64.8	42	20.32	193.4	64.41	69.93	99.99	76.14	62.38
14	35.9	155.68	73.03	79.85	100.0	78.72	64.83	43	20.16	193.97	64.3	69.81	99.99	76.06	62.32
15	34.6	157.89	72.46	79.17	100.0	78.75	64.85	44	20.02	194.51	64.19	69.7	99.99	75.99	62.25
16	33.4	160.05	71.92	78.51	100.0	78.77	64.86	45	19.88	195.01	64.09	69.6	99.99	75.93	62.2
17	32.29	162.13	71.4	77.88	100.0	78.78	64.87	46	19.75	195.49	64.0	69.5	99.99	75.87	62.14
18	31.26	164.15	70.9	77.29	100.0	78.79	64.88	47	19.63	195.93	63.91	69.41	99.99	75.82	62.09
19	30.31	166.11	70.43	76.73	100.0	78.85	64.92	48	19.52	196.35	63.83	69.32	99.99	75.77	62.05
20	29.43	167.99	69.98	76.19	100.0	78.65	64.72	49	19.42	196.74	63.75	69.25	99.99	75.73	62.01
21	28.61	169.8	69.55	75.68	100.0	78.5	64.58	50	19.33	197.1	63.68	69.18	99.99	75.69	61.97
22	27.86	171.55	69.15	75.19	100.0	78.36	64.45	51	19.24	197.45	63.62	69.11	99.99	75.65	61.94
23	27.16	173.23	68.75	74.75	100.0	78.22	64.32	52	19.16	197.77	63.55	69.05	99.99	75.63	61.92
24	26.51	174.83	68.38	74.32	100.0	78.09	64.19	53	19.08	198.07	63.5	69.0	99.99	75.58	61.87
25	25.91	176.37	68.03	73.92	100.0	77.96	64.07	54	19.01	198.34	63.44	68.94	99.99	75.53	61.83
26	25.35	177.84	67.7	73.54	100.0	77.84	63.96	55	18.94	198.61	63.39	68.9	99.99	75.49	61.79
27	24.83	179.25	67.39	73.18	100.0	77.73	63.85	56	18.88	198.85	63.35	68.85	99.99	75.45	61.75
28	24.35	180.58	67.1	72.84	100.0	77.62	63.74	57	18.82	199.08	63.3	68.81	99.99	75.41	61.71
29	23.91	181.86	66.83	72.52	100.0	77.51	63.64	58	18.77	199.29	63.26	68.77	99.99	75.37	61.68
30	23.49	183.07	66.56	72.24	100.0	77.41	63.55	59	18.72	199.49	63.22	68.73	99.99	75.34	61.65

Table A.41.: Ne^{8+}

Step	$\hat{E}$	$\hat{T}$	P_1	P_2	P_T	P_S	P_{AS}	Step	$\hat{E}$	$\hat{T}$	P_1	P_2	P_T	P_S	P_{AS}
2	0.0	90.37	92.53	97.72	100.0	74.14	61.1	31	27.49	172.42	68.94	74.96	100.0	79.81	65.64
3	121.99	95.19	91.22	97.01	100.0	74.63	61.51	32	27.07	173.43	68.71	74.69	100.0	79.8	65.62
4	108.01	100.1	89.79	96.14	100.0	75.14	61.92	33	26.68	174.39	68.48	74.44	100.0	79.68	65.51
5	96.06	105.1	88.27	95.09	100.0	75.66	62.35	34	26.32	175.3	68.28	74.2	100.0	79.57	65.41
6	85.84	110.13	86.68	93.91	100.0	76.35	62.92	35	25.99	176.16	68.08	73.97	100.0	79.46	65.31
7	77.08	115.18	85.06	92.59	100.0	77.1	63.53	36	25.68	176.98	67.9	73.76	100.0	79.36	65.22
8	69.34	120.2	83.44	91.16	100.0	77.81	64.12	37	25.39	177.74	67.73	73.57	100.0	79.27	65.14
9	62.59	125.16	81.86	89.67	100.0	78.47	64.66	38	25.12	178.46	67.57	73.38	100.0	79.19	65.06
10	56.82	130.03	80.33	88.15	100.0	79.08	65.15	39	24.87	179.14	67.42	73.2	100.0	79.11	64.99
11	51.89	134.77	78.88	86.63	100.0	79.58	65.56	40	24.64	179.79	67.28	73.04	100.0	79.03	64.92
12	47.68	139.35	77.52	85.13	100.0	79.83	65.77	41	24.42	180.39	67.14	72.89	100.0	78.97	64.86
13	44.07	143.74	76.26	83.69	100.0	80.05	65.94	42	24.22	180.96	67.02	72.74	100.0	78.9	64.8
14	42.46	145.86	75.67	83.0	100.0	80.15	66.02	43	24.04	181.49	66.91	72.61	100.0	78.85	64.75
15	40.98	147.92	75.1	82.33	100.0	80.24	66.1	44	23.86	181.99	66.8	72.49	100.0	78.79	64.7
16	39.59	149.93	74.56	81.68	100.0	80.33	66.16	45	23.7	182.46	66.69	72.38	100.0	78.75	64.66
17	38.29	151.87	74.03	81.06	100.0	80.4	66.22	46	23.55	182.9	66.6	72.28	100.0	78.7	64.62
18	37.08	153.75	73.54	80.46	100.0	80.48	66.28	47	23.41	183.31	66.51	72.18	100.0	78.66	64.58
19	35.96	155.57	73.06	79.88	100.0	80.62	66.4	48	23.28	183.7	66.42	72.09	100.0	78.63	64.55
20	34.93	157.32	72.61	79.34	100.0	80.53	66.32	49	23.16	184.06	66.35	72.01	99.99	78.6	64.52
21	33.97	159.01	72.18	78.83	100.0	80.45	66.25	50	23.05	184.4	66.27	71.93	99.99	78.57	64.49
22	33.08	160.64	71.77	78.33	100.0	80.39	66.2	51	22.94	184.72	66.21	71.85	99.99	78.54	64.47
23	32.25	162.2	71.39	77.86	100.0	80.33	66.16	52	22.85	185.01	66.14	71.79	99.99	78.54	64.46
24	31.49	163.69	71.02	77.42	100.0	80.29	66.12	53	22.76	185.29	66.08	71.72	99.99	78.49	64.42
25	30.78	165.12	70.67	77.01	100.0	80.27	66.1	54	22.67	185.55	66.03	71.66	99.99	78.45	64.38
26	30.13	166.49	70.34	76.62	100.0	80.25	66.08	55	22.6	185.79	65.98	71.61	99.99	78.42	64.35
27	29.52	167.8	70.02	76.25	100.0	80.05	65.88	56	22.52	186.02	65.93	71.55	99.99	78.38	64.32
28	28.95	169.04	69.73	75.89	100.0	79.99	65.81	57	22.45	186.23	65.88	71.51	99.99	78.35	64.29
29	28.43	170.23	69.45	75.56	100.0	79.92	65.75	58	22.39	186.43	65.84	71.46	99.99	78.32	64.26
30	27.94	171.35	69.19	75.25	100.0	79.86	65.69	59	22.33	186.61	65.8	71.42	99.99	78.3	64.23

Table A.42.: Ne^{9+}

Step	$\hat{E}$	$\hat{T}$	P_1	P_2	P_T	P_S	P_{AS}	Step	$\hat{E}$	$\hat{T}$	P_1	P_2	P_T	P_S	P_{AS}
2	0.0	85.53	93.76	98.31	100.0	74.39	61.32	31	32.0	162.7	71.26	77.71	100.0	81.72	67.3
3	0.0	90.07	92.61	97.76	100.0	74.92	61.75	32	31.51	163.65	71.03	77.43	100.0	81.79	67.35
4	123.5	94.7	91.36	97.09	100.0	75.46	62.2	33	31.06	164.55	70.81	77.17	100.0	81.74	67.31
5	109.86	99.4	90.0	96.27	100.0	76.03	62.66	34	30.65	165.41	70.6	76.93	100.0	81.7	67.28
6	98.18	104.15	88.57	95.3	100.0	76.77	63.27	35	30.26	166.21	70.4	76.7	100.0	81.67	67.25
7	88.19	108.9	87.07	94.21	100.0	77.6	63.95	36	29.9	166.97	70.22	76.48	100.0	81.64	67.23
8	79.64	113.63	85.56	93.01	100.0	78.4	64.6	37	29.57	167.69	70.05	76.28	100.0	81.34	66.95
9	72.21	118.3	84.06	91.72	100.0	79.15	65.22	38	29.26	168.37	69.89	76.08	100.0	81.27	66.89
10	65.58	122.88	82.59	90.37	100.0	79.86	65.8	39	28.97	169.01	69.74	75.9	100.0	81.21	66.83
11	59.92	127.33	81.17	89.0	100.0	80.46	66.3	40	28.7	169.61	69.6	75.73	100.0	81.16	66.78
12	55.08	131.64	79.84	87.64	100.0	80.81	66.58	41	28.45	170.18	69.46	75.58	100.0	81.1	66.73
13	50.93	135.77	78.58	86.3	100.0	81.12	66.84	42	28.22	170.71	69.34	75.43	100.0	81.06	66.68
14	49.09	137.76	77.99	85.65	100.0	81.27	66.95	43	28.0	171.21	69.23	75.29	100.0	81.01	66.64
15	47.38	139.69	77.42	85.01	100.0	81.41	67.07	44	27.8	171.68	69.12	75.16	100.0	80.97	66.61
16	45.8	141.58	76.88	84.4	100.0	81.54	67.17	45	27.62	172.12	69.01	75.04	100.0	80.94	66.57
17	44.34	143.4	76.36	83.8	100.0	81.67	67.28	46	27.45	172.53	68.92	74.93	100.0	80.91	66.54
18	42.98	145.17	75.86	83.22	100.0	81.79	67.37	47	27.29	172.92	68.83	74.83	100.0	80.88	66.51
19	41.72	146.88	75.39	82.67	100.0	81.99	67.54	48	27.14	173.28	68.74	74.73	100.0	80.85	66.49
20	40.56	148.53	74.94	82.13	100.0	81.91	67.48	49	27.0	173.62	68.66	74.64	100.0	80.83	66.47
21	39.47	150.11	74.51	81.62	100.0	81.85	67.42	50	26.87	173.94	68.59	74.56	100.0	80.81	66.45
22	38.44	151.64	74.1	81.13	100.0	81.79	67.37	51	26.75	174.24	68.52	74.48	100.0	80.79	66.43
23	37.49	153.1	73.71	80.67	100.0	81.74	67.33	52	26.64	174.51	68.46	74.41	100.0	80.8	66.43
24	36.61	154.51	73.34	80.22	100.0	81.71	67.3	53	26.53	174.78	68.4	74.34	100.0	80.76	66.4
25	35.79	155.85	72.99	79.8	100.0	81.68	67.28	54	26.44	175.02	68.34	74.27	100.0	80.73	66.37
26	35.04	157.14	72.66	79.4	100.0	81.67	67.27	55	26.35	175.25	68.29	74.21	100.0	80.7	66.34
27	34.33	158.36	72.34	79.03	100.0	81.66	67.26	56	26.26	175.46	68.24	74.16	100.0	80.67	66.31
28	33.68	159.53	72.05	78.67	100.0	81.66	67.26	57	26.18	175.66	68.2	74.11	100.0	80.64	66.29
29	33.08	160.64	71.77	78.33	100.0	81.67	67.27	58	26.11	175.84	68.15	74.06	100.0	80.62	66.26
30	32.52	161.7	71.51	78.01	100.0	81.69	67.28	59	26.05	176.02	68.11	74.01	100.0	80.6	66.24

Table A.43.: Ne^{10+}

Step	$\hat{E}$	$\hat{T}$	P_1	P_2	P_T	P_S	P_{AS}	Step	$\hat{E}$	$\hat{T}$	P_1	P_2	P_T	P_S	P_{AS}
2	0.0	80.88	0.0	0.0	0.0	0.0	0.0	31	36.61	154.51	73.34	80.22	100.0	82.85	68.24
3	0.0	85.74	93.7	98.29	100.0	75.15	61.94	32	36.06	155.41	73.1	79.93	100.0	82.91	68.3
4	0.0	90.14	92.59	97.75	100.0	75.72	62.41	33	35.55	156.26	72.88	79.67	100.0	82.87	68.26
5	123.85	94.59	91.39	97.1	100.0	76.32	62.9	34	35.07	157.07	72.68	79.42	100.0	82.84	68.23
6	110.71	99.09	90.09	96.32	100.0	77.11	63.55	35	34.64	157.83	72.48	79.19	100.0	82.8	68.2
7	99.46	103.59	88.75	95.43	100.0	78.0	64.28	36	34.23	158.55	72.3	78.97	100.0	82.78	68.18
8	89.83	108.07	87.33	94.41	100.0	78.86	64.99	37	33.85	159.23	72.12	78.76	100.0	82.76	68.16
9	81.57	112.5	85.93	93.31	100.0	79.69	65.67	38	33.49	159.87	71.96	78.57	100.0	82.74	68.15
10	74.49	116.83	84.53	92.13	100.0	80.48	66.32	39	33.17	160.47	71.81	78.38	100.0	82.72	68.13
11	68.11	121.06	83.17	90.91	100.0	81.17	66.89	40	32.86	161.04	71.67	78.21	100.0	82.71	68.13
12	62.63	125.13	81.87	89.68	100.0	81.59	67.23	41	32.58	161.58	71.54	78.05	100.0	82.7	68.12
13	57.94	129.04	80.64	88.46	100.0	81.98	67.55	42	32.32	162.08	71.41	77.9	100.0	82.7	68.11
14	55.85	130.92	80.06	87.87	100.0	82.16	67.7	43	32.07	162.55	71.3	77.76	100.0	82.7	68.11
15	53.92	132.75	79.49	87.28	100.0	82.34	67.84	44	31.84	162.99	71.19	77.62	100.0	82.7	68.11
16	52.13	134.54	78.95	86.7	100.0	82.51	67.98	45	31.63	163.41	71.09	77.5	100.0	82.7	68.11
17	50.47	136.26	78.43	86.14	100.0	82.68	68.12	46	31.44	163.8	70.99	77.39	100.0	82.7	68.11
18	48.93	137.93	77.94	85.59	100.0	82.84	68.25	47	31.25	164.17	70.9	77.28	100.0	82.71	68.12
19	47.51	139.55	77.47	85.06	100.0	83.1	68.46	48	31.08	164.51	70.82	77.19	100.0	82.71	68.12
20	46.19	141.11	77.01	84.55	100.0	83.03	68.4	49	30.93	164.83	70.74	77.09	100.0	82.72	68.13
21	44.96	142.61	76.58	84.06	100.0	82.96	68.35	50	30.78	165.13	70.66	77.01	100.0	82.73	68.14
22	43.83	144.05	76.18	83.59	100.0	82.91	68.31	51	30.64	165.41	70.6	76.93	100.0	82.75	68.15
23	42.78	145.44	75.79	83.13	100.0	82.87	68.27	52	30.52	165.68	70.53	76.85	100.0	82.78	68.18
24	41.8	146.77	75.42	82.7	100.0	82.84	68.25	53	30.4	165.92	70.47	76.78	100.0	82.76	68.16
25	40.9	148.04	75.07	82.29	100.0	82.82	68.23	54	30.29	166.15	70.42	76.71	100.0	82.75	68.15
26	40.06	149.25	74.74	81.89	100.0	82.81	68.21	55	30.19	166.37	70.37	76.65	100.0	82.74	68.14
27	39.26	150.41	74.43	81.52	100.0	82.8	68.21	56	30.09	166.57	70.32	76.6	100.0	82.74	68.13
28	38.52	151.51	74.13	81.17	100.0	82.8	68.21	57	30.0	166.75	70.27	76.54	100.0	82.73	68.13
29	37.84	152.56	73.85	80.84	100.0	82.81	68.22	58	29.92	166.93	70.23	76.49	100.0	82.72	68.12
30	37.2	153.56	73.59	80.52	100.0	82.83	68.23	59	29.84	167.09	70.19	76.45	100.0	82.72	68.11

Table A.44.: Mg^{1+}

Step	$\hat{E}$	$\hat{T}$	P_1	P_2	P_T	P_S	P_{AS}	Step	$\hat{E}$	$\hat{T}$	P_1	P_2	P_T	P_S	P_{AS}
2	9.46	272.5	40.43	47.6	93.22	50.58	40.81	31	1.48	0.0	11.08	10.92	0.07	16.45	13.04
3	8.09	288.68	38.1	45.52	82.03	47.82	38.47	32	1.46	0.0	10.9	10.75	0.07	16.19	12.83
4	6.96	305.4	35.85	43.33	64.97	45.46	36.51	33	1.43	0.0	10.73	10.58	0.06	15.98	12.67
5	6.02	322.58	33.58	40.74	45.69	42.83	34.33	34	1.42	0.0	10.58	10.43	0.06	15.77	12.51
6	5.22	340.11	31.36	37.76	28.88	40.1	32.08	35	1.4	0.0	10.44	10.29	0.06	15.58	12.35
7	4.56	357.9	28.96	33.93	16.91	37.68	30.1	36	1.38	0.0	10.31	10.16	0.05	15.39	12.2
8	4.03	375.81	26.36	29.2	9.77	35.08	27.98	37	1.37	0.0	10.19	10.04	0.05	15.21	12.06
9	3.59	393.67	23.71	24.4	5.58	32.9	26.21	38	1.35	0.0	10.07	9.93	0.05	15.05	11.93
10	3.22	411.45	21.57	21.31	3.22	30.67	24.41	39	1.34	0.0	9.97	9.82	0.05	14.89	11.8
11	2.9	429.09	20.01	19.76	1.9	28.72	22.84	40	1.33	0.0	9.87	9.72	0.05	14.73	11.68
12	2.63	446.48	18.63	18.39	1.16	26.85	21.34	41	1.32	0.0	9.77	9.63	0.05	14.59	11.57
13	2.41	463.45	17.38	17.16	0.74	25.2	20.01	42	1.31	0.0	9.68	9.54	0.04	14.49	11.49
14	2.32	471.74	16.81	16.6	0.6	24.45	19.41	43	1.3	0.0	9.6	9.46	0.04	14.38	11.4
15	2.23	479.87	16.27	16.07	0.5	23.69	18.81	44	1.29	0.0	9.53	9.39	0.04	14.28	11.32
16	2.15	487.84	15.77	15.57	0.42	22.95	18.21	45	1.28	0.0	9.45	9.32	0.04	14.18	11.25
17	2.07	495.63	15.29	15.1	0.35	22.35	17.73	46	1.27	0.0	9.39	9.25	0.04	14.09	11.17
18	2.01	503.24	14.85	14.66	0.3	21.76	17.26	47	1.27	0.0	9.33	9.19	0.04	14.01	11.11
19	1.94	510.65	14.43	14.24	0.26	21.18	16.8	48	1.26	0.0	9.27	9.13	0.04	13.93	11.04
20	1.88	0.0	14.04	13.86	0.22	20.6	16.34	49	1.25	0.0	9.22	9.08	0.04	13.85	10.98
21	1.83	0.0	13.68	13.5	0.2	20.08	15.92	50	1.25	0.0	9.17	9.03	0.04	13.78	10.93
22	1.78	0.0	13.33	13.15	0.17	19.63	15.56	51	1.24	0.0	9.12	8.99	0.04	13.71	10.88
23	1.74	0.0	13.0	12.83	0.15	19.19	15.21	52	1.24	0.0	9.08	8.95	0.04	13.65	10.83
24	1.69	0.0	12.7	12.53	0.14	18.76	14.87	53	1.23	0.0	9.04	8.91	0.03	13.59	10.78
25	1.65	0.0	12.42	12.25	0.12	18.34	14.54	54	1.23	0.0	9.01	8.87	0.03	13.54	10.74
26	1.62	0.0	12.16	11.99	0.11	17.96	14.24	55	1.22	0.0	8.97	8.84	0.03	13.49	10.7
27	1.58	0.0	11.91	11.74	0.1	17.63	13.98	56	1.22	0.0	8.94	8.81	0.03	13.44	10.66
28	1.55	0.0	11.68	11.52	0.09	17.32	13.73	57	1.22	0.0	8.91	8.78	0.03	13.39	10.62
29	1.53	0.0	11.47	11.31	0.08	17.02	13.49	58	1.21	0.0	8.88	8.75	0.03	13.35	10.59
30	1.5	0.0	11.27	11.11	0.08	16.73	13.26	59	1.21	0.0	8.86	8.73	0.03	13.31	10.56

Table A.45.: Mg^{2+}

Step	$\hat{E}$	$\hat{T}$	P_1	P_2	P_T	P_S	P_{AS}	Step	$\hat{E}$	$\hat{T}$	P_1	P_2	P_T	P_S	P_{AS}
2	24.28	191.91	57.86	63.84	100.0	64.64	52.97	31	3.77	386.08	24.77	26.2	7.08	35.18	28.04
3	20.99	202.77	54.75	60.69	99.99	63.43	51.86	32	3.71	388.62	24.4	25.49	6.54	34.86	27.79
4	18.2	213.9	51.82	57.8	99.99	62.04	50.6	33	3.65	391.02	24.06	24.91	6.06	34.54	27.53
5	15.84	225.25	49.11	55.28	99.97	60.47	49.17	34	3.6	393.29	23.76	24.47	5.65	34.24	27.29
6	13.85	236.78	46.64	53.04	99.85	58.65	47.53	35	3.55	395.45	23.48	24.07	5.28	33.95	27.05
7	12.17	248.4	44.42	51.08	99.29	57.13	46.26	36	3.51	397.49	23.22	23.69	4.95	33.68	26.83
8	10.75	260.04	42.4	49.31	97.58	55.36	44.76	37	3.47	399.42	22.98	23.34	4.66	33.42	26.62
9	9.55	271.62	40.56	47.72	93.64	53.45	43.13	38	3.43	401.24	22.76	23.01	4.41	33.17	26.42
10	8.53	283.06	38.88	46.23	86.59	51.4	41.4	39	3.39	402.96	22.55	22.71	4.18	32.93	26.23
11	7.69	294.28	37.33	44.81	76.81	49.54	39.84	40	3.36	404.57	22.36	22.42	3.97	32.71	26.05
12	6.98	305.19	35.87	43.35	65.2	47.85	38.44	41	3.33	406.1	22.18	22.16	3.79	32.5	25.88
13	6.37	315.72	34.48	41.8	53.26	46.12	37.01	42	3.3	407.54	22.01	21.91	3.63	32.31	25.72
14	6.11	320.82	33.81	41.0	47.59	45.25	36.28	43	3.27	408.89	21.85	21.68	3.48	32.12	25.57
15	5.86	325.8	33.18	40.25	42.28	44.38	35.56	44	3.24	410.16	21.71	21.47	3.35	31.94	25.43
16	5.63	330.66	32.59	39.54	37.39	43.51	34.84	45	3.22	411.35	21.58	21.32	3.23	31.78	25.29
17	5.42	335.38	31.96	38.64	32.96	42.64	34.13	46	3.2	412.47	21.47	21.21	3.12	31.62	25.17
18	5.23	339.97	31.37	37.79	29.0	42.01	33.61	47	3.18	413.53	21.38	21.11	3.02	31.48	25.05
19	5.05	344.41	30.79	36.91	25.51	41.4	33.11	48	3.16	414.51	21.28	21.02	2.93	31.34	24.94
20	4.89	348.71	30.2	35.96	22.44	40.76	32.6	49	3.14	415.44	21.2	20.94	2.85	31.21	24.83
21	4.73	352.86	29.64	35.06	19.76	40.14	32.09	50	3.13	416.31	21.12	20.86	2.77	31.09	24.74
22	4.59	356.86	29.11	34.21	17.45	39.54	31.59	51	3.11	417.12	21.05	20.79	2.71	30.98	24.64
23	4.47	360.7	28.55	33.19	15.55	38.94	31.11	52	3.1	417.88	20.98	20.72	2.65	30.87	24.56
24	4.36	364.4	28.02	32.24	13.9	38.37	30.64	53	3.09	418.59	20.91	20.66	2.59	30.84	24.54
25	4.25	367.94	27.52	31.35	12.47	37.8	30.18	54	3.07	419.26	20.85	20.6	2.54	30.77	24.48
26	4.16	371.33	27.06	30.52	11.23	37.26	29.74	55	3.06	419.88	20.8	20.54	2.49	30.7	24.42
27	4.07	374.57	26.56	29.58	10.15	36.74	29.31	56	3.05	420.47	20.75	20.49	2.45	30.63	24.37
28	3.99	377.66	26.06	28.64	9.22	36.23	28.89	57	3.04	421.01	20.7	20.44	2.41	30.57	24.32
29	3.91	380.61	25.6	27.77	8.4	35.87	28.6	58	3.03	421.52	20.65	20.4	2.37	30.52	24.27
30	3.84	383.42	25.17	26.96	7.7	35.52	28.32	59	3.02	422.0	20.61	20.36	2.34	30.46	24.23

Table A.46.: Mg^{3+}

Step	$\hat{E}$	$\hat{T}$	P_1	P_2	P_T	P_S	P_{AS}	Step	$\hat{E}$	$\hat{T}$	P_1	P_2	P_T	P_S	P_{AS}
2	40.94	157.24	69.0	76.26	100.0	69.38	57.12	31	6.69	310.05	35.26	42.73	59.71	48.84	39.22
3	35.55	165.98	66.06	72.87	100.0	69.24	57.0	32	6.58	312.0	34.99	42.41	57.48	48.52	38.95
4	30.99	174.93	63.13	69.55	100.0	68.59	56.37	33	6.47	313.86	34.73	42.1	55.37	48.17	38.67
5	27.13	184.02	60.25	66.38	100.0	67.87	55.7	34	6.38	315.62	34.49	41.82	53.38	47.85	38.4
6	23.85	193.22	57.47	63.44	99.99	67.02	54.9	35	6.29	317.29	34.27	41.56	51.51	47.54	38.14
7	21.07	202.47	54.83	60.77	99.99	66.02	53.99	36	6.21	318.86	34.06	41.31	49.75	47.24	37.9
8	18.71	211.7	52.38	58.34	99.99	64.89	52.96	37	6.13	320.35	33.87	41.08	48.11	46.96	37.67
9	16.7	220.86	50.12	56.22	99.99	63.64	51.82	38	6.06	321.75	33.69	40.86	46.58	46.69	37.45
10	15.0	229.88	48.09	54.34	99.95	62.26	50.57	39	5.99	323.07	33.52	40.66	45.16	46.44	37.24
11	13.56	238.69	46.26	52.71	99.8	60.96	49.43	40	5.93	324.32	33.37	40.47	43.83	46.21	37.04
12	12.33	247.23	44.63	51.27	99.39	59.71	48.37	41	5.87	325.49	33.22	40.3	42.6	45.98	36.86
13	11.28	255.46	43.17	49.98	98.45	58.43	47.28	42	5.82	326.6	33.08	40.14	41.46	45.77	36.68
14	10.82	259.44	42.5	49.4	97.71	57.78	46.73	43	5.77	327.63	32.96	39.98	40.4	45.57	36.52
15	10.39	263.32	41.87	48.85	96.74	57.13	46.17	44	5.73	328.61	32.84	39.84	39.41	45.38	36.36
16	9.99	267.1	41.27	48.33	95.52	56.47	45.62	45	5.68	329.52	32.73	39.71	38.5	45.21	36.22
17	9.63	270.77	40.69	47.83	94.03	55.82	45.06	46	5.65	330.38	32.63	39.59	37.66	45.04	36.08
18	9.29	274.33	40.16	47.36	92.28	55.17	44.51	47	5.61	331.19	32.52	39.44	36.87	44.89	35.95
19	8.98	277.78	39.65	46.92	90.27	54.54	43.98	48	5.57	331.94	32.42	39.29	36.15	44.74	35.83
20	8.69	281.12	39.16	46.48	88.03	53.86	43.41	49	5.54	332.65	32.33	39.16	35.48	44.6	35.72
21	8.43	284.33	38.7	46.06	85.62	53.2	42.84	50	5.51	333.31	32.24	39.03	34.86	44.48	35.62
22	8.19	287.43	38.27	45.68	83.11	52.55	42.29	51	5.49	333.93	32.15	38.91	34.28	44.36	35.52
23	7.97	290.41	37.86	45.31	80.48	51.91	41.75	52	5.46	334.52	32.08	38.8	33.75	44.25	35.43
24	7.76	293.27	37.48	44.95	77.8	51.58	41.49	53	5.44	335.06	32.01	38.7	33.25	44.14	35.34
25	7.57	296.01	37.09	44.57	75.07	51.15	41.13	54	5.42	335.57	31.94	38.6	32.8	44.03	35.25
26	7.39	298.63	36.73	44.21	72.36	50.73	40.78	55	5.39	336.04	31.88	38.51	32.37	43.94	35.17
27	7.23	301.14	36.4	43.88	69.67	50.32	40.45	56	5.38	336.48	31.82	38.43	31.98	43.84	35.09
28	7.08	303.53	36.09	43.57	67.05	49.93	40.12	57	5.36	336.9	31.77	38.35	31.61	43.76	35.02
29	6.94	305.81	35.79	43.27	64.5	49.55	39.81	58	5.34	337.29	31.72	38.28	31.28	43.68	34.95
30	6.81	307.98	35.52	43.0	62.05	49.19	39.51	59	5.33	337.65	31.67	38.21	30.96	43.73	35.0

Table A.47.: Mg^{4+}

Step	$\hat{E}$	$\hat{T}$	P_1	P_2	P_T	P_S	P_{AS}	Step	$\hat{E}$	$\hat{T}$	P_1	P_2	P_T	P_S	P_{AS}
2	58.57	136.77	76.22	84.36	100.0	71.12	58.58	31	10.03	266.71	41.33	48.38	95.66	58.43	47.21
3	51.11	144.29	73.51	81.4	100.0	71.21	58.65	32	9.87	268.35	41.07	48.16	95.05	58.15	46.97
4	44.73	151.98	70.81	78.34	100.0	71.29	58.7	33	9.71	269.9	40.83	47.95	94.41	57.83	46.7
5	39.26	159.79	68.13	75.26	100.0	71.33	58.72	34	9.57	271.38	40.6	47.75	93.76	57.53	46.44
6	34.62	167.68	65.5	72.22	100.0	71.32	58.7	35	9.44	272.77	40.39	47.57	93.09	57.24	46.2
7	30.68	175.61	62.91	69.31	100.0	70.72	58.12	36	9.31	274.09	40.19	47.39	92.41	56.97	45.97
8	27.34	183.5	60.41	66.55	100.0	70.15	57.58	37	9.2	275.33	40.01	47.23	91.73	56.71	45.75
9	24.48	191.32	58.03	64.02	100.0	69.5	56.97	38	9.09	276.51	39.84	47.08	91.05	56.46	45.54
10	22.06	199.01	55.8	61.73	99.99	68.76	56.28	39	8.99	277.61	39.68	46.95	90.37	56.23	45.35
11	19.99	206.5	53.74	59.68	99.99	67.92	55.5	40	8.9	278.65	39.52	46.81	89.71	56.01	45.16
12	18.23	213.76	51.86	57.83	99.99	66.93	54.6	41	8.82	279.64	39.38	46.68	89.06	55.81	44.99
13	16.73	220.73	50.15	56.25	99.99	65.89	53.66	42	8.74	280.56	39.24	46.55	88.43	55.61	44.83
14	16.06	224.1	49.37	55.53	99.98	65.36	53.18	43	8.67	281.43	39.12	46.44	87.81	55.43	44.67
15	15.45	227.38	48.63	54.84	99.96	64.82	52.7	44	8.6	282.24	39.0	46.33	87.21	55.26	44.53
16	14.88	230.58	47.94	54.21	99.94	64.28	52.21	45	8.53	283.0	38.89	46.23	86.63	55.1	44.39
17	14.35	233.68	47.28	53.61	99.9	63.73	51.72	46	8.48	283.72	38.79	46.14	86.09	54.95	44.26
18	13.87	236.68	46.66	53.06	99.85	63.19	51.23	47	8.42	284.4	38.69	46.06	85.57	54.81	44.14
19	13.42	239.59	46.08	52.55	99.77	62.96	51.06	48	8.37	285.03	38.6	45.98	85.08	54.68	44.03
20	13.0	242.4	45.54	52.07	99.67	62.53	50.69	49	8.33	285.62	38.52	45.9	84.6	54.55	43.93
21	12.62	245.11	45.03	51.62	99.53	62.1	50.32	50	8.28	286.17	38.44	45.83	84.15	54.44	43.83
22	12.26	247.72	44.54	51.19	99.35	61.68	49.97	51	8.24	286.69	38.37	45.77	83.73	54.33	43.74
23	11.93	250.22	44.09	50.79	99.13	61.27	49.62	52	8.21	287.17	38.3	45.71	83.32	54.24	43.66
24	11.63	252.63	43.66	50.41	98.85	60.88	49.28	53	8.17	287.63	38.24	45.65	82.94	54.13	43.57
25	11.34	254.93	43.26	50.06	98.53	60.49	48.95	54	8.14	288.05	38.18	45.6	82.58	54.03	43.49
26	11.08	257.13	42.88	49.73	98.17	60.11	48.64	55	8.11	288.45	38.13	45.55	82.23	53.94	43.41
27	10.84	259.24	42.53	49.43	97.76	59.75	48.33	56	8.08	288.82	38.08	45.5	81.91	53.85	43.33
28	10.61	261.25	42.2	49.14	97.3	59.4	48.03	57	8.06	289.16	38.03	45.46	81.6	53.77	43.27
29	10.41	263.16	41.89	48.87	96.79	59.06	47.74	58	8.03	289.49	37.99	45.42	81.32	53.7	43.2
30	10.21	264.98	41.61	48.62	96.24	58.74	47.47	59	8.01	289.79	37.95	45.39	81.05	53.63	43.14

Table A.48.: Mg^{5+}

Step	$\hat{E}$	$\hat{T}$	P_1	P_2	P_T	P_S	P_{AS}	Step	$\hat{E}$	$\hat{T}$	P_1	P_2	P_T	P_S	P_{AS}
2	76.92	122.87	81.41	89.54	100.0	72.17	59.46	31	13.68	237.9	46.42	52.85	99.82	64.96	52.69
3	67.21	129.57	78.89	87.12	100.0	72.4	59.64	32	13.46	239.34	46.13	52.6	99.78	64.79	52.54
4	58.96	136.42	76.35	84.5	100.0	72.63	59.82	33	13.25	240.7	45.87	52.36	99.74	64.56	52.35
5	51.95	143.37	73.84	81.77	100.0	72.84	59.99	34	13.06	241.99	45.62	52.14	99.68	64.34	52.16
6	45.97	150.39	71.36	78.98	100.0	73.07	60.17	35	12.88	243.21	45.38	51.94	99.63	64.14	51.99
7	40.81	157.43	68.94	76.18	100.0	73.24	60.3	36	12.72	244.37	45.16	51.74	99.57	63.94	51.82
8	36.42	164.45	66.57	73.45	100.0	73.29	60.34	37	12.57	245.46	44.96	51.56	99.51	63.76	51.67
9	32.7	171.39	64.28	70.84	100.0	73.02	60.06	38	12.43	246.48	44.77	51.39	99.44	63.58	51.52
10	29.52	178.21	62.09	68.38	100.0	72.66	59.7	39	12.3	247.45	44.59	51.23	99.37	63.42	51.38
11	26.81	184.85	60.0	66.1	100.0	72.21	59.27	40	12.17	248.37	44.42	51.09	99.3	63.27	51.25
12	24.5	191.27	58.05	64.04	100.0	71.62	58.71	41	12.06	249.22	44.27	50.95	99.22	63.12	51.13
13	22.53	197.44	56.25	62.18	99.99	70.98	58.12	42	11.96	250.03	44.12	50.82	99.14	62.99	51.01
14	21.65	200.41	55.41	61.34	99.99	70.66	57.82	43	11.86	250.79	43.98	50.7	99.07	62.86	50.91
15	20.84	203.31	54.6	60.54	99.99	70.32	57.51	44	11.77	251.5	43.86	50.59	98.99	62.74	50.81
16	20.09	206.13	53.84	59.78	99.99	69.99	57.2	45	11.68	252.17	43.74	50.48	98.91	62.63	50.71
17	19.39	208.86	53.12	59.07	99.99	69.65	56.89	46	11.6	252.8	43.63	50.38	98.83	62.53	50.63
18	18.75	211.51	52.43	58.39	99.99	69.3	56.58	47	11.53	253.39	43.53	50.29	98.75	62.43	50.54
19	18.16	214.07	51.78	57.75	99.99	69.0	56.29	48	11.46	253.94	43.43	50.21	98.68	62.34	50.47
20	17.61	216.54	51.16	57.18	99.99	68.58	55.92	49	11.4	254.46	43.34	50.13	98.6	62.26	50.4
21	17.1	218.93	50.58	56.65	99.99	68.18	55.56	50	11.34	254.94	43.26	50.06	98.53	62.18	50.33
22	16.63	221.22	50.03	56.14	99.98	67.78	55.2	51	11.29	255.39	43.18	49.99	98.46	62.11	50.27
23	16.19	223.43	49.52	55.67	99.98	67.4	54.86	52	11.24	255.82	43.11	49.93	98.4	62.06	50.23
24	15.79	225.54	49.04	55.22	99.97	67.02	54.52	53	11.19	256.21	43.04	49.87	98.33	61.98	50.16
25	15.42	227.56	48.59	54.8	99.96	66.66	54.2	54	11.15	256.58	42.98	49.81	98.27	61.91	50.1
26	15.07	229.5	48.17	54.42	99.95	66.31	53.88	55	11.1	256.93	42.92	49.76	98.21	61.84	50.04
27	14.75	231.35	47.77	54.06	99.93	65.97	53.58	56	11.07	257.25	42.86	49.71	98.15	61.77	49.98
28	14.45	233.11	47.4	53.72	99.91	65.65	53.29	57	11.03	257.56	42.81	49.67	98.09	61.71	49.93
29	14.17	234.79	47.05	53.41	99.89	65.34	53.01	58	11.0	257.84	42.77	49.63	98.04	61.66	49.88
30	13.92	236.38	46.72	53.11	99.86	65.04	52.74	59	10.97	258.1	42.72	49.59	97.99	61.61	49.84

Table A.49.: Mg^{6+}

Step	$\hat{E}$	$\hat{T}$	P_1	P_2	P_T	P_S	P_{AS}	Step	$\hat{E}$	$\hat{T}$	P_1	P_2	P_T	P_S	P_{AS}
2	95.49	112.65	85.29	92.89	100.0	72.87	60.04	31	17.52	216.98	51.06	57.08	99.99	70.17	57.21
3	83.91	118.74	82.98	90.96	100.0	73.2	60.31	32	17.24	218.27	50.74	56.79	99.99	70.0	57.06
4	73.68	124.97	80.62	88.8	100.0	73.52	60.57	33	16.98	219.5	50.44	56.52	99.99	69.77	56.85
5	64.99	131.3	78.24	86.47	100.0	73.85	60.83	34	16.74	220.67	50.17	56.27	99.99	69.55	56.65
6	57.59	137.68	75.88	84.01	100.0	74.24	61.15	35	16.52	221.77	49.91	56.03	99.98	69.34	56.46
7	51.29	144.09	73.58	81.48	100.0	74.62	61.45	36	16.31	222.8	49.67	55.8	99.98	69.14	56.29
8	45.91	150.46	71.34	78.95	100.0	74.91	61.69	37	16.12	223.79	49.44	55.59	99.98	68.95	56.12
9	41.26	156.77	69.17	76.44	100.0	75.1	61.84	38	15.95	224.71	49.23	55.4	99.97	68.78	55.96
10	37.3	162.96	67.08	74.02	100.0	75.2	61.91	39	15.78	225.58	49.03	55.21	99.97	68.61	55.82
11	33.92	168.99	65.07	71.73	100.0	75.17	61.88	40	15.63	226.4	48.85	55.04	99.97	68.46	55.68
12	31.05	174.81	63.17	69.59	100.0	74.74	61.45	41	15.49	227.18	48.68	54.88	99.96	68.31	55.55
13	28.59	180.4	61.39	67.62	100.0	74.38	61.09	42	15.35	227.9	48.52	54.73	99.96	68.18	55.43
14	27.5	183.1	60.54	66.69	100.0	74.18	60.91	43	15.23	228.59	48.37	54.6	99.96	68.06	55.32
15	26.48	185.72	59.73	65.8	100.0	73.99	60.72	44	15.12	229.23	48.23	54.47	99.95	67.94	55.21
16	25.54	188.27	58.95	64.97	100.0	73.78	60.53	45	15.01	229.83	48.1	54.35	99.95	67.83	55.12
17	24.68	190.75	58.2	64.2	100.0	73.58	60.33	46	14.91	230.39	47.98	54.24	99.94	67.73	55.03
18	23.88	193.15	57.49	63.47	99.99	73.37	60.13	47	14.82	230.92	47.86	54.14	99.94	67.64	54.94
19	23.13	195.46	56.81	62.77	99.99	73.21	59.97	48	14.73	231.42	47.76	54.04	99.93	67.55	54.87
20	22.45	197.7	56.17	62.11	99.99	72.91	59.7	49	14.66	231.88	47.66	53.96	99.93	67.47	54.79
21	21.81	199.86	55.56	61.49	99.99	72.62	59.44	50	14.58	232.32	47.57	53.87	99.92	67.4	54.73
22	21.22	201.93	54.98	60.92	99.99	72.33	59.18	51	14.51	232.73	47.48	53.79	99.92	67.33	54.67
23	20.67	203.92	54.43	60.38	99.99	72.05	58.93	52	14.45	233.11	47.4	53.72	99.91	67.28	54.62
24	20.17	205.83	53.92	59.86	99.99	71.78	58.68	53	14.39	233.46	47.33	53.65	99.91	67.21	54.55
25	19.7	207.65	53.43	59.38	99.99	71.52	58.44	54	14.33	233.8	47.26	53.59	99.9	67.13	54.49
26	19.26	209.4	52.97	58.93	99.99	71.27	58.22	55	14.28	234.11	47.19	53.53	99.9	67.06	54.43
27	18.86	211.07	52.54	58.5	99.99	71.03	58.0	56	14.24	234.4	47.13	53.48	99.89	67.0	54.37
28	18.48	212.66	52.14	58.1	99.99	70.8	57.79	57	14.19	234.67	47.08	53.43	99.89	66.94	54.32
29	18.14	214.17	51.75	57.73	99.99	70.58	57.59	58	14.15	234.93	47.02	53.38	99.88	66.89	54.27
30	17.81	215.61	51.39	57.4	99.99	70.37	57.39	59	14.11	235.16	46.97	53.34	99.88	66.84	54.22

Table A.50.: Mg^{7+}

Step	$\hat{E}$	$\hat{T}$	P_1	P_2	P_T	P_S	P_{AS}	Step	$\hat{E}$	$\hat{T}$	P_1	P_2	P_T	P_S	P_{AS}
2	114.0	104.71	88.2	95.07	100.0	73.38	60.47	31	21.51	200.89	55.27	61.21	99.99	74.03	60.58
3	100.38	110.35	86.14	93.56	100.0	73.77	60.78	32	21.18	202.08	54.94	60.88	99.99	73.92	60.48
4	88.75	116.1	83.98	91.82	100.0	74.17	61.11	33	20.87	203.21	54.63	60.57	99.99	73.73	60.31
5	78.42	121.95	81.76	89.87	100.0	74.57	61.44	34	20.58	204.27	54.34	60.28	99.99	73.56	60.16
6	69.55	127.84	79.54	87.76	100.0	75.08	61.85	35	20.31	205.28	54.06	60.01	99.99	73.39	60.01
7	61.99	133.75	77.33	85.53	100.0	75.61	62.28	36	20.06	206.24	53.81	59.76	99.99	73.23	59.86
8	55.56	139.64	75.17	83.24	100.0	76.06	62.65	37	19.83	207.14	53.57	59.52	99.99	73.08	59.73
9	50.07	145.46	73.1	80.94	100.0	76.45	62.96	38	19.61	207.98	53.35	59.29	99.99	72.94	59.61
10	45.36	151.17	71.09	78.67	100.0	76.74	63.21	39	19.41	208.78	53.14	59.08	99.99	72.81	59.49
11	41.29	156.72	69.18	76.46	100.0	76.93	63.35	40	19.23	209.54	52.94	58.89	99.99	72.69	59.38
12	37.82	162.1	67.36	74.36	100.0	76.91	63.33	41	19.06	210.25	52.76	58.71	99.99	72.58	59.28
13	34.86	167.25	65.64	72.39	100.0	76.85	63.27	42	18.9	210.91	52.58	58.54	99.99	72.48	59.19
14	33.54	169.73	64.83	71.45	100.0	76.7	63.11	43	18.75	211.54	52.42	58.38	99.99	72.38	59.1
15	32.32	172.15	64.03	70.56	100.0	76.6	63.01	44	18.61	212.12	52.27	58.24	99.99	72.29	59.02
16	31.2	174.5	63.27	69.71	100.0	76.5	62.9	45	18.48	212.68	52.13	58.1	99.99	72.2	58.94
17	30.15	176.77	62.54	68.89	100.0	76.39	62.79	46	18.36	213.19	52.0	57.97	99.99	72.13	58.87
18	29.19	178.98	61.84	68.11	100.0	76.28	62.68	47	18.25	213.68	51.88	57.85	99.99	72.06	58.8
19	28.3	181.11	61.16	67.37	100.0	76.22	62.6	48	18.14	214.13	51.76	57.74	99.99	71.99	58.75
20	27.47	183.17	60.52	66.67	100.0	76.0	62.4	49	18.05	214.56	51.66	57.64	99.99	71.93	58.69
21	26.7	185.15	59.91	66.0	100.0	75.79	62.21	50	17.96	214.96	51.56	57.54	99.99	71.87	58.64
22	25.99	187.06	59.33	65.36	100.0	75.58	62.01	51	17.88	215.33	51.46	57.46	99.99	71.82	58.59
23	25.33	188.89	58.77	64.78	100.0	75.38	61.83	52	17.8	215.68	51.38	57.38	99.99	71.79	58.57
24	24.71	190.64	58.23	64.23	100.0	75.18	61.65	53	17.73	216.01	51.3	57.3	99.99	71.73	58.51
25	24.15	192.32	57.73	63.72	99.99	74.99	61.48	54	17.66	216.31	51.22	57.24	99.99	71.67	58.45
26	23.62	193.93	57.26	63.23	99.99	74.81	61.31	55	17.6	216.6	51.15	57.17	99.99	71.61	58.4
27	23.13	195.46	56.81	62.77	99.99	74.64	61.15	56	17.54	216.86	51.08	57.11	99.99	71.56	58.36
28	22.68	196.92	56.4	62.34	99.99	74.47	61.0	57	17.49	217.11	51.02	57.05	99.99	71.52	58.31
29	22.26	198.31	56.0	61.93	99.99	74.32	60.85	58	17.44	217.35	50.97	57.0	99.99	71.47	58.27
30	21.88	199.63	55.62	61.56	99.99	74.17	60.71	59	17.39	217.56	50.91	56.95	99.99	71.43	58.23

Table A.51.: Mg^{8+}

Step	$\hat{E}$	$\hat{T}$	P_1	P_2	P_T	P_S	P_{AS}	Step	$\hat{E}$	$\hat{T}$	P_1	P_2	P_T	P_S	P_{AS}
2	0.0	98.32	90.44	96.53	100.0	73.76	60.78	31	25.64	188.01	59.04	65.05	100.0	76.92	63.11
3	117.02	103.59	88.61	95.35	100.0	74.2	61.14	32	25.25	189.12	58.7	64.71	100.0	76.86	63.05
4	103.5	108.97	86.66	93.96	100.0	74.65	61.51	33	24.88	190.16	58.38	64.38	100.0	76.71	62.91
5	91.94	114.42	84.62	92.35	100.0	75.11	61.89	34	24.54	191.16	58.08	64.08	100.0	76.56	62.78
6	81.82	119.93	82.53	90.56	100.0	75.71	62.38	35	24.22	192.1	57.8	63.79	99.99	76.43	62.66
7	72.98	125.45	80.44	88.63	100.0	76.35	62.9	36	23.93	192.98	57.54	63.52	99.99	76.3	62.54
8	65.44	130.94	78.37	86.6	100.0	76.93	63.38	37	23.66	193.82	57.29	63.26	99.99	76.18	62.44
9	59.01	136.37	76.37	84.52	100.0	77.46	63.81	38	23.4	194.61	57.06	63.03	99.99	76.07	62.34
10	53.53	141.69	74.44	82.43	100.0	77.91	64.18	39	23.17	195.35	56.85	62.8	99.99	75.96	62.24
11	48.85	146.87	72.6	80.38	100.0	78.25	64.45	40	22.95	196.05	56.64	62.59	99.99	75.87	62.15
12	44.81	151.88	70.84	78.38	100.0	78.37	64.54	41	22.75	196.71	56.46	62.4	99.99	75.78	62.07
13	41.32	156.68	69.19	76.48	100.0	78.45	64.6	42	22.56	197.33	56.28	62.22	99.99	75.69	62.0
14	39.77	159.0	68.4	75.57	100.0	78.47	64.62	43	22.38	197.91	56.11	62.04	99.99	75.62	61.93
15	38.34	161.25	67.64	74.69	100.0	78.49	64.64	44	22.22	198.45	55.96	61.89	99.99	75.54	61.86
16	37.01	163.44	66.91	73.84	100.0	78.5	64.64	45	22.07	198.97	55.81	61.74	99.99	75.48	61.8
17	35.79	165.56	66.2	73.03	100.0	78.51	64.65	46	21.93	199.45	55.68	61.61	99.99	75.42	61.75
18	34.65	167.62	65.52	72.25	100.0	78.51	64.64	47	21.8	199.9	55.55	61.48	99.99	75.36	61.7
19	33.6	169.6	64.87	71.5	100.0	78.47	64.58	48	21.68	200.32	55.43	61.36	99.99	75.31	61.65
20	32.63	171.52	64.24	70.79	100.0	78.32	64.43	49	21.56	200.72	55.32	61.25	99.99	75.27	61.61
21	31.73	173.37	63.64	70.12	100.0	78.16	64.28	50	21.46	201.09	55.22	61.15	99.99	75.23	61.57
22	30.89	175.14	63.06	69.48	100.0	78.01	64.14	51	21.36	201.43	55.12	61.06	99.99	75.19	61.53
23	30.12	176.85	62.52	68.86	100.0	77.87	64.01	52	21.27	201.76	55.03	60.97	99.99	75.17	61.52
24	29.4	178.48	62.0	68.28	100.0	77.73	63.88	53	21.18	202.06	54.94	60.88	99.99	75.12	61.47
25	28.74	180.04	61.5	67.74	100.0	77.59	63.75	54	21.11	202.34	54.87	60.81	99.99	75.07	61.42
26	28.12	181.54	61.03	67.23	100.0	77.47	63.63	55	21.03	202.61	54.79	60.73	99.99	75.02	61.38
27	27.55	182.96	60.58	66.74	100.0	77.34	63.51	56	20.96	202.86	54.72	60.67	99.99	74.98	61.34
28	27.02	184.32	60.16	66.28	100.0	77.23	63.4	57	20.9	203.09	54.66	60.6	99.99	74.94	61.3
29	26.52	185.61	59.77	65.84	100.0	77.12	63.3	58	20.84	203.3	54.6	60.54	99.99	74.9	61.27
30	26.07	186.84	59.39	65.43	100.0	77.01	63.2	59	20.79	203.51	54.55	60.49	99.99	74.87	61.24

Table A.52.: Mg^{9+}

Step	$\hat{E}$	$\hat{T}$	P_1	P_2	P_T	P_S	P_{AS}	Step	$\hat{E}$	$\hat{T}$	P_1	P_2	P_T	P_S	P_{AS}
2	0.0	93.04	92.18	97.52	100.0	74.05	61.03	31	29.88	177.39	62.35	68.67	100.0	79.17	65.07
3	0.0	98.0	90.55	96.6	100.0	74.53	61.42	32	29.42	178.43	62.02	68.3	100.0	79.15	65.05
4	118.48	103.06	88.8	95.48	100.0	75.03	61.83	33	29.0	179.42	61.7	67.96	100.0	79.02	64.93
5	105.28	108.2	86.94	94.16	100.0	75.54	62.25	34	28.61	180.35	61.4	67.63	100.0	78.9	64.82
6	93.99	113.39	85.01	92.67	100.0	76.21	62.79	35	28.25	181.23	61.12	67.33	100.0	78.79	64.72
7	84.21	118.58	83.04	91.01	100.0	76.93	63.39	36	27.91	182.06	60.86	67.05	100.0	78.68	64.63
8	75.55	123.75	81.08	89.23	100.0	77.61	63.95	37	27.6	182.85	60.62	66.78	100.0	78.59	64.54
9	68.17	128.85	79.16	87.38	100.0	78.24	64.46	38	27.3	183.59	60.39	66.53	100.0	78.5	64.46
10	61.86	133.86	77.29	85.49	100.0	78.81	64.93	39	27.03	184.29	60.17	66.29	100.0	78.41	64.38
11	56.48	138.74	75.5	83.6	100.0	79.28	65.31	40	26.78	184.94	59.97	66.07	100.0	78.33	64.31
12	51.87	143.45	73.81	81.74	100.0	79.5	65.49	41	26.54	185.56	59.78	65.86	100.0	78.26	64.24
13	47.94	147.96	72.21	79.95	100.0	79.69	65.64	42	26.33	186.14	59.61	65.66	100.0	78.19	64.18
14	46.17	150.14	71.45	79.08	100.0	79.77	65.71	43	26.12	186.69	59.44	65.48	100.0	78.13	64.13
15	44.52	152.26	70.71	78.23	100.0	79.85	65.77	44	25.93	187.2	59.29	65.31	100.0	78.08	64.08
16	42.99	154.31	70.0	77.42	100.0	79.92	65.82	45	25.76	187.68	59.14	65.16	100.0	78.03	64.03
17	41.58	156.31	69.32	76.63	100.0	79.98	65.87	46	25.6	188.13	59.0	65.02	100.0	77.98	63.98
18	40.27	158.24	68.66	75.87	100.0	80.03	65.91	47	25.45	188.55	58.87	64.88	100.0	77.94	63.95
19	39.06	160.11	68.03	75.13	100.0	80.15	66.01	48	25.3	188.95	58.75	64.76	100.0	77.9	63.91
20	37.93	161.91	67.42	74.43	100.0	80.06	65.93	49	25.17	189.32	58.64	64.64	100.0	77.86	63.88
21	36.89	163.64	66.84	73.76	100.0	79.98	65.86	50	25.05	189.67	58.53	64.54	100.0	77.83	63.85
22	35.93	165.31	66.28	73.12	100.0	79.91	65.81	51	24.94	189.99	58.43	64.44	100.0	77.8	63.82
23	35.04	166.91	65.75	72.52	100.0	79.86	65.76	52	24.83	190.3	58.34	64.34	100.0	77.8	63.81
24	34.21	168.45	65.25	71.94	100.0	79.82	65.73	53	24.74	190.58	58.25	64.25	100.0	77.75	63.77
25	33.44	169.91	64.77	71.38	100.0	79.62	65.52	54	24.64	190.85	58.17	64.17	100.0	77.71	63.73
26	32.73	171.32	64.31	70.87	100.0	79.53	65.43	55	24.56	191.09	58.1	64.1	100.0	77.67	63.69
27	32.07	172.66	63.87	70.38	100.0	79.45	65.35	56	24.48	191.33	58.03	64.02	100.0	77.63	63.66
28	31.46	173.93	63.45	69.91	100.0	79.37	65.28	57	24.41	191.54	57.96	63.96	100.0	77.6	63.63
29	30.89	175.14	63.06	69.48	100.0	79.3	65.2	58	24.34	191.75	57.9	63.89	100.0	77.57	63.6
30	30.37	176.3	62.69	69.06	100.0	79.23	65.14	59	24.28	191.93	57.85	63.84	100.0	77.54	63.57

Table A.53.: Mg^{10+}

Step	$\hat{E}$	$\hat{T}$	P_1	P_2	P_T	P_S	P_{AS}	Step	$\hat{E}$	$\hat{T}$	P_1	P_2	P_T	P_S	P_{AS}
2	0.0	87.99	0.0	0.0	0.0	0.0	0.0	31	34.21	168.45	65.25	71.93	100.0	81.15	66.82
3	0.0	93.27	92.11	97.48	100.0	74.8	61.65	32	33.69	169.43	64.93	71.56	100.0	80.98	66.64
4	0.0	98.07	90.53	96.58	100.0	75.33	62.08	33	33.21	170.36	64.62	71.22	100.0	80.87	66.55
5	118.82	102.94	88.84	95.51	100.0	75.88	62.53	34	32.77	171.24	64.33	70.89	100.0	80.77	66.46
6	106.1	107.86	87.06	94.26	100.0	76.6	63.12	35	32.36	172.08	64.06	70.59	100.0	80.68	66.37
7	95.22	112.78	85.24	92.85	100.0	77.39	63.78	36	31.97	172.86	63.8	70.3	100.0	80.59	66.3
8	85.86	117.67	83.39	91.31	100.0	78.16	64.4	37	31.62	173.6	63.56	70.03	100.0	80.51	66.22
9	77.5	122.51	81.55	89.67	100.0	78.87	64.99	38	31.29	174.3	63.33	69.78	100.0	80.44	66.16
10	70.37	127.26	79.76	87.97	100.0	79.54	65.54	39	30.98	174.96	63.12	69.54	100.0	80.37	66.09
11	64.27	131.87	78.03	86.25	100.0	80.1	66.0	40	30.69	175.58	62.92	69.32	100.0	80.31	66.03
12	59.05	136.33	76.38	84.54	100.0	80.41	66.25	41	30.43	176.17	62.74	69.11	100.0	80.25	65.98
13	54.59	140.6	74.83	82.86	100.0	80.69	66.47	42	30.18	176.72	62.56	68.91	100.0	80.2	65.93
14	52.61	142.66	74.09	82.05	100.0	80.81	66.57	43	29.95	177.23	62.4	68.73	100.0	80.15	65.89
15	50.77	144.67	73.38	81.25	100.0	80.93	66.67	44	29.74	177.72	62.25	68.55	100.0	80.1	65.85
16	49.07	146.61	72.69	80.48	100.0	81.05	66.76	45	29.54	178.17	62.1	68.39	100.0	80.06	65.81
17	47.49	148.5	72.02	79.73	100.0	81.15	66.85	46	29.35	178.6	61.96	68.24	100.0	80.03	65.77
18	46.02	150.33	71.38	79.0	100.0	81.25	66.93	47	29.18	179.0	61.84	68.1	100.0	79.99	65.74
19	44.64	152.1	70.77	78.3	100.0	81.44	67.08	48	29.02	179.37	61.72	67.97	100.0	79.97	65.72
20	43.37	153.8	70.18	77.62	100.0	81.35	67.01	49	28.88	179.72	61.6	67.85	100.0	79.94	65.69
21	42.18	155.44	69.62	76.97	100.0	81.28	66.95	50	28.74	180.05	61.5	67.74	100.0	79.92	65.67
22	41.09	157.02	69.08	76.34	100.0	81.22	66.9	51	28.61	180.36	61.4	67.63	100.0	79.9	65.65
23	40.08	158.53	68.56	75.75	100.0	81.17	66.86	52	28.49	180.64	61.31	67.53	100.0	79.9	65.65
24	39.13	159.99	68.07	75.18	100.0	81.14	66.82	53	28.38	180.91	61.23	67.44	100.0	79.86	65.61
25	38.26	161.37	67.6	74.64	100.0	81.11	66.8	54	28.28	181.16	61.15	67.35	100.0	79.82	65.58
26	37.45	162.7	67.16	74.12	100.0	81.1	66.79	55	28.18	181.4	61.07	67.27	100.0	79.79	65.55
27	36.7	163.97	66.73	73.63	100.0	81.09	66.78	56	28.09	181.62	61.0	67.2	100.0	79.76	65.52
28	36.01	165.17	66.33	73.17	100.0	81.09	66.78	57	28.01	181.82	60.94	67.13	100.0	79.73	65.49
29	35.36	166.32	65.95	72.74	100.0	81.1	66.79	58	27.93	182.01	60.88	67.06	100.0	79.7	65.47
30	34.76	167.41	65.59	72.33	100.0	81.12	66.8	59	27.86	182.19	60.82	67.0	100.0	79.68	65.44

Table A.54.: Mg^{11+}

Step	$\hat{E}$	$\hat{T}$	P_1	P_2	P_T	P_S	P_{AS}	Step	$\hat{E}$	$\hat{T}$	P_1	P_2	P_T	P_S	P_{AS}
2	0.0	84.2	0.0	0.0	0.0	0.0	0.0	31	38.64	160.78	67.8	74.87	100.0	82.23	67.72
3	0.0	88.62	0.0	0.0	0.0	0.0	0.0	32	38.06	161.71	67.49	74.51	100.0	82.29	67.78
4	0.0	93.78	91.94	97.39	100.0	75.58	62.29	33	37.52	162.6	67.2	74.16	100.0	82.25	67.74
5	0.0	98.42	90.41	96.51	100.0	76.15	62.76	34	37.02	163.43	66.92	73.84	100.0	82.21	67.71
6	118.37	103.1	88.78	95.47	100.0	76.92	63.39	35	36.55	164.22	66.65	73.54	100.0	82.18	67.68
7	106.25	107.79	87.09	94.27	100.0	77.78	64.1	36	36.12	164.97	66.4	73.25	100.0	82.15	67.66
8	95.88	112.46	85.36	92.95	100.0	78.6	64.77	37	35.72	165.68	66.16	72.98	100.0	82.13	67.64
9	87.0	117.06	83.62	91.51	100.0	79.39	65.42	38	35.35	166.34	65.94	72.73	100.0	82.11	67.62
10	79.02	121.58	81.9	89.99	100.0	80.13	66.03	39	35.01	166.97	65.73	72.49	100.0	82.09	67.61
11	72.2	125.97	80.24	88.44	100.0	80.78	66.56	40	34.69	167.56	65.54	72.27	100.0	82.08	67.6
12	66.37	130.22	78.64	86.87	100.0	81.15	66.87	41	34.39	168.11	65.36	72.06	100.0	82.07	67.59
13	61.37	134.29	77.14	85.33	100.0	81.5	67.15	42	34.11	168.64	65.18	71.86	100.0	82.07	67.58
14	59.15	136.24	76.41	84.57	100.0	81.67	67.29	43	33.85	169.13	65.03	71.68	100.0	81.8	67.33
15	57.09	138.15	75.71	83.83	100.0	81.82	67.41	44	33.61	169.59	64.88	71.51	100.0	81.76	67.3
16	55.19	140.01	75.04	83.1	100.0	81.97	67.54	45	33.39	170.02	64.74	71.34	100.0	81.73	67.27
17	53.42	141.8	74.4	82.39	100.0	82.12	67.65	46	33.18	170.42	64.6	71.19	100.0	81.7	67.24
18	51.79	143.54	73.78	81.7	100.0	82.26	67.76	47	32.99	170.8	64.48	71.06	100.0	81.68	67.22
19	50.27	145.22	73.18	81.03	100.0	82.49	67.95	48	32.81	171.16	64.36	70.93	100.0	81.66	67.2
20	48.87	146.84	72.61	80.39	100.0	82.41	67.89	49	32.64	171.49	64.25	70.8	100.0	81.64	67.18
21	47.57	148.4	72.06	79.77	100.0	82.35	67.84	50	32.49	171.8	64.15	70.69	100.0	81.62	67.16
22	46.36	149.91	71.53	79.17	100.0	82.29	67.79	51	32.35	172.1	64.05	70.58	100.0	81.61	67.15
23	45.22	151.35	71.03	78.59	100.0	82.25	67.75	52	32.21	172.37	63.96	70.48	100.0	81.62	67.15
24	44.16	152.73	70.55	78.05	100.0	82.22	67.73	53	32.09	172.62	63.88	70.39	100.0	81.58	67.12
25	43.19	154.05	70.09	77.52	100.0	82.19	67.7	54	31.97	172.86	63.8	70.3	100.0	81.55	67.09
26	42.28	155.31	69.66	77.02	100.0	82.18	67.69	55	31.86	173.09	63.73	70.22	100.0	81.52	67.06
27	41.44	156.51	69.25	76.54	100.0	82.17	67.69	56	31.76	173.3	63.66	70.15	100.0	81.5	67.04
28	40.66	157.66	68.86	76.09	100.0	82.18	67.69	57	31.67	173.49	63.6	70.07	100.0	81.47	67.01
29	39.93	158.75	68.49	75.66	100.0	82.19	67.69	58	31.58	173.67	63.54	70.01	100.0	81.45	66.99
30	39.26	159.79	68.13	75.26	100.0	82.2	67.71	59	31.5	173.84	63.48	69.95	100.0	81.43	66.97

Table A.55.: Mg^{12+}

Step	$\hat{E}$	$\hat{T}$	P_1	P_2	P_T	P_S	P_{AS}	Step	$\hat{E}$	$\hat{T}$	P_1	P_2	P_T	P_S	P_{AS}
2	0.0	80.88	0.0	0.0	0.0	0.0	0.0	31	43.15	154.1	70.08	77.5	100.0	83.13	68.48
3	0.0	85.12	0.0	0.0	0.0	0.0	0.0	32	42.5	154.99	69.77	77.15	100.0	83.19	68.53
4	0.0	89.45	0.0	0.0	0.0	0.0	0.0	33	41.91	155.84	69.48	76.81	100.0	83.15	68.49
5	0.0	94.48	91.72	97.27	100.0	76.39	62.96	34	41.35	156.64	69.21	76.5	100.0	83.11	68.46
6	0.0	98.96	90.22	96.4	100.0	77.19	63.62	35	40.84	157.39	68.95	76.2	100.0	83.08	68.44
7	117.41	103.45	88.66	95.39	100.0	78.09	64.36	36	40.36	158.11	68.71	75.92	100.0	83.06	68.42
8	105.97	107.91	87.04	94.24	100.0	78.97	65.08	37	39.91	158.78	68.48	75.65	100.0	83.04	68.4
9	96.17	112.32	85.41	92.99	100.0	79.82	65.78	38	39.5	159.42	68.26	75.4	100.0	83.02	68.38
10	87.77	116.64	83.78	91.65	100.0	80.63	66.45	39	39.12	160.02	68.06	75.17	100.0	83.01	68.37
11	80.26	120.84	82.18	90.25	100.0	81.34	67.03	40	38.76	160.58	67.87	74.95	100.0	82.99	68.36
12	73.8	124.9	80.65	88.83	100.0	81.78	67.39	41	38.43	161.11	67.69	74.74	100.0	82.99	68.36
13	68.26	128.78	79.18	87.41	100.0	82.19	67.72	42	38.12	161.61	67.52	74.55	100.0	82.98	68.35
14	65.8	130.66	78.48	86.71	100.0	82.38	67.88	43	37.83	162.08	67.37	74.36	100.0	82.98	68.35
15	63.52	132.48	77.8	86.02	100.0	82.57	68.03	44	37.57	162.52	67.22	74.19	100.0	82.98	68.35
16	61.41	134.25	77.15	85.34	100.0	82.75	68.18	45	37.32	162.93	67.09	74.03	100.0	82.98	68.35
17	59.45	135.97	76.51	84.68	100.0	82.92	68.32	46	37.09	163.31	66.96	73.88	100.0	82.99	68.35
18	57.64	137.63	75.9	84.03	100.0	83.09	68.46	47	36.87	163.68	66.83	73.74	100.0	82.99	68.36
19	55.96	139.24	75.32	83.4	100.0	83.36	68.68	48	36.68	164.02	66.72	73.62	100.0	83.0	68.36
20	54.41	140.79	74.76	82.79	100.0	83.29	68.63	49	36.49	164.34	66.61	73.49	100.0	83.01	68.37
21	52.97	142.28	74.23	82.2	100.0	83.24	68.58	50	36.32	164.63	66.51	73.38	100.0	83.02	68.38
22	51.63	143.71	73.71	81.63	100.0	83.19	68.53	51	36.16	164.91	66.42	73.27	100.0	83.03	68.39
23	50.39	145.09	73.23	81.09	100.0	83.15	68.5	52	36.01	165.17	66.33	73.18	100.0	83.06	68.41
24	49.24	146.41	72.76	80.56	100.0	83.12	68.48	53	35.87	165.42	66.25	73.08	100.0	83.05	68.4
25	48.18	147.67	72.31	80.06	100.0	83.1	68.46	54	35.74	165.64	66.17	73.0	100.0	83.04	68.39
26	47.19	148.88	71.89	79.58	100.0	83.08	68.45	55	35.62	165.86	66.1	72.91	100.0	83.03	68.38
27	46.26	150.03	71.49	79.12	100.0	83.08	68.44	56	35.51	166.06	66.03	72.84	100.0	83.02	68.37
28	45.39	151.12	71.11	78.68	100.0	83.08	68.44	57	35.41	166.24	65.97	72.77	100.0	83.01	68.37
29	44.59	152.17	70.74	78.27	100.0	83.09	68.45	58	35.31	166.42	65.91	72.7	100.0	83.01	68.36
30	43.84	153.16	70.4	77.88	100.0	83.1	68.46	59	35.22	166.58	65.86	72.64	100.0	83.0	68.35

Table A.56.: Si^{1+}

Step	$\hat{E}$	$\hat{T}$	P_1	P_2	P_T	P_S	P_{AS}	Step	$\hat{E}$	$\hat{T}$	P_1	P_2	P_T	P_S	P_{AS}
2	8.4	298.92	65.77	72.44	85.13	46.72	37.57	31	1.23	0.0	29.35	29.04	0.03	13.16	10.44
3	7.16	317.23	63.15	70.05	68.32	44.13	35.42	32	1.21	0.0	28.97	28.66	0.03	12.96	10.28
4	6.12	336.23	60.59	67.21	47.96	41.24	33.02	33	1.19	0.0	28.61	28.3	0.03	12.76	10.12
5	5.25	355.89	58.31	63.88	29.59	38.58	30.84	34	1.17	0.0	28.27	27.97	0.03	12.57	9.97
6	4.56	376.21	56.75	60.05	16.94	35.84	28.61	35	1.16	0.0	27.96	27.66	0.03	12.39	9.83
7	3.97	397.24	55.87	56.12	9.1	33.23	26.48	36	1.14	0.0	27.67	27.37	0.03	12.21	9.69
8	3.47	418.74	53.5	53.14	4.76	30.73	24.46	37	1.13	0.0	27.39	27.09	0.03	12.06	9.57
9	3.06	440.17	50.84	50.47	2.52	28.46	22.63	38	1.12	0.0	27.12	26.83	0.02	11.93	9.46
10	2.73	461.48	48.31	47.94	1.39	26.3	20.89	39	1.11	0.0	26.88	26.59	0.02	11.8	9.36
11	2.46	482.71	45.93	45.56	0.82	24.44	19.4	40	1.1	0.0	26.65	26.36	0.02	11.68	9.27
12	2.23	503.7	43.68	43.32	0.5	22.63	17.95	41	1.09	0.0	26.44	26.15	0.02	11.56	9.18
13	2.04	0.0	41.57	41.22	0.32	21.12	16.75	42	1.08	0.0	26.23	25.95	0.02	11.45	9.09
14	1.95	0.0	40.58	40.23	0.27	20.36	16.14	43	1.07	0.0	26.04	25.76	0.02	11.35	9.01
15	1.87	0.0	39.63	39.28	0.22	19.7	15.62	44	1.06	0.0	25.87	25.58	0.02	11.25	8.93
16	1.8	0.0	38.71	38.37	0.18	19.09	15.13	45	1.05	0.0	25.71	25.42	0.02	11.16	8.86
17	1.74	0.0	37.85	37.5	0.15	18.47	14.65	46	1.05	0.0	25.55	25.27	0.02	11.08	8.79
18	1.68	0.0	37.01	36.66	0.13	17.89	14.18	47	1.04	0.0	25.41	25.13	0.02	11.01	8.74
19	1.62	0.0	36.21	35.87	0.11	17.39	13.79	48	1.03	0.0	25.28	25.0	0.02	10.95	8.69
20	1.58	0.0	35.47	35.13	0.1	16.9	13.4	49	1.03	0.0	25.15	24.87	0.02	10.88	8.64
21	1.53	0.0	34.74	34.4	0.09	16.42	13.02	50	1.02	0.0	25.03	24.75	0.02	10.83	8.6
22	1.49	0.0	34.05	33.72	0.08	15.98	12.67	51	1.02	0.0	24.92	24.64	0.02	10.77	8.55
23	1.45	0.0	33.41	33.08	0.07	15.59	12.36	52	1.02	0.0	24.82	24.54	0.02	10.72	8.51
24	1.41	0.0	32.8	32.48	0.06	15.21	12.06	53	1.01	0.0	24.73	24.45	0.02	10.67	8.47
25	1.38	0.0	32.21	31.88	0.06	14.85	11.77	54	1.01	0.0	24.64	24.36	0.02	10.63	8.44
26	1.35	0.0	31.65	31.33	0.05	14.51	11.5	55	1.0	0.0	24.55	24.28	0.02	10.58	8.4
27	1.32	0.0	31.13	30.82	0.05	14.21	11.27	56	1.0	0.0	24.48	24.2	0.02	10.55	8.37
28	1.29	0.0	30.65	30.34	0.04	13.93	11.05	57	1.0	0.0	24.41	24.13	0.02	10.51	8.34
29	1.27	0.0	30.2	29.89	0.04	13.66	10.83	58	1.0	0.0	24.34	24.07	0.02	10.47	8.32
30	1.25	0.0	29.76	29.45	0.04	13.4	10.63	59	0.99	0.0	24.28	24.01	0.02	10.44	8.29

Table A.57.: Si^{2+}

Step	$\hat{E}$	$\hat{T}$	P_1	P_2	P_T	P_S	P_{AS}	Step	$\hat{E}$	$\hat{T}$	P_1	P_2	P_T	P_S	P_{AS}
2	22.22	208.46	76.83	81.07	99.99	62.37	50.96	31	3.23	431.07	51.94	51.58	3.29	30.32	24.12
3	19.11	220.55	75.54	79.96	99.99	60.83	49.56	32	3.17	434.11	51.57	51.2	3.01	30.02	23.87
4	16.49	233.0	74.19	78.9	99.98	59.06	47.97	33	3.12	436.99	51.22	50.85	2.77	29.71	23.63
5	14.28	245.73	72.76	77.8	99.87	57.33	46.46	34	3.07	439.72	50.89	50.53	2.56	29.42	23.4
6	12.43	258.68	71.19	76.64	99.37	55.51	44.91	35	3.03	442.3	50.59	50.22	2.37	29.14	23.17
7	10.86	271.75	69.52	75.39	97.68	53.48	43.18	36	2.99	444.74	50.29	49.92	2.21	28.88	22.96
8	9.55	284.87	67.75	74.04	93.48	51.27	41.31	37	2.95	447.04	50.01	49.64	2.07	28.63	22.76
9	8.47	297.94	65.9	72.55	85.85	49.1	39.49	38	2.91	449.23	49.75	49.38	1.95	28.39	22.57
10	7.56	310.87	64.05	70.9	74.75	47.22	37.93	39	2.88	451.28	49.5	49.13	1.84	28.17	22.39
11	6.79	323.58	62.26	69.1	61.55	45.23	36.28	40	2.85	453.23	49.27	48.9	1.74	27.96	22.22
12	6.13	335.99	60.62	67.25	48.21	43.14	34.55	41	2.82	455.06	49.05	48.68	1.65	27.76	22.06
13	5.58	348.02	59.19	65.19	36.34	41.3	33.04	42	2.79	456.78	48.85	48.48	1.57	27.57	21.91
14	5.34	353.87	58.53	64.21	31.23	40.5	32.39	43	2.77	458.41	48.66	48.29	1.5	27.39	21.76
15	5.11	359.61	57.96	63.2	26.83	39.7	31.74	44	2.75	459.93	48.49	48.11	1.45	27.22	21.63
16	4.92	365.22	57.48	62.15	23.07	38.9	31.08	45	2.73	461.37	48.32	47.95	1.39	27.06	21.5
17	4.73	370.7	57.05	61.13	19.82	38.11	30.43	46	2.71	462.71	48.17	47.8	1.35	26.91	21.38
18	4.56	376.04	56.76	60.08	17.03	37.32	29.79	47	2.69	463.98	48.02	47.65	1.3	26.77	21.27
19	4.41	381.25	56.49	59.08	14.64	36.55	29.16	48	2.68	465.17	47.89	47.52	1.26	26.64	21.16
20	4.26	386.32	56.26	58.12	12.61	35.76	28.52	49	2.66	466.28	47.77	47.39	1.23	26.52	21.06
21	4.13	391.23	56.08	57.21	10.9	35.21	28.07	50	2.65	467.32	47.65	47.28	1.2	26.46	21.02
22	4.0	395.99	55.91	56.35	9.45	34.64	27.61	51	2.63	468.3	47.54	47.17	1.17	26.38	20.95
23	3.89	400.6	55.76	55.52	8.22	34.07	27.15	52	2.62	469.21	47.44	47.07	1.14	26.3	20.89
24	3.78	405.03	55.25	54.89	7.19	33.53	26.71	53	2.61	470.07	47.34	46.97	1.12	26.22	20.83
25	3.68	409.29	54.7	54.34	6.32	33.0	26.28	54	2.6	470.87	47.25	46.88	1.09	26.15	20.77
26	3.59	413.36	54.17	53.81	5.59	32.48	25.87	55	2.59	471.62	47.17	46.8	1.07	26.08	20.71
27	3.5	417.25	53.68	53.32	4.97	31.99	25.46	56	2.58	472.32	47.09	46.72	1.05	26.02	20.66
28	3.43	420.97	53.22	52.86	4.45	31.51	25.08	57	2.57	472.98	47.01	46.64	1.04	25.96	20.62
29	3.36	424.5	52.77	52.41	4.0	31.05	24.7	58	2.57	473.59	46.94	46.57	1.02	25.91	20.57
30	3.29	427.87	52.34	51.98	3.62	30.6	24.34	59	2.56	474.16	46.88	46.51	1.01	25.86	20.53

Table A.58.: Si^{3+}

Step	$\hat{E}$	$\hat{T}$	P_1	P_2	P_T	P_S	P_{AS}	Step	$\hat{E}$	$\hat{T}$	P_1	P_2	P_T	P_S	P_{AS}
2	37.98	170.11	81.35	85.89	100.0	68.36	56.27	31	5.87	341.53	59.95	66.29	42.55	43.53	34.84
3	32.89	179.73	80.1	84.41	100.0	67.5	55.46	32	5.77	343.76	59.68	65.91	40.35	43.12	34.5
4	28.56	189.61	78.92	83.11	100.0	66.66	54.67	33	5.67	345.89	59.44	65.55	38.32	42.93	34.35
5	24.9	199.69	77.79	81.95	99.99	65.67	53.76	34	5.59	347.9	59.2	65.21	36.45	42.64	34.11
6	21.81	209.92	76.68	80.93	99.99	64.52	52.7	35	5.5	349.81	58.98	64.89	34.72	42.36	33.88
7	19.19	220.23	75.57	79.99	99.99	63.19	51.5	36	5.43	351.62	58.78	64.59	33.14	42.09	33.67
8	16.97	230.55	74.47	79.11	99.98	61.7	50.15	37	5.36	353.33	58.59	64.3	31.69	41.84	33.46
9	15.09	240.8	73.32	78.23	99.94	60.19	48.81	38	5.29	354.94	58.41	64.04	30.36	41.6	33.27
10	13.5	250.92	72.13	77.34	99.75	58.83	47.65	39	5.23	356.46	58.24	63.79	29.13	41.37	33.08
11	12.15	260.82	70.92	76.44	99.21	57.37	46.41	40	5.18	357.9	58.11	63.52	28.06	41.16	32.91
12	11.01	270.44	69.68	75.51	97.94	55.79	45.07	41	5.13	359.25	57.99	63.26	27.09	40.95	32.74
13	10.04	279.71	68.44	74.57	95.51	54.16	43.69	42	5.08	360.52	57.88	63.02	26.19	40.76	32.58
14	9.61	284.19	67.84	74.1	93.77	53.34	42.99	43	5.04	361.72	57.78	62.8	25.36	40.58	32.44
15	9.23	288.57	67.22	73.61	91.71	52.51	42.29	44	5.0	362.85	57.68	62.59	24.61	40.41	32.3
16	8.87	292.83	66.61	73.12	89.29	51.68	41.59	45	4.96	363.9	57.59	62.39	23.91	40.25	32.17
17	8.54	296.98	66.03	72.65	86.54	51.06	41.07	46	4.93	364.9	57.51	62.21	23.27	40.1	32.05
18	8.24	301.0	65.47	72.17	83.52	50.47	40.58	47	4.9	365.83	57.43	62.03	22.69	39.96	31.93
19	7.96	304.9	64.9	71.66	80.27	49.9	40.11	48	4.87	366.71	57.36	61.87	22.15	39.83	31.82
20	7.7	308.67	64.36	71.18	76.86	49.29	39.6	49	4.84	367.53	57.29	61.72	21.65	39.71	31.72
21	7.47	312.31	63.85	70.71	73.35	48.69	39.11	50	4.81	368.29	57.23	61.58	21.2	39.59	31.63
22	7.25	315.82	63.36	70.26	69.8	48.1	38.62	51	4.79	369.01	57.17	61.45	20.78	39.48	31.54
23	7.04	319.19	62.88	69.75	66.26	47.53	38.15	52	4.77	369.69	57.11	61.33	20.39	39.39	31.46
24	6.85	322.43	62.42	69.27	62.79	46.97	37.69	53	4.75	370.32	57.07	61.2	20.03	39.28	31.38
25	6.68	325.55	61.99	68.81	59.42	46.43	37.24	54	4.73	370.91	57.04	61.09	19.7	39.19	31.3
26	6.52	328.53	61.59	68.38	56.19	45.9	36.81	55	4.71	371.46	57.01	60.98	19.4	39.1	31.23
27	6.37	331.38	61.21	67.97	53.11	45.39	36.38	56	4.69	371.98	56.98	60.88	19.12	39.02	31.16
28	6.23	334.1	60.85	67.58	50.21	44.9	35.98	57	4.68	372.46	56.96	60.78	18.86	38.94	31.1
29	6.1	336.7	60.53	67.13	47.47	44.43	35.59	58	4.66	372.91	56.93	60.69	18.62	38.87	31.04
30	5.98	339.17	60.23	66.7	44.92	43.97	35.21	59	4.65	373.33	56.91	60.61	18.4	38.8	30.98

Table A.59.: Si^{4+}

Step	$\hat{E}$	$\hat{T}$	P_1	P_2	P_T	P_S	P_{AS}	Step	$\hat{E}$	$\hat{T}$	P_1	P_2	P_T	P_S	P_{AS}
2	54.85	147.68	84.86	90.14	100.0	70.36	57.94	31	8.91	292.39	66.67	73.17	89.56	53.32	42.91
3	47.67	155.9	83.45	88.47	100.0	70.35	57.93	32	8.76	294.24	66.41	72.96	88.4	52.95	42.6
4	41.56	164.32	82.17	86.88	100.0	70.31	57.88	33	8.62	296.0	66.17	72.76	87.23	52.72	42.42
5	36.39	172.91	80.98	85.44	100.0	69.95	57.53	34	8.49	297.66	65.94	72.58	86.06	52.45	42.19
6	32.01	181.61	79.87	84.14	100.0	69.35	56.96	35	8.37	299.23	65.73	72.4	84.89	52.2	41.98
7	28.27	190.36	78.84	83.02	100.0	68.64	56.29	36	8.26	300.72	65.51	72.21	83.74	51.95	41.78
8	25.09	199.12	77.85	82.02	99.99	67.81	55.52	37	8.16	302.13	65.3	72.02	82.61	51.72	41.59
9	22.4	207.8	76.9	81.13	99.99	66.87	54.66	38	8.06	303.46	65.11	71.85	81.51	51.5	41.41
10	20.12	216.36	75.99	80.34	99.99	65.83	53.71	39	7.98	304.71	64.92	71.69	80.44	51.29	41.24
11	18.17	224.73	75.1	79.61	99.99	64.68	52.66	40	7.89	305.88	64.75	71.53	79.4	51.1	41.08
12	16.52	232.85	74.21	78.91	99.98	63.37	51.49	41	7.82	306.99	64.6	71.39	78.4	50.92	40.92
13	15.11	240.66	73.33	78.24	99.94	62.16	50.41	42	7.75	308.04	64.45	71.26	77.45	50.74	40.78
14	14.49	244.44	72.9	77.91	99.89	61.64	49.97	43	7.68	309.02	64.31	71.13	76.53	50.58	40.65
15	13.91	248.12	72.47	77.59	99.83	61.13	49.53	44	7.62	309.94	64.18	71.01	75.65	50.43	40.52
16	13.38	251.71	72.04	77.27	99.73	60.61	49.09	45	7.56	310.81	64.06	70.9	74.82	50.28	40.4
17	12.89	255.19	71.62	76.96	99.58	60.09	48.65	46	7.51	311.62	63.94	70.8	74.03	50.15	40.29
18	12.44	258.57	71.2	76.65	99.38	59.57	48.21	47	7.46	312.38	63.84	70.71	73.27	50.02	40.18
19	12.02	261.84	70.8	76.35	99.12	59.08	47.8	48	7.42	313.09	63.74	70.62	72.56	49.9	40.09
20	11.63	265.0	70.39	76.05	98.78	58.53	47.33	49	7.37	313.76	63.64	70.53	71.89	49.79	40.0
21	11.28	268.05	69.99	75.75	98.35	57.99	46.87	50	7.33	314.39	63.56	70.46	71.26	49.69	39.91
22	10.95	270.98	69.62	75.46	97.84	57.46	46.42	51	7.3	314.98	63.48	70.38	70.66	49.59	39.83
23	10.64	273.8	69.26	75.19	97.23	56.94	45.98	52	7.26	315.52	63.4	70.31	70.09	49.51	39.76
24	10.36	276.51	68.88	74.9	96.52	56.44	45.55	53	7.23	316.04	63.33	70.23	69.56	49.42	39.68
25	10.1	279.11	68.52	74.63	95.72	55.94	45.14	54	7.2	316.52	63.26	70.16	69.07	49.33	39.61
26	9.86	281.59	68.18	74.37	94.83	55.47	44.73	55	7.17	316.97	63.19	70.09	68.6	49.25	39.54
27	9.63	283.96	67.87	74.13	93.87	55.0	44.34	56	7.15	317.39	63.13	70.02	68.16	49.17	39.48
28	9.43	286.23	67.56	73.89	92.86	54.56	43.96	57	7.13	317.78	63.08	69.97	67.75	49.1	39.42
29	9.24	288.38	67.25	73.64	91.8	54.13	43.6	58	7.1	318.15	63.03	69.91	67.36	49.03	39.36
30	9.07	290.44	66.95	73.4	90.7	53.71	43.25	59	7.08	318.49	62.98	69.86	67.0	48.97	39.31

Table A.60.: Si^{5+}

Step	$\hat{E}$	$\hat{T}$	P_1	P_2	P_T	P_S	P_{AS}	Step	$\hat{E}$	$\hat{T}$	P_1	P_2	P_T	P_S	P_{AS}
2	72.35	132.52	87.88	93.36	100.0	71.56	58.95	31	12.26	259.94	71.03	76.52	99.28	60.95	49.32
3	63.09	139.81	86.35	91.81	100.0	71.72	59.07	32	12.06	261.55	70.83	76.38	99.14	60.71	49.12
4	55.22	147.28	84.93	90.22	100.0	71.85	59.17	33	11.87	263.09	70.64	76.24	98.99	60.42	48.87
5	48.48	154.89	83.62	88.66	100.0	71.96	59.25	34	11.69	264.54	70.45	76.1	98.83	60.15	48.64
6	42.73	162.58	82.42	87.19	100.0	72.05	59.31	35	11.53	265.92	70.27	75.96	98.66	59.89	48.43
7	37.86	170.32	81.33	85.85	100.0	72.03	59.29	36	11.37	267.21	70.1	75.83	98.48	59.65	48.22
8	33.71	178.04	80.32	84.65	100.0	71.46	58.73	37	11.23	268.44	69.94	75.71	98.29	59.41	48.02
9	30.18	185.7	79.38	83.6	100.0	70.94	58.23	38	11.1	269.6	69.79	75.6	98.09	59.19	47.84
10	27.17	193.24	78.51	82.67	100.0	70.35	57.67	39	10.98	270.69	69.65	75.49	97.89	58.99	47.66
11	24.6	200.61	77.69	81.86	99.99	69.66	57.03	40	10.87	271.71	69.52	75.39	97.69	58.79	47.49
12	22.42	207.74	76.91	81.14	99.99	68.82	56.26	41	10.76	272.68	69.4	75.3	97.48	58.61	47.34
13	20.56	214.61	76.18	80.5	99.99	67.93	55.45	42	10.66	273.59	69.28	75.21	97.28	58.43	47.19
14	19.73	217.93	75.82	80.2	99.99	67.47	55.03	43	10.57	274.44	69.17	75.12	97.07	58.27	47.05
15	18.97	221.16	75.47	79.91	99.99	67.01	54.61	44	10.49	275.25	69.06	75.04	96.86	58.12	46.93
16	18.26	224.31	75.15	79.64	99.99	66.55	54.19	45	10.41	276.0	68.95	74.96	96.66	57.97	46.8
17	17.61	227.36	74.81	79.38	99.99	66.08	53.77	46	10.34	276.71	68.85	74.88	96.46	57.84	46.69
18	17.01	230.33	74.49	79.13	99.98	65.6	53.34	47	10.27	277.37	68.76	74.81	96.27	57.71	46.59
19	16.46	233.2	74.17	78.88	99.98	65.16	52.94	48	10.21	277.99	68.67	74.75	96.08	57.6	46.49
20	15.94	235.97	73.87	78.64	99.97	64.64	52.47	49	10.15	278.57	68.59	74.68	95.89	57.49	46.39
21	15.46	238.64	73.57	78.42	99.95	64.12	52.01	50	10.1	279.12	68.52	74.63	95.71	57.39	46.31
22	15.02	241.21	73.27	78.19	99.93	63.81	51.76	51	10.05	279.63	68.45	74.57	95.54	57.29	46.23
23	14.61	243.68	72.99	77.98	99.91	63.45	51.45	52	10.0	280.11	68.38	74.52	95.37	57.22	46.16
24	14.23	246.05	72.72	77.77	99.87	63.1	51.15	53	9.96	280.55	68.32	74.48	95.21	57.12	46.08
25	13.88	248.32	72.44	77.57	99.82	62.76	50.86	54	9.91	280.97	68.27	74.43	95.06	57.03	46.0
26	13.56	250.5	72.18	77.37	99.76	62.43	50.58	55	9.88	281.36	68.21	74.39	94.92	56.94	45.93
27	13.26	252.57	71.94	77.19	99.69	62.11	50.31	56	9.84	281.73	68.17	74.36	94.78	56.87	45.86
28	12.98	254.55	71.71	77.02	99.61	61.8	50.05	57	9.81	282.07	68.12	74.32	94.64	56.79	45.8
29	12.72	256.44	71.47	76.84	99.51	61.51	49.8	58	9.78	282.39	68.08	74.29	94.52	56.72	45.74
30	12.48	258.23	71.24	76.68	99.4	61.22	49.55	59	9.75	282.68	68.04	74.26	94.4	56.66	45.69

Table A.61.: Si^{6+}

Step	$\hat{E}$	$\hat{T}$	P_1	P_2	P_T	P_S	P_{AS}	Step	$\hat{E}$	$\hat{T}$	P_1	P_2	P_T	P_S	P_{AS}
2	90.5	121.39	90.39	95.59	100.0	72.37	59.62	31	15.85	236.45	73.81	78.6	99.97	66.06	53.62
3	79.02	128.02	88.87	94.29	100.0	72.63	59.83	32	15.59	237.9	73.66	78.48	99.96	65.83	53.41
4	69.26	134.8	87.39	92.87	100.0	72.88	60.03	33	15.35	239.28	73.5	78.36	99.95	65.54	53.15
5	60.97	141.7	85.98	91.4	100.0	73.12	60.22	34	15.13	240.58	73.34	78.24	99.94	65.42	53.07
6	53.91	148.67	84.68	89.93	100.0	73.39	60.44	35	14.92	241.82	73.2	78.14	99.93	65.23	52.91
7	47.84	155.67	83.49	88.51	100.0	73.61	60.61	36	14.73	242.98	73.07	78.04	99.91	65.04	52.75
8	42.68	162.66	82.41	87.18	100.0	73.73	60.7	37	14.55	244.08	72.94	77.94	99.9	64.87	52.6
9	38.28	169.59	81.43	85.97	100.0	73.73	60.7	38	14.38	245.12	72.83	77.86	99.88	64.7	52.46
10	34.54	176.4	80.53	84.89	100.0	73.35	60.3	39	14.23	246.1	72.71	77.77	99.87	64.55	52.33
11	31.35	183.05	79.7	83.94	100.0	72.97	59.93	40	14.08	247.02	72.6	77.69	99.85	64.4	52.21
12	28.61	189.49	78.94	83.12	100.0	72.43	59.43	41	13.95	247.89	72.49	77.61	99.83	64.27	52.09
13	26.28	195.68	78.23	82.4	100.0	71.86	58.89	42	13.83	248.71	72.4	77.53	99.81	64.14	51.98
14	25.25	198.67	77.9	82.07	99.99	71.56	58.61	43	13.71	249.47	72.31	77.46	99.79	64.02	51.88
15	24.29	201.58	77.59	81.75	99.99	71.26	58.33	44	13.6	250.19	72.22	77.4	99.77	63.91	51.79
16	23.4	204.41	77.27	81.47	99.99	70.95	58.05	45	13.5	250.87	72.14	77.34	99.75	63.8	51.7
17	22.59	207.17	76.97	81.19	99.99	70.64	57.76	46	13.41	251.5	72.07	77.28	99.73	63.71	51.62
18	21.83	209.83	76.69	80.94	99.99	70.33	57.47	47	13.33	252.1	72.0	77.23	99.71	63.62	51.54
19	21.13	212.41	76.42	80.7	99.99	70.06	57.22	48	13.25	252.65	71.93	77.18	99.69	63.53	51.47
20	20.48	214.91	76.15	80.47	99.99	69.67	56.87	49	13.17	253.18	71.87	77.14	99.67	63.46	51.4
21	19.88	217.31	75.88	80.25	99.99	69.29	56.52	50	13.1	253.66	71.82	77.1	99.65	63.38	51.34
22	19.33	219.62	75.64	80.05	99.99	68.91	56.19	51	13.04	254.12	71.76	77.06	99.63	63.32	51.28
23	18.81	221.84	75.4	79.85	99.99	68.55	55.86	52	12.98	254.55	71.71	77.02	99.61	63.27	51.24
24	18.34	223.97	75.18	79.67	99.99	68.2	55.55	53	12.93	254.95	71.66	76.98	99.59	63.19	51.18
25	17.9	226.02	74.96	79.49	99.99	67.85	55.24	54	12.87	255.33	71.61	76.94	99.57	63.12	51.12
26	17.49	227.97	74.75	79.33	99.99	67.52	54.94	55	12.83	255.68	71.56	76.91	99.55	63.06	51.06
27	17.11	229.83	74.54	79.17	99.99	67.21	54.65	56	12.78	256.0	71.52	76.88	99.54	63.0	51.01
28	16.76	231.61	74.35	79.02	99.98	66.9	54.38	57	12.74	256.31	71.48	76.85	99.52	62.94	50.96
29	16.43	233.31	74.16	78.87	99.98	66.61	54.12	58	12.7	256.59	71.45	76.83	99.51	62.89	50.92
30	16.13	234.92	73.98	78.73	99.97	66.33	53.86	59	12.67	256.86	71.41	76.8	99.49	62.84	50.87

Table A.62.: Si^{7+}

Step	$\hat{E}$	$\hat{T}$	P_1	P_2	P_T	P_S	P_{AS}	Step	$\hat{E}$	$\hat{T}$	P_1	P_2	P_T	P_S	P_{AS}
2	108.75	112.78	92.39	97.06	100.0	72.94	60.1	31	19.6	218.46	75.76	80.15	99.99	70.55	57.54
3	95.43	118.9	90.97	96.04	100.0	73.28	60.37	32	19.29	219.79	75.62	80.03	99.99	70.39	57.39
4	83.73	125.15	89.52	94.86	100.0	73.61	60.65	33	19.0	221.05	75.48	79.92	99.99	70.15	57.19
5	73.78	131.51	88.09	93.57	100.0	73.95	60.91	34	18.72	222.24	75.36	79.82	99.99	69.93	56.99
6	65.32	137.93	86.73	92.21	100.0	74.36	61.24	35	18.47	223.37	75.24	79.72	99.99	69.72	56.8
7	58.11	144.38	85.46	90.83	100.0	74.75	61.56	36	18.24	224.43	75.13	79.63	99.99	69.53	56.63
8	51.96	150.81	84.31	89.49	100.0	75.06	61.81	37	18.02	225.44	75.02	79.54	99.99	69.34	56.46
9	46.67	157.17	83.25	88.22	100.0	75.27	61.99	38	17.82	226.39	74.92	79.46	99.99	69.17	56.31
10	42.16	163.43	82.3	87.04	100.0	75.39	62.08	39	17.63	227.28	74.82	79.39	99.99	69.01	56.16
11	38.31	169.54	81.43	85.98	100.0	75.39	62.07	40	17.46	228.12	74.73	79.31	99.99	68.85	56.03
12	35.03	175.45	80.65	85.03	100.0	75.01	61.68	41	17.3	228.91	74.64	79.25	99.99	68.71	55.9
13	32.23	181.13	79.93	84.21	100.0	74.66	61.34	42	17.15	229.66	74.56	79.19	99.99	68.58	55.78
14	30.98	183.87	79.6	83.84	100.0	74.48	61.16	43	17.01	230.36	74.49	79.13	99.98	68.45	55.67
15	29.82	186.54	79.28	83.49	100.0	74.29	60.98	44	16.88	231.02	74.42	79.07	99.98	68.34	55.56
16	28.75	189.14	78.98	83.17	100.0	74.09	60.8	45	16.76	231.63	74.35	79.02	99.98	68.23	55.47
17	27.76	191.66	78.69	82.86	100.0	73.9	60.61	46	16.64	232.21	74.28	78.97	99.98	68.13	55.38
18	26.85	194.1	78.41	82.58	100.0	73.7	60.42	47	16.54	232.76	74.22	78.92	99.98	68.04	55.29
19	26.0	196.46	78.15	82.31	100.0	73.54	60.26	48	16.44	233.27	74.16	78.88	99.98	67.95	55.22
20	25.22	198.75	77.89	82.06	99.99	73.25	60.0	49	16.35	233.74	74.11	78.83	99.98	67.87	55.15
21	24.49	200.95	77.66	81.82	99.99	72.96	59.74	50	16.27	234.19	74.06	78.8	99.97	67.8	55.08
22	23.82	203.06	77.42	81.6	99.99	72.68	59.48	51	16.19	234.61	74.02	78.76	99.97	67.73	55.02
23	23.2	205.1	77.2	81.4	99.99	72.4	59.23	52	16.12	235.0	73.97	78.73	99.97	67.69	54.98
24	22.62	207.05	76.98	81.21	99.99	72.14	58.99	53	16.05	235.36	73.93	78.7	99.97	67.61	54.91
25	22.09	208.92	76.78	81.03	99.99	71.88	58.76	54	15.99	235.71	73.89	78.67	99.97	67.54	54.84
26	21.59	210.7	76.59	80.86	99.99	71.64	58.53	55	15.93	236.03	73.86	78.64	99.97	67.47	54.78
27	21.13	212.41	76.42	80.7	99.99	71.4	58.32	56	15.87	236.32	73.83	78.61	99.97	67.41	54.72
28	20.7	214.04	76.25	80.55	99.99	71.17	58.11	57	15.82	236.6	73.8	78.59	99.96	67.35	54.67
29	20.31	215.58	76.07	80.41	99.99	70.95	57.91	58	15.78	236.86	73.77	78.57	99.96	67.3	54.62
30	19.94	217.06	75.91	80.27	99.99	70.74	57.72	59	15.73	237.11	73.74	78.55	99.96	67.25	54.58

Table A.63.: Si^{8+}

Step	$\hat{E}$	$\hat{T}$	P_1	P_2	P_T	P_S	P_{AS}	Step	$\hat{E}$	$\hat{T}$	P_1	P_2	P_T	P_S	P_{AS}
2	127.0	105.85	93.95	98.02	100.0	73.37	60.46	31	23.49	204.12	77.3	81.49	99.99	73.9	60.47
3	111.67	111.56	92.67	97.24	100.0	73.77	60.78	32	23.12	205.35	77.17	81.37	99.99	73.8	60.37
4	98.57	117.4	91.32	96.3	100.0	74.16	61.11	33	22.78	206.51	77.04	81.26	99.99	73.6	60.2
5	86.93	123.33	89.94	95.22	100.0	74.57	61.43	34	22.45	207.62	76.92	81.15	99.99	73.42	60.04
6	77.02	129.31	88.58	94.02	100.0	75.08	61.85	35	22.16	208.66	76.7	81.05	99.99	73.25	59.88
7	68.59	135.32	87.28	92.77	100.0	75.6	62.28	36	21.88	209.65	76.7	80.96	99.99	73.09	59.74
8	61.4	141.3	86.06	91.49	100.0	76.05	62.65	37	21.62	210.58	76.61	80.87	99.99	72.94	59.6
9	55.27	147.23	84.94	90.23	100.0	76.43	62.95	38	21.38	211.46	76.51	80.79	99.99	72.8	59.48
10	50.0	153.05	83.92	89.02	100.0	76.73	63.19	39	21.16	212.29	76.43	80.71	99.99	72.66	59.36
11	45.49	158.73	83.01	87.92	100.0	76.9	63.33	40	20.96	213.07	76.35	80.64	99.99	72.54	59.25
12	41.63	164.22	82.18	86.9	100.0	76.88	63.3	41	20.77	213.8	76.27	80.57	99.99	72.42	59.14
13	38.34	169.49	81.44	85.99	100.0	76.81	63.24	42	20.59	214.49	76.2	80.51	99.99	72.32	59.05
14	36.88	172.04	81.09	85.58	100.0	76.66	63.07	43	20.42	215.14	76.12	80.45	99.99	72.22	58.96
15	35.52	174.52	80.77	85.18	100.0	76.55	62.96	44	20.27	215.75	76.06	80.39	99.99	72.12	58.87
16	34.27	176.93	80.46	84.82	100.0	76.44	62.85	45	20.13	216.32	75.99	80.34	99.99	72.04	58.79
17	33.11	179.27	80.16	84.48	100.0	76.33	62.74	46	19.99	216.85	75.93	80.29	99.99	71.96	58.72
18	32.04	181.54	79.88	84.15	100.0	76.21	62.62	47	19.87	217.36	75.88	80.25	99.99	71.89	58.66
19	31.04	183.73	79.62	83.85	100.0	76.15	62.54	48	19.76	217.83	75.83	80.2	99.99	71.82	58.6
20	30.12	185.85	79.36	83.58	100.0	75.92	62.34	49	19.65	218.27	75.78	80.16	99.99	71.76	58.54
21	29.26	187.89	79.12	83.32	100.0	75.71	62.14	50	19.55	218.68	75.74	80.13	99.99	71.7	58.49
22	28.47	189.85	78.9	83.08	100.0	75.49	61.94	51	19.46	219.07	75.69	80.09	99.99	71.65	58.44
23	27.73	191.74	78.69	82.85	100.0	75.29	61.75	52	19.37	219.43	75.66	80.06	99.99	71.62	58.41
24	27.05	193.54	78.48	82.64	100.0	75.09	61.57	53	19.29	219.77	75.62	80.03	99.99	71.55	58.35
25	26.42	195.28	78.28	82.44	100.0	74.9	61.39	54	19.22	220.08	75.59	80.0	99.99	71.49	58.3
26	25.84	196.93	78.09	82.26	100.0	74.71	61.22	55	19.15	220.38	75.55	79.98	99.99	71.43	58.24
27	25.3	198.51	77.92	82.08	99.99	74.53	61.06	56	19.09	220.66	75.53	79.95	99.99	71.38	58.2
28	24.79	200.02	77.76	81.92	99.99	74.36	60.9	57	19.03	220.91	75.5	79.93	99.99	71.33	58.15
29	24.33	201.46	77.6	81.76	99.99	74.2	60.75	58	18.97	221.16	75.47	79.91	99.99	71.29	58.11
30	23.9	202.82	77.45	81.62	99.99	74.05	60.61	59	18.92	221.38	75.45	79.89	99.99	71.25	58.07

Table A.64.: Si^{9+}

Step	$\hat{E}$	$\hat{T}$	P_1	P_2	P_T	P_S	P_{AS}	Step	$\hat{E}$	$\hat{T}$	P_1	P_2	P_T	P_S	P_{AS}
2	0.0	100.12	95.14	98.64	100.0	73.71	60.75	31	27.5	192.34	78.61	82.78	100.0	76.5	62.75
3	0.0	105.5	94.02	98.06	100.0	74.15	61.1	32	27.07	193.49	78.48	82.65	100.0	76.44	62.68
4	113.08	110.99	92.8	97.33	100.0	74.59	61.47	33	26.67	194.59	78.36	82.52	100.0	76.28	62.54
5	100.31	116.57	91.51	96.44	100.0	75.05	61.84	34	26.3	195.62	78.24	82.4	100.0	76.13	62.4
6	88.99	122.2	90.21	95.43	100.0	75.64	62.32	35	25.96	196.59	78.13	82.3	100.0	75.99	62.27
7	79.3	127.84	88.91	94.32	100.0	76.26	62.83	36	25.64	197.52	78.03	82.19	99.99	75.85	62.15
8	71.04	133.47	87.67	93.16	100.0	76.83	63.29	37	25.34	198.39	77.93	82.1	99.99	75.73	62.04
9	64.0	139.03	86.51	91.97	100.0	77.33	63.7	38	25.06	199.21	77.84	82.01	99.99	75.61	61.94
10	57.99	144.5	85.44	90.8	100.0	77.76	64.06	39	24.81	199.98	77.76	81.92	99.99	75.5	61.84
11	52.85	149.82	84.48	89.69	100.0	78.08	64.32	40	24.57	200.71	77.68	81.84	99.99	75.4	61.74
12	48.41	154.97	83.6	88.65	100.0	78.18	64.39	41	24.35	201.4	77.61	81.77	99.99	75.3	61.66
13	44.61	159.92	82.82	87.69	100.0	78.24	64.43	42	24.14	202.04	77.54	81.7	99.99	75.22	61.58
14	42.92	162.31	82.46	87.24	100.0	78.26	64.44	43	23.95	202.65	77.47	81.64	99.99	75.13	61.51
15	41.36	164.63	82.12	86.83	100.0	78.27	64.45	44	23.77	203.22	77.41	81.58	99.99	75.06	61.44
16	39.92	166.89	81.8	86.43	100.0	78.27	64.45	45	23.61	203.75	77.35	81.53	99.99	74.99	61.38
17	38.58	169.08	81.49	86.06	100.0	78.26	64.44	46	23.45	204.25	77.29	81.48	99.99	74.93	61.32
18	37.35	171.21	81.21	85.71	100.0	78.17	64.33	47	23.31	204.72	77.24	81.43	99.99	74.87	61.26
19	36.2	173.26	80.93	85.38	100.0	78.17	64.31	48	23.18	205.16	77.19	81.39	99.99	74.82	61.22
20	35.14	175.24	80.68	85.07	100.0	78.0	64.16	49	23.05	205.57	77.14	81.35	99.99	74.77	61.17
21	34.16	177.15	80.43	84.78	100.0	77.84	64.0	50	22.94	205.96	77.1	81.31	99.99	74.72	61.13
22	33.25	178.99	80.2	84.52	100.0	77.68	63.85	51	22.83	206.32	77.06	81.28	99.99	74.68	61.09
23	32.4	180.76	79.98	84.26	100.0	77.53	63.71	52	22.73	206.66	77.02	81.24	99.99	74.66	61.07
24	31.62	182.45	79.77	84.03	100.0	77.38	63.57	53	22.64	206.98	76.99	81.21	99.99	74.61	61.02
25	30.89	184.07	79.58	83.81	100.0	77.23	63.43	54	22.55	207.27	76.96	81.18	99.99	74.55	60.97
26	30.21	185.62	79.39	83.61	100.0	77.1	63.31	55	22.48	207.55	76.93	81.16	99.99	74.51	60.93
27	29.59	187.1	79.22	83.42	100.0	76.96	63.18	56	22.4	207.81	76.9	81.13	99.99	74.46	60.89
28	29.01	188.51	79.05	83.25	100.0	76.84	63.06	57	22.33	208.05	76.87	81.11	99.99	74.42	60.85
29	28.47	189.85	78.9	83.08	100.0	76.72	62.95	58	22.27	208.27	76.85	81.09	99.99	74.38	60.82
30	27.97	191.13	78.75	82.92	100.0	76.61	62.85	59	22.21	208.48	76.83	81.07	99.99	74.35	60.78

Table A.65.: Si^{10+}

Step	$\hat{E}$	$\hat{T}$	P_1	P_2	P_T	P_S	P_{AS}	Step	$\hat{E}$	$\hat{T}$	P_1	P_2	P_T	P_S	P_{AS}
2	0.0	94.53	0.0	0.0	0.0	0.0	0.0	31	31.62	182.45	79.77	84.03	100.0	78.58	64.56
3	0.0	100.37	95.09	98.62	100.0	74.45	61.36	32	31.13	183.54	79.64	83.88	100.0	78.55	64.53
4	127.8	105.58	94.01	98.05	100.0	74.94	61.76	33	30.67	184.57	79.52	83.75	100.0	78.42	64.41
5	113.41	110.86	92.83	97.35	100.0	75.44	62.16	34	30.25	185.54	79.4	83.62	100.0	78.29	64.29
6	101.11	116.19	91.6	96.51	100.0	76.09	62.7	35	29.86	186.46	79.29	83.5	100.0	78.17	64.18
7	90.23	121.54	90.36	95.56	100.0	76.79	63.27	36	29.49	187.33	79.19	83.39	100.0	78.06	64.08
8	80.88	126.86	89.13	94.52	100.0	77.45	63.81	37	29.15	188.15	79.09	83.29	100.0	77.95	63.99
9	72.91	132.12	87.96	93.44	100.0	78.05	64.31	38	28.84	188.92	79.0	83.19	100.0	77.86	63.9
10	66.1	137.29	86.86	92.34	100.0	78.6	64.75	39	28.55	189.65	78.92	83.1	100.0	77.77	63.82
11	60.28	142.32	85.86	91.27	100.0	79.03	65.1	40	28.28	190.34	78.84	83.02	100.0	77.68	63.74
12	55.31	147.19	84.95	90.24	100.0	79.22	65.26	41	28.02	190.99	78.77	82.94	100.0	77.6	63.67
13	51.03	151.86	84.12	89.27	100.0	79.39	65.39	42	27.79	191.59	78.7	82.87	100.0	77.53	63.6
14	49.11	154.11	83.74	88.81	100.0	79.45	65.44	43	27.57	192.16	78.64	82.8	100.0	77.47	63.54
15	47.34	156.31	83.39	88.39	100.0	79.51	65.49	44	27.37	192.7	78.57	82.74	100.0	77.4	63.49
16	45.7	158.44	83.05	87.97	100.0	79.57	65.53	45	27.18	193.2	78.51	82.68	100.0	77.35	63.44
17	44.18	160.51	82.73	87.58	100.0	79.61	65.57	46	27.01	193.67	78.46	82.62	100.0	77.3	63.39
18	42.78	162.52	82.43	87.2	100.0	79.65	65.6	47	26.84	194.12	78.41	82.57	100.0	77.25	63.35
19	41.48	164.46	82.15	86.86	100.0	79.75	65.67	48	26.69	194.53	78.36	82.53	100.0	77.21	63.31
20	40.27	166.33	81.88	86.53	100.0	79.65	65.59	49	26.55	194.92	78.32	82.48	100.0	77.17	63.27
21	39.16	168.13	81.63	86.22	100.0	79.57	65.52	50	26.42	195.28	78.28	82.44	100.0	77.14	63.24
22	38.12	169.86	81.39	85.93	100.0	79.5	65.46	51	26.3	195.62	78.24	82.4	100.0	77.1	63.21
23	37.16	171.53	81.16	85.66	100.0	79.32	65.27	52	26.19	195.94	78.2	82.37	100.0	77.09	63.2
24	36.27	173.13	80.95	85.4	100.0	79.21	65.17	53	26.08	196.24	78.17	82.33	100.0	77.05	63.15
25	35.45	174.65	80.75	85.16	100.0	79.1	65.07	54	25.98	196.52	78.14	82.3	100.0	77.0	63.11
26	34.69	176.12	80.56	84.94	100.0	79.0	64.97	55	25.89	196.78	78.11	82.27	100.0	76.96	63.07
27	33.98	177.51	80.38	84.73	100.0	78.91	64.88	56	25.81	197.02	78.08	82.25	100.0	76.92	63.04
28	33.32	178.84	80.22	84.54	100.0	78.82	64.79	57	25.73	197.25	78.06	82.22	100.0	76.89	63.01
29	32.71	180.11	80.06	84.36	100.0	78.74	64.71	58	25.66	197.46	78.03	82.2	99.99	76.85	62.98
30	32.14	181.31	79.91	84.19	100.0	78.66	64.64	59	25.59	197.66	78.01	82.18	99.99	76.83	62.95

Table A.66.: Si^{11+}

Step	$\hat{E}$	$\hat{T}$	P_1	P_2	P_T	P_S	P_{AS}	Step	$\hat{E}$	$\hat{T}$	P_1	P_2	P_T	P_S	P_{AS}
2	0.0	90.43	0.0	0.0	0.0	0.0	0.0	31	35.8	174.0	80.84	85.26	100.0	80.28	66.05
3	0.0	95.21	0.0	0.0	0.0	0.0	0.0	32	35.25	175.02	80.7	85.1	100.0	80.28	66.04
4	0.0	100.92	94.98	98.56	100.0	75.22	61.99	33	34.75	176.0	80.58	84.95	100.0	80.16	65.93
5	126.68	105.96	93.92	98.0	100.0	75.75	62.43	34	34.27	176.92	80.46	84.82	100.0	80.06	65.83
6	112.97	111.03	92.79	97.32	100.0	76.46	63.01	35	33.84	177.79	80.35	84.69	100.0	79.96	65.74
7	101.26	116.12	91.62	96.52	100.0	77.23	63.64	36	33.43	178.62	80.24	84.57	100.0	79.86	65.66
8	90.89	121.19	90.44	95.62	100.0	77.96	64.24	37	33.05	179.4	80.15	84.46	100.0	79.77	65.58
9	81.97	126.19	89.28	94.65	100.0	78.65	64.8	38	32.7	180.13	80.06	84.35	100.0	79.69	65.5
10	74.36	131.11	88.18	93.65	100.0	79.28	65.32	39	32.37	180.82	79.97	84.26	100.0	79.62	65.43
11	67.85	135.89	87.15	92.64	100.0	79.8	65.75	40	32.07	181.47	79.89	84.16	100.0	79.55	65.37
12	62.28	140.52	86.21	91.66	100.0	80.08	65.97	41	31.79	182.09	79.82	84.08	100.0	79.48	65.31
13	57.52	144.96	85.35	90.71	100.0	80.32	66.17	42	31.52	182.66	79.75	84.0	100.0	79.42	65.26
14	55.4	147.1	84.96	90.26	100.0	80.43	66.26	43	31.28	183.2	79.68	83.92	100.0	79.37	65.21
15	53.44	149.18	84.59	89.83	100.0	80.53	66.34	44	31.05	183.71	79.62	83.86	100.0	79.32	65.16
16	51.6	151.21	84.24	89.41	100.0	80.63	66.42	45	30.84	184.19	79.56	83.79	100.0	79.27	65.12
17	49.9	153.17	83.9	89.0	100.0	80.72	66.49	46	30.64	184.63	79.51	83.74	100.0	79.23	65.08
18	48.33	155.08	83.59	88.63	100.0	80.8	66.55	47	30.46	185.05	79.46	83.68	100.0	79.2	65.05
19	46.87	156.92	83.29	88.27	100.0	80.96	66.68	48	30.29	185.45	79.41	83.63	100.0	79.16	65.02
20	45.51	158.69	83.01	87.93	100.0	80.87	66.61	49	30.13	185.82	79.37	83.59	100.0	79.13	64.99
21	44.26	160.4	82.75	87.6	100.0	80.8	66.54	50	29.98	186.16	79.33	83.54	100.0	79.11	64.96
22	43.1	162.05	82.5	87.29	100.0	80.73	66.49	51	29.85	186.48	79.29	83.5	100.0	79.08	64.94
23	42.02	163.63	82.27	87.0	100.0	80.68	66.45	52	29.72	186.78	79.25	83.46	100.0	79.08	64.94
24	41.03	165.15	82.05	86.74	100.0	80.64	66.41	53	29.6	187.07	79.22	83.43	100.0	79.04	64.9
25	40.1	166.6	81.84	86.48	100.0	80.62	66.39	54	29.49	187.33	79.19	83.39	100.0	79.0	64.86
26	39.24	167.98	81.65	86.24	100.0	80.6	66.37	55	29.39	187.58	79.16	83.36	100.0	78.96	64.83
27	38.45	169.31	81.46	86.02	100.0	80.59	66.36	56	29.29	187.81	79.13	83.33	100.0	78.93	64.79
28	37.71	170.57	81.29	85.81	100.0	80.59	66.36	57	29.21	188.02	79.11	83.31	100.0	78.9	64.77
29	37.03	171.77	81.13	85.62	100.0	80.38	66.15	58	29.12	188.22	79.08	83.28	100.0	78.87	64.74
30	36.39	172.91	80.98	85.44	100.0	80.33	66.1	59	29.05	188.41	79.06	83.26	100.0	78.85	64.72

Table A.67.: Si^{12+}

Step	$\hat{E}$	$\hat{T}$	P_1	P_2	P_T	P_S	P_{AS}	Step	$\hat{E}$	$\hat{T}$	P_1	P_2	P_T	P_S	P_{AS}
2	0.0	86.85	0.0	0.0	0.0	0.0	0.0	31	40.07	166.65	81.83	86.47	100.0	81.68	67.27
3	0.0	91.43	0.0	0.0	0.0	0.0	0.0	32	39.46	167.63	81.7	86.3	100.0	81.75	67.32
4	0.0	96.1	0.0	0.0	0.0	0.0	0.0	33	38.89	168.56	81.57	86.14	100.0	81.71	67.28
5	0.0	101.68	94.83	98.49	100.0	76.02	62.65	34	38.37	169.44	81.45	86.0	100.0	81.67	67.25
6	124.99	106.54	93.8	97.93	100.0	76.77	63.26	35	37.88	170.27	81.33	85.86	100.0	81.63	67.22
7	112.05	111.41	92.71	97.27	100.0	77.59	63.94	36	37.43	171.06	81.23	85.73	100.0	81.6	67.2
8	100.99	116.25	91.59	96.5	100.0	78.38	64.59	37	37.01	171.8	81.13	85.61	100.0	81.29	66.9
9	91.19	121.03	90.48	95.65	100.0	79.14	65.21	38	36.62	172.5	81.03	85.5	100.0	81.22	66.84
10	82.75	125.73	89.39	94.75	100.0	79.84	65.79	39	36.26	173.16	80.95	85.4	100.0	81.16	66.78
11	75.54	130.3	88.36	93.82	100.0	80.45	66.29	40	35.92	173.78	80.87	85.3	100.0	81.1	66.73
12	69.37	134.72	87.4	92.89	100.0	80.79	66.56	41	35.6	174.36	80.79	85.21	100.0	81.05	66.68
13	64.09	138.95	86.52	91.99	100.0	81.1	66.82	42	35.31	174.91	80.72	85.12	100.0	81.0	66.63
14	61.74	141.0	86.12	91.55	100.0	81.25	66.94	43	35.04	175.43	80.65	85.04	100.0	80.95	66.59
15	59.57	142.99	85.73	91.13	100.0	81.39	67.05	44	34.79	175.91	80.59	84.97	100.0	80.91	66.55
16	57.56	144.92	85.36	90.71	100.0	81.52	67.15	45	34.56	176.37	80.53	84.9	100.0	80.88	66.52
17	55.69	146.8	85.02	90.33	100.0	81.64	67.26	46	34.34	176.79	80.48	84.84	100.0	80.85	66.49
18	53.97	148.61	84.69	89.95	100.0	81.76	67.35	47	34.14	177.19	80.42	84.78	100.0	80.82	66.46
19	52.35	150.37	84.38	89.58	100.0	81.97	67.52	48	33.95	177.57	80.38	84.72	100.0	80.79	66.44
20	50.85	152.06	84.09	89.23	100.0	81.89	67.45	49	33.78	177.92	80.33	84.67	100.0	80.77	66.42
21	49.46	153.69	83.81	88.9	100.0	81.82	67.39	50	33.61	178.25	80.29	84.63	100.0	80.75	66.4
22	48.17	155.26	83.56	88.59	100.0	81.76	67.35	51	33.46	178.55	80.25	84.58	100.0	80.73	66.38
23	46.98	156.77	83.31	88.3	100.0	81.71	67.31	52	33.32	178.84	80.22	84.54	100.0	80.73	66.38
24	45.87	158.22	83.09	88.02	100.0	81.68	67.28	53	33.19	179.11	80.18	84.5	100.0	80.7	66.35
25	44.84	159.6	82.87	87.75	100.0	81.65	67.25	54	33.07	179.36	80.15	84.46	100.0	80.66	66.31
26	43.89	160.92	82.67	87.5	100.0	81.64	67.24	55	32.96	179.6	80.12	84.43	100.0	80.63	66.28
27	43.01	162.18	82.48	87.27	100.0	81.63	67.23	56	32.85	179.82	80.09	84.4	100.0	80.6	66.26
28	42.19	163.39	82.3	87.05	100.0	81.63	67.23	57	32.75	180.02	80.07	84.37	100.0	80.58	66.23
29	41.43	164.53	82.14	86.84	100.0	81.64	67.24	58	32.66	180.21	80.04	84.34	100.0	80.55	66.21
30	40.72	165.62	81.98	86.65	100.0	81.66	67.25	59	32.58	180.39	80.02	84.32	100.0	80.53	66.19

Table A.68.: Si^{13+}

Step	$\hat{E}$	$\hat{T}$	P_1	P_2	P_T	P_S	P_{AS}	Step	$\hat{E}$	$\hat{T}$	P_1	P_2	P_T	P_S	P_{AS}
2	0.0	83.7	0.0	0.0	0.0	0.0	0.0	31	44.41	160.2	82.78	87.64	100.0	82.56	68.0
3	0.0	88.1	0.0	0.0	0.0	0.0	0.0	32	43.74	161.14	82.64	87.46	100.0	82.62	68.05
4	0.0	92.58	0.0	0.0	0.0	0.0	0.0	33	43.11	162.03	82.5	87.3	100.0	82.58	68.02
5	0.0	97.13	0.0	0.0	0.0	0.0	0.0	34	42.54	162.87	82.38	87.14	100.0	82.54	67.99
6	0.0	102.58	94.64	98.39	100.0	77.03	63.48	35	42.0	163.67	82.26	87.0	100.0	82.51	67.96
7	122.97	107.25	93.64	97.84	100.0	77.9	64.2	36	41.5	164.42	82.15	86.86	100.0	82.48	67.94
8	110.85	111.9	92.59	97.19	100.0	78.74	64.89	37	41.04	165.13	82.05	86.74	100.0	82.46	67.92
9	100.48	116.49	91.53	96.46	100.0	79.56	65.56	38	40.61	165.8	81.95	86.62	100.0	82.44	67.9
10	91.27	120.99	90.48	95.66	100.0	80.32	66.19	39	40.21	166.43	81.87	86.51	100.0	82.43	67.89
11	83.34	125.38	89.47	94.82	100.0	80.99	66.74	40	39.84	167.02	81.78	86.41	100.0	82.41	67.88
12	76.57	129.61	88.52	93.96	100.0	81.39	67.07	41	39.49	167.58	81.7	86.31	100.0	82.41	67.87
13	70.76	133.67	87.63	93.11	100.0	81.76	67.37	42	39.17	168.11	81.63	86.22	100.0	82.4	67.86
14	68.18	135.63	87.21	92.7	100.0	81.94	67.51	43	38.87	168.6	81.56	86.14	100.0	82.4	67.86
15	65.79	137.54	86.81	92.29	100.0	82.11	67.65	44	38.59	169.06	81.5	86.06	100.0	82.4	67.86
16	63.58	139.39	86.44	91.9	100.0	82.27	67.78	45	38.34	169.5	81.44	85.99	100.0	82.4	67.86
17	61.53	141.19	86.08	91.51	100.0	82.42	67.91	46	38.1	169.9	81.38	85.92	100.0	82.4	67.86
18	59.63	142.93	85.74	91.14	100.0	82.57	68.03	47	37.87	170.29	81.33	85.86	100.0	82.41	67.87
19	57.87	144.61	85.42	90.78	100.0	82.82	68.23	48	37.67	170.64	81.28	85.8	100.0	82.42	67.87
20	56.24	146.23	85.12	90.44	100.0	82.74	68.17	49	37.47	170.98	81.24	85.75	100.0	82.43	67.88
21	54.73	147.8	84.84	90.12	100.0	82.68	68.11	50	37.3	171.29	81.19	85.7	100.0	82.14	67.61
22	53.33	149.3	84.57	89.8	100.0	82.63	68.07	51	37.13	171.59	81.16	85.65	100.0	82.12	67.6
23	52.02	150.74	84.32	89.5	100.0	82.59	68.03	52	36.97	171.86	81.12	85.6	100.0	82.13	67.6
24	50.8	152.13	84.08	89.21	100.0	82.55	68.01	53	36.83	172.12	81.08	85.56	100.0	82.1	67.57
25	49.67	153.45	83.85	88.95	100.0	82.53	67.98	54	36.7	172.36	81.05	85.52	100.0	82.07	67.54
26	48.62	154.71	83.65	88.7	100.0	82.51	67.97	55	36.57	172.59	81.02	85.49	100.0	82.04	67.52
27	47.65	155.92	83.45	88.46	100.0	82.51	67.97	56	36.45	172.8	80.99	85.46	100.0	82.02	67.49
28	46.74	157.07	83.27	88.24	100.0	82.51	67.97	57	36.35	172.99	80.97	85.42	100.0	82.0	67.47
29	45.91	158.17	83.09	88.02	100.0	82.52	67.97	58	36.25	173.18	80.94	85.39	100.0	81.97	67.45
30	45.13	159.21	82.93	87.83	100.0	82.54	67.98	59	36.15	173.35	80.92	85.37	100.0	81.96	67.43

Table A.69.: Si^{14+}

Step	$\hat{E}$	$\hat{T}$	P_1	P_2	P_T	P_S	P_{AS}	Step	$\hat{E}$	$\hat{T}$	P_1	P_2	P_T	P_S	P_{AS}
2	0.0	80.88	0.0	0.0	0.0	0.0	0.0	31	48.82	154.48	83.68	88.74	100.0	83.31	68.63
3	0.0	85.12	0.0	0.0	0.0	0.0	0.0	32	48.08	155.38	83.54	88.57	100.0	83.37	68.68
4	0.0	89.45	0.0	0.0	0.0	0.0	0.0	33	47.4	156.23	83.4	88.4	100.0	83.33	68.65
5	0.0	93.83	0.0	0.0	0.0	0.0	0.0	34	46.77	157.04	83.27	88.24	100.0	83.3	68.62
6	0.0	98.25	0.0	0.0	0.0	0.0	0.0	35	46.18	157.8	83.15	88.09	100.0	83.27	68.59
7	0.0	103.55	94.44	98.29	100.0	78.16	64.42	36	45.64	158.53	83.04	87.96	100.0	83.24	68.57
8	120.82	108.03	93.47	97.74	100.0	79.05	65.15	37	45.13	159.21	82.93	87.83	100.0	83.22	68.55
9	109.53	112.45	92.47	97.11	100.0	79.91	65.86	38	44.66	159.85	82.83	87.71	100.0	83.2	68.54
10	99.87	116.78	91.46	96.41	100.0	80.74	66.54	39	44.22	160.45	82.74	87.59	100.0	83.19	68.52
11	91.25	121.0	90.48	95.66	100.0	81.46	67.13	40	43.82	161.02	82.65	87.48	100.0	83.18	68.51
12	83.86	125.07	89.54	94.88	100.0	81.91	67.5	41	43.44	161.56	82.57	87.38	100.0	83.17	68.51
13	77.53	128.98	88.66	94.09	100.0	82.33	67.84	42	43.09	162.06	82.5	87.29	100.0	83.16	68.5
14	74.71	130.86	88.24	93.7	100.0	82.53	68.0	43	42.76	162.54	82.43	87.2	100.0	83.16	68.5
15	72.11	132.69	87.84	93.32	100.0	82.72	68.16	44	42.46	162.98	82.36	87.12	100.0	83.16	68.5
16	69.69	134.48	87.46	92.94	100.0	82.91	68.32	45	42.18	163.4	82.3	87.04	100.0	83.17	68.5
17	67.45	136.2	87.09	92.58	100.0	83.09	68.46	46	41.92	163.79	82.24	86.97	100.0	83.17	68.5
18	65.38	137.88	86.74	92.22	100.0	83.27	68.61	47	41.67	164.16	82.19	86.91	100.0	83.17	68.51
19	63.46	139.49	86.42	91.88	100.0	83.55	68.84	48	41.45	164.5	82.14	86.85	100.0	83.18	68.51
20	61.68	141.05	86.11	91.54	100.0	83.48	68.78	49	41.24	164.83	82.09	86.79	100.0	83.19	68.52
21	60.03	142.55	85.81	91.22	100.0	83.42	68.73	50	41.04	165.13	82.05	86.74	100.0	83.2	68.53
22	58.5	144.0	85.53	90.91	100.0	83.37	68.69	51	40.86	165.41	82.01	86.69	100.0	83.21	68.54
23	57.09	145.39	85.28	90.62	100.0	83.33	68.66	52	40.69	165.67	81.97	86.64	100.0	83.24	68.56
24	55.77	146.72	85.03	90.34	100.0	83.3	68.63	53	40.53	165.92	81.94	86.6	100.0	83.23	68.55
25	54.55	147.99	84.8	90.08	100.0	83.28	68.61	54	40.38	166.15	81.9	86.56	100.0	83.21	68.54
26	53.42	149.2	84.59	89.82	100.0	83.27	68.6	55	40.25	166.37	81.87	86.52	100.0	83.21	68.53
27	52.36	150.37	84.38	89.58	100.0	83.26	68.6	56	40.12	166.57	81.85	86.49	100.0	83.2	68.52
28	51.37	151.47	84.19	89.35	100.0	83.26	68.6	57	40.0	166.76	81.82	86.46	100.0	83.19	68.51
29	50.45	152.52	84.01	89.13	100.0	83.27	68.6	58	39.89	166.93	81.79	86.42	100.0	83.19	68.51
30	49.61	153.52	83.84	88.93	100.0	83.29	68.61	59	39.79	167.1	81.77	86.4	100.0	83.18	68.5

Table A.70.: S^{1+}

Step	$\hat{E}$	$\hat{T}$	P_1	P_2	P_T	P_S	P_{AS}	Step	$\hat{E}$	$\hat{T}$	P_1	P_2	P_T	P_S	P_{AS}
2	7.77	320.56	64.15	70.92	77.5	43.78	35.14	31	1.09	0.0	27.75	27.45	0.02	11.07	8.79
3	6.6	340.64	62.23	68.51	57.75	40.77	32.64	32	1.08	0.0	27.36	27.06	0.02	10.89	8.65
4	5.62	361.64	60.71	65.51	37.35	38.03	30.4	33	1.06	0.0	26.99	26.69	0.02	10.71	8.51
5	4.83	383.58	59.69	61.85	21.65	35.14	28.03	34	1.04	0.0	26.65	26.35	0.02	10.54	8.37
6	4.16	406.39	58.24	58.05	11.46	32.48	25.88	35	1.03	0.0	26.32	26.02	0.02	10.38	8.24
7	3.61	429.62	55.44	55.06	5.83	29.78	23.69	36	1.02	0.0	26.01	25.72	0.02	10.23	8.12
8	3.15	453.03	52.63	52.25	2.96	27.5	21.85	37	1.0	0.0	25.72	25.43	0.02	10.1	8.02
9	2.78	476.71	49.92	49.56	1.58	25.25	20.05	38	0.99	0.0	25.45	25.17	0.02	9.98	7.93
10	2.48	500.57	47.33	46.96	0.88	23.23	18.44	39	0.98	0.0	25.2	24.92	0.02	9.86	7.83
11	2.23	0.0	44.85	44.49	0.51	21.44	17.0	40	0.97	0.0	24.97	24.68	0.01	9.75	7.75
12	2.02	0.0	42.53	42.17	0.32	19.77	15.67	41	0.97	0.0	24.75	24.46	0.01	9.65	7.67
13	1.84	0.0	40.36	40.0	0.2	18.31	14.52	42	0.96	0.0	24.54	24.26	0.01	9.55	7.59
14	1.76	0.0	39.33	38.98	0.17	17.64	13.99	43	0.95	0.0	24.35	24.07	0.01	9.46	7.52
15	1.69	0.0	38.35	38.0	0.14	17.04	13.51	44	0.94	0.0	24.17	23.89	0.01	9.38	7.45
16	1.63	0.0	37.42	37.06	0.12	16.43	13.03	45	0.94	0.0	24.0	23.72	0.01	9.31	7.4
17	1.57	0.0	36.5	36.16	0.1	15.88	12.59	46	0.93	0.0	23.85	23.57	0.01	9.24	7.34
18	1.51	0.0	35.64	35.3	0.09	15.38	12.2	47	0.92	0.0	23.7	23.42	0.01	9.18	7.29
19	1.46	0.0	34.82	34.49	0.07	14.89	11.81	48	0.92	0.0	23.56	23.28	0.01	9.11	7.24
20	1.42	0.0	34.03	33.7	0.06	14.43	11.44	49	0.91	0.0	23.43	23.16	0.01	9.06	7.2
21	1.37	0.0	33.29	32.97	0.06	14.02	11.12	50	0.91	0.0	23.31	23.04	0.01	9.0	7.16
22	1.33	0.0	32.59	32.28	0.05	13.63	10.81	51	0.91	0.0	23.2	22.93	0.01	8.95	7.12
23	1.3	0.0	31.91	31.6	0.05	13.24	10.5	52	0.9	0.0	23.1	22.82	0.01	8.91	7.08
24	1.26	0.0	31.28	30.96	0.04	12.91	10.24	53	0.9	0.0	23.0	22.73	0.01	8.86	7.05
25	1.23	0.0	30.68	30.37	0.04	12.6	9.99	54	0.9	0.0	22.91	22.64	0.01	8.82	7.01
26	1.21	0.0	30.13	29.82	0.03	12.29	9.75	55	0.89	0.0	22.83	22.56	0.01	8.78	6.98
27	1.18	0.0	29.59	29.28	0.03	12.01	9.53	56	0.89	0.0	22.75	22.48	0.01	8.75	6.95
28	1.15	0.0	29.08	28.78	0.03	11.76	9.33	57	0.89	0.0	22.68	22.41	0.01	8.72	6.93
29	1.13	0.0	28.61	28.3	0.03	11.52	9.14	58	0.88	0.0	22.61	22.34	0.01	8.69	6.91
30	1.11	0.0	28.16	27.86	0.02	11.29	8.96	59	0.88	0.0	22.55	22.28	0.01	8.67	6.89

Table A.71.: S^{2+}

Step	$\hat{E}$	$\hat{T}$	P_1	P_2	P_T	P_S	P_{AS}	Step	$\hat{E}$	$\hat{T}$	P_1	P_2	P_T	P_S	P_{AS}
2	20.76	222.88	76.84	81.15	99.99	60.23	49.07	31	2.93	466.6	51.06	50.69	2.05	26.86	21.34
3	17.84	235.86	74.98	79.63	99.99	58.39	47.41	32	2.88	469.97	50.68	50.31	1.88	26.5	21.05
4	15.37	249.23	73.1	78.17	99.93	56.59	45.85	33	2.83	473.17	50.33	49.96	1.73	26.23	20.84
5	13.29	262.92	71.22	76.74	99.64	54.69	44.23	34	2.79	476.2	49.98	49.61	1.6	25.97	20.62
6	11.54	276.87	69.36	75.33	98.52	52.54	42.4	35	2.75	479.08	49.65	49.29	1.49	25.71	20.42
7	10.08	291.01	67.56	73.94	95.39	50.15	40.38	36	2.72	481.81	49.35	48.98	1.39	25.47	20.23
8	8.87	305.24	65.85	72.53	88.91	47.99	38.57	37	2.68	484.39	49.06	48.69	1.3	25.24	20.04
9	7.85	319.48	64.26	71.05	78.44	45.89	36.84	38	2.65	486.83	48.79	48.42	1.23	25.02	19.87
10	6.98	333.65	62.85	69.4	64.95	43.66	34.99	39	2.62	489.14	48.54	48.17	1.16	24.82	19.7
11	6.25	347.64	61.67	67.55	50.56	41.45	33.16	40	2.59	491.32	48.3	47.93	1.1	24.62	19.55
12	5.63	361.38	60.72	65.56	37.57	39.61	31.66	41	2.57	493.37	48.08	47.71	1.05	24.44	19.4
13	5.13	374.78	60.04	63.35	27.21	37.73	30.13	42	2.55	495.3	47.88	47.51	1.0	24.26	19.26
14	4.9	381.32	59.74	62.29	22.98	36.78	29.35	43	2.52	497.12	47.69	47.32	0.96	24.1	19.13
15	4.69	387.75	59.6	61.05	19.34	35.83	28.58	44	2.5	498.83	47.51	47.14	0.92	23.94	19.0
16	4.5	394.06	59.46	59.86	16.26	35.07	27.96	45	2.49	500.44	47.34	46.97	0.88	23.8	18.89
17	4.33	400.21	58.88	58.93	13.68	34.35	27.38	46	2.47	501.96	47.19	46.81	0.85	23.66	18.78
18	4.16	406.2	58.26	58.07	11.53	33.65	26.81	47	2.45	503.38	47.03	46.66	0.82	23.53	18.67
19	4.02	412.01	57.64	57.27	9.75	32.96	26.25	48	2.44	504.71	46.89	46.52	0.8	23.41	18.58
20	3.88	417.62	56.92	56.55	8.28	32.26	25.69	49	2.42	505.96	46.76	46.39	0.78	23.3	18.48
21	3.75	423.04	56.24	55.87	7.06	31.58	25.14	50	2.41	507.13	46.63	46.27	0.76	23.19	18.4
22	3.64	428.26	55.61	55.23	6.07	30.91	24.6	51	2.4	508.23	46.52	46.15	0.74	23.09	18.32
23	3.53	433.27	54.99	54.61	5.24	30.34	24.14	52	2.39	509.26	46.41	46.04	0.72	23.0	18.29
24	3.43	438.09	54.4	54.02	4.55	29.85	23.75	53	2.38	510.22	46.31	45.94	0.7	22.97	18.23
25	3.34	442.72	53.85	53.46	3.98	29.38	23.36	54	2.37	511.12	46.21	45.85	0.69	22.91	18.18
26	3.26	447.15	53.33	52.94	3.5	28.92	23.0	55	2.36	511.96	46.13	45.76	0.68	22.84	18.13
27	3.18	451.41	52.82	52.44	3.1	28.48	22.64	56	2.35	0.0	46.04	45.68	0.66	22.79	18.08
28	3.11	455.47	52.34	51.96	2.76	28.05	22.29	57	2.34	0.0	45.97	45.61	0.65	22.73	18.03
29	3.04	459.36	51.88	51.51	2.48	27.64	21.96	58	2.33	0.0	45.9	45.54	0.64	22.68	17.99
30	2.98	463.07	51.46	51.08	2.25	27.24	21.64	59	2.33	0.0	45.83	45.47	0.63	22.63	17.95

Table A.72.: S^{3+}

Step	$\hat{E}$	$\hat{T}$	P_1	P_2	P_T	P_S	P_{AS}	Step	$\hat{E}$	$\hat{T}$	P_1	P_2	P_T	P_S	P_{AS}
2	35.67	181.74	82.94	86.79	100.0	66.8	54.88	31	5.39	367.54	60.4	64.54	32.54	39.89	31.87
3	30.83	192.07	81.4	85.23	100.0	65.88	54.02	32	5.3	370.03	60.27	64.13	30.63	39.53	31.58
4	26.74	202.67	79.82	83.73	99.99	64.81	53.04	33	5.21	372.4	60.15	63.74	28.89	39.17	31.29
5	23.29	213.48	78.23	82.31	99.99	63.59	51.92	34	5.13	374.65	60.04	63.38	27.3	38.82	31.0
6	20.38	224.45	76.62	80.96	99.99	62.17	50.63	35	5.06	376.78	59.94	63.03	25.86	38.49	30.73
7	17.91	235.51	75.03	79.67	99.99	60.55	49.17	36	4.99	378.8	59.84	62.71	24.55	38.18	30.48
8	15.82	246.59	73.47	78.45	99.95	59.0	47.82	37	4.92	380.71	59.75	62.41	23.35	37.88	30.23
9	14.05	257.62	71.94	77.28	99.81	57.48	46.52	38	4.86	382.51	59.71	62.06	22.27	37.59	30.0
10	12.55	268.51	70.47	76.17	99.34	55.84	45.13	39	4.81	384.22	59.67	61.73	21.28	37.32	29.78
11	11.28	279.19	69.06	75.1	98.17	54.08	43.65	40	4.76	385.83	59.64	61.42	20.38	37.07	29.58
12	10.22	289.59	67.74	74.08	95.83	52.2	42.05	41	4.71	387.35	59.6	61.13	19.56	36.83	29.38
13	9.32	299.63	66.51	73.08	91.93	50.48	40.6	42	4.66	388.78	59.57	60.86	18.81	36.6	29.19
14	8.93	304.51	65.93	72.6	89.34	49.76	40.01	43	4.62	390.12	59.55	60.6	18.13	36.39	29.02
15	8.56	309.27	65.39	72.1	86.35	49.05	39.42	44	4.58	391.39	59.52	60.36	17.51	36.28	28.94
16	8.23	313.91	64.86	71.62	82.99	48.33	38.83	45	4.55	392.58	59.49	60.14	16.94	36.14	28.82
17	7.92	318.43	64.37	71.16	79.34	47.62	38.24	46	4.51	393.69	59.47	59.93	16.43	36.01	28.71
18	7.63	322.83	63.91	70.65	75.47	46.92	37.65	47	4.48	394.74	59.45	59.73	15.95	35.88	28.61
19	7.36	327.1	63.48	70.15	71.46	46.23	37.08	48	4.45	395.73	59.36	59.58	15.52	35.76	28.52
20	7.12	331.23	63.08	69.68	67.39	45.51	36.49	49	4.43	396.65	59.26	59.44	15.12	35.65	28.43
21	6.89	335.22	62.7	69.23	63.34	44.8	35.91	50	4.4	397.51	59.17	59.32	14.76	35.55	28.34
22	6.68	339.08	62.36	68.72	59.37	44.11	35.33	51	4.38	398.32	59.08	59.2	14.43	35.45	28.27
23	6.49	342.8	62.06	68.21	55.53	43.44	34.78	52	4.36	399.08	59.0	59.09	14.12	35.37	28.2
24	6.31	346.37	61.77	67.72	51.85	42.78	34.23	53	4.34	399.79	58.92	58.99	13.84	35.28	28.12
25	6.14	349.81	61.5	67.26	48.38	42.4	33.92	54	4.32	400.45	58.85	58.89	13.58	35.2	28.06
26	5.99	353.11	61.25	66.82	45.12	41.94	33.55	55	4.3	401.07	58.79	58.8	13.35	35.12	27.99
27	5.85	356.26	61.01	66.41	42.09	41.5	33.19	56	4.29	401.65	58.73	58.72	13.13	35.04	27.93
28	5.72	359.28	60.84	65.91	39.39	41.07	32.84	57	4.27	402.19	58.67	58.64	12.93	34.98	27.88
29	5.6	362.17	60.68	65.43	36.91	40.66	32.51	58	4.26	402.7	58.62	58.57	12.74	34.91	27.83
30	5.49	364.92	60.54	64.97	34.63	40.27	32.18	59	4.25	403.17	58.57	58.5	12.57	34.85	27.78

Table A.73.: S^{4+}

Step	$\hat{E}$	$\hat{T}$	P_1	P_2	P_T	P_S	P_{AS}	Step	$\hat{E}$	$\hat{T}$	P_1	P_2	P_T	P_S	P_{AS}
2	51.67	157.64	86.51	90.8	100.0	69.63	57.33	31	8.26	313.43	64.92	71.67	83.36	49.76	39.97
3	44.84	166.48	85.2	89.28	100.0	69.52	57.23	32	8.12	315.45	64.7	71.46	81.79	49.44	39.72
4	39.06	175.53	83.86	87.78	100.0	69.05	56.78	33	7.99	317.36	64.49	71.26	80.24	49.11	39.44
5	34.16	184.75	82.49	86.32	100.0	68.39	56.15	34	7.87	319.18	64.29	71.08	78.7	48.79	39.18
6	29.99	194.08	81.1	84.94	100.0	67.59	55.4	35	7.75	320.9	64.11	70.88	77.2	48.49	38.93
7	26.46	203.47	79.71	83.62	99.99	66.65	54.54	36	7.65	322.53	63.94	70.69	75.75	48.2	38.69
8	23.47	212.86	78.31	82.39	99.99	65.59	53.57	37	7.55	324.07	63.79	70.51	74.33	47.93	38.46
9	20.94	222.18	76.94	81.23	99.99	64.4	52.49	38	7.46	325.52	63.64	70.34	72.97	47.67	38.25
10	18.79	231.36	75.62	80.15	99.99	63.09	51.3	39	7.38	326.89	63.5	70.18	71.66	47.42	38.05
11	16.96	240.34	74.35	79.13	99.98	61.66	50.01	40	7.3	328.18	63.38	70.03	70.41	47.19	37.85
12	15.4	249.06	73.12	78.19	99.93	60.5	49.03	41	7.23	329.39	63.26	69.89	69.22	46.97	37.67
13	14.07	257.46	71.96	77.3	99.81	59.27	47.99	42	7.16	330.54	63.15	69.76	68.08	46.77	37.5
14	13.48	261.53	71.41	76.88	99.69	58.65	47.45	43	7.1	331.61	63.04	69.63	67.01	46.57	37.34
15	12.94	265.49	70.87	76.47	99.52	58.02	46.92	44	7.04	332.62	62.94	69.52	65.99	46.39	37.19
16	12.44	269.36	70.35	76.08	99.28	57.39	46.39	45	6.98	333.57	62.85	69.41	65.02	46.22	37.05
17	11.98	273.11	69.86	75.71	98.96	56.76	45.85	46	6.93	334.47	62.77	69.31	64.12	46.05	36.92
18	11.55	276.76	69.38	75.34	98.53	56.14	45.32	47	6.89	335.3	62.69	69.22	63.26	45.9	36.79
19	11.16	280.29	68.92	74.99	97.99	55.53	44.81	48	6.84	336.09	62.62	69.13	62.45	45.76	36.67
20	10.79	283.7	68.48	74.65	97.32	54.88	44.26	49	6.8	336.82	62.55	69.04	61.7	45.63	36.56
21	10.46	287.0	68.06	74.33	96.55	54.24	43.72	50	6.77	337.51	62.49	68.94	60.99	45.5	36.46
22	10.16	290.17	67.67	74.02	95.65	53.61	43.18	51	6.73	338.16	62.44	68.85	60.32	45.39	36.36
23	9.88	293.23	67.29	73.72	94.62	52.99	42.66	52	6.7	338.76	62.39	68.77	59.7	45.28	36.28
24	9.62	296.17	66.93	73.42	93.49	52.39	42.15	53	6.67	339.33	62.34	68.69	59.11	45.17	36.19
25	9.38	298.98	66.59	73.14	92.24	52.0	41.83	54	6.64	339.86	62.3	68.62	58.57	45.07	36.1
26	9.15	301.68	66.27	72.88	90.9	51.59	41.49	55	6.61	340.35	62.26	68.55	58.06	44.97	36.02
27	8.95	304.26	65.96	72.63	89.48	51.19	41.16	56	6.59	340.81	62.22	68.48	57.58	44.8	35.95
28	8.76	306.72	65.68	72.37	88.01	50.81	40.85	57	6.57	341.24	62.18	68.42	57.13	44.8	35.88
29	8.58	309.07	65.41	72.12	86.48	50.45	40.55	58	6.55	341.65	62.15	68.37	56.71	44.72	35.81
30	8.41	311.3	65.16	71.89	84.93	50.09	40.25	59	6.53	342.02	62.12	68.32	56.32	44.65	35.75

Table A.74.: S^{5+}

Step	$\hat{E}$	$\hat{T}$	P_1	P_2	P_T	P_S	P_{AS}	Step	$\hat{E}$	$\hat{T}$	P_1	P_2	P_T	P_S	P_{AS}
2	68.47	141.36	89.01	93.62	100.0	70.98	58.46	31	11.38	278.23	69.19	75.19	98.32	57.28	46.24
3	59.6	149.2	87.79	92.27	100.0	71.05	58.51	32	11.19	279.98	68.96	75.02	98.04	56.98	45.98
4	52.03	157.22	86.57	90.87	100.0	71.1	58.54	33	11.01	281.64	68.75	74.86	97.74	56.64	45.7
5	45.61	165.39	85.36	89.47	100.0	71.12	58.54	34	10.84	283.21	68.55	74.7	97.43	56.32	45.43
6	40.17	173.66	84.15	88.09	100.0	70.83	58.26	35	10.69	284.69	68.36	74.56	97.11	56.01	45.17
7	35.55	181.96	82.91	86.76	100.0	70.3	57.75	36	10.55	286.1	68.18	74.42	96.78	55.72	44.92
8	31.61	190.26	81.67	85.49	100.0	69.68	57.16	37	10.42	287.42	68.01	74.29	96.44	55.45	44.69
9	28.27	198.47	80.44	84.31	100.0	68.96	56.49	38	10.3	288.67	67.85	74.17	96.09	55.18	44.47
10	25.42	206.56	79.24	83.21	99.99	68.15	55.75	39	10.19	289.86	67.7	74.05	95.75	54.94	44.26
11	23.01	214.46	78.08	82.19	99.99	67.24	54.91	40	10.09	290.97	67.57	73.95	95.4	54.71	44.07
12	20.95	222.12	76.95	81.24	99.99	66.18	53.95	41	9.99	292.01	67.44	73.85	95.05	54.49	43.88
13	19.2	229.48	75.9	80.36	99.99	65.07	52.94	42	9.9	293.0	67.32	73.75	94.71	54.28	43.71
14	18.43	233.04	75.38	79.95	99.99	64.49	52.43	43	9.82	293.93	67.2	73.65	94.37	54.08	43.54
15	17.71	236.51	74.88	79.56	99.99	63.92	51.91	44	9.74	294.8	67.09	73.56	94.04	53.9	43.39
16	17.04	239.89	74.41	79.18	99.98	63.33	51.38	45	9.67	295.61	66.99	73.48	93.71	53.73	43.24
17	16.43	243.17	73.95	78.82	99.97	62.93	51.04	46	9.6	296.38	66.9	73.4	93.4	53.57	43.1
18	15.86	246.36	73.5	78.48	99.95	62.51	50.68	47	9.54	297.1	66.81	73.33	93.09	53.42	42.98
19	15.33	249.44	73.07	78.15	99.93	62.12	50.34	48	9.48	297.77	66.73	73.26	92.79	53.28	42.86
20	14.85	252.42	72.66	77.83	99.9	61.65	49.95	49	9.43	298.4	66.66	73.2	92.51	53.31	42.9
21	14.4	255.29	72.26	77.53	99.85	61.2	49.56	50	9.38	299.0	66.58	73.14	92.23	53.23	42.83
22	13.98	258.05	71.88	77.24	99.8	60.75	49.19	51	9.33	299.55	66.52	73.09	91.97	53.15	42.76
23	13.6	260.71	71.52	76.96	99.72	60.32	48.82	52	9.29	300.07	66.46	73.03	91.72	53.08	42.71
24	13.24	263.26	71.17	76.7	99.63	59.89	48.46	53	9.25	300.55	66.4	72.99	91.48	53.0	42.64
25	12.91	265.71	70.84	76.45	99.51	59.48	48.11	54	9.21	301.01	66.34	72.94	91.25	52.92	42.57
26	12.61	268.05	70.53	76.21	99.37	59.08	47.77	55	9.17	301.43	66.29	72.9	91.03	52.85	42.51
27	12.32	270.29	70.23	75.99	99.21	58.69	47.44	56	9.14	301.83	66.25	72.86	90.82	52.79	42.46
28	12.06	272.42	69.95	75.78	99.03	58.32	47.12	57	9.11	302.2	66.2	72.83	90.63	52.72	42.41
29	11.82	274.46	69.68	75.57	98.81	57.96	46.81	58	9.08	302.54	66.16	72.79	90.44	52.67	42.36
30	11.59	276.39	69.42	75.38	98.58	57.61	46.52	59	9.06	302.87	66.13	72.76	90.26	52.61	42.31

Table A.75.: S^{6+}

Step	$\hat{E}$	$\hat{T}$	P_1	P_2	P_T	P_S	P_{AS}	Step	$\hat{E}$	$\hat{T}$	P_1	P_2	P_T	P_S	P_{AS}
2	85.87	129.41	90.98	95.57	100.0	71.88	59.21	31	14.76	252.94	72.59	77.77	99.89	62.96	51.01
3	74.85	136.53	89.79	94.43	100.0	72.07	59.36	32	14.52	254.5	72.37	77.61	99.87	62.75	50.83
4	65.5	143.81	88.62	93.2	100.0	72.25	59.5	33	14.29	255.98	72.17	77.45	99.84	62.49	50.61
5	57.55	151.22	87.48	91.92	100.0	72.41	59.63	34	14.08	257.38	71.97	77.31	99.81	62.25	50.4
6	50.77	158.71	86.35	90.62	100.0	72.57	59.75	35	13.89	258.71	71.79	77.17	99.78	62.01	50.21
7	45.01	166.24	85.24	89.32	100.0	72.64	59.8	36	13.7	259.96	71.62	77.04	99.74	61.79	50.02
8	40.12	173.75	84.13	88.07	100.0	72.4	59.56	37	13.54	261.15	71.46	76.92	99.71	61.58	49.84
9	35.96	181.18	83.03	86.88	100.0	72.0	59.16	38	13.38	262.26	71.31	76.8	99.67	61.38	49.68
10	32.4	188.49	81.94	85.75	100.0	71.52	58.7	39	13.23	263.32	71.17	76.7	99.62	61.2	49.52
11	29.37	195.63	80.88	84.72	100.0	70.95	58.16	40	13.1	264.31	71.03	76.59	99.58	61.02	49.37
12	26.79	202.54	79.84	83.75	99.99	70.23	57.5	41	12.97	265.24	70.9	76.5	99.54	60.86	49.23
13	24.59	209.17	78.85	82.86	99.99	69.47	56.8	42	12.86	266.12	70.79	76.41	99.49	60.7	49.1
14	23.62	212.38	78.38	82.45	99.99	69.08	56.44	43	12.75	266.95	70.67	76.33	99.44	60.56	48.98
15	22.71	215.5	77.93	82.06	99.99	68.68	56.08	44	12.65	267.72	70.57	76.25	99.4	60.42	48.86
16	21.88	218.54	77.48	81.68	99.99	68.28	55.71	45	12.55	268.45	70.47	76.17	99.35	60.29	48.75
17	21.11	221.5	77.04	81.31	99.99	67.87	55.34	46	12.47	269.14	70.38	76.11	99.3	60.17	48.65
18	20.4	224.36	76.63	80.97	99.99	67.47	54.97	47	12.39	269.78	70.3	76.04	99.25	60.06	48.56
19	19.74	227.13	76.24	80.64	99.99	67.09	54.63	48	12.31	270.38	70.22	75.98	99.21	59.96	48.47
20	19.13	229.8	75.85	80.33	99.99	66.62	54.21	49	12.24	270.94	70.15	75.93	99.16	59.86	48.39
21	18.57	232.38	75.47	80.03	99.99	66.16	53.8	50	12.18	271.47	70.08	75.88	99.11	59.77	48.31
22	18.05	234.86	75.12	79.74	99.99	65.71	53.39	51	12.12	271.96	70.01	75.82	99.07	59.69	48.24
23	17.56	237.25	74.78	79.47	99.98	65.27	53.0	52	12.06	272.42	69.95	75.78	99.03	59.63	48.19
24	17.11	239.53	74.46	79.22	99.98	64.85	52.62	53	12.01	272.85	69.89	75.73	98.99	59.54	48.11
25	16.69	241.73	74.15	78.98	99.97	64.43	52.25	54	11.96	273.26	69.84	75.69	98.94	59.45	48.04
26	16.31	243.82	73.85	78.75	99.97	64.26	52.12	55	11.92	273.63	69.79	75.65	98.9	59.38	47.97
27	15.95	245.83	73.57	78.53	99.96	63.98	51.88	56	11.87	273.99	69.74	75.61	98.87	59.31	47.91
28	15.62	247.74	73.31	78.33	99.94	63.71	51.65	57	11.83	274.32	69.7	75.59	98.83	59.24	47.86
29	15.31	249.56	73.05	78.13	99.93	63.44	51.42	58	11.8	274.63	69.66	75.55	98.8	59.18	47.8
30	15.03	251.29	72.81	77.95	99.91	63.2	51.21	59	11.76	274.91	69.62	75.53	98.76	59.12	47.75

Table A.76.: S^{7+}

Step	$\hat{E}$	$\hat{T}$	P_1	P_2	P_T	P_S	P_{AS}	Step	$\hat{E}$	$\hat{T}$	P_1	P_2	P_T	P_S	P_{AS}
2	103.82	120.16	92.56	96.89	100.0	72.52	59.75	31	18.31	233.61	75.3	79.89	99.99	67.29	54.7
3	90.6	126.73	91.44	95.97	100.0	72.8	59.98	32	18.01	235.04	75.09	79.72	99.99	67.08	54.5
4	79.37	133.45	90.3	94.94	100.0	73.07	60.19	33	17.73	236.39	74.9	79.57	99.99	66.8	54.26
5	69.83	140.27	89.18	93.81	100.0	73.34	60.41	34	17.48	237.67	74.72	79.43	99.98	66.55	54.03
6	61.73	147.17	88.1	92.62	100.0	73.65	60.65	35	17.24	238.88	74.55	79.29	99.98	66.3	53.81
7	54.81	154.1	87.05	91.42	100.0	73.92	60.87	36	17.02	240.02	74.39	79.17	99.98	66.07	53.61
8	48.91	161.01	86.01	90.22	100.0	74.08	61.0	37	16.81	241.1	74.24	79.05	99.98	65.85	53.41
9	43.89	167.85	85.0	89.05	100.0	74.14	61.04	38	16.62	242.12	74.09	78.94	99.97	65.65	53.23
10	39.62	174.57	84.01	87.94	100.0	73.92	60.81	39	16.44	243.08	73.96	78.83	99.97	65.64	53.24
11	35.99	181.13	83.03	86.89	100.0	73.6	60.48	40	16.28	243.99	73.83	78.73	99.97	65.5	53.13
12	32.87	187.47	82.09	85.91	100.0	73.12	60.03	41	16.13	244.84	73.71	78.64	99.96	65.37	53.02
13	30.2	193.56	81.18	85.01	100.0	72.61	59.55	42	15.98	245.64	73.6	78.55	99.96	65.26	52.92
14	29.02	196.5	80.74	84.59	100.0	72.35	59.3	43	15.85	246.39	73.5	78.47	99.95	65.15	52.83
15	27.93	199.37	80.31	84.19	100.0	72.08	59.05	44	15.73	247.1	73.4	78.4	99.95	65.04	52.74
16	26.92	202.16	79.9	83.8	99.99	71.8	58.79	45	15.62	247.76	73.3	78.33	99.94	64.95	52.66
17	25.99	204.86	79.5	83.43	99.99	71.52	58.53	46	15.51	248.38	73.22	78.26	99.94	64.86	52.58
18	25.13	207.48	79.11	83.09	99.99	71.24	58.27	47	15.41	248.97	73.13	78.2	99.93	64.77	52.51
19	24.33	210.02	78.73	82.76	99.99	71.0	58.04	48	15.32	249.51	73.06	78.14	99.93	64.7	52.44
20	23.59	212.47	78.37	82.44	99.99	70.64	57.72	49	15.24	250.03	72.99	78.08	99.92	64.62	52.38
21	22.91	214.83	78.03	82.14	99.99	70.28	57.4	50	15.16	250.51	72.92	78.03	99.92	64.56	52.33
22	22.27	217.1	77.69	81.86	99.99	69.94	57.08	51	15.08	250.95	72.86	77.98	99.92	64.5	52.28
23	21.69	219.28	77.37	81.59	99.99	69.6	56.78	52	15.01	251.37	72.8	77.94	99.91	64.46	52.24
24	21.14	221.37	77.06	81.33	99.99	69.27	56.48	53	14.95	251.77	72.75	77.9	99.91	64.38	52.18
25	20.64	223.37	76.77	81.09	99.99	68.95	56.2	54	14.89	252.14	72.7	77.86	99.9	64.32	52.12
26	20.18	225.29	76.5	80.86	99.99	68.65	55.92	55	14.84	252.48	72.65	77.82	99.9	64.26	52.07
27	19.74	227.12	76.24	80.64	99.99	68.35	55.66	56	14.79	252.8	72.61	77.79	99.89	64.2	52.02
28	19.34	228.87	75.99	80.44	99.99	68.07	55.4	57	14.74	253.1	72.56	77.76	99.89	64.15	51.97
29	18.97	230.53	75.74	80.24	99.99	67.8	55.15	58	14.69	253.38	72.53	77.73	99.88	64.1	51.93
30	18.63	232.11	75.51	80.06	99.99	67.54	54.92	59	14.65	253.64	72.49	77.7	99.88	64.05	51.89

Table A.77.: S^{8+}

Step	$\hat{E}$	$\hat{T}$	P_1	P_2	P_T	P_S	P_{AS}	Step	$\hat{E}$	$\hat{T}$	P_1	P_2	P_T	P_S	P_{AS}
2	121.8	112.73	93.85	97.8	100.0	73.01	60.16	31	21.97	218.23	77.52	81.72	99.99	71.05	57.98
3	106.76	118.86	92.79	97.07	100.0	73.35	60.43	32	21.62	219.55	77.33	81.55	99.99	70.9	57.84
4	93.61	125.12	91.71	96.21	100.0	73.69	60.71	33	21.29	220.8	77.15	81.4	99.99	70.67	57.64
5	82.44	131.48	90.63	95.25	100.0	74.04	60.99	34	20.99	221.98	76.97	81.26	99.99	70.46	57.45
6	72.94	137.91	89.56	94.2	100.0	74.46	61.33	35	20.71	223.1	76.81	81.12	99.99	70.26	57.27
7	64.86	144.37	88.53	93.11	100.0	74.87	61.67	36	20.45	224.16	76.66	80.99	99.99	70.07	57.1
8	57.97	150.8	87.54	91.99	100.0	75.2	61.93	37	20.21	225.16	76.52	80.87	99.99	69.89	56.94
9	52.08	157.17	86.58	90.89	100.0	75.44	62.13	38	19.98	226.1	76.38	80.76	99.99	69.72	56.79
10	47.06	163.42	85.66	89.8	100.0	75.58	62.24	39	19.77	226.99	76.26	80.66	99.99	69.56	56.65
11	42.78	169.52	84.76	88.77	100.0	75.61	62.25	40	19.58	227.83	76.14	80.56	99.99	69.41	56.52
12	39.13	175.42	83.88	87.8	100.0	75.29	61.93	41	19.4	228.61	76.02	80.47	99.99	69.28	56.39
13	36.01	181.08	83.04	86.89	100.0	74.97	61.61	42	19.23	229.35	75.92	80.38	99.99	69.15	56.28
14	34.62	183.81	82.63	86.47	100.0	74.79	61.44	43	19.08	230.05	75.81	80.3	99.99	69.03	56.17
15	33.33	186.47	82.24	86.06	100.0	74.62	61.27	44	18.93	230.7	75.72	80.22	99.99	68.91	56.07
16	32.14	189.06	81.85	85.67	100.0	74.44	61.1	45	18.8	231.31	75.63	80.15	99.99	68.81	55.97
17	31.04	191.57	81.47	85.3	100.0	74.25	60.92	46	18.68	231.89	75.54	80.08	99.99	68.71	55.89
18	30.02	194.01	81.12	84.95	100.0	74.07	60.74	47	18.56	232.43	75.47	80.02	99.99	68.63	55.81
19	29.08	196.36	80.76	84.61	100.0	73.92	60.6	48	18.45	232.93	75.39	79.96	99.99	68.54	55.73
20	28.21	198.63	80.42	84.29	100.0	73.64	60.34	49	18.35	233.41	75.33	79.91	99.99	68.47	55.66
21	27.4	200.82	80.1	83.99	99.99	73.36	60.09	50	18.26	233.85	75.26	79.86	99.99	68.4	55.6
22	26.65	202.92	79.79	83.7	99.99	73.09	59.84	51	18.17	234.27	75.2	79.81	99.99	68.33	55.54
23	25.96	204.95	79.49	83.42	99.99	72.83	59.61	52	18.09	234.66	75.15	79.77	99.99	68.29	55.5
24	25.32	206.89	79.2	83.16	99.99	72.58	59.37	53	18.01	235.02	75.1	79.73	99.99	68.21	55.43
25	24.72	208.74	78.92	82.92	99.99	72.33	59.15	54	17.94	235.36	75.05	79.69	99.99	68.14	55.37
26	24.17	210.52	78.66	82.69	99.99	72.09	58.93	55	17.88	235.68	75.0	79.65	99.99	68.08	55.31
27	23.66	212.22	78.41	82.47	99.99	71.87	58.73	56	17.82	235.97	74.96	79.62	99.99	68.02	55.25
28	23.19	213.83	78.17	82.27	99.99	71.65	58.53	57	17.76	236.25	74.92	79.59	99.99	67.96	55.2
29	22.75	215.37	77.95	82.07	99.99	71.44	58.34	58	17.71	236.51	74.88	79.56	99.99	67.91	55.16
30	22.34	216.84	77.73	81.89	99.99	71.24	58.16	59	17.66	236.75	74.85	79.53	99.99	67.86	55.11

Table A.78.: S^{9+}

Step	$\hat{E}$	$\hat{T}$	P_1	P_2	P_T	P_S	P_{AS}	Step	$\hat{E}$	$\hat{T}$	P_1	P_2	P_T	P_S	P_{AS}
2	0.0	106.59	94.89	98.42	100.0	73.38	60.47	31	25.74	205.6	79.39	83.34	99.99	73.97	60.53
3	122.81	112.36	93.91	97.84	100.0	73.78	60.79	32	25.34	206.83	79.2	83.17	99.99	73.87	60.43
4	108.18	118.25	92.9	97.14	100.0	74.18	61.12	33	24.96	208.0	79.03	83.02	99.99	73.68	60.26
5	95.34	124.23	91.86	96.34	100.0	74.58	61.44	34	24.61	209.11	78.86	82.87	99.99	73.49	60.1
6	84.42	130.27	90.84	95.44	100.0	75.09	61.86	35	24.29	210.16	78.71	82.74	99.99	73.32	59.95
7	75.13	136.34	89.82	94.46	100.0	75.62	62.29	36	23.98	211.15	78.56	82.61	99.99	73.17	59.81
8	67.21	142.38	88.85	93.45	100.0	76.07	62.66	37	23.7	212.08	78.43	82.49	99.99	73.01	59.67
9	60.47	148.36	87.92	92.42	100.0	76.45	62.97	38	23.44	212.96	78.3	82.38	99.99	72.87	59.55
10	54.69	154.23	87.03	91.4	100.0	76.75	63.21	39	23.2	213.79	78.18	82.27	99.99	72.74	59.43
11	49.75	159.95	86.17	90.4	100.0	76.93	63.35	40	22.98	214.57	78.07	82.17	99.99	72.62	59.32
12	45.54	165.49	85.35	89.45	100.0	76.91	63.33	41	22.77	215.31	77.96	82.08	99.99	72.51	59.21
13	41.95	170.8	84.56	88.56	100.0	76.84	63.27	42	22.58	216.0	77.86	81.99	99.99	72.4	59.12
14	40.35	173.36	84.19	88.14	100.0	76.7	63.11	43	22.4	216.65	77.76	81.91	99.99	72.3	59.03
15	38.87	175.86	83.82	87.73	100.0	76.59	63.0	44	22.23	217.26	77.67	81.84	99.99	72.21	58.95
16	37.51	178.28	83.46	87.34	100.0	76.49	62.89	45	22.07	217.83	77.58	81.76	99.99	72.12	58.87
17	36.24	180.64	83.11	86.96	100.0	76.37	62.77	46	21.93	218.37	77.5	81.7	99.99	72.04	58.8
18	35.07	182.92	82.77	86.61	100.0	76.26	62.66	47	21.79	218.87	77.43	81.64	99.99	71.97	58.73
19	33.98	185.12	82.44	86.26	100.0	76.2	62.58	48	21.67	219.35	77.36	81.58	99.99	71.91	58.67
20	32.97	187.25	82.13	85.94	100.0	75.97	62.38	49	21.55	219.79	77.29	81.52	99.99	71.84	58.62
21	32.03	189.3	81.82	85.63	100.0	75.76	62.18	50	21.44	220.2	77.23	81.47	99.99	71.79	58.56
22	31.17	191.27	81.52	85.34	100.0	75.55	61.99	51	21.34	220.59	77.18	81.42	99.99	71.74	58.52
23	30.37	193.17	81.24	85.07	100.0	75.34	61.8	52	21.25	220.95	77.12	81.38	99.99	71.71	58.49
24	29.62	194.98	80.97	84.81	100.0	75.15	61.62	53	21.16	221.29	77.07	81.34	99.99	71.64	58.43
25	28.94	196.72	80.71	84.56	100.0	74.95	61.44	54	21.08	221.61	77.03	81.3	99.99	71.58	58.37
26	28.3	198.39	80.46	84.33	100.0	74.77	61.27	55	21.01	221.91	76.98	81.26	99.99	71.52	58.32
27	27.71	199.97	80.22	84.1	100.0	74.59	61.11	56	20.94	222.18	76.94	81.23	99.99	71.47	58.28
28	27.16	201.49	80.0	83.89	99.99	74.43	60.96	57	20.87	222.44	76.91	81.2	99.99	71.42	58.23
29	26.65	202.93	79.79	83.7	99.99	74.27	60.81	58	20.81	222.68	76.87	81.17	99.99	71.38	58.19
30	26.18	204.3	79.59	83.51	99.99	74.11	60.67	59	20.76	222.91	76.84	81.14	99.99	71.34	58.15

Table A.79.: S^{10+}

Step	$\hat{E}$	$\hat{T}$	P_1	P_2	P_T	P_S	P_{AS}	Step	$\hat{E}$	$\hat{T}$	P_1	P_2	P_T	P_S	P_{AS}
2	0.0	100.61	0.0	0.0	0.0	0.0	0.0	31	29.62	194.99	80.97	84.81	100.0	76.3	62.57
3	0.0	106.86	94.84	98.39	100.0	74.12	61.08	32	29.16	196.15	80.8	84.64	100.0	76.24	62.5
4	122.58	112.44	93.9	97.83	100.0	74.56	61.44	33	28.73	197.26	80.63	84.48	100.0	76.07	62.36
5	108.51	118.11	92.92	97.16	100.0	75.01	61.81	34	28.33	198.3	80.47	84.34	100.0	75.92	62.22
6	96.14	123.83	91.93	96.39	100.0	75.6	62.28	35	27.96	199.29	80.32	84.2	100.0	75.78	62.09
7	85.61	129.56	90.96	95.55	100.0	76.21	62.79	36	27.62	200.22	80.18	84.07	100.0	75.64	61.97
8	76.64	135.28	90.0	94.64	100.0	76.77	63.24	37	27.3	201.1	80.05	83.95	99.99	75.51	61.85
9	69.0	140.93	89.08	93.69	100.0	77.26	63.65	38	27.0	201.93	79.93	83.83	99.99	75.39	61.75
10	62.48	146.48	88.21	92.74	100.0	77.68	63.99	39	26.73	202.71	79.82	83.73	99.99	75.28	61.65
11	56.9	151.89	87.38	91.8	100.0	77.99	64.24	40	26.47	203.45	79.71	83.62	99.99	75.18	61.55
12	52.11	157.12	86.59	90.89	100.0	78.08	64.3	41	26.23	204.14	79.61	83.53	99.99	75.08	61.47
13	48.03	162.14	85.85	90.02	100.0	78.13	64.34	42	26.01	204.79	79.51	83.44	99.99	75.0	61.39
14	46.21	164.56	85.49	89.61	100.0	78.14	64.35	43	25.81	205.41	79.42	83.36	99.99	74.91	61.31
15	44.53	166.92	85.14	89.21	100.0	78.14	64.35	44	25.62	205.98	79.33	83.28	99.99	74.84	61.24
16	42.98	169.21	84.8	88.83	100.0	78.14	64.34	45	25.44	206.52	79.25	83.21	99.99	74.77	61.18
17	41.54	171.44	84.47	88.46	100.0	78.13	64.33	46	25.27	207.03	79.17	83.15	99.99	74.7	61.12
18	40.21	173.59	84.16	88.1	100.0	78.01	64.19	47	25.12	207.5	79.1	83.08	99.99	74.64	61.07
19	38.98	175.67	83.84	87.76	100.0	78.01	64.17	48	24.98	207.95	79.04	83.03	99.99	74.59	61.02
20	37.84	177.68	83.54	87.44	100.0	77.84	64.01	49	24.85	208.36	78.97	82.97	99.99	74.54	60.97
21	36.78	179.62	83.26	87.13	100.0	77.67	63.85	50	24.72	208.75	78.92	82.92	99.99	74.49	60.93
22	35.81	181.48	82.98	86.83	100.0	77.51	63.7	51	24.61	209.12	78.86	82.87	99.99	74.45	60.89
23	34.89	183.26	82.71	86.55	100.0	77.35	63.55	52	24.5	209.46	78.81	82.83	99.99	74.43	60.87
24	34.05	184.98	82.46	86.29	100.0	77.2	63.41	53	24.4	209.78	78.76	82.79	99.99	74.38	60.82
25	33.26	186.62	82.22	86.03	100.0	77.05	63.27	54	24.31	210.08	78.72	82.75	99.99	74.32	60.77
26	32.54	188.19	81.98	85.8	100.0	76.91	63.14	55	24.22	210.36	78.68	82.71	99.99	74.28	60.73
27	31.86	189.69	81.76	85.58	100.0	76.77	63.02	56	24.14	210.62	78.64	82.68	99.99	74.23	60.69
28	31.24	191.11	81.54	85.37	100.0	76.65	62.9	57	24.07	210.86	78.61	82.65	99.99	74.19	60.65
29	30.66	192.47	81.34	85.17	100.0	76.53	62.78	58	24.0	211.09	78.57	82.62	99.99	74.15	60.61
30	30.12	193.76	81.15	84.98	100.0	76.41	62.67	59	23.94	211.3	78.54	82.59	99.99	74.12	60.58

Table A.80.: S^{11+}

Step	$\hat{E}$	$\hat{T}$	P_1	P_2	P_T	P_S	P_{AS}	Step	$\hat{E}$	$\hat{T}$	P_1	P_2	P_T	P_S	P_{AS}
2	0.0	96.23	0.0	0.0	0.0	0.0	0.0	31	33.6	185.91	82.32	86.14	100.0	78.21	64.24
3	0.0	101.34	0.0	0.0	0.0	0.0	0.0	32	33.08	187.02	82.16	85.97	100.0	78.17	64.19
4	0.0	107.46	94.74	98.34	100.0	74.88	61.7	33	32.59	188.06	82.0	85.82	100.0	78.03	64.07
5	121.49	112.85	93.83	97.79	100.0	75.37	62.11	34	32.15	189.05	81.85	85.67	100.0	77.9	63.95
6	108.07	118.29	92.89	97.14	100.0	76.01	62.63	35	31.73	189.99	81.71	85.53	100.0	77.78	63.84
7	96.29	123.75	91.94	96.4	100.0	76.7	63.19	36	31.34	190.87	81.58	85.4	100.0	77.66	63.74
8	86.25	129.19	91.02	95.6	100.0	77.34	63.72	37	30.98	191.71	81.45	85.28	100.0	77.55	63.64
9	77.69	134.56	90.12	94.75	100.0	77.92	64.2	38	30.65	192.5	81.34	85.17	100.0	77.45	63.55
10	70.39	139.84	89.25	93.88	100.0	78.45	64.62	39	30.34	193.24	81.23	85.06	100.0	77.36	63.46
11	64.15	144.98	88.44	93.0	100.0	78.86	64.96	40	30.05	193.94	81.13	84.96	100.0	77.27	63.38
12	58.82	149.96	87.67	92.14	100.0	79.04	65.1	41	29.78	194.59	81.03	84.86	100.0	77.19	63.31
13	54.24	154.72	86.95	91.31	100.0	79.18	65.21	42	29.53	195.21	80.94	84.78	100.0	77.12	63.24
14	52.2	157.02	86.6	90.91	100.0	79.24	65.26	43	29.3	195.79	80.85	84.69	100.0	77.05	63.18
15	50.31	159.26	86.27	90.52	100.0	79.29	65.3	44	29.09	196.34	80.77	84.61	100.0	76.99	63.12
16	48.57	161.44	85.95	90.14	100.0	79.33	65.33	45	28.89	196.85	80.69	84.54	100.0	76.93	63.07
17	46.96	163.55	85.64	89.78	100.0	79.37	65.36	46	28.7	197.33	80.62	84.47	100.0	76.87	63.02
18	45.46	165.6	85.33	89.43	100.0	79.4	65.38	47	28.53	197.78	80.55	84.41	100.0	76.83	62.97
19	44.08	167.57	85.04	89.1	100.0	79.48	65.45	48	28.37	198.2	80.49	84.35	100.0	76.78	62.93
20	42.8	169.48	84.76	88.78	100.0	79.38	65.37	49	28.22	198.59	80.43	84.3	100.0	76.74	62.9
21	41.61	171.32	84.49	88.47	100.0	79.3	65.3	50	28.08	198.96	80.37	84.24	100.0	76.71	62.86
22	40.52	173.09	84.23	88.18	100.0	79.11	65.1	51	27.95	199.31	80.32	84.2	100.0	76.67	62.83
23	39.5	174.78	83.98	87.9	100.0	78.99	64.99	52	27.83	199.63	80.27	84.15	100.0	76.66	62.82
24	38.55	176.41	83.73	87.64	100.0	78.88	64.88	53	27.72	199.94	80.23	84.11	100.0	76.61	62.77
25	37.68	177.97	83.5	87.39	100.0	78.76	64.77	54	27.62	200.22	80.18	84.07	100.0	76.57	62.73
26	36.87	179.46	83.28	87.15	100.0	78.66	64.67	55	27.52	200.49	80.14	84.03	99.99	76.52	62.69
27	36.12	180.88	83.07	86.93	100.0	78.56	64.57	56	27.43	200.73	80.11	84.0	99.99	76.48	62.66
28	35.42	182.23	82.87	86.71	100.0	78.46	64.48	57	27.35	200.96	80.07	83.97	99.99	76.45	62.62
29	34.76	183.52	82.68	86.51	100.0	78.37	64.39	58	27.27	201.18	80.04	83.94	99.99	76.42	62.59
30	34.16	184.75	82.49	86.32	100.0	78.29	64.31	59	27.2	201.38	80.01	83.91	99.99	76.38	62.56

Table A.81.: S^{12+}

Step	$\hat{E}$	$\hat{T}$	P_1	P_2	P_T	P_S	P_{AS}	Step	$\hat{E}$	$\hat{T}$	P_1	P_2	P_T	P_S	P_{AS}
2	0.0	92.41	0.0	0.0	0.0	0.0	0.0	31	37.64	178.03	83.49	87.38	100.0	79.8	65.62
3	0.0	97.3	0.0	0.0	0.0	0.0	0.0	32	37.07	179.08	83.34	87.21	100.0	79.79	65.6
4	0.0	102.3	0.0	0.0	0.0	0.0	0.0	33	36.54	180.08	83.19	87.05	100.0	79.67	65.5
5	0.0	108.27	94.61	98.26	100.0	75.67	62.35	34	36.04	181.03	83.05	86.9	100.0	79.55	65.39
6	119.85	113.48	93.72	97.71	100.0	76.35	62.92	35	35.58	181.92	82.92	86.76	100.0	79.45	65.3
7	107.14	118.69	92.82	97.09	100.0	77.11	63.54	36	35.15	182.76	82.79	86.63	100.0	79.35	65.21
8	96.02	123.89	91.92	96.39	100.0	77.82	64.12	37	34.75	183.56	82.67	86.51	100.0	79.25	65.12
9	86.53	129.02	91.05	95.63	100.0	78.48	64.66	38	34.38	184.31	82.56	86.39	100.0	79.17	65.04
10	78.43	134.07	90.2	94.84	100.0	79.08	65.16	39	34.03	185.01	82.45	86.28	100.0	79.09	64.97
11	71.52	138.98	89.39	94.02	100.0	79.58	65.56	40	33.71	185.68	82.36	86.18	100.0	79.01	64.91
12	65.61	143.72	88.64	93.22	100.0	79.83	65.77	41	33.41	186.31	82.27	86.08	100.0	78.95	64.84
13	60.56	148.27	87.93	92.43	100.0	80.05	65.94	42	33.13	186.9	82.18	85.99	100.0	78.88	64.79
14	58.3	150.47	87.59	92.05	100.0	80.15	66.02	43	32.88	187.45	82.1	85.91	100.0	78.83	64.73
15	56.21	152.61	87.27	91.68	100.0	80.24	66.09	44	32.64	187.97	82.02	85.83	100.0	78.77	64.68
16	54.27	154.68	86.96	91.32	100.0	80.33	66.16	45	32.41	188.46	81.94	85.76	100.0	78.73	64.64
17	52.48	156.7	86.65	90.97	100.0	80.4	66.22	46	32.21	188.91	81.87	85.69	100.0	78.68	64.6
18	50.82	158.65	86.36	90.63	100.0	80.47	66.28	47	32.02	189.34	81.81	85.63	100.0	78.64	64.56
19	49.28	160.54	86.08	90.3	100.0	80.61	66.39	48	31.84	189.74	81.75	85.57	100.0	78.61	64.53
20	47.86	162.36	85.81	89.98	100.0	80.52	66.32	49	31.67	190.12	81.69	85.51	100.0	78.58	64.5
21	46.54	164.11	85.55	89.68	100.0	80.44	66.25	50	31.52	190.47	81.64	85.46	100.0	78.55	64.47
22	45.32	165.8	85.3	89.4	100.0	80.38	66.2	51	31.37	190.8	81.59	85.41	100.0	78.52	64.45
23	44.19	167.42	85.07	89.13	100.0	80.33	66.15	52	31.24	191.11	81.54	85.37	100.0	78.52	64.44
24	43.14	168.97	84.84	88.87	100.0	80.29	66.12	53	31.11	191.4	81.5	85.33	100.0	78.47	64.4
25	42.17	170.46	84.62	88.62	100.0	80.26	66.09	54	31.0	191.67	81.46	85.29	100.0	78.43	64.36
26	41.26	171.88	84.41	88.38	100.0	80.24	66.07	55	30.89	191.92	81.42	85.25	100.0	78.39	64.33
27	40.43	173.23	84.21	88.16	100.0	80.04	65.87	56	30.79	192.16	81.39	85.22	100.0	78.36	64.3
28	39.65	174.52	84.02	87.95	100.0	79.97	65.8	57	30.7	192.38	81.35	85.18	100.0	78.33	64.27
29	38.93	175.75	83.83	87.75	100.0	79.91	65.74	58	30.61	192.58	81.32	85.15	100.0	78.3	64.24
30	38.26	176.92	83.66	87.56	100.0	79.85	65.68	59	30.53	192.77	81.3	85.13	100.0	78.27	64.21

Table A.82.: S^{13+}

Step	$\hat{E}$	$\hat{T}$	P_1	P_2	P_T	P_S	P_{AS}	Step	$\hat{E}$	$\hat{T}$	P_1	P_2	P_T	P_S	P_{AS}
2	0.0	89.03	0.0	0.0	0.0	0.0	0.0	31	41.75	171.1	84.52	88.51	100.0	81.27	66.93
3	0.0	93.74	0.0	0.0	0.0	0.0	0.0	32	41.12	172.11	84.37	88.34	100.0	81.35	66.98
4	0.0	98.53	0.0	0.0	0.0	0.0	0.0	33	40.53	173.07	84.23	88.19	100.0	81.05	66.7
5	0.0	103.4	0.0	0.0	0.0	0.0	0.0	34	39.98	173.97	84.1	88.04	100.0	80.95	66.61
6	0.0	109.23	94.45	98.17	100.0	76.65	63.16	35	39.47	174.82	83.97	87.9	100.0	80.86	66.53
7	117.89	114.24	93.59	97.63	100.0	77.45	63.82	36	39.0	175.63	83.85	87.77	100.0	80.77	66.45
8	105.93	119.22	92.73	97.02	100.0	78.22	64.46	37	38.56	176.39	83.74	87.64	100.0	80.69	66.38
9	95.51	124.15	91.88	96.35	100.0	78.95	65.05	38	38.16	177.11	83.63	87.53	100.0	80.62	66.31
10	86.6	128.98	91.06	95.64	100.0	79.62	65.6	39	37.78	177.79	83.53	87.42	100.0	80.55	66.25
11	79.0	133.69	90.26	94.9	100.0	80.19	66.07	40	37.43	178.43	83.43	87.32	100.0	80.49	66.19
12	72.5	138.24	89.51	94.15	100.0	80.51	66.33	41	37.1	179.03	83.35	87.22	100.0	80.43	66.14
13	66.95	142.6	88.81	93.41	100.0	80.8	66.56	42	36.8	179.59	83.26	87.13	100.0	80.38	66.09
14	64.47	144.7	88.48	93.05	100.0	80.93	66.67	43	36.52	180.12	83.19	87.04	100.0	80.33	66.05
15	62.19	146.75	88.17	92.7	100.0	81.05	66.77	44	36.25	180.62	83.11	86.97	100.0	80.29	66.01
16	60.07	148.74	87.86	92.35	100.0	81.17	66.86	45	36.01	181.08	83.04	86.89	100.0	80.25	65.97
17	58.1	150.67	87.56	92.02	100.0	81.28	66.95	46	35.78	181.52	82.98	86.82	100.0	80.21	65.94
18	56.27	152.54	87.28	91.69	100.0	81.38	67.04	47	35.57	181.93	82.91	86.76	100.0	80.18	65.91
19	54.58	154.35	87.01	91.37	100.0	81.57	67.19	48	35.37	182.32	82.86	86.7	100.0	80.15	65.88
20	53.01	156.09	86.74	91.07	100.0	81.48	67.12	49	35.19	182.68	82.8	86.64	100.0	80.13	65.85
21	51.56	157.77	86.49	90.78	100.0	81.41	67.06	50	35.02	183.01	82.75	86.59	100.0	80.1	65.83
22	50.21	159.39	86.25	90.5	100.0	81.35	67.01	51	34.86	183.33	82.7	86.54	100.0	80.08	65.81
23	48.96	160.94	86.02	90.23	100.0	81.31	66.97	52	34.71	183.62	82.66	86.5	100.0	80.08	65.81
24	47.81	162.43	85.8	89.97	100.0	81.27	66.93	53	34.58	183.9	82.62	86.45	100.0	80.05	65.78
25	46.74	163.85	85.59	89.73	100.0	81.24	66.91	54	34.45	184.16	82.58	86.41	100.0	80.01	65.74
26	45.74	165.21	85.39	89.5	100.0	81.23	66.9	55	34.33	184.4	82.55	86.38	100.0	79.98	65.71
27	44.82	166.51	85.2	89.28	100.0	81.22	66.89	56	34.22	184.62	82.51	86.34	100.0	79.95	65.68
28	43.97	167.74	85.02	89.07	100.0	81.22	66.89	57	34.12	184.84	82.48	86.31	100.0	79.92	65.66
29	43.17	168.92	84.85	88.87	100.0	81.23	66.89	58	34.02	185.03	82.45	86.28	100.0	79.89	65.63
30	42.44	170.04	84.68	88.69	100.0	81.25	66.91	59	33.93	185.22	82.43	86.25	100.0	79.87	65.61

Table A.83.: S^{14+}

Step	$\hat{E}$	$\hat{T}$	P_1	P_2	P_T	P_S	P_{AS}	Step	$\hat{E}$	$\hat{T}$	P_1	P_2	P_T	P_S	P_{AS}
2	0.0	86.03	0.0	0.0	0.0	0.0	0.0	31	45.93	164.95	85.43	89.54	100.0	82.12	67.63
3	0.0	90.56	0.0	0.0	0.0	0.0	0.0	32	45.23	165.92	85.29	89.38	100.0	82.18	67.69
4	0.0	95.18	0.0	0.0	0.0	0.0	0.0	33	44.59	166.84	85.15	89.22	100.0	82.14	67.65
5	0.0	99.87	0.0	0.0	0.0	0.0	0.0	34	43.99	167.71	85.03	89.08	100.0	82.1	67.61
6	0.0	104.59	0.0	0.0	0.0	0.0	0.0	35	43.44	168.53	84.9	88.94	100.0	82.07	67.59
7	0.0	110.27	94.27	98.06	100.0	77.75	64.07	36	42.92	169.3	84.79	88.81	100.0	82.04	67.56
8	115.8	115.07	93.44	97.53	100.0	78.57	64.74	37	42.44	170.03	84.68	88.69	100.0	82.01	67.54
9	104.61	119.81	92.62	96.94	100.0	79.35	65.39	38	41.99	170.72	84.58	88.57	100.0	81.99	67.52
10	94.89	124.46	91.82	96.31	100.0	80.08	65.99	39	41.58	171.37	84.48	88.47	100.0	81.98	67.51
11	86.59	128.99	91.06	95.64	100.0	80.72	66.51	40	41.2	171.99	84.39	88.36	100.0	81.97	67.5
12	79.5	133.36	90.32	94.95	100.0	81.09	66.81	41	40.84	172.56	84.3	88.27	100.0	81.96	67.49
13	73.43	137.56	89.62	94.26	100.0	81.43	67.09	42	40.51	173.1	84.23	88.18	100.0	81.66	67.21
14	70.73	139.58	89.29	93.92	100.0	81.59	67.22	43	40.2	173.61	84.15	88.1	100.0	81.62	67.17
15	68.23	141.55	88.98	93.59	100.0	81.74	67.35	44	39.91	174.09	84.08	88.02	100.0	81.58	67.14
16	65.92	143.46	88.68	93.26	100.0	81.89	67.46	45	39.64	174.54	84.01	87.94	100.0	81.55	67.11
17	63.77	145.32	88.39	92.94	100.0	82.03	67.58	46	39.4	174.96	83.95	87.88	100.0	81.52	67.08
18	61.79	147.11	88.11	92.63	100.0	82.16	67.69	47	39.16	175.35	83.89	87.81	100.0	81.5	67.06
19	59.95	148.85	87.84	92.33	100.0	82.39	67.87	48	38.95	175.72	83.84	87.75	100.0	81.47	67.03
20	58.24	150.53	87.58	92.04	100.0	82.31	67.81	49	38.75	176.07	83.78	87.7	100.0	81.45	67.02
21	56.65	152.14	87.34	91.76	100.0	82.24	67.75	50	38.57	176.39	83.74	87.64	100.0	81.44	67.0
22	55.18	153.7	87.11	91.49	100.0	82.19	67.7	51	38.39	176.69	83.69	87.59	100.0	81.42	66.98
23	53.82	155.19	86.88	91.23	100.0	82.15	67.67	52	38.23	176.98	83.65	87.55	100.0	81.43	66.99
24	52.55	156.61	86.67	90.98	100.0	82.11	67.64	53	38.08	177.24	83.61	87.51	100.0	81.39	66.95
25	51.38	157.98	86.46	90.74	100.0	82.09	67.62	54	37.94	177.49	83.57	87.47	100.0	81.36	66.92
26	50.29	159.29	86.26	90.52	100.0	82.07	67.6	55	37.82	177.72	83.54	87.43	100.0	81.33	66.9
27	49.29	160.54	86.08	90.3	100.0	82.06	67.59	56	37.7	177.94	83.51	87.39	100.0	81.31	66.87
28	48.35	161.72	85.91	90.09	100.0	82.07	67.59	57	37.58	178.14	83.48	87.36	100.0	81.28	66.85
29	47.48	162.85	85.74	89.9	100.0	82.08	67.6	58	37.48	178.33	83.45	87.33	100.0	81.26	66.82
30	46.68	163.93	85.58	89.71	100.0	82.09	67.61	59	37.38	178.51	83.42	87.3	100.0	81.24	66.8

Table A.84.: S^{15+}

Step	$\hat{E}$	$\hat{T}$	P_1	P_2	P_T	P_S	P_{AS}	Step	$\hat{E}$	$\hat{T}$	P_1	P_2	P_T	P_S	P_{AS}
2	0.0	83.33	0.0	0.0	0.0	0.0	0.0	31	50.17	159.44	86.24	90.49	100.0	82.85	68.24
3	0.0	87.71	0.0	0.0	0.0	0.0	0.0	32	49.41	160.37	86.1	90.33	100.0	82.91	68.29
4	0.0	92.17	0.0	0.0	0.0	0.0	0.0	33	48.71	161.26	85.97	90.17	100.0	82.87	68.26
5	0.0	96.7	0.0	0.0	0.0	0.0	0.0	34	48.06	162.09	85.85	90.03	100.0	82.83	68.23
6	0.0	101.26	0.0	0.0	0.0	0.0	0.0	35	47.46	162.89	85.74	89.89	100.0	82.8	68.2
7	0.0	106.72	94.87	98.41	100.0	78.0	64.29	36	46.9	163.63	85.63	89.76	100.0	82.77	68.18
8	125.58	111.34	94.09	97.95	100.0	78.87	65.0	37	46.38	164.34	85.52	89.65	100.0	82.75	68.16
9	113.72	115.92	93.3	97.43	100.0	79.7	65.68	38	45.89	165.0	85.42	89.53	100.0	82.73	68.14
10	103.29	120.4	92.52	96.86	100.0	80.48	66.33	39	45.44	165.63	85.33	89.43	100.0	82.72	68.13
11	94.29	124.77	91.77	96.26	100.0	81.17	66.89	40	45.02	166.22	85.24	89.33	100.0	82.71	68.12
12	86.59	128.99	91.06	95.63	100.0	81.59	67.23	41	44.63	166.77	85.16	89.23	100.0	82.7	68.11
13	80.0	133.04	90.37	95.0	100.0	81.98	67.55	42	44.27	167.3	85.09	89.15	100.0	82.69	68.11
14	77.07	134.99	90.05	94.69	100.0	82.17	67.7	43	43.94	167.79	85.01	89.07	100.0	82.69	68.11
15	74.36	136.88	89.73	94.37	100.0	82.34	67.85	44	43.62	168.25	84.95	88.99	100.0	82.69	68.11
16	71.85	138.73	89.43	94.07	100.0	82.52	67.99	45	43.33	168.68	84.88	88.92	100.0	82.69	68.11
17	69.52	140.52	89.14	93.76	100.0	82.68	68.12	46	43.06	169.08	84.82	88.85	100.0	82.7	68.11
18	67.37	142.25	88.87	93.47	100.0	82.84	68.25	47	42.81	169.46	84.76	88.78	100.0	82.7	68.11
19	65.37	143.93	88.6	93.18	100.0	83.1	68.46	48	42.58	169.82	84.71	88.72	100.0	82.71	68.12
20	63.52	145.54	88.35	92.91	100.0	83.03	68.4	49	42.36	170.15	84.66	88.67	100.0	82.72	68.13
21	61.81	147.1	88.11	92.64	100.0	82.97	68.35	50	42.16	170.46	84.61	88.62	100.0	82.73	68.13
22	60.22	148.59	87.88	92.38	100.0	82.91	68.31	51	41.97	170.75	84.57	88.57	100.0	82.74	68.14
23	58.75	150.03	87.66	92.13	100.0	82.87	68.27	52	41.8	171.03	84.53	88.52	100.0	82.77	68.17
24	57.37	151.41	87.45	91.89	100.0	82.84	68.25	53	41.64	171.28	84.49	88.48	100.0	82.76	68.16
25	56.1	152.72	87.25	91.66	100.0	82.82	68.23	54	41.49	171.52	84.46	88.44	100.0	82.75	68.15
26	54.91	153.98	87.07	91.44	100.0	82.8	68.21	55	41.35	171.75	84.42	88.4	100.0	82.74	68.14
27	53.82	155.19	86.88	91.23	100.0	82.8	68.21	56	41.22	171.95	84.39	88.37	100.0	82.73	68.13
28	52.8	156.33	86.71	91.03	100.0	82.8	68.21	57	41.09	172.15	84.37	88.34	100.0	82.72	68.12
29	51.86	157.42	86.54	90.84	100.0	82.81	68.21	58	40.98	172.33	84.34	88.31	100.0	82.72	68.11
30	50.98	158.46	86.39	90.66	100.0	82.82	68.23	59	40.88	172.5	84.31	88.28	100.0	82.71	68.11

Table A.85.: S^{16+}

Step	$\hat{E}$	$\hat{T}$	P_1	P_2	P_T	P_S	P_{AS}	Step	$\hat{E}$	$\hat{T}$	P_1	P_2	P_T	P_S	P_{AS}
2	0.0	80.88	0.0	0.0	0.0	0.0	0.0	31	54.47	154.47	86.99	91.35	100.0	83.48	68.78
3	0.0	85.12	0.0	0.0	0.0	0.0	0.0	32	53.65	155.37	86.85	91.2	100.0	83.54	68.83
4	0.0	89.45	0.0	0.0	0.0	0.0	0.0	33	52.9	156.22	86.72	91.05	100.0	83.51	68.79
5	0.0	93.83	0.0	0.0	0.0	0.0	0.0	34	52.19	157.03	86.6	90.91	100.0	83.47	68.76
6	0.0	98.25	0.0	0.0	0.0	0.0	0.0	35	51.54	157.8	86.49	90.78	100.0	83.44	68.74
7	0.0	102.67	0.0	0.0	0.0	0.0	0.0	36	50.93	158.52	86.38	90.65	100.0	83.42	68.72
8	0.0	107.98	94.66	98.29	100.0	79.13	65.21	37	50.37	159.2	86.28	90.53	100.0	83.4	68.7
9	122.69	112.4	93.91	97.83	100.0	80.0	65.93	38	49.84	159.84	86.18	90.42	100.0	83.38	68.69
10	111.75	116.74	93.16	97.33	100.0	80.84	66.62	39	49.36	160.45	86.09	90.32	100.0	83.36	68.67
11	102.07	120.96	92.42	96.79	100.0	81.57	67.23	40	48.91	161.01	86.01	90.22	100.0	83.35	68.66
12	93.76	125.04	91.72	96.22	100.0	82.03	67.6	41	48.48	161.55	85.93	90.12	100.0	83.35	68.66
13	86.65	128.95	91.06	95.64	100.0	82.47	67.95	42	48.09	162.05	85.86	90.04	100.0	83.34	68.65
14	83.49	130.84	90.74	95.35	100.0	82.67	68.12	43	47.73	162.53	85.79	89.95	100.0	83.34	68.65
15	80.56	132.67	90.43	95.06	100.0	82.87	68.28	44	47.39	162.97	85.73	89.88	100.0	83.34	68.65
16	77.85	134.46	90.13	94.77	100.0	83.06	68.44	45	47.08	163.39	85.66	89.81	100.0	83.34	68.65
17	75.34	136.19	89.85	94.49	100.0	83.25	68.59	46	46.79	163.78	85.6	89.74	100.0	83.34	68.65
18	73.01	137.86	89.57	94.21	100.0	83.43	68.74	47	46.52	164.15	85.55	89.68	100.0	83.35	68.66
19	70.86	139.48	89.31	93.94	100.0	83.72	68.98	48	46.26	164.49	85.5	89.62	100.0	83.36	68.66
20	68.86	141.04	89.06	93.68	100.0	83.65	68.92	49	46.03	164.81	85.45	89.57	100.0	83.37	68.67
21	67.01	142.54	88.82	93.42	100.0	83.6	68.88	50	45.81	165.11	85.41	89.51	100.0	83.37	68.68
22	65.3	143.99	88.59	93.17	100.0	83.55	68.84	51	45.61	165.4	85.36	89.47	100.0	83.39	68.69
23	63.71	145.38	88.38	92.93	100.0	83.51	68.8	52	45.42	165.66	85.33	89.42	100.0	83.41	68.71
24	62.23	146.71	88.17	92.7	100.0	83.48	68.78	53	45.24	165.91	85.29	89.38	100.0	83.4	68.7
25	60.87	147.98	87.97	92.48	100.0	83.46	68.76	54	45.08	166.14	85.25	89.34	100.0	83.39	68.69
26	59.6	149.2	87.79	92.27	100.0	83.45	68.75	55	44.93	166.35	85.22	89.31	100.0	83.38	68.68
27	58.41	150.36	87.61	92.07	100.0	83.44	68.74	56	44.79	166.55	85.19	89.27	100.0	83.38	68.67
28	57.32	151.46	87.44	91.88	100.0	83.44	68.74	57	44.66	166.74	85.17	89.24	100.0	83.37	68.66
29	56.3	152.52	87.28	91.69	100.0	83.45	68.75	58	44.53	166.92	85.14	89.21	100.0	83.37	68.66
30	55.35	153.52	87.14	91.52	100.0	83.46	68.76	59	44.42	167.08	85.12	89.18	100.0	83.36	68.65

Table A.86.: Ca^{1+}

Step	$\hat{E}$	$\hat{T}$	P_1	P_2	P_T	P_S	P_{AS}	Step	$\hat{E}$	$\hat{T}$	P_1	P_2	P_T	P_S	P_{AS}
2	6.68	360.78	57.38	62.46	58.89	38.42	30.72	31	0.91	0.0	18.48	18.26	0.01	8.26	6.57
3	5.68	384.04	55.85	57.87	38.92	35.46	28.3	32	0.0	0.0	18.15	17.93	0.0	8.1	6.44
4	4.83	408.64	54.05	53.72	22.43	32.57	25.95	33	0.0	0.0	17.83	17.61	0.0	7.96	6.33
5	4.14	434.06	50.88	50.51	11.74	29.71	23.64	34	0.0	0.0	17.55	17.32	0.0	7.82	6.22
6	3.56	460.2	47.77	47.4	5.83	27.19	21.61	35	0.0	0.0	17.28	17.05	0.0	7.69	6.12
7	3.1	487.19	44.73	44.37	2.92	24.74	19.64	36	0.0	0.0	17.02	16.8	0.0	7.57	6.03
8	2.72	0.0	41.83	41.47	1.49	22.46	17.82	37	0.0	0.0	16.78	16.56	0.0	7.47	5.94
9	2.39	0.0	39.06	38.71	0.78	20.47	16.23	38	0.0	0.0	16.56	16.34	0.0	7.37	5.87
10	2.12	0.0	36.48	36.14	0.43	18.67	14.8	39	0.0	0.0	16.35	16.14	0.0	7.28	5.79
11	1.9	0.0	34.05	33.73	0.25	17.04	13.51	40	0.0	0.0	16.16	15.95	0.0	7.19	5.72
12	1.71	0.0	31.81	31.49	0.16	15.59	12.36	41	0.0	0.0	15.98	15.77	0.0	7.11	5.66
13	1.56	0.0	29.76	29.44	0.1	14.31	11.35	42	0.0	0.0	15.81	15.6	0.0	7.03	5.6
14	1.49	0.0	28.8	28.49	0.09	13.75	10.91	43	0.0	0.0	15.65	15.44	0.0	6.97	5.55
15	1.43	0.0	27.88	27.58	0.07	13.19	10.46	44	0.0	0.0	15.5	15.3	0.0	6.9	5.5
16	1.37	0.0	27.01	26.72	0.06	12.71	10.08	45	0.0	0.0	15.36	15.16	0.0	6.84	5.45
17	1.32	0.0	26.19	25.9	0.05	12.24	9.71	46	0.0	0.0	15.24	15.03	0.0	6.78	5.4
18	1.27	0.0	25.4	25.11	0.04	11.8	9.37	47	0.0	0.0	15.12	14.92	0.0	6.73	5.36
19	1.23	0.0	24.67	24.39	0.04	11.4	9.05	48	0.0	0.0	15.01	14.81	0.0	6.68	5.32
20	1.19	0.0	23.96	23.68	0.03	11.01	8.74	49	0.0	0.0	14.91	14.71	0.0	6.64	5.29
21	1.15	0.0	23.29	23.02	0.03	10.67	8.47	50	0.0	0.0	14.81	14.61	0.0	6.6	5.26
22	1.12	0.0	22.67	22.41	0.03	10.34	8.21	51	0.0	0.0	14.72	14.52	0.0	6.56	5.23
23	1.09	0.0	22.09	21.83	0.02	10.03	7.97	52	0.0	0.0	14.63	14.43	0.0	6.53	5.2
24	1.06	0.0	21.52	21.27	0.02	9.75	7.75	53	0.0	0.0	14.56	14.36	0.0	6.49	5.17
25	1.03	0.0	21.0	20.75	0.02	9.48	7.53	54	0.0	0.0	14.48	14.28	0.0	6.46	5.15
26	1.01	0.0	20.52	20.27	0.02	9.24	7.34	55	0.0	0.0	14.41	14.22	0.0	6.43	5.12
27	0.98	0.0	20.06	19.82	0.02	9.02	7.17	56	0.0	0.0	14.35	14.15	0.0	6.4	5.1
28	0.96	0.0	19.63	19.39	0.02	8.8	6.99	57	0.0	0.0	14.29	14.1	0.0	6.38	5.08
29	0.95	0.0	19.22	18.99	0.01	8.61	6.84	58	0.0	0.0	14.24	14.04	0.0	6.36	5.06
30	0.93	0.0	18.84	18.61	0.01	8.43	6.7	59	0.0	0.0	14.19	13.99	0.0	6.33	5.05

Table A.87.: Ca^{2+}

Step	$\hat{E}$	$\hat{T}$	P_1	P_2	P_T	P_S	P_{AS}	Step	$\hat{E}$	$\hat{T}$	P_1	P_2	P_T	P_S	P_{AS}
2	17.85	249.66	76.75	81.4	99.96	56.21	45.57	31	2.52	0.0	40.24	39.88	1.02	21.77	17.27
3	15.3	264.35	73.98	79.21	99.83	54.24	43.88	32	2.48	0.0	39.84	39.48	0.93	21.48	17.04
4	13.16	279.49	71.02	76.86	99.29	52.0	41.98	33	2.44	0.0	39.47	39.12	0.86	21.19	16.81
5	11.4	295.01	67.96	74.34	97.64	49.5	39.86	34	2.4	0.0	39.12	38.77	0.79	20.92	16.59
6	9.92	310.85	64.9	71.69	93.64	47.17	37.91	35	2.36	0.0	38.79	38.45	0.73	20.66	16.38
7	8.68	326.93	62.03	68.89	85.99	44.83	35.97	36	2.33	0.0	38.49	38.15	0.68	20.41	16.18
8	7.62	343.19	59.51	65.87	74.33	42.29	33.87	37	2.3	0.0	38.21	37.87	0.64	20.22	16.03
9	6.74	359.54	57.49	62.71	59.99	40.0	31.99	38	2.27	0.0	37.94	37.6	0.6	20.03	15.89
10	6.0	375.9	56.09	59.5	45.6	37.83	30.22	39	2.25	0.0	37.7	37.36	0.57	19.86	15.75
11	5.38	392.22	55.62	56.27	32.76	35.55	28.35	40	2.22	0.0	37.46	37.13	0.54	19.69	15.62
12	4.84	408.33	54.09	53.77	22.6	33.66	26.83	41	2.2	0.0	37.24	36.9	0.51	19.54	15.49
13	4.4	423.92	52.14	51.78	15.3	31.82	25.34	42	2.18	0.0	37.04	36.7	0.49	19.39	15.38
14	4.2	431.46	51.2	50.83	12.58	30.9	24.59	43	2.16	0.0	36.84	36.5	0.47	19.25	15.27
15	4.02	438.84	50.3	49.94	10.34	30.06	23.91	44	2.14	0.0	36.66	36.32	0.45	19.12	15.16
16	3.86	446.06	49.43	49.06	8.53	29.35	23.34	45	2.13	0.0	36.49	36.15	0.43	19.0	15.07
17	3.7	453.11	48.59	48.23	7.05	28.65	22.78	46	2.11	0.0	36.34	35.99	0.42	18.88	14.97
18	3.56	459.98	47.8	47.43	5.87	27.95	22.22	47	2.1	0.0	36.19	35.85	0.41	18.78	14.89
19	3.44	466.68	47.02	46.65	4.93	27.27	21.67	48	2.08	0.0	36.06	35.71	0.39	18.67	14.81
20	3.33	473.18	46.28	45.92	4.18	26.59	21.12	49	2.07	0.0	35.93	35.58	0.38	18.58	14.73
21	3.22	479.48	45.58	45.22	3.55	26.01	20.65	50	2.06	0.0	35.8	35.46	0.37	18.49	14.66
22	3.13	485.59	44.9	44.54	3.05	25.49	20.24	51	2.05	0.0	35.69	35.35	0.36	18.4	14.59
23	3.04	491.48	44.27	43.91	2.63	24.98	19.83	52	2.04	0.0	35.58	35.24	0.35	18.32	14.53
24	2.95	497.17	43.67	43.31	2.28	24.49	19.44	53	2.03	0.0	35.48	35.14	0.35	18.25	14.47
25	2.88	502.64	43.1	42.74	1.99	24.01	19.05	54	2.02	0.0	35.39	35.05	0.34	18.18	14.41
26	2.81	507.91	42.54	42.19	1.75	23.54	18.68	55	2.01	0.0	35.3	34.96	0.33	18.11	14.36
27	2.74	0.0	42.02	41.67	1.55	23.09	18.32	56	2.01	0.0	35.22	34.88	0.33	18.07	14.33
28	2.68	0.0	41.54	41.18	1.39	22.74	18.04	57	2.0	0.0	35.15	34.81	0.32	18.03	14.29
29	2.62	0.0	41.08	40.72	1.24	22.41	17.78	58	1.99	0.0	35.08	34.74	0.32	17.98	14.26
30	2.57	0.0	40.65	40.29	1.12	22.08	17.52	59	1.99	0.0	35.01	34.67	0.31	17.94	14.22

Table A.88.: Ca^{3+}

Step	$\hat{E}$	$\hat{T}$	P_1	P_2	P_T	P_S	P_{AS}	Step	$\hat{E}$	$\hat{T}$	P_1	P_2	P_T	P_S	P_{AS}
2	30.87	203.13	84.48	87.79	99.99	64.01	52.41	31	4.63	415.52	53.17	52.83	18.94	33.59	26.76
3	26.64	214.81	82.72	86.26	99.99	62.7	51.22	32	4.55	418.41	52.81	52.46	17.61	33.24	26.48
4	23.08	226.79	80.79	84.65	99.99	61.21	49.86	33	4.47	421.16	52.47	52.12	16.42	32.89	26.19
5	20.06	239.02	78.69	82.95	99.99	59.5	48.32	34	4.4	423.77	52.16	51.8	15.36	32.56	25.92
6	17.51	251.43	76.43	81.14	99.96	57.82	46.86	35	4.34	426.23	51.85	51.49	14.42	32.24	25.67
7	15.37	263.95	74.05	79.27	99.84	56.09	45.38	36	4.28	428.56	51.56	51.19	13.57	31.94	25.42
8	13.55	276.5	71.61	77.33	99.46	54.19	43.77	37	4.22	430.76	51.28	50.92	12.81	31.65	25.19
9	12.04	288.99	69.14	75.33	98.47	52.13	42.03	38	4.17	432.83	51.03	50.66	12.13	31.38	24.97
10	10.77	301.35	66.72	73.29	96.4	49.94	40.17	39	4.12	434.79	50.79	50.42	11.52	31.12	24.76
11	9.7	313.48	64.41	71.25	92.66	48.29	38.81	40	4.07	436.64	50.56	50.2	10.97	30.88	24.57
12	8.79	325.32	62.3	69.18	86.94	46.47	37.3	41	4.03	438.38	50.36	49.99	10.47	30.72	24.44
13	8.02	336.78	60.45	67.07	79.35	44.62	35.77	42	3.99	440.01	50.16	49.8	10.03	30.56	24.31
14	7.67	342.35	59.62	66.04	75.01	43.68	34.99	43	3.96	441.55	49.97	49.61	9.62	30.4	24.18
15	7.36	347.8	58.89	64.98	70.44	42.74	34.22	44	3.93	443.0	49.8	49.43	9.26	30.25	24.06
16	7.06	353.13	58.2	63.96	65.74	41.98	33.59	45	3.89	444.36	49.63	49.27	8.92	30.11	23.95
17	6.8	358.33	57.6	62.95	61.07	41.29	33.03	46	3.87	445.64	49.48	49.11	8.62	29.98	23.85
18	6.55	363.4	57.14	61.94	56.55	40.61	32.47	47	3.84	446.84	49.33	48.97	8.35	29.86	23.75
19	6.33	368.32	56.71	60.97	52.18	39.94	31.93	48	3.81	447.97	49.2	48.83	8.1	29.74	23.65
20	6.12	373.1	56.3	60.04	48.0	39.26	31.37	49	3.79	449.03	49.07	48.71	7.87	29.64	23.57
21	5.93	377.73	56.03	59.13	44.05	38.58	30.82	50	3.77	450.01	48.96	48.59	7.66	29.53	23.49
22	5.75	382.22	55.9	58.23	40.37	37.92	30.28	51	3.75	450.94	48.85	48.48	7.48	29.44	23.41
23	5.58	386.55	55.78	57.37	36.96	37.28	29.75	52	3.73	451.81	48.74	48.38	7.3	29.35	23.34
24	5.43	390.74	55.66	56.55	33.83	36.64	29.24	53	3.71	452.62	48.65	48.28	7.14	29.27	23.27
25	5.29	394.76	55.55	55.78	30.98	36.03	28.73	54	3.7	453.38	48.56	48.19	7.0	29.19	23.21
26	5.16	398.63	55.38	55.08	28.4	35.6	28.39	55	3.68	454.09	48.48	48.11	6.87	29.11	23.14
27	5.03	402.33	54.88	54.57	26.07	35.17	28.04	56	3.67	454.76	48.4	48.03	6.74	29.04	23.09
28	4.92	405.87	54.41	54.09	23.98	34.75	27.7	57	3.66	455.38	48.33	47.96	6.63	28.97	23.03
29	4.82	409.25	53.97	53.64	22.11	34.35	27.37	58	3.64	455.96	48.26	47.9	6.53	28.91	22.98
30	4.72	412.46	53.56	53.22	20.43	33.96	27.06	59	3.63	456.5	48.2	47.83	6.43	28.85	22.94

Table A.89.: Ca^{4+}

Step	$\hat{E}$	$\hat{T}$	P_1	P_2	P_T	P_S	P_{AS}	Step	$\hat{E}$	$\hat{T}$	P_1	P_2	P_T	P_S	P_{AS}
2	45.11	175.93	88.11	91.32	100.0	67.99	55.93	31	7.09	352.58	58.27	64.06	66.24	43.03	34.43
3	39.02	185.9	86.86	90.02	100.0	67.23	55.22	32	6.97	354.9	57.98	63.62	64.15	42.72	34.18
4	33.88	196.12	85.48	88.7	99.99	66.35	54.4	33	6.86	357.1	57.72	63.2	62.16	42.41	33.93
5	29.55	206.53	83.98	87.35	99.99	65.33	53.46	34	6.75	359.19	57.52	62.78	60.31	42.11	33.68
6	25.91	217.08	82.37	85.97	99.99	64.14	52.37	35	6.66	361.17	57.34	62.38	58.54	41.82	33.45
7	22.83	227.7	80.65	84.53	99.99	62.77	51.12	36	6.57	363.05	57.17	62.01	56.87	41.55	33.22
8	20.22	238.32	78.81	83.05	99.99	61.24	49.74	37	6.49	364.82	57.02	61.66	55.28	41.29	33.01
9	18.0	248.86	76.89	81.51	99.97	59.77	48.45	38	6.41	366.5	56.87	61.33	53.79	41.04	32.81
10	16.13	259.26	74.95	79.98	99.9	58.37	47.27	39	6.34	368.08	56.73	61.02	52.39	40.81	32.62
11	14.54	269.43	73.0	78.44	99.72	56.88	45.99	40	6.27	369.57	56.6	60.73	51.08	40.59	32.44
12	13.19	279.3	71.06	76.89	99.3	55.25	44.62	41	6.21	370.98	56.48	60.45	49.84	40.38	32.27
13	12.06	288.82	69.17	75.35	98.49	53.59	43.21	42	6.15	372.3	56.37	60.19	48.69	40.18	32.11
14	11.56	293.43	68.27	74.6	97.89	52.75	42.49	43	6.1	373.55	56.26	59.95	47.61	40.0	31.96
15	11.1	297.93	67.38	73.86	97.12	51.9	41.78	44	6.05	374.72	56.16	59.73	46.61	39.82	31.82
16	10.68	302.31	66.53	73.13	96.17	51.05	41.06	45	6.01	375.82	56.09	59.51	45.67	39.66	31.69
17	10.29	306.58	65.71	72.41	95.03	50.57	40.67	46	5.96	376.85	56.06	59.3	44.79	39.51	31.56
18	9.93	310.72	64.93	71.71	93.69	49.96	40.16	47	5.92	377.82	56.03	59.11	43.98	39.36	31.44
19	9.6	314.73	64.18	71.03	92.16	49.38	39.68	48	5.89	378.74	56.0	58.92	43.22	39.23	31.33
20	9.29	318.62	63.48	70.34	90.45	48.75	39.16	49	5.85	379.59	55.98	58.75	42.51	39.1	31.23
21	9.01	322.37	62.82	69.69	88.57	48.14	38.66	50	5.82	380.39	55.95	58.59	41.85	38.98	31.13
22	8.74	325.99	62.19	69.06	86.55	47.54	38.16	51	5.79	381.14	55.93	58.44	41.24	38.87	31.04
23	8.5	329.47	61.62	68.41	84.42	46.96	37.68	52	5.76	381.85	55.91	58.3	40.67	38.77	30.96
24	8.27	332.82	61.08	67.8	82.19	46.38	37.2	53	5.74	382.51	55.89	58.17	40.14	38.66	30.87
25	8.06	336.04	60.56	67.21	79.9	45.83	36.75	54	5.71	383.12	55.87	58.05	39.65	38.57	30.79
26	7.87	339.12	60.08	66.65	77.57	45.29	36.3	55	5.69	383.7	55.86	57.93	39.19	38.48	30.72
27	7.69	342.06	59.66	66.09	75.24	44.77	35.87	56	5.67	384.24	55.84	57.83	38.76	38.39	30.65
28	7.52	344.88	59.28	65.54	72.92	44.26	35.45	57	5.65	384.74	55.83	57.73	38.37	38.31	30.58
29	7.37	347.57	58.92	65.02	70.64	43.78	35.05	58	5.63	385.21	55.81	57.64	38.0	38.24	30.52
30	7.23	350.14	58.59	64.53	68.41	43.31	34.66	59	5.62	385.65	55.8	57.55	37.66	38.17	30.47

Table A.90.: Ca^{5+}

Step	$\hat{E}$	$\hat{T}$	P_1	P_2	P_T	P_S	P_{AS}	Step	$\hat{E}$	$\hat{T}$	P_1	P_2	P_T	P_S	P_{AS}
2	60.25	157.57	90.29	93.73	100.0	69.83	57.5	31	9.79	312.4	64.61	71.43	93.08	50.8	40.83
3	52.22	166.4	89.25	92.57	100.0	69.75	57.43	32	9.63	314.38	64.25	71.09	92.3	50.5	40.59
4	45.43	175.46	88.17	91.38	100.0	69.43	57.12	33	9.48	316.27	63.91	70.76	91.51	50.19	40.33
5	39.7	184.67	87.02	90.18	100.0	68.82	56.53	34	9.34	318.05	63.59	70.44	90.71	49.88	40.08
6	34.86	194.0	85.78	88.98	99.99	68.08	55.83	35	9.2	319.74	63.28	70.15	89.91	49.59	39.84
7	30.77	203.39	84.44	87.76	99.99	67.2	55.03	36	9.08	321.34	63.0	69.87	89.11	49.32	39.61
8	27.33	212.76	83.03	86.53	99.99	66.21	54.11	37	8.97	322.85	62.73	69.6	88.32	49.06	39.4
9	24.41	222.05	81.56	85.29	99.99	65.09	53.09	38	8.87	324.28	62.48	69.36	87.53	48.82	39.19
10	21.93	231.19	80.04	84.04	99.99	63.86	51.98	39	8.77	325.62	62.25	69.12	86.77	48.58	39.0
11	19.81	240.13	78.5	82.8	99.99	62.51	50.76	40	8.68	326.89	62.04	68.89	86.02	48.36	38.82
12	18.02	248.79	76.9	81.52	99.97	61.25	49.66	41	8.59	328.08	61.84	68.67	85.29	48.16	38.65
13	16.49	257.13	75.36	80.3	99.92	60.09	48.67	42	8.52	329.21	61.66	68.46	84.59	47.96	38.49
14	15.81	261.16	74.58	79.69	99.88	59.5	48.17	43	8.44	330.26	61.49	68.27	83.9	47.78	38.34
15	15.19	265.09	73.84	79.1	99.82	58.9	47.67	44	8.38	331.26	61.33	68.08	83.25	47.6	38.19
16	14.61	268.91	73.1	78.52	99.73	58.31	47.16	45	8.31	332.19	61.18	67.91	82.62	47.44	38.06
17	14.08	272.63	72.37	77.94	99.62	57.72	46.66	46	8.26	333.06	61.04	67.75	82.02	47.29	37.93
18	13.59	276.23	71.66	77.37	99.47	57.13	46.16	47	8.2	333.88	60.91	67.6	81.45	47.14	37.81
19	13.13	279.73	70.97	76.82	99.28	56.56	45.67	48	8.15	334.65	60.78	67.46	80.9	47.01	37.7
20	12.71	283.1	70.31	76.29	99.04	55.94	45.15	49	8.11	335.38	60.67	67.33	80.38	46.88	37.6
21	12.33	286.35	69.66	75.76	98.75	55.33	44.63	50	8.06	336.05	60.56	67.21	79.89	46.77	37.5
22	11.98	289.49	69.04	75.25	98.41	54.73	44.13	51	8.02	336.68	60.46	67.09	79.42	46.66	37.41
23	11.66	292.5	68.45	74.76	98.02	54.14	43.63	52	7.98	337.28	60.37	66.98	78.98	46.56	37.33
24	11.36	295.4	67.88	74.28	97.57	53.57	43.15	53	7.95	337.83	60.28	66.88	78.56	46.46	37.25
25	11.08	298.17	67.34	73.81	97.07	53.02	42.68	54	7.92	338.35	60.2	66.79	78.16	46.36	37.16
26	10.82	300.83	66.82	73.38	96.51	52.48	42.22	55	7.89	338.83	60.13	66.7	77.79	46.27	37.09
27	10.58	303.37	66.33	72.95	95.91	52.15	41.96	56	7.86	339.29	60.06	66.62	77.44	46.18	37.02
28	10.36	305.79	65.86	72.54	95.25	51.79	41.66	57	7.83	339.71	59.99	66.54	77.11	46.1	36.95
29	10.16	308.1	65.42	72.15	94.56	51.45	41.37	58	7.81	340.11	59.93	66.47	76.8	46.02	36.89
30	9.97	310.3	65.01	71.78	93.83	51.11	41.1	59	7.79	340.48	59.88	66.4	76.51	45.96	36.83

Table A.91.: Ca^{6+}

Step	$\hat{E}$	$\hat{T}$	P_1	P_2	P_T	P_S	P_{AS}	Step	$\hat{E}$	$\hat{T}$	P_1	P_2	P_T	P_S	P_{AS}
2	76.11	144.12	91.86	95.47	100.0	70.92	58.41	31	12.64	283.69	70.19	76.19	98.99	56.96	45.97
3	66.04	152.13	90.92	94.44	100.0	70.99	58.46	32	12.43	285.46	69.84	75.9	98.84	56.66	45.71
4	57.56	160.33	89.96	93.37	100.0	71.03	58.48	33	12.24	287.14	69.51	75.63	98.67	56.31	45.43
5	50.39	168.69	88.99	92.27	100.0	71.04	58.48	34	12.07	288.73	69.19	75.37	98.5	55.99	45.15
6	44.31	177.14	87.96	91.16	100.0	70.7	58.14	35	11.9	290.23	68.9	75.13	98.32	55.68	44.89
7	39.17	185.63	86.89	90.06	100.0	70.15	57.62	36	11.75	291.65	68.62	74.9	98.14	55.39	44.64
8	34.82	194.1	85.76	88.97	99.99	69.51	57.02	37	11.61	293.0	68.35	74.68	97.95	55.11	44.41
9	31.13	202.5	84.57	87.87	99.99	68.77	56.33	38	11.47	294.26	68.1	74.46	97.76	54.85	44.19
10	28.01	210.76	83.34	86.8	99.99	67.95	55.56	39	11.35	295.46	67.87	74.27	97.56	54.6	43.98
11	25.37	218.83	82.09	85.73	99.99	67.02	54.71	40	11.24	296.59	67.65	74.08	97.37	54.36	43.78
12	23.12	226.64	80.82	84.67	99.99	65.93	53.73	41	11.13	297.64	67.44	73.9	97.17	54.14	43.59
13	21.2	234.15	79.52	83.62	99.99	64.8	52.7	42	11.03	298.64	67.24	73.74	96.98	53.93	43.42
14	20.34	237.77	78.9	83.12	99.99	64.22	52.18	43	10.94	299.58	67.06	73.58	96.79	53.74	43.25
15	19.56	241.31	78.28	82.62	99.98	63.63	51.65	44	10.86	300.46	66.89	73.44	96.6	53.55	43.09
16	18.83	244.75	77.64	82.11	99.98	63.04	51.12	45	10.78	301.29	66.73	73.3	96.41	53.38	42.95
17	18.16	248.09	77.03	81.63	99.97	62.69	50.83	46	10.71	302.06	66.58	73.17	96.23	53.22	42.81
18	17.53	251.33	76.45	81.16	99.96	62.26	50.47	47	10.64	302.79	66.44	73.05	96.05	53.24	42.84
19	16.96	254.46	75.88	80.71	99.94	61.86	50.13	48	10.57	303.47	66.31	72.94	95.88	53.14	42.75
20	16.43	257.49	75.29	80.25	99.92	61.39	49.73	49	10.52	304.11	66.19	72.83	95.72	53.05	42.68
21	15.94	260.41	74.73	79.8	99.89	60.93	49.34	50	10.46	304.71	66.07	72.73	95.56	52.96	42.61
22	15.48	263.22	74.19	79.38	99.85	60.48	48.95	51	10.41	305.27	65.96	72.63	95.4	52.88	42.54
23	15.06	265.92	73.68	78.98	99.8	60.03	48.58	52	10.36	305.79	65.86	72.54	95.25	52.81	42.48
24	14.67	268.51	73.18	78.59	99.75	59.6	48.21	53	10.32	306.28	65.77	72.46	95.11	52.73	42.42
25	14.31	270.99	72.69	78.2	99.68	59.19	47.86	54	10.28	306.74	65.68	72.38	94.98	52.65	42.35
26	13.98	273.37	72.23	77.83	99.59	58.78	47.52	55	10.24	307.17	65.6	72.31	94.85	52.58	42.29
27	13.67	275.63	71.78	77.47	99.5	58.39	47.18	56	10.2	307.57	65.52	72.24	94.73	52.52	42.23
28	13.38	277.8	71.35	77.12	99.39	58.01	46.86	57	10.17	307.95	65.45	72.18	94.61	52.45	42.18
29	13.11	279.86	70.94	76.8	99.27	57.65	46.55	58	10.14	308.3	65.39	72.12	94.5	52.39	42.13
30	12.87	281.82	70.56	76.49	99.13	57.3	46.26	59	10.11	308.62	65.32	72.06	94.4	52.34	42.09

Table A.92.: Ca^{7+}

Step	$\hat{E}$	$\hat{T}$	P_1	P_2	P_T	P_S	P_{AS}	Step	$\hat{E}$	$\hat{T}$	P_1	P_2	P_T	P_S	P_{AS}
2	92.62	133.72	93.16	96.73	100.0	71.7	59.07	31	15.71	261.8	74.46	79.59	99.87	61.86	50.09
3	80.46	141.1	92.23	95.84	100.0	71.87	59.2	32	15.45	263.42	74.15	79.35	99.85	61.64	49.9
4	70.15	148.66	91.33	94.89	100.0	72.03	59.32	33	15.21	264.95	73.87	79.12	99.82	61.37	49.67
5	61.49	156.35	90.43	93.89	100.0	72.16	59.42	34	14.99	266.4	73.59	78.91	99.79	61.11	49.45
6	54.15	164.12	89.52	92.87	100.0	72.28	59.51	35	14.78	267.77	73.33	78.7	99.76	60.86	49.24
7	47.92	171.93	88.61	91.84	100.0	72.3	59.51	36	14.59	269.06	73.07	78.5	99.73	60.63	49.04
8	42.64	179.73	87.65	90.83	100.0	71.87	59.09	37	14.41	270.29	72.83	78.31	99.7	60.41	48.86
9	38.17	187.45	86.66	89.82	100.0	71.4	58.64	38	14.25	271.44	72.61	78.13	99.66	60.2	48.68
10	34.38	195.04	85.63	88.84	99.99	70.86	58.12	39	14.09	272.53	72.39	77.96	99.62	60.0	48.51
11	31.15	202.44	84.58	87.88	99.99	70.23	57.53	40	13.95	273.55	72.19	77.8	99.59	59.82	48.36
12	28.42	209.61	83.52	86.95	99.99	69.44	56.8	41	13.82	274.51	72.01	77.65	99.55	59.64	48.21
13	26.1	216.5	82.46	86.04	99.99	68.61	56.05	42	13.7	275.42	71.83	77.5	99.51	59.48	48.07
14	25.07	219.82	81.93	85.59	99.99	68.18	55.66	43	13.58	276.27	71.66	77.37	99.47	59.32	47.94
15	24.11	223.06	81.4	85.15	99.99	67.75	55.26	44	13.47	277.07	71.5	77.24	99.43	59.18	47.82
16	23.23	226.21	80.88	84.73	99.99	67.31	54.87	45	13.38	277.82	71.35	77.12	99.39	59.04	47.7
17	22.42	229.27	80.37	84.31	99.99	66.88	54.47	46	13.28	278.53	71.21	77.01	99.35	58.92	47.59
18	21.67	232.24	79.86	83.89	99.99	66.43	54.07	47	13.2	279.19	71.08	76.9	99.31	58.8	47.49
19	20.97	235.1	79.36	83.49	99.99	66.02	53.69	48	13.12	279.81	70.95	76.81	99.27	58.69	47.4
20	20.32	237.87	78.89	83.11	99.99	65.53	53.25	49	13.05	280.39	70.84	76.71	99.23	58.59	47.31
21	19.72	240.54	78.42	82.73	99.99	65.04	52.81	50	12.98	280.93	70.73	76.63	99.2	58.49	47.23
22	19.17	243.11	77.94	82.35	99.98	64.56	52.38	51	12.91	281.44	70.63	76.55	99.16	58.4	47.16
23	18.66	245.58	77.49	81.99	99.98	64.09	51.97	52	12.86	281.92	70.54	76.47	99.13	58.33	47.1
24	18.18	247.95	77.06	81.65	99.97	63.89	51.81	53	12.8	282.37	70.45	76.4	99.09	58.24	47.02
25	17.74	250.21	76.65	81.32	99.96	63.57	51.54	54	12.75	282.78	70.37	76.34	99.06	58.15	46.94
26	17.34	252.38	76.26	81.01	99.95	63.26	51.27	55	12.7	283.17	70.29	76.28	99.03	58.07	46.88
27	16.96	254.46	75.88	80.71	99.94	62.95	51.02	56	12.66	283.54	70.22	76.22	99.0	57.99	46.81
28	16.61	256.43	75.49	80.41	99.93	62.66	50.77	57	12.62	283.88	70.15	76.16	98.97	57.92	46.75
29	16.29	258.31	75.13	80.12	99.91	62.39	50.53	58	12.58	284.19	70.09	76.11	98.95	57.86	46.7
30	15.99	260.1	74.79	79.85	99.89	62.12	50.31	59	12.55	284.49	70.03	76.06	98.92	57.8	46.64

Table A.93.: Ca^{8+}

Step	$\hat{E}$	$\hat{T}$	P_1	P_2	P_T	P_S	P_{AS}	Step	$\hat{E}$	$\hat{T}$	P_1	P_2	P_T	P_S	P_{AS}
2	109.62	125.38	94.26	97.64	100.0	72.29	59.56	31	18.9	244.39	77.71	82.17	99.98	65.46	53.1
3	95.34	132.26	93.35	96.9	100.0	72.54	59.75	32	18.6	245.88	77.43	81.95	99.98	65.22	52.88
4	83.23	139.29	92.45	96.07	100.0	72.78	59.94	33	18.31	247.3	77.18	81.74	99.97	65.14	52.83
5	72.96	146.45	91.59	95.17	100.0	73.0	60.12	34	18.05	248.64	76.93	81.55	99.97	64.93	52.66
6	64.3	153.69	90.74	94.24	100.0	73.26	60.33	35	17.8	249.91	76.7	81.36	99.96	64.73	52.49
7	56.98	160.96	89.89	93.29	100.0	73.45	60.48	36	17.58	251.1	76.49	81.19	99.96	64.54	52.32
8	50.76	168.21	89.04	92.33	100.0	73.54	60.55	37	17.36	252.23	76.28	81.03	99.95	64.36	52.17
9	45.48	175.39	88.18	91.39	100.0	73.37	60.37	38	17.17	253.3	76.09	80.88	99.95	64.19	52.03
10	40.99	182.45	87.31	90.47	100.0	73.05	60.04	39	16.99	254.31	75.91	80.73	99.94	64.03	51.9
11	37.18	189.33	86.4	89.58	100.0	72.63	59.64	40	16.82	255.25	75.72	80.59	99.94	63.88	51.77
12	33.94	195.99	85.5	88.72	99.99	72.07	59.11	41	16.66	256.14	75.55	80.45	99.93	63.74	51.65
13	31.17	202.39	84.59	87.89	99.99	71.47	58.55	42	16.52	256.98	75.39	80.32	99.92	63.61	51.54
14	29.96	205.47	84.13	87.49	99.99	71.16	58.26	43	16.38	257.77	75.24	80.2	99.92	63.49	51.44
15	28.83	208.48	83.7	87.1	99.99	70.84	57.96	44	16.25	258.51	75.09	80.09	99.91	63.37	51.34
16	27.79	211.41	83.24	86.71	99.99	70.52	57.67	45	16.14	259.2	74.96	79.99	99.9	63.27	51.25
17	26.83	214.24	82.81	86.34	99.99	70.19	57.37	46	16.03	259.85	74.83	79.89	99.89	63.17	51.16
18	25.94	216.99	82.39	85.98	99.99	69.87	57.07	47	15.93	260.46	74.72	79.79	99.89	63.07	51.08
19	25.12	219.65	81.95	85.62	99.99	69.58	56.8	48	15.83	261.04	74.61	79.71	99.88	62.99	51.01
20	24.35	222.22	81.53	85.27	99.99	69.18	56.44	49	15.75	261.57	74.51	79.63	99.87	62.91	50.94
21	23.65	224.7	81.13	84.93	99.99	68.78	56.08	50	15.66	262.07	74.41	79.55	99.87	62.83	50.88
22	23.0	227.08	80.75	84.62	99.99	68.4	55.74	51	15.59	262.54	74.32	79.48	99.86	62.76	50.82
23	22.39	229.37	80.36	84.3	99.99	68.02	55.4	52	15.52	262.98	74.24	79.42	99.85	62.71	50.78
24	21.84	231.56	79.97	83.99	99.99	67.66	55.08	53	15.45	263.39	74.16	79.36	99.85	62.64	50.71
25	21.32	233.66	79.61	83.69	99.99	67.31	54.76	54	15.39	263.78	74.09	79.3	99.84	62.56	50.65
26	20.83	235.67	79.26	83.41	99.99	66.97	54.46	55	15.34	264.14	74.02	79.24	99.84	62.5	50.59
27	20.39	237.59	78.93	83.15	99.99	66.64	54.16	56	15.28	264.47	73.95	79.19	99.83	62.44	50.54
28	19.97	239.42	78.62	82.9	99.99	66.33	53.88	57	15.23	264.79	73.9	79.15	99.82	62.38	50.49
29	19.59	241.16	78.31	82.64	99.98	66.03	53.61	58	15.19	265.08	73.84	79.1	99.82	62.32	50.44
30	19.23	242.82	78.0	82.4	99.98	65.74	53.35	59	15.15	265.36	73.79	79.06	99.81	62.27	50.4

Table A.94.: Ca^{9+}

Step	$\hat{E}$	$\hat{T}$	P_1	P_2	P_T	P_S	P_{AS}	Step	$\hat{E}$	$\hat{T}$	P_1	P_2	P_T	P_S	P_{AS}
2	127.03	118.49	95.19	98.3	100.0	72.74	59.94	31	22.2	230.1	80.23	84.19	99.99	69.01	56.2
3	110.59	124.96	94.32	97.69	100.0	73.05	60.19	32	21.85	231.5	79.98	84.0	99.99	68.83	56.03
4	96.65	131.57	93.44	96.98	100.0	73.36	60.43	33	21.52	232.82	79.75	83.81	99.99	68.57	55.81
5	84.82	138.29	92.58	96.19	100.0	73.66	60.67	34	21.22	234.08	79.54	83.63	99.99	68.34	55.6
6	74.78	145.09	91.75	95.34	100.0	74.02	60.97	35	20.93	235.26	79.33	83.47	99.99	68.11	55.4
7	66.28	151.91	90.95	94.47	100.0	74.35	61.23	36	20.67	236.38	79.14	83.31	99.99	67.9	55.21
8	59.11	158.72	90.15	93.58	100.0	74.6	61.43	37	20.42	237.44	78.96	83.17	99.99	67.7	55.03
9	53.01	165.46	89.36	92.69	100.0	74.74	61.54	38	20.19	238.43	78.79	83.03	99.99	67.51	54.86
10	47.82	172.08	88.6	91.82	100.0	74.77	61.56	39	19.98	239.37	78.63	82.9	99.99	67.34	54.7
11	43.4	178.53	87.79	90.98	100.0	74.51	61.28	40	19.79	240.26	78.47	82.78	99.99	67.17	54.56
12	39.64	184.78	87.0	90.17	100.0	74.11	60.9	41	19.6	241.09	78.32	82.65	99.98	67.02	54.42
13	36.44	190.78	86.21	89.39	100.0	73.69	60.49	42	19.44	241.87	78.17	82.54	99.98	66.87	54.29
14	35.02	193.67	85.82	89.02	100.0	73.47	60.28	43	19.28	242.61	78.04	82.43	99.98	66.74	54.17
15	33.71	196.49	85.43	88.65	99.99	73.24	60.06	44	19.13	243.3	77.91	82.33	99.98	66.61	54.06
16	32.5	199.23	85.04	88.3	99.99	73.0	59.84	45	19.0	243.95	77.79	82.23	99.98	66.5	53.95
17	31.38	201.89	84.66	87.95	99.99	72.77	59.62	46	18.87	244.55	77.68	82.14	99.98	66.39	53.86
18	30.35	204.46	84.28	87.62	99.99	72.53	59.4	47	18.75	245.12	77.57	82.06	99.98	66.29	53.77
19	29.39	206.96	83.92	87.3	99.99	72.34	59.21	48	18.64	245.66	77.48	81.98	99.98	66.2	53.68
20	28.51	209.36	83.56	86.98	99.99	72.01	58.92	49	18.54	246.16	77.38	81.91	99.97	66.11	53.6
21	27.7	211.68	83.2	86.67	99.99	71.69	58.63	50	18.45	246.63	77.3	81.84	99.97	66.2	53.7
22	26.94	213.91	82.86	86.38	99.99	71.38	58.34	51	18.36	247.07	77.22	81.77	99.97	66.14	53.66
23	26.24	216.05	82.53	86.1	99.99	71.08	58.07	52	18.28	247.48	77.14	81.72	99.97	66.11	53.63
24	25.59	218.1	82.21	85.83	99.99	70.78	57.8	53	18.2	247.86	77.07	81.66	99.97	66.05	53.57
25	24.99	220.07	81.89	85.56	99.99	70.5	57.55	54	18.13	248.22	77.01	81.61	99.97	65.98	53.52
26	24.43	221.95	81.58	85.3	99.99	70.22	57.3	55	18.06	248.55	76.95	81.56	99.97	65.93	53.47
27	23.92	223.74	81.28	85.06	99.99	69.96	57.06	56	18.0	248.87	76.89	81.51	99.97	65.88	53.43
28	23.44	225.45	81.01	84.83	99.99	69.7	56.83	57	17.95	249.16	76.84	81.47	99.97	65.83	53.38
29	23.0	227.08	80.74	84.61	99.99	69.46	56.61	58	17.89	249.43	76.79	81.43	99.96	65.78	53.35
30	22.59	228.63	80.48	84.4	99.99	69.23	56.4	59	17.84	249.69	76.74	81.39	99.96	65.74	53.31

Table A.95.: Ca^{10+}

Step	$\hat{E}$	$\hat{T}$	P_1	P_2	P_T	P_S	P_{AS}	Step	$\hat{E}$	$\hat{T}$	P_1	P_2	P_T	P_S	P_{AS}
2	0.0	111.73	0.0	0.0	0.0	0.0	0.0	31	25.59	218.11	82.21	85.83	99.99	71.84	58.67
3	126.18	118.8	95.15	98.27	100.0	73.47	60.53	32	25.19	219.42	81.99	85.65	99.99	71.7	58.54
4	110.37	125.05	94.31	97.68	100.0	73.83	60.82	33	24.81	220.67	81.79	85.48	99.99	71.49	58.35
5	96.95	131.41	93.46	96.99	100.0	74.19	61.11	34	24.46	221.85	81.59	85.32	99.99	71.28	58.17
6	85.55	137.84	92.63	96.24	100.0	74.63	61.48	35	24.14	222.97	81.41	85.17	99.99	71.09	58.0
7	75.87	144.29	91.84	95.45	100.0	75.08	61.84	36	23.84	224.02	81.24	85.02	99.99	70.91	57.83
8	67.66	150.72	91.09	94.62	100.0	75.44	62.13	37	23.56	225.02	81.08	84.89	99.99	70.74	57.68
9	60.73	157.09	90.34	93.79	100.0	75.72	62.36	38	23.3	225.95	80.93	84.77	99.99	70.58	57.54
10	54.82	163.34	89.61	92.97	100.0	75.9	62.5	39	23.06	226.84	80.78	84.65	99.99	70.43	57.4
11	49.8	169.44	88.9	92.17	100.0	75.97	62.55	40	22.84	227.67	80.65	84.54	99.99	70.28	57.28
12	45.51	175.34	88.18	91.4	100.0	75.75	62.33	41	22.63	228.46	80.52	84.43	99.99	70.15	57.16
13	41.85	181.01	87.49	90.66	100.0	75.46	62.05	42	22.44	229.19	80.39	84.32	99.99	70.03	57.05
14	40.24	183.74	87.14	90.31	100.0	75.31	61.9	43	22.26	229.89	80.26	84.22	99.99	69.92	56.95
15	38.74	186.4	86.79	89.96	100.0	75.15	61.74	44	22.09	230.54	80.15	84.13	99.99	69.81	56.85
16	37.36	188.98	86.45	89.63	100.0	74.99	61.58	45	21.94	231.15	80.04	84.05	99.99	69.71	56.76
17	36.08	191.49	86.11	89.3	100.0	74.83	61.42	46	21.8	231.72	79.94	83.97	99.99	69.62	56.68
18	34.9	193.93	85.79	88.99	99.99	74.66	61.26	47	21.66	232.26	79.85	83.89	99.99	69.54	56.6
19	33.81	196.28	85.46	88.68	99.99	74.54	61.14	48	21.54	232.76	79.76	83.82	99.99	69.46	56.53
20	32.79	198.55	85.14	88.39	99.99	74.27	60.89	49	21.42	233.23	79.68	83.75	99.99	69.39	56.47
21	31.86	200.73	84.84	88.1	99.99	74.01	60.66	50	21.31	233.67	79.61	83.69	99.99	69.32	56.41
22	30.99	202.84	84.52	87.83	99.99	73.76	60.43	51	21.21	234.08	79.54	83.63	99.99	69.26	56.35
23	30.19	204.86	84.22	87.57	99.99	73.51	60.2	52	21.12	234.47	79.47	83.58	99.99	69.22	56.32
24	29.45	206.79	83.94	87.32	99.99	73.27	59.98	53	21.03	234.83	79.41	83.53	99.99	69.15	56.25
25	28.77	208.65	83.67	87.08	99.99	73.04	59.77	54	20.95	235.17	79.35	83.48	99.99	69.08	56.19
26	28.13	210.42	83.4	86.84	99.99	72.82	59.57	55	20.88	235.49	79.29	83.44	99.99	69.02	56.13
27	27.55	212.11	83.13	86.62	99.99	72.61	59.37	56	20.81	235.78	79.24	83.4	99.99	68.96	56.08
28	27.0	213.72	82.88	86.4	99.99	72.4	59.19	57	20.74	236.06	79.2	83.36	99.99	68.9	56.03
29	26.49	215.26	82.65	86.2	99.99	72.21	59.01	58	20.68	236.31	79.15	83.32	99.99	68.85	55.98
30	26.03	216.72	82.43	86.01	99.99	72.02	58.84	59	20.63	236.56	79.11	83.29	99.99	68.81	55.94

Table A.96.: Ca^{11+}

Step	$\hat{E}$	$\hat{T}$	P_1	P_2	P_T	P_S	P_{AS}	Step	$\hat{E}$	$\hat{T}$	P_1	P_2	P_T	P_S	P_{AS}
2	0.0	106.83	0.0	0.0	0.0	0.0	0.0	31	29.06	207.85	83.79	87.18	99.99	74.16	60.7
3	0.0	112.55	0.0	0.0	0.0	0.0	0.0	32	28.61	209.1	83.6	87.02	99.99	74.06	60.6
4	124.36	119.46	95.06	98.21	100.0	74.21	61.14	33	28.18	210.28	83.42	86.86	99.99	73.87	60.43
5	109.32	125.51	94.24	97.63	100.0	74.62	61.47	34	27.79	211.4	83.24	86.71	99.99	73.69	60.27
6	96.55	131.62	93.43	96.97	100.0	75.13	61.9	35	27.43	212.46	83.08	86.57	99.99	73.52	60.12
7	85.69	137.75	92.65	96.25	100.0	75.67	62.33	36	27.09	213.45	82.93	86.44	99.99	73.36	59.98
8	76.46	143.87	91.89	95.5	100.0	76.13	62.71	37	26.78	214.4	82.78	86.32	99.99	73.22	59.85
9	68.61	149.92	91.19	94.73	100.0	76.52	63.03	38	26.49	215.29	82.65	86.2	99.99	73.08	59.72
10	61.99	155.86	90.49	93.95	100.0	76.83	63.27	39	26.21	216.13	82.52	86.09	99.99	72.95	59.61
11	56.34	161.65	89.81	93.19	100.0	77.02	63.43	40	25.96	216.92	82.4	85.99	99.99	72.83	59.5
12	51.52	167.26	89.15	92.46	100.0	77.0	63.41	41	25.73	217.66	82.28	85.89	99.99	72.71	59.4
13	47.41	172.64	88.53	91.75	100.0	76.95	63.36	42	25.51	218.36	82.17	85.79	99.99	72.61	59.3
14	45.59	175.23	88.2	91.41	100.0	76.91	63.32	43	25.31	219.01	82.06	85.7	99.99	72.51	59.21
15	43.9	177.76	87.89	91.08	100.0	76.72	63.11	44	25.12	219.63	81.96	85.62	99.99	72.42	59.13
16	42.34	180.21	87.59	90.76	100.0	76.62	63.01	45	24.95	220.21	81.86	85.54	99.99	72.34	59.06
17	40.9	182.6	87.29	90.45	100.0	76.51	62.9	46	24.79	220.75	81.77	85.47	99.99	72.26	58.99
18	39.57	184.9	86.99	90.15	100.0	76.4	62.78	47	24.64	221.26	81.69	85.4	99.99	72.19	58.92
19	38.34	187.14	86.7	89.87	100.0	76.34	62.71	48	24.5	221.74	81.61	85.33	99.99	72.12	58.86
20	37.2	189.29	86.41	89.59	100.0	76.13	62.51	49	24.37	222.18	81.54	85.27	99.99	72.06	58.81
21	36.15	191.36	86.13	89.32	100.0	75.91	62.32	50	24.25	222.6	81.47	85.22	99.99	72.01	58.76
22	35.17	193.36	85.87	89.06	100.0	75.71	62.13	51	24.13	222.99	81.41	85.16	99.99	71.96	58.71
23	34.27	195.28	85.6	88.81	99.99	75.51	61.94	52	24.03	223.36	81.35	85.11	99.99	71.93	58.68
24	33.43	197.11	85.34	88.57	99.99	75.31	61.76	53	23.93	223.7	81.29	85.07	99.99	71.86	58.62
25	32.65	198.87	85.09	88.34	99.99	75.12	61.59	54	23.84	224.02	81.24	85.02	99.99	71.8	58.57
26	31.93	200.55	84.86	88.13	99.99	74.94	61.42	55	23.76	224.32	81.19	84.98	99.99	71.75	58.52
27	31.27	202.16	84.62	87.92	99.99	74.77	61.26	56	23.68	224.6	81.14	84.95	99.99	71.7	58.47
28	30.65	203.69	84.4	87.72	99.99	74.61	61.11	57	23.6	224.86	81.1	84.91	99.99	71.65	58.43
29	30.08	205.15	84.18	87.53	99.99	74.45	60.97	58	23.54	225.11	81.06	84.88	99.99	71.61	58.39
30	29.55	206.53	83.98	87.35	99.99	74.3	60.83	59	23.47	225.33	81.03	84.85	99.99	71.56	58.35

Table A.97.: Ca^{12+}

Step	$\hat{E}$	$\hat{T}$	P_1	P_2	P_T	P_S	P_{AS}	Step	$\hat{E}$	$\hat{T}$	P_1	P_2	P_T	P_S	P_{AS}
2	0.0	102.56	0.0	0.0	0.0	0.0	0.0	31	32.62	198.94	85.08	88.33	99.99	76.09	62.38
3	0.0	108.03	0.0	0.0	0.0	0.0	0.0	32	32.11	200.13	84.92	88.18	99.99	76.02	62.31
4	0.0	113.61	0.0	0.0	0.0	0.0	0.0	33	31.64	201.26	84.76	88.03	99.99	75.85	62.16
5	121.91	120.38	94.94	98.13	100.0	74.97	61.78	34	31.2	202.33	84.6	87.89	99.99	75.69	62.02
6	107.74	126.21	94.15	97.56	100.0	75.55	62.25	35	30.79	203.33	84.45	87.76	99.99	75.55	61.89
7	95.69	132.07	93.37	96.92	100.0	76.16	62.74	36	30.42	204.29	84.31	87.64	99.99	75.41	61.77
8	85.44	137.91	92.63	96.23	100.0	76.71	63.19	37	30.07	205.19	84.18	87.52	99.99	75.28	61.65
9	76.72	143.68	91.91	95.52	100.0	77.19	63.59	38	29.74	206.03	84.05	87.41	99.99	75.16	61.54
10	69.29	149.36	91.25	94.8	100.0	77.6	63.92	39	29.44	206.83	83.94	87.31	99.99	75.05	61.44
11	63.01	154.89	90.6	94.08	100.0	77.89	64.16	40	29.16	207.58	83.83	87.22	99.99	74.94	61.35
12	57.66	160.23	89.97	93.38	100.0	77.97	64.22	41	28.9	208.29	83.73	87.12	99.99	74.85	61.26
13	53.09	165.36	89.38	92.71	100.0	78.01	64.24	42	28.66	208.96	83.62	87.04	99.99	74.75	61.18
14	51.06	167.84	89.09	92.38	100.0	78.02	64.24	43	28.43	209.58	83.53	86.95	99.99	74.67	61.1
15	49.18	170.25	88.81	92.06	100.0	78.01	64.24	44	28.22	210.17	83.43	86.88	99.99	74.59	61.03
16	47.44	172.59	88.53	91.76	100.0	78.0	64.23	45	28.03	210.72	83.35	86.8	99.99	74.52	60.97
17	45.84	174.86	88.24	91.46	100.0	77.99	64.21	46	27.85	211.24	83.27	86.73	99.99	74.46	60.91
18	44.35	177.07	87.97	91.17	100.0	77.85	64.05	47	27.68	211.72	83.19	86.67	99.99	74.4	60.85
19	42.98	179.19	87.71	90.89	100.0	77.84	64.03	48	27.52	212.18	83.12	86.61	99.99	74.34	60.8
20	41.71	181.25	87.46	90.63	100.0	77.67	63.86	49	27.38	212.6	83.06	86.55	99.99	74.29	60.75
21	40.53	183.23	87.2	90.37	100.0	77.5	63.7	50	27.24	213.0	83.0	86.5	99.99	74.24	60.71
22	39.44	185.13	86.96	90.12	100.0	77.33	63.54	51	27.12	213.37	82.94	86.45	99.99	74.2	60.67
23	38.44	186.96	86.72	89.89	100.0	77.16	63.39	52	27.0	213.72	82.89	86.4	99.99	74.18	60.65
24	37.5	188.71	86.49	89.66	100.0	77.01	63.25	53	26.89	214.05	82.83	86.36	99.99	74.12	60.6
25	36.64	190.39	86.26	89.44	100.0	76.86	63.1	54	26.79	214.35	82.79	86.32	99.99	74.07	60.55
26	35.84	191.99	86.05	89.24	100.0	76.71	62.97	55	26.7	214.64	82.74	86.28	99.99	74.02	60.51
27	35.09	193.52	85.84	89.04	100.0	76.57	62.84	56	26.61	214.91	82.7	86.25	99.99	73.98	60.46
28	34.4	194.98	85.64	88.85	99.99	76.44	62.72	57	26.53	215.15	82.67	86.22	99.99	73.93	60.42
29	33.76	196.37	85.44	88.67	99.99	76.32	62.6	58	26.45	215.39	82.63	86.19	99.99	73.89	60.39
30	33.17	197.69	85.26	88.5	99.99	76.2	62.49	59	26.38	215.6	82.6	86.16	99.99	73.86	60.36

Table A.98.: Ca^{13+}

Step	$\hat{E}$	$\hat{T}$	P_1	P_2	P_T	P_S	P_{AS}	Step	$\hat{E}$	$\hat{T}$	P_1	P_2	P_T	P_S	P_{AS}
2	0.0	98.78	0.0	0.0	0.0	0.0	0.0	31	36.27	191.12	86.16	89.35	100.0	77.72	63.81
3	0.0	104.04	0.0	0.0	0.0	0.0	0.0	32	35.71	192.26	86.01	89.2	100.0	77.67	63.76
4	0.0	109.41	0.0	0.0	0.0	0.0	0.0	33	35.18	193.34	85.87	89.07	100.0	77.53	63.63
5	0.0	114.85	0.0	0.0	0.0	0.0	0.0	34	34.7	194.36	85.73	88.93	99.99	77.39	63.5
6	119.11	121.45	94.79	98.03	100.0	75.9	62.54	35	34.25	195.32	85.59	88.81	99.99	77.26	63.39
7	105.86	127.07	94.03	97.47	100.0	76.57	63.09	36	33.83	196.23	85.46	88.69	99.99	77.14	63.28
8	94.57	132.66	93.29	96.85	100.0	77.2	63.6	37	33.44	197.09	85.34	88.57	99.99	77.03	63.18
9	84.97	138.2	92.59	96.2	100.0	77.76	64.06	38	33.08	197.9	85.23	88.47	99.99	76.92	63.08
10	76.79	143.63	91.92	95.53	100.0	78.25	64.46	39	32.74	198.67	85.12	88.37	99.99	76.82	62.99
11	69.81	148.93	91.3	94.85	100.0	78.64	64.78	40	32.43	199.39	85.02	88.28	99.99	76.73	62.91
12	63.91	154.05	90.7	94.19	100.0	78.79	64.9	41	32.14	200.07	84.93	88.19	99.99	76.65	62.83
13	58.87	158.97	90.12	93.55	100.0	78.91	64.99	42	31.87	200.7	84.84	88.11	99.99	76.57	62.76
14	56.63	161.34	89.85	93.24	100.0	78.96	65.03	43	31.62	201.3	84.75	88.03	99.99	76.5	62.7
15	54.56	163.65	89.58	92.93	100.0	78.99	65.06	44	31.39	201.86	84.67	87.96	99.99	76.43	62.64
16	52.65	165.89	89.31	92.64	100.0	79.02	65.08	45	31.17	202.39	84.59	87.89	99.99	76.37	62.58
17	50.88	168.07	89.06	92.35	100.0	79.05	65.1	46	30.97	202.88	84.52	87.82	99.99	76.31	62.53
18	49.24	170.18	88.82	92.07	100.0	79.07	65.11	47	30.79	203.35	84.45	87.76	99.99	76.26	62.48
19	47.72	172.21	88.58	91.81	100.0	79.13	65.16	48	30.61	203.78	84.38	87.71	99.99	76.22	62.44
20	46.31	174.18	88.33	91.55	100.0	79.03	65.08	49	30.45	204.19	84.32	87.65	99.99	76.17	62.4
21	45.01	176.08	88.09	91.3	100.0	78.83	64.87	50	30.3	204.57	84.27	87.6	99.99	76.13	62.36
22	43.81	177.9	87.87	91.06	100.0	78.7	64.74	51	30.17	204.93	84.21	87.56	99.99	76.1	62.33
23	42.69	179.65	87.65	90.84	100.0	78.57	64.62	52	30.04	205.26	84.17	87.51	99.99	76.09	62.32
24	41.66	181.33	87.45	90.62	100.0	78.44	64.5	53	29.92	205.57	84.12	87.47	99.99	76.03	62.27
25	40.7	182.93	87.24	90.41	100.0	78.32	64.39	54	29.81	205.86	84.08	87.44	99.99	75.99	62.23
26	39.82	184.47	87.04	90.21	100.0	78.21	64.28	55	29.7	206.14	84.04	87.4	99.99	75.94	62.18
27	39.0	185.93	86.85	90.02	100.0	78.1	64.17	56	29.61	206.39	84.0	87.37	99.99	75.9	62.15
28	38.24	187.33	86.67	89.84	100.0	77.99	64.07	57	29.52	206.63	83.97	87.34	99.99	75.86	62.11
29	37.53	188.66	86.49	89.67	100.0	77.9	63.98	58	29.43	206.85	83.93	87.31	99.99	75.83	62.08
30	36.88	189.92	86.32	89.5	100.0	77.8	63.89	59	29.35	207.06	83.9	87.28	99.99	75.8	62.05

Table A.99.: Ca^{14+}

Step	$\hat{E}$	$\hat{T}$	P_1	P_2	P_T	P_S	P_{AS}	Step	$\hat{E}$	$\hat{T}$	P_1	P_2	P_T	P_S	P_{AS}
2	0.0	95.42	0.0	0.0	0.0	0.0	0.0	31	39.98	184.18	87.08	90.25	100.0	79.11	65.03
3	0.0	100.49	0.0	0.0	0.0	0.0	0.0	32	39.37	185.27	86.94	90.11	100.0	79.09	65.0
4	0.0	105.66	0.0	0.0	0.0	0.0	0.0	33	38.79	186.3	86.81	89.97	100.0	78.96	64.88
5	0.0	110.9	0.0	0.0	0.0	0.0	0.0	34	38.26	187.28	86.68	89.85	100.0	78.84	64.77
6	0.0	116.18	0.0	0.0	0.0	0.0	0.0	35	37.77	188.21	86.55	89.73	100.0	78.73	64.67
7	116.18	122.62	94.63	97.92	100.0	76.93	63.39	36	37.31	189.09	86.44	89.61	100.0	78.62	64.57
8	103.85	128.0	93.91	97.37	100.0	77.61	63.95	37	36.88	189.91	86.32	89.51	100.0	78.52	64.48
9	93.35	133.32	93.21	96.78	100.0	78.24	64.46	38	36.48	190.69	86.22	89.4	100.0	78.43	64.4
10	84.41	138.55	92.55	96.16	100.0	78.81	64.93	39	36.12	191.42	86.12	89.31	100.0	78.34	64.32
11	76.78	143.64	91.92	95.53	100.0	79.27	65.31	40	35.78	192.12	86.03	89.22	100.0	78.26	64.25
12	70.26	148.56	91.34	94.9	100.0	79.49	65.48	41	35.46	192.77	85.94	89.14	100.0	78.19	64.18
13	64.74	153.29	90.79	94.29	100.0	79.68	65.63	42	35.16	193.38	85.86	89.06	100.0	78.12	64.12
14	62.3	155.56	90.53	93.99	100.0	79.76	65.7	43	34.89	193.95	85.78	88.99	99.99	78.06	64.06
15	60.03	157.78	90.26	93.7	100.0	79.83	65.75	44	34.63	194.49	85.71	88.91	99.99	78.0	64.01
16	57.94	159.94	90.01	93.42	100.0	79.9	65.81	45	34.4	195.0	85.64	88.85	99.99	77.95	63.96
17	56.0	162.03	89.77	93.14	100.0	79.96	65.85	46	34.18	195.47	85.57	88.79	99.99	77.9	63.92
18	54.2	164.06	89.53	92.88	100.0	80.01	65.9	47	33.97	195.92	85.51	88.73	99.99	77.86	63.88
19	52.54	166.01	89.3	92.62	100.0	80.13	65.99	48	33.78	196.33	85.45	88.67	99.99	77.82	63.84
20	51.0	167.9	89.08	92.37	100.0	80.03	65.91	49	33.6	196.72	85.39	88.62	99.99	77.79	63.81
21	49.58	169.72	88.87	92.13	100.0	79.95	65.84	50	33.44	197.09	85.34	88.57	99.99	77.75	63.78
22	48.26	171.48	88.67	91.9	100.0	79.89	65.78	51	33.29	197.43	85.29	88.53	99.99	77.73	63.75
23	47.04	173.16	88.46	91.68	100.0	79.83	65.74	52	33.14	197.75	85.25	88.49	99.99	77.72	63.74
24	45.91	174.77	88.26	91.47	100.0	79.79	65.7	53	33.01	198.05	85.21	88.45	99.99	77.67	63.7
25	44.86	176.31	88.06	91.27	100.0	79.58	65.48	54	32.89	198.33	85.17	88.41	99.99	77.63	63.66
26	43.88	177.78	87.88	91.08	100.0	79.49	65.4	55	32.77	198.59	85.13	88.38	99.99	77.59	63.62
27	42.98	179.19	87.71	90.9	100.0	79.4	65.31	56	32.67	198.84	85.1	88.35	99.99	77.55	63.59
28	42.14	180.53	87.55	90.72	100.0	79.32	65.23	57	32.57	199.07	85.07	88.32	99.99	77.52	63.56
29	41.37	181.81	87.39	90.56	100.0	79.25	65.16	58	32.48	199.28	85.04	88.29	99.99	77.49	63.53
30	40.65	183.02	87.23	90.4	100.0	79.18	65.09	59	32.39	199.48	85.01	88.26	99.99	77.46	63.5

Table A.100.: Ca^{15+}

Step	$\hat{E}$	$\hat{T}$	P_1	P_2	P_T	P_S	P_{AS}	Step	$\hat{E}$	$\hat{T}$	P_1	P_2	P_T	P_S	P_{AS}
2	0.0	92.41	0.0	0.0	0.0	0.0	0.0	31	43.77	177.96	87.86	91.06	100.0	80.33	66.09
3	0.0	97.3	0.0	0.0	0.0	0.0	0.0	32	43.1	179.01	87.73	90.92	100.0	80.32	66.07
4	0.0	102.3	0.0	0.0	0.0	0.0	0.0	33	42.47	180.01	87.61	90.79	100.0	80.21	65.97
5	0.0	107.36	0.0	0.0	0.0	0.0	0.0	34	41.89	180.95	87.5	90.67	100.0	80.1	65.87
6	0.0	112.46	0.0	0.0	0.0	0.0	0.0	35	41.35	181.84	87.39	90.55	100.0	80.0	65.78
7	126.64	118.63	95.17	98.29	100.0	77.24	63.65	36	40.85	182.69	87.28	90.44	100.0	79.91	65.7
8	113.26	123.82	94.47	97.8	100.0	77.98	64.25	37	40.38	183.48	87.17	90.34	100.0	79.82	65.62
9	101.86	128.95	93.78	97.27	100.0	78.66	64.82	38	39.95	184.23	87.07	90.24	100.0	79.74	65.54
10	92.14	133.99	93.12	96.7	100.0	79.3	65.33	39	39.55	184.94	86.98	90.15	100.0	79.66	65.47
11	83.85	138.9	92.5	96.11	100.0	79.82	65.77	40	39.18	185.61	86.9	90.06	100.0	79.59	65.41
12	76.77	143.64	91.92	95.53	100.0	80.1	65.99	41	38.83	186.23	86.82	89.98	100.0	79.53	65.35
13	70.72	148.2	91.39	94.95	100.0	80.35	66.19	42	38.51	186.82	86.74	89.91	100.0	79.47	65.3
14	68.05	150.39	91.13	94.67	100.0	80.46	66.28	43	38.21	187.37	86.67	89.83	100.0	79.42	65.25
15	65.59	152.53	90.88	94.39	100.0	80.56	66.36	44	37.94	187.89	86.6	89.77	100.0	79.37	65.2
16	63.31	154.61	90.64	94.12	100.0	80.66	66.44	45	37.68	188.38	86.53	89.7	100.0	79.32	65.16
17	61.2	156.62	90.4	93.85	100.0	80.75	66.51	46	37.44	188.84	86.47	89.64	100.0	79.28	65.12
18	59.25	158.58	90.17	93.6	100.0	80.83	66.58	47	37.21	189.27	86.41	89.59	100.0	79.25	65.09
19	57.44	160.46	89.95	93.35	100.0	80.99	66.71	48	37.01	189.67	86.36	89.54	100.0	79.21	65.06
20	55.77	162.28	89.74	93.11	100.0	80.9	66.63	49	36.81	190.04	86.31	89.49	100.0	79.18	65.03
21	54.22	164.04	89.53	92.88	100.0	80.83	66.57	50	36.63	190.4	86.26	89.44	100.0	79.16	65.01
22	52.79	165.72	89.33	92.66	100.0	80.76	66.52	51	36.47	190.73	86.22	89.4	100.0	79.13	64.98
23	51.46	167.34	89.14	92.45	100.0	80.71	66.47	52	36.31	191.03	86.17	89.36	100.0	79.13	64.98
24	50.22	168.89	88.97	92.24	100.0	80.67	66.44	53	36.17	191.32	86.14	89.32	100.0	79.09	64.94
25	49.08	170.38	88.8	92.05	100.0	80.65	66.41	54	36.03	191.59	86.1	89.29	100.0	79.05	64.9
26	48.02	171.8	88.63	91.86	100.0	80.63	66.4	55	35.91	191.84	86.07	89.26	100.0	79.01	64.87
27	47.04	173.16	88.46	91.68	100.0	80.62	66.39	56	35.79	192.08	86.04	89.23	100.0	78.98	64.84
28	46.13	174.45	88.3	91.51	100.0	80.62	66.39	57	35.69	192.3	86.01	89.2	100.0	78.95	64.81
29	45.28	175.68	88.14	91.35	100.0	80.42	66.19	58	35.58	192.5	85.98	89.17	100.0	78.92	64.78
30	44.5	176.85	88.0	91.2	100.0	80.37	66.13	59	35.49	192.7	85.95	89.15	100.0	78.9	64.76

Table A.101.: Ca^{16+}

Step	$\hat{E}$	$\hat{T}$	P_1	P_2	P_T	P_S	P_{AS}	Step	$\hat{E}$	$\hat{T}$	P_1	P_2	P_T	P_S	P_{AS}
2	0.0	89.67	0.0	0.0	0.0	0.0	0.0	31	47.62	172.35	88.56	91.79	100.0	81.45	67.07
3	0.0	94.42	0.0	0.0	0.0	0.0	0.0	32	46.89	173.36	88.43	91.66	100.0	81.52	67.13
4	0.0	99.25	0.0	0.0	0.0	0.0	0.0	33	46.21	174.33	88.31	91.53	100.0	81.48	67.09
5	0.0	104.15	0.0	0.0	0.0	0.0	0.0	34	45.58	175.24	88.2	91.41	100.0	81.43	67.06
6	0.0	109.09	0.0	0.0	0.0	0.0	0.0	35	45.0	176.1	88.09	91.3	100.0	81.11	66.75
7	0.0	114.04	0.0	0.0	0.0	0.0	0.0	36	44.45	176.91	87.99	91.19	100.0	81.03	66.68
8	122.78	120.05	94.98	98.16	100.0	78.29	64.52	37	43.95	177.68	87.89	91.09	100.0	80.95	66.61
9	110.47	125.01	94.31	97.68	100.0	79.03	65.12	38	43.48	178.41	87.81	91.0	100.0	80.88	66.54
10	99.97	129.88	93.66	97.16	100.0	79.72	65.69	39	43.05	179.09	87.72	90.91	100.0	80.82	66.48
11	91.02	134.62	93.04	96.63	100.0	80.31	66.17	40	42.64	179.73	87.64	90.83	100.0	80.75	66.43
12	83.37	139.21	92.46	96.08	100.0	80.63	66.44	41	42.26	180.34	87.57	90.75	100.0	80.7	66.37
13	76.83	143.6	91.92	95.53	100.0	80.93	66.68	42	41.92	180.91	87.5	90.67	100.0	80.65	66.33
14	73.92	145.72	91.67	95.26	100.0	81.07	66.79	43	41.59	181.44	87.44	90.61	100.0	80.6	66.28
15	71.24	147.79	91.43	95.0	100.0	81.2	66.89	44	41.29	181.94	87.37	90.54	100.0	80.56	66.25
16	68.76	149.8	91.2	94.74	100.0	81.32	66.99	45	41.01	182.41	87.31	90.48	100.0	80.52	66.21
17	66.48	151.74	90.97	94.49	100.0	81.44	67.09	46	40.75	182.85	87.25	90.42	100.0	80.49	66.18
18	64.37	153.63	90.75	94.25	100.0	81.55	67.18	47	40.51	183.27	87.2	90.37	100.0	80.46	66.15
19	62.41	155.45	90.54	94.01	100.0	81.74	67.33	48	40.28	183.65	87.15	90.32	100.0	80.43	66.12
20	60.61	157.21	90.33	93.78	100.0	81.66	67.26	49	40.08	184.02	87.1	90.27	100.0	80.41	66.1
21	58.93	158.9	90.13	93.56	100.0	81.59	67.21	50	39.88	184.36	87.06	90.22	100.0	80.38	66.08
22	57.38	160.53	89.94	93.34	100.0	81.53	67.16	51	39.7	184.68	87.02	90.18	100.0	80.37	66.06
23	55.94	162.1	89.76	93.14	100.0	81.48	67.12	52	39.53	184.97	86.98	90.14	100.0	80.37	66.06
24	54.6	163.6	89.58	92.94	100.0	81.45	67.08	53	39.38	185.25	86.94	90.11	100.0	80.33	66.02
25	53.37	165.03	89.41	92.75	100.0	81.42	67.06	54	39.23	185.51	86.91	90.07	100.0	80.29	65.99
26	52.22	166.4	89.25	92.57	100.0	81.41	67.05	55	39.1	185.76	86.88	90.04	100.0	80.26	65.96
27	51.16	167.71	89.1	92.4	100.0	81.4	67.04	56	38.97	185.98	86.85	90.01	100.0	80.23	65.93
28	50.17	168.96	88.96	92.23	100.0	81.4	67.04	57	38.85	186.2	86.82	89.99	100.0	80.21	65.91
29	49.26	170.15	88.82	92.08	100.0	81.41	67.04	58	38.74	186.39	86.79	89.96	100.0	80.18	65.88
30	48.41	171.28	88.7	91.93	100.0	81.43	67.06	59	38.64	186.58	86.77	89.94	100.0	80.16	65.86

Table A.102.: Ca^{17+}

Step	$\hat{E}$	$\hat{T}$	P_1	P_2	P_T	P_S	P_{AS}	Step	$\hat{E}$	$\hat{T}$	P_1	P_2	P_T	P_S	P_{AS}
2	0.0	87.19	0.0	0.0	0.0	0.0	0.0	31	51.53	167.25	89.16	92.46	100.0	82.13	67.65
3	0.0	91.79	0.0	0.0	0.0	0.0	0.0	32	50.74	168.24	89.04	92.33	100.0	82.2	67.7
4	0.0	96.48	0.0	0.0	0.0	0.0	0.0	33	50.01	169.17	88.93	92.21	100.0	82.16	67.66
5	0.0	101.23	0.0	0.0	0.0	0.0	0.0	34	49.33	170.05	88.83	92.09	100.0	82.12	67.63
6	0.0	106.03	0.0	0.0	0.0	0.0	0.0	35	48.7	170.89	88.74	91.98	100.0	82.09	67.6
7	0.0	110.82	0.0	0.0	0.0	0.0	0.0	36	48.11	171.67	88.65	91.88	100.0	82.06	67.58
8	0.0	115.59	0.0	0.0	0.0	0.0	0.0	37	47.57	172.42	88.55	91.78	100.0	82.03	67.56
9	119.19	121.42	94.8	98.03	100.0	79.36	65.4	38	47.07	173.12	88.46	91.69	100.0	82.01	67.54
10	107.9	126.14	94.16	97.56	100.0	80.1	66.0	39	46.6	173.78	88.38	91.6	100.0	82.0	67.53
11	98.27	130.73	93.54	97.07	100.0	80.73	66.52	40	46.16	174.4	88.3	91.52	100.0	81.98	67.52
12	90.05	135.17	92.97	96.56	100.0	81.11	66.83	41	45.76	174.99	88.23	91.44	100.0	81.98	67.51
13	83.02	139.43	92.44	96.05	100.0	81.45	67.11	42	45.38	175.54	88.16	91.37	100.0	81.69	67.24
14	79.89	141.48	92.18	95.8	100.0	81.61	67.24	43	45.03	176.05	88.1	91.3	100.0	81.65	67.2
15	77.0	143.48	91.94	95.55	100.0	81.76	67.36	44	44.7	176.54	88.04	91.24	100.0	81.61	67.16
16	74.32	145.42	91.71	95.3	100.0	81.91	67.48	45	44.4	176.99	87.98	91.18	100.0	81.58	67.13
17	71.85	147.31	91.49	95.06	100.0	82.05	67.59	46	44.12	177.42	87.93	91.13	100.0	81.55	67.11
18	69.56	149.14	91.28	94.83	100.0	82.18	67.7	47	43.86	177.82	87.88	91.07	100.0	81.53	67.08
19	67.45	150.9	91.07	94.6	100.0	82.41	67.89	48	43.62	178.2	87.83	91.02	100.0	81.5	67.06
20	65.5	152.6	90.87	94.38	100.0	82.33	67.82	49	43.39	178.55	87.79	90.98	100.0	81.48	67.04
21	63.7	154.24	90.68	94.17	100.0	82.27	67.77	50	43.18	178.88	87.75	90.94	100.0	81.47	67.02
22	62.03	155.82	90.5	93.96	100.0	82.21	67.72	51	42.99	179.18	87.71	90.9	100.0	81.45	67.01
23	60.48	157.33	90.32	93.76	100.0	82.17	67.68	52	42.8	179.47	87.68	90.86	100.0	81.46	67.01
24	59.05	158.78	90.14	93.57	100.0	82.13	67.65	53	42.64	179.74	87.64	90.82	100.0	81.42	66.98
25	57.72	160.17	89.98	93.39	100.0	82.11	67.63	54	42.48	179.99	87.61	90.79	100.0	81.39	66.95
26	56.48	161.5	89.83	93.21	100.0	82.09	67.62	55	42.33	180.23	87.58	90.76	100.0	81.36	66.92
27	55.34	162.77	89.68	93.05	100.0	82.08	67.61	56	42.2	180.45	87.56	90.73	100.0	81.34	66.9
28	54.28	163.97	89.54	92.89	100.0	82.09	67.61	57	42.07	180.65	87.53	90.71	100.0	81.31	66.87
29	53.29	165.12	89.4	92.74	100.0	82.1	67.62	58	41.95	180.85	87.51	90.68	100.0	81.29	66.85
30	52.38	166.22	89.28	92.59	100.0	82.11	67.63	59	41.84	181.02	87.49	90.66	100.0	81.27	66.83

Table A.103.: Ca^{18+}

Step	$\hat{E}$	$\hat{T}$	P_1	P_2	P_T	P_S	P_{AS}	Step	$\hat{E}$	$\hat{T}$	P_1	P_2	P_T	P_S	P_{AS}
2	0.0	84.91	0.0	0.0	0.0	0.0	0.0	31	55.49	162.6	89.7	93.07	100.0	82.74	68.16
3	0.0	89.38	0.0	0.0	0.0	0.0	0.0	32	54.64	163.55	89.59	92.94	100.0	82.81	68.21
4	0.0	93.94	0.0	0.0	0.0	0.0	0.0	33	53.86	164.46	89.48	92.82	100.0	82.76	68.17
5	0.0	98.56	0.0	0.0	0.0	0.0	0.0	34	53.13	165.31	89.38	92.71	100.0	82.73	68.14
6	0.0	103.22	0.0	0.0	0.0	0.0	0.0	35	52.45	166.12	89.29	92.61	100.0	82.7	68.11
7	0.0	107.88	0.0	0.0	0.0	0.0	0.0	36	51.83	166.89	89.2	92.51	100.0	82.67	68.09
8	0.0	112.52	0.0	0.0	0.0	0.0	0.0	37	51.24	167.61	89.11	92.41	100.0	82.65	68.07
9	0.0	117.09	0.0	0.0	0.0	0.0	0.0	38	50.7	168.29	89.04	92.32	100.0	82.63	68.06
10	115.93	122.72	94.62	97.91	100.0	80.43	66.28	39	50.2	168.93	88.96	92.24	100.0	82.61	68.04
11	105.62	127.18	94.02	97.46	100.0	81.11	66.84	40	49.73	169.53	88.89	92.16	100.0	82.6	68.03
12	96.81	131.49	93.45	96.99	100.0	81.52	67.18	41	49.3	170.1	88.83	92.08	100.0	82.59	68.03
13	89.28	135.62	92.92	96.51	100.0	81.91	67.49	42	48.89	170.63	88.77	92.01	100.0	82.59	68.02
14	85.93	137.61	92.66	96.27	100.0	82.09	67.64	43	48.52	171.13	88.71	91.95	100.0	82.58	68.02
15	82.83	139.55	92.42	96.04	100.0	82.26	67.78	44	48.17	171.6	88.66	91.89	100.0	82.58	68.02
16	79.97	141.43	92.19	95.8	100.0	82.43	67.91	45	47.84	172.04	88.6	91.83	100.0	82.59	68.02
17	77.31	143.26	91.96	95.57	100.0	82.59	68.04	46	47.54	172.46	88.55	91.77	100.0	82.59	68.02
18	74.86	145.03	91.75	95.35	100.0	82.74	68.17	47	47.26	172.85	88.5	91.72	100.0	82.6	68.02
19	72.58	146.74	91.55	95.13	100.0	83.0	68.38	48	47.0	173.21	88.45	91.68	100.0	82.6	68.03
20	70.48	148.39	91.36	94.92	100.0	82.93	68.32	49	46.76	173.55	88.41	91.63	100.0	82.61	68.04
21	68.53	149.98	91.18	94.72	100.0	82.86	68.27	50	46.53	173.87	88.37	91.59	100.0	82.62	68.05
22	66.74	151.51	91.0	94.52	100.0	82.81	68.22	51	46.32	174.17	88.33	91.55	100.0	82.63	68.05
23	65.08	152.98	90.82	94.33	100.0	82.77	68.19	52	46.13	174.45	88.3	91.51	100.0	82.67	68.08
24	63.54	154.39	90.66	94.15	100.0	82.74	68.16	53	45.95	174.71	88.26	91.48	100.0	82.65	68.07
25	62.12	155.73	90.51	93.97	100.0	82.72	68.14	54	45.78	174.95	88.23	91.45	100.0	82.64	68.06
26	60.8	157.02	90.35	93.8	100.0	82.7	68.13	55	45.62	175.18	88.2	91.42	100.0	82.63	68.05
27	59.57	158.25	90.21	93.64	100.0	82.7	68.12	56	45.48	175.39	88.18	91.39	100.0	82.32	67.75
28	58.43	159.42	90.07	93.49	100.0	82.7	68.12	57	45.34	175.59	88.15	91.36	100.0	82.29	67.73
29	57.37	160.54	89.94	93.34	100.0	82.71	68.13	58	45.21	175.78	88.13	91.34	100.0	82.27	67.71
30	56.39	161.59	89.82	93.2	100.0	82.72	68.14	59	45.1	175.95	88.11	91.32	100.0	82.26	67.69

Table A.104.: Ca^{19+}

Step	$\hat{E}$	$\hat{T}$	P_1	P_2	P_T	P_S	P_{AS}	Step	$\hat{E}$	$\hat{T}$	P_1	P_2	P_T	P_S	P_{AS}
2	0.0	82.82	0.0	0.0	0.0	0.0	0.0	31	59.49	158.33	90.2	93.63	100.0	83.29	68.61
3	0.0	87.17	0.0	0.0	0.0	0.0	0.0	32	58.59	159.26	90.09	93.51	100.0	83.35	68.66
4	0.0	91.61	0.0	0.0	0.0	0.0	0.0	33	57.75	160.13	89.99	93.39	100.0	83.31	68.63
5	0.0	96.1	0.0	0.0	0.0	0.0	0.0	34	56.97	160.96	89.89	93.28	100.0	83.27	68.6
6	0.0	100.64	0.0	0.0	0.0	0.0	0.0	35	56.25	161.75	89.8	93.18	100.0	83.24	68.57
7	0.0	105.18	0.0	0.0	0.0	0.0	0.0	36	55.58	162.49	89.71	93.08	100.0	83.22	68.55
8	0.0	109.69	0.0	0.0	0.0	0.0	0.0	37	54.96	163.19	89.63	92.99	100.0	83.2	68.53
9	0.0	114.14	0.0	0.0	0.0	0.0	0.0	38	54.38	163.85	89.55	92.9	100.0	83.18	68.52
10	124.04	119.58	95.05	98.2	100.0	80.73	66.53	39	53.84	164.47	89.48	92.82	100.0	83.16	68.51
11	113.04	123.91	94.46	97.79	100.0	81.45	67.12	40	53.34	165.06	89.41	92.75	100.0	83.15	68.5
12	103.64	128.1	93.89	97.36	100.0	81.9	67.49	41	52.88	165.61	89.35	92.67	100.0	83.15	68.49
13	95.61	132.11	93.36	96.91	100.0	82.32	67.83	42	52.45	166.13	89.29	92.6	100.0	83.14	68.48
14	92.03	134.05	93.12	96.69	100.0	82.52	67.99	43	52.05	166.62	89.23	92.54	100.0	83.14	68.48
15	88.73	135.93	92.88	96.47	100.0	82.71	68.15	44	51.67	167.07	89.18	92.48	100.0	83.14	68.48
16	85.67	137.77	92.64	96.25	100.0	82.89	68.3	45	51.33	167.5	89.13	92.42	100.0	83.14	68.48
17	82.84	139.54	92.42	96.04	100.0	83.07	68.45	46	51.01	167.9	89.08	92.37	100.0	83.14	68.48
18	80.22	141.26	92.21	95.82	100.0	83.25	68.59	47	50.71	168.28	89.04	92.32	100.0	83.15	68.49
19	77.79	142.92	92.0	95.62	100.0	83.53	68.82	48	50.43	168.63	89.0	92.28	100.0	83.16	68.49
20	75.54	144.53	91.81	95.42	100.0	83.46	68.76	49	50.17	168.96	88.96	92.23	100.0	83.16	68.5
21	73.46	146.07	91.63	95.22	100.0	83.4	68.71	50	49.93	169.27	88.92	92.19	100.0	83.17	68.51
22	71.53	147.56	91.46	95.03	100.0	83.35	68.67	51	49.7	169.56	88.89	92.15	100.0	83.18	68.52
23	69.74	148.98	91.3	94.85	100.0	83.31	68.64	52	49.5	169.84	88.86	92.12	100.0	83.21	68.54
24	68.09	150.35	91.13	94.67	100.0	83.28	68.61	53	49.3	170.09	88.83	92.08	100.0	83.2	68.53
25	66.57	151.66	90.98	94.5	100.0	83.26	68.6	54	49.12	170.33	88.8	92.05	100.0	83.19	68.52
26	65.16	152.91	90.83	94.34	100.0	83.25	68.58	55	48.95	170.55	88.78	92.02	100.0	83.18	68.51
27	63.85	154.1	90.69	94.18	100.0	83.24	68.58	56	48.8	170.76	88.75	92.0	100.0	83.18	68.5
28	62.63	155.24	90.56	94.04	100.0	83.24	68.58	57	48.65	170.95	88.73	91.97	100.0	83.17	68.5
29	61.51	156.32	90.44	93.89	100.0	83.25	68.58	58	48.52	171.13	88.71	91.95	100.0	83.16	68.49
30	60.46	157.35	90.31	93.76	100.0	83.27	68.6	59	48.39	171.3	88.69	91.93	100.0	83.16	68.48

Table A.105.: Ca^{20+}

Step	$\hat{E}$	$\hat{T}$	P_1	P_2	P_T	P_S	P_{AS}	Step	$\hat{E}$	$\hat{T}$	P_1	P_2	P_T	P_S	P_{AS}
2	0.0	80.88	0.0	0.0	0.0	0.0	0.0	31	63.54	154.39	90.66	94.15	100.0	83.78	69.02
3	0.0	85.12	0.0	0.0	0.0	0.0	0.0	32	62.58	155.29	90.56	94.03	100.0	83.83	69.07
4	0.0	89.45	0.0	0.0	0.0	0.0	0.0	33	61.69	156.15	90.46	93.92	100.0	83.8	69.04
5	0.0	93.83	0.0	0.0	0.0	0.0	0.0	34	60.86	156.95	90.36	93.81	100.0	83.76	69.01
6	0.0	98.25	0.0	0.0	0.0	0.0	0.0	35	60.09	157.72	90.27	93.71	100.0	83.74	68.99
7	0.0	102.67	0.0	0.0	0.0	0.0	0.0	36	59.38	158.44	90.18	93.62	100.0	83.71	68.96
8	0.0	107.07	0.0	0.0	0.0	0.0	0.0	37	58.72	159.12	90.1	93.53	100.0	83.69	68.95
9	0.0	111.41	0.0	0.0	0.0	0.0	0.0	38	58.1	159.76	90.03	93.44	100.0	83.67	68.93
10	0.0	115.66	0.0	0.0	0.0	0.0	0.0	39	57.53	160.37	89.96	93.36	100.0	83.66	68.92
11	120.54	120.9	94.87	98.08	100.0	81.76	67.38	40	57.0	160.94	89.89	93.29	100.0	83.65	68.91
12	110.55	124.98	94.32	97.68	100.0	82.24	67.77	41	56.5	161.47	89.83	93.22	100.0	83.64	68.91
13	102.0	128.88	93.79	97.27	100.0	82.69	68.14	42	56.05	161.98	89.77	93.15	100.0	83.64	68.9
14	98.21	130.77	93.54	97.07	100.0	82.9	68.32	43	55.62	162.45	89.72	93.09	100.0	83.63	68.9
15	94.69	132.6	93.3	96.86	100.0	83.11	68.49	44	55.22	162.9	89.67	93.03	100.0	83.63	68.9
16	91.44	134.38	93.07	96.65	100.0	83.31	68.65	45	54.85	163.31	89.62	92.98	100.0	83.64	68.9
17	88.43	136.11	92.85	96.45	100.0	83.51	68.81	46	54.51	163.7	89.57	92.92	100.0	83.64	68.9
18	85.64	137.78	92.64	96.25	100.0	83.7	68.97	47	54.19	164.07	89.53	92.88	100.0	83.64	68.91
19	83.06	139.4	92.44	96.05	100.0	84.01	69.22	48	53.89	164.41	89.49	92.83	100.0	83.65	68.91
20	80.67	140.96	92.24	95.86	100.0	83.94	69.16	49	53.62	164.74	89.45	92.79	100.0	83.66	68.92
21	78.45	142.47	92.06	95.67	100.0	83.88	69.12	50	53.36	165.04	89.41	92.75	100.0	83.67	68.93
22	76.4	143.91	91.88	95.49	100.0	83.84	69.08	51	53.12	165.32	89.38	92.71	100.0	83.68	68.93
23	74.49	145.3	91.72	95.32	100.0	83.8	69.05	52	52.9	165.58	89.35	92.68	100.0	83.71	68.96
24	72.73	146.63	91.57	95.15	100.0	83.77	69.02	53	52.7	165.83	89.32	92.64	100.0	83.7	68.95
25	71.09	147.9	91.42	94.99	100.0	83.75	69.0	54	52.5	166.06	89.29	92.61	100.0	83.69	68.94
26	69.58	149.12	91.28	94.83	100.0	83.74	68.99	55	52.33	166.28	89.27	92.59	100.0	83.68	68.93
27	68.18	150.28	91.14	94.68	100.0	83.73	68.99	56	52.16	166.48	89.25	92.56	100.0	83.67	68.92
28	66.89	151.39	91.01	94.54	100.0	83.73	68.99	57	52.01	166.67	89.22	92.53	100.0	83.67	68.91
29	65.69	152.44	90.89	94.4	100.0	83.74	68.99	58	51.86	166.84	89.2	92.51	100.0	83.66	68.9
30	64.57	153.44	90.77	94.27	100.0	83.76	69.01	59	51.73	167.01	89.18	92.49	100.0	83.66	68.9

Table A.106.: Fe^{1+}

Step	$\hat{E}$	$\hat{T}$	P_1	P_2	P_T	P_S	P_{AS}	Step	$\hat{E}$	$\hat{T}$	P_1	P_2	P_T	P_S	P_{AS}
2	5.33	432.94	45.8	45.44	31.5	32.12	25.59	31	0.0	0.0	9.25	9.12	0.0	5.68	4.53
3	4.53	461.91	42.39	42.03	17.04	29.04	23.1	32	0.0	0.0	9.04	8.91	0.0	5.56	4.44
4	3.87	492.42	39.07	38.72	8.42	26.37	20.95	33	0.0	0.0	8.84	8.71	0.0	5.46	4.35
5	3.31	0.0	35.91	35.57	3.97	23.79	18.88	34	0.0	0.0	8.65	8.52	0.0	5.36	4.27
6	2.85	0.0	32.89	32.57	1.86	21.39	16.96	35	0.0	0.0	8.47	8.34	0.0	5.27	4.2
7	2.46	0.0	30.08	29.77	1.03	19.19	15.22	36	0.0	0.0	8.3	8.18	0.0	5.18	4.13
8	2.13	0.0	27.43	27.14	0.51	17.23	13.66	37	0.0	0.0	8.15	8.03	0.0	5.1	4.07
9	1.86	0.0	25.02	24.74	0.27	15.48	12.27	38	0.0	0.0	8.01	7.89	0.0	5.03	4.01
10	1.65	0.0	22.8	22.54	0.15	13.93	11.05	39	0.0	0.0	7.88	7.76	0.0	4.96	3.96
11	1.48	0.0	20.79	20.54	0.09	12.58	9.98	40	0.0	0.0	7.75	7.63	0.0	4.9	3.91
12	1.33	0.0	18.99	18.75	0.06	11.39	9.04	41	0.0	0.0	7.63	7.52	0.0	4.84	3.87
13	1.21	0.0	17.37	17.15	0.04	10.36	8.22	42	0.0	0.0	7.53	7.41	0.0	4.79	3.82
14	1.16	0.0	16.63	16.42	0.03	9.9	7.86	43	0.0	0.0	7.43	7.32	0.0	4.74	3.78
15	1.11	0.0	15.93	15.72	0.03	9.47	7.52	44	0.0	0.0	7.33	7.23	0.0	4.69	3.75
16	1.07	0.0	15.29	15.08	0.02	9.08	7.21	45	0.0	0.0	7.25	7.14	0.0	4.65	3.71
17	0.0	0.0	14.66	14.47	0.0	8.7	6.92	46	0.0	0.0	7.17	7.06	0.0	4.61	3.68
18	0.0	0.0	14.08	13.89	0.0	8.37	6.65	47	0.0	0.0	7.09	6.99	0.0	4.57	3.65
19	0.0	0.0	13.55	13.37	0.0	8.05	6.4	48	0.0	0.0	7.02	6.92	0.0	4.54	3.63
20	0.0	0.0	13.04	12.86	0.0	7.76	6.17	49	0.0	0.0	6.96	6.86	0.0	4.51	3.6
21	0.0	0.0	12.57	12.39	0.0	7.49	5.96	50	0.0	0.0	6.9	6.8	0.0	4.48	3.58
22	0.0	0.0	12.13	11.96	0.0	7.24	5.76	51	0.0	0.0	6.84	6.74	0.0	4.45	3.56
23	0.0	0.0	11.71	11.54	0.0	7.0	5.58	52	0.0	0.0	6.79	6.69	0.0	4.43	3.54
24	0.0	0.0	11.32	11.16	0.0	6.79	5.41	53	0.0	0.0	6.74	6.65	0.0	4.4	3.52
25	0.0	0.0	10.97	10.81	0.0	6.59	5.25	54	0.0	0.0	6.7	6.6	0.0	4.38	3.5
26	0.0	0.0	10.63	10.48	0.0	6.41	5.1	55	0.0	0.0	6.66	6.56	0.0	0.0	0.0
27	0.0	0.0	10.31	10.17	0.0	6.24	4.97	56	0.0	0.0	6.62	6.52	0.0	0.0	0.0
28	0.0	0.0	10.02	9.88	0.0	6.08	4.85	57	0.0	0.0	6.59	6.49	0.0	0.0	0.0
29	0.0	0.0	9.74	9.61	0.0	5.93	4.73	58	0.0	0.0	6.55	6.46	0.0	0.0	0.0
30	0.0	0.0	9.49	9.36	0.0	5.8	4.63	59	0.0	0.0	6.52	6.43	0.0	0.0	0.0

Table A.107.: Fe^{2+}

Step	$\hat{E}$	$\hat{T}$	P_1	P_2	P_T	P_S	P_{AS}	Step	$\hat{E}$	$\hat{T}$	P_1	P_2	P_T	P_S	P_{AS}
2	13.97	295.59	65.35	72.0	99.7	51.09	41.24	31	1.97	0.0	26.01	25.73	0.35	16.41	13.01
3	12.02	313.61	63.76	70.62	98.73	48.37	38.93	32	1.93	0.0	25.68	25.4	0.32	16.15	12.8
4	10.38	332.28	61.95	68.64	95.81	45.92	36.89	33	1.9	0.0	25.37	25.09	0.29	15.93	12.63
5	9.0	351.51	59.66	65.48	89.14	43.3	34.72	34	1.86	0.0	25.07	24.79	0.27	15.72	12.46
6	7.84	371.17	56.6	60.63	77.79	40.39	32.31	35	1.83	0.0	24.79	24.51	0.25	15.52	12.3
7	6.88	391.08	52.31	53.51	62.78	38.07	30.42	36	1.81	0.0	24.52	24.25	0.23	15.33	12.15
8	6.06	411.11	48.56	48.2	46.81	35.48	28.31	37	1.79	0.0	24.28	24.0	0.22	15.15	12.01
9	5.38	431.39	45.99	45.63	32.47	33.21	26.46	38	1.76	0.0	24.05	23.78	0.21	14.97	11.87
10	4.79	451.79	43.55	43.18	21.3	30.96	24.64	39	1.74	0.0	23.84	23.56	0.2	14.81	11.74
11	4.29	472.06	41.27	40.91	13.53	28.93	23.0	40	1.73	0.0	23.63	23.36	0.19	14.66	11.62
12	3.87	492.03	39.11	38.76	8.49	27.04	21.48	41	1.71	0.0	23.44	23.18	0.18	14.53	11.52
13	3.52	511.56	37.15	36.8	5.36	25.33	20.11	42	1.69	0.0	23.27	23.0	0.17	14.42	11.43
14	3.36	0.0	36.23	35.89	4.28	24.57	19.5	43	1.68	0.0	23.11	22.84	0.16	14.3	11.34
15	3.22	0.0	35.34	35.0	3.44	23.8	18.89	44	1.66	0.0	22.95	22.69	0.16	14.2	11.26
16	3.09	0.0	34.5	34.16	2.79	23.05	18.29	45	1.65	0.0	22.81	22.55	0.15	14.1	11.18
17	2.97	0.0	33.69	33.35	2.27	22.42	17.78	46	1.64	0.0	22.68	22.42	0.15	14.01	11.11
18	2.85	0.0	32.92	32.59	1.87	21.82	17.31	47	1.63	0.0	22.56	22.3	0.14	13.92	11.04
19	2.75	0.0	32.19	31.87	1.81	21.23	16.84	48	1.62	0.0	22.44	22.18	0.14	13.84	10.98
20	2.65	0.0	31.5	31.18	1.51	20.64	16.37	49	1.61	0.0	22.33	22.07	0.14	13.76	10.92
21	2.56	0.0	30.84	30.53	1.27	20.1	15.94	50	1.6	0.0	22.23	21.97	0.13	13.69	10.86
22	2.48	0.0	30.24	29.92	1.08	19.64	15.58	51	1.59	0.0	22.13	21.88	0.13	13.62	10.8
23	2.4	0.0	29.64	29.33	0.92	19.19	15.22	52	1.58	0.0	22.05	21.79	0.13	13.56	10.75
24	2.33	0.0	29.08	28.78	0.79	18.76	14.87	53	1.58	0.0	21.96	21.71	0.12	13.5	10.71
25	2.27	0.0	28.56	28.26	0.69	18.33	14.53	54	1.57	0.0	21.89	21.63	0.12	13.44	10.66
26	2.21	0.0	28.07	27.78	0.6	17.94	14.23	55	1.56	0.0	21.82	21.56	0.12	13.39	10.62
27	2.15	0.0	27.61	27.32	0.53	17.61	13.96	56	1.56	0.0	21.75	21.49	0.12	13.34	10.58
28	2.1	0.0	27.17	26.88	0.47	17.29	13.71	57	1.55	0.0	21.69	21.43	0.12	13.3	10.55
29	2.05	0.0	26.76	26.47	0.43	16.99	13.47	58	1.55	0.0	21.63	21.38	0.11	13.25	10.51
30	2.01	0.0	26.37	26.08	0.38	16.69	13.23	59	1.54	0.0	21.58	21.32	0.11	13.23	10.49

Table A.108.: Fe^{3+}

Step	$\hat{E}$	$\hat{T}$	P_1	P_2	P_T	P_S	P_{AS}	Step	$\hat{E}$	$\hat{T}$	P_1	P_2	P_T	P_S	P_{AS}
2	24.21	239.33	71.28	76.38	99.99	60.05	48.91	31	3.71	501.0	38.2	37.86	6.87	26.61	21.13
3	20.87	253.34	69.52	75.04	99.99	58.18	47.22	32	3.64	504.64	37.84	37.49	6.31	26.31	20.9
4	18.04	267.79	67.94	73.89	99.98	56.38	45.68	33	3.58	508.09	37.49	37.14	5.82	26.03	20.67
5	15.66	282.62	66.52	72.88	99.91	54.45	44.03	34	3.52	511.37	37.16	36.82	5.38	25.75	20.45
6	13.71	297.76	65.16	71.87	99.64	52.25	42.16	35	3.47	0.0	36.86	36.52	5.0	25.5	20.25
7	12.07	313.11	63.8	70.66	98.78	49.82	40.1	36	3.42	0.0	36.58	36.23	4.67	25.25	20.05
8	10.68	328.58	62.32	69.09	96.62	47.69	38.33	37	3.38	0.0	36.32	35.97	4.37	25.02	19.86
9	9.5	344.05	60.64	66.92	92.26	45.55	36.56	38	3.34	0.0	36.06	35.72	4.11	24.8	19.69
10	8.5	359.38	58.54	63.77	85.12	43.28	34.68	39	3.3	0.0	35.82	35.48	3.88	24.59	19.52
11	7.67	374.44	55.93	59.51	75.51	41.13	32.91	40	3.26	0.0	35.6	35.26	3.68	24.39	19.36
12	6.96	389.08	52.79	54.28	64.37	39.28	31.39	41	3.23	0.0	35.39	35.05	3.49	24.21	19.21
13	6.37	403.21	49.61	49.24	53.02	37.4	29.86	42	3.2	0.0	35.2	34.86	3.33	24.03	19.07
14	6.1	410.08	48.7	48.33	47.61	36.45	29.09	43	3.17	0.0	35.02	34.68	3.18	23.86	18.94
15	5.86	416.82	47.83	47.47	42.5	35.5	28.31	44	3.14	0.0	34.85	34.51	3.05	23.71	18.81
16	5.63	423.42	46.99	46.63	37.76	34.82	27.76	45	3.12	0.0	34.69	34.36	2.93	23.56	18.69
17	5.42	429.89	46.18	45.81	33.43	34.11	27.18	46	3.09	0.0	34.55	34.21	2.82	23.42	18.58
18	5.23	436.2	45.41	45.04	29.52	33.4	26.61	47	3.07	0.0	34.41	34.07	2.72	23.29	18.48
19	5.05	442.34	44.68	44.31	26.04	32.71	26.05	48	3.05	0.0	34.28	33.94	2.64	23.16	18.38
20	4.88	448.3	43.96	43.6	22.97	32.01	25.48	49	3.04	0.0	34.16	33.82	2.56	23.09	18.32
21	4.73	454.07	43.28	42.92	20.27	31.32	24.93	50	3.02	0.0	34.04	33.71	2.49	23.0	18.25
22	4.59	459.64	42.64	42.28	17.92	30.65	24.38	51	3.0	0.0	33.93	33.6	2.42	22.92	18.18
23	4.46	465.03	42.04	41.68	15.88	30.13	23.97	52	2.99	0.0	33.83	33.5	2.36	22.84	18.13
24	4.34	470.22	41.48	41.12	14.12	29.64	23.57	53	2.97	0.0	33.74	33.41	2.31	22.77	18.07
25	4.22	475.2	40.91	40.55	12.59	29.16	23.19	54	2.96	0.0	33.65	33.32	2.26	22.7	18.01
26	4.12	479.99	40.38	40.03	11.26	28.69	22.81	55	2.95	0.0	33.57	33.24	2.21	22.64	17.96
27	4.02	484.58	39.89	39.53	10.12	28.25	22.45	56	2.94	0.0	33.5	33.17	2.17	22.58	17.91
28	3.93	488.98	39.42	39.07	9.13	27.81	22.1	57	2.93	0.0	33.43	33.1	2.13	22.52	17.87
29	3.85	493.17	38.99	38.64	8.27	27.39	21.77	58	2.92	0.0	33.36	33.03	2.1	22.47	17.83
30	3.78	497.18	38.58	38.23	7.52	26.99	21.44	59	2.91	0.0	33.3	32.97	2.06	22.42	17.79

Table A.109.: Fe^{4+}

Step	$\hat{E}$	$\hat{T}$	P_1	P_2	P_T	P_S	P_{AS}	Step	$\hat{E}$	$\hat{T}$	P_1	P_2	P_T	P_S	P_{AS}
2	35.38	206.9	76.35	80.64	100.0	65.02	53.31	31	5.66	422.73	47.08	46.72	38.24	35.52	28.32
3	30.61	218.76	74.34	78.88	99.99	63.85	52.24	32	5.56	425.61	46.71	46.35	36.26	35.21	28.07
4	26.57	230.94	72.46	77.32	99.99	62.51	51.01	33	5.47	428.35	46.37	46.0	34.43	34.88	27.81
5	23.17	243.4	70.74	75.97	99.99	60.98	49.62	34	5.39	430.96	46.04	45.68	32.74	34.58	27.56
6	20.29	256.08	69.2	74.81	99.99	59.21	48.03	35	5.31	433.42	45.74	45.38	31.2	34.29	27.32
7	17.85	268.89	67.83	73.81	99.98	57.64	46.69	36	5.24	435.76	45.46	45.09	29.78	34.01	27.1
8	15.78	281.77	66.59	72.94	99.92	55.9	45.21	37	5.18	437.97	45.19	44.83	28.48	33.75	26.89
9	14.09	294.62	65.43	72.07	99.72	54.02	43.62	38	5.11	440.06	44.94	44.58	27.29	33.5	26.68
10	12.65	307.35	64.3	71.11	99.21	52.01	41.91	39	5.06	442.04	44.71	44.35	26.2	33.26	26.49
11	11.43	319.85	63.18	70.05	98.05	50.03	40.24	40	5.0	443.9	44.49	44.13	25.21	33.04	26.31
12	10.4	332.05	61.97	68.67	95.86	48.35	38.85	41	4.96	445.65	44.28	43.92	24.29	32.82	26.14
13	9.51	343.83	60.66	66.95	92.34	46.64	37.43	42	4.91	447.3	44.08	43.72	23.46	32.63	25.98
14	9.12	349.55	59.92	65.86	90.03	45.77	36.72	43	4.87	448.85	43.89	43.53	22.7	32.44	25.83
15	8.76	355.13	59.18	64.77	87.38	44.91	36.0	44	4.83	450.31	43.72	43.36	21.99	32.26	25.68
16	8.43	360.57	58.35	63.46	84.45	44.04	35.29	45	4.79	451.68	43.56	43.2	21.35	32.09	25.55
17	8.13	365.87	57.5	62.1	81.27	43.18	34.58	46	4.76	452.97	43.41	43.05	20.76	31.94	25.42
18	7.85	371.01	56.64	60.69	77.9	42.33	33.87	47	4.73	454.18	43.27	42.91	20.22	31.79	25.3
19	7.59	375.98	55.61	58.98	74.4	41.82	33.46	48	4.7	455.31	43.14	42.77	19.73	31.65	25.19
20	7.35	380.79	54.64	57.32	70.83	41.19	32.94	49	4.67	456.38	43.01	42.65	19.27	31.52	25.08
21	7.13	385.44	53.68	55.69	67.25	40.57	32.44	50	4.64	457.37	42.9	42.54	18.85	31.4	24.98
22	6.93	389.91	52.59	53.96	63.71	39.97	31.94	51	4.62	458.31	42.79	42.43	18.46	31.28	24.89
23	6.74	394.2	51.56	52.3	60.26	39.38	31.46	52	4.6	459.18	42.69	42.33	18.11	31.18	24.81
24	6.56	398.33	50.58	50.7	56.94	38.8	31.0	53	4.58	460.0	42.6	42.24	17.78	31.07	24.72
25	6.4	402.29	49.73	49.37	53.76	38.25	30.54	54	4.56	460.77	42.52	42.16	17.48	30.98	24.64
26	6.25	406.09	49.22	48.86	50.73	37.71	30.1	55	4.54	461.48	42.44	42.08	17.2	30.89	24.57
27	6.12	409.72	48.74	48.38	47.88	37.18	29.67	56	4.53	462.15	42.36	42.0	16.95	30.87	24.56
28	5.99	413.2	48.29	47.93	45.21	36.68	29.26	57	4.51	462.78	42.29	41.93	16.71	30.81	24.51
29	5.87	416.53	47.87	47.5	42.71	36.19	28.86	58	4.5	463.36	42.23	41.87	16.49	30.75	24.46
30	5.76	419.71	47.47	47.1	40.39	35.86	28.59	59	4.48	463.91	42.17	41.81	16.29	30.7	24.42

Table A.110.: Fe^{5+}

Step	$\hat{E}$	$\hat{T}$	P_1	P_2	P_T	P_S	P_{AS}	Step	$\hat{E}$	$\hat{T}$	P_1	P_2	P_T	P_S	P_{AS}
2	47.39	185.13	80.35	84.46	100.0	68.0	55.94	31	7.74	373.09	56.21	59.97	76.46	42.91	34.34
3	40.99	195.6	78.39	82.54	100.0	67.24	55.23	32	7.61	375.55	55.7	59.13	74.71	42.61	34.09
4	35.63	206.34	76.45	80.73	100.0	66.37	54.41	33	7.49	377.89	55.23	58.33	73.0	42.29	33.83
5	31.14	217.3	74.58	79.08	99.99	65.35	53.47	34	7.39	380.1	54.78	57.56	71.35	41.99	33.58
6	27.34	228.42	72.84	77.62	99.99	64.16	52.38	35	7.28	382.19	54.36	56.84	69.76	41.7	33.35
7	24.13	239.63	71.24	76.35	99.99	62.79	51.14	36	7.19	384.17	53.97	56.15	68.24	41.43	33.13
8	21.41	250.87	69.81	75.26	99.99	61.25	49.76	37	7.1	386.03	53.53	55.45	66.78	41.17	32.92
9	19.1	262.06	68.54	74.33	99.99	59.78	48.46	38	7.02	387.8	53.1	54.78	65.39	40.92	32.71
10	17.13	273.12	67.41	73.51	99.97	58.37	47.27	39	6.95	389.46	52.7	54.13	64.07	40.69	32.52
11	15.46	283.97	66.39	72.79	99.9	56.87	45.99	40	6.88	391.02	52.32	53.53	62.82	40.47	32.35
12	14.1	294.54	65.44	72.07	99.73	55.23	44.6	41	6.81	392.49	51.97	52.96	61.64	40.26	32.18
13	12.93	304.74	64.53	71.32	99.35	53.55	43.17	42	6.75	393.88	51.64	52.42	60.53	40.06	32.02
14	12.41	309.68	64.1	70.93	99.05	52.69	42.45	43	6.7	395.18	51.33	51.92	59.48	39.88	31.87
15	11.93	314.51	63.68	70.56	98.65	51.84	41.72	44	6.65	396.4	51.04	51.44	58.49	39.71	31.72
16	11.49	319.22	63.24	70.11	98.13	51.12	41.13	45	6.6	397.55	50.76	51.0	57.57	39.54	31.59
17	11.08	323.81	62.81	69.68	97.48	50.5	40.61	46	6.55	398.63	50.51	50.58	56.7	39.39	31.47
18	10.7	328.26	62.36	69.13	96.68	49.89	40.1	47	6.51	399.64	50.27	50.19	55.88	39.25	31.35
19	10.36	332.57	61.92	68.6	95.74	49.3	39.61	48	6.47	400.59	50.05	49.82	55.12	39.11	31.24
20	10.03	336.75	61.46	68.01	94.64	48.67	39.09	49	6.44	401.48	49.84	49.48	54.41	38.98	31.14
21	9.73	340.78	61.0	67.4	93.4	48.05	38.58	50	6.4	402.31	49.73	49.36	53.74	38.87	31.04
22	9.46	344.66	60.57	66.83	92.03	47.44	38.08	51	6.37	403.09	49.62	49.26	53.12	38.76	30.95
23	9.2	348.4	60.07	66.09	90.53	46.85	37.59	52	6.34	403.82	49.53	49.16	52.54	38.66	30.87
24	8.96	351.99	59.59	65.38	88.92	46.27	37.11	53	6.32	404.5	49.43	49.07	51.99	38.55	30.78
25	8.74	355.44	59.14	64.71	87.23	45.71	36.64	54	6.29	405.14	49.35	48.98	51.48	38.46	30.7
26	8.54	358.74	58.65	63.93	85.48	45.16	36.19	55	6.27	405.74	49.27	48.9	51.01	38.37	30.63
27	8.36	361.89	58.14	63.12	83.69	44.63	35.76	56	6.25	406.3	49.19	48.83	50.57	38.28	30.56
28	8.18	364.9	57.66	62.35	81.88	44.12	35.34	57	6.23	406.82	49.12	48.76	50.16	38.2	30.5
29	8.02	367.76	57.2	61.62	80.06	43.63	34.93	58	6.21	407.31	49.06	48.69	49.77	38.13	30.44
30	7.88	370.49	56.74	60.86	78.25	43.16	34.54	59	6.19	407.76	49.0	48.63	49.42	38.06	30.38

Table A.111.: Fe^{6+}

Step	$\hat{E}$	$\hat{T}$	P_1	P_2	P_T	P_S	P_{AS}	Step	$\hat{E}$	$\hat{T}$	P_1	P_2	P_T	P_S	P_{AS}
2	60.42	169.21	83.35	87.62	100.0	69.56	57.28	31	9.98	337.48	61.38	67.9	94.43	49.39	39.67
3	52.1	178.69	81.56	85.71	100.0	69.45	57.17	32	9.81	339.67	61.13	67.57	93.76	49.07	39.41
4	45.25	188.41	79.73	83.85	100.0	68.93	56.67	33	9.66	341.75	60.89	67.26	93.08	48.73	39.13
5	39.53	198.31	77.89	82.07	100.0	68.25	56.03	34	9.52	343.72	60.68	66.97	92.38	48.41	38.86
6	34.75	208.34	76.1	80.41	100.0	67.44	55.27	35	9.39	345.58	60.45	66.65	91.67	48.1	38.61
7	30.72	218.43	74.4	78.92	99.99	66.48	54.39	36	9.27	347.35	60.21	66.3	90.97	47.81	38.36
8	27.31	228.54	72.82	77.6	99.99	65.4	53.4	37	9.16	349.01	59.99	65.97	90.26	47.53	38.13
9	24.41	238.57	71.38	76.46	99.99	64.19	52.3	38	9.06	350.59	59.78	65.66	89.57	47.26	37.92
10	21.95	248.48	70.1	75.48	99.99	62.85	51.09	39	8.96	352.07	59.58	65.37	88.88	47.01	37.71
11	19.86	258.18	68.96	74.63	99.99	61.39	49.78	40	8.87	353.47	59.4	65.09	88.21	46.78	37.52
12	18.07	267.61	67.96	73.91	99.98	60.26	48.83	41	8.79	354.78	59.23	64.84	87.56	46.56	37.33
13	16.55	276.7	67.06	73.27	99.95	59.01	47.76	42	8.71	356.02	59.07	64.6	86.92	46.35	37.16
14	15.88	281.11	66.65	72.98	99.92	58.37	47.22	43	8.64	357.18	58.9	64.33	86.31	46.15	36.99
15	15.27	285.41	66.26	72.69	99.88	57.73	46.68	44	8.57	358.27	58.72	64.05	85.73	45.96	36.84
16	14.71	289.6	65.87	72.4	99.82	57.09	46.13	45	8.51	359.3	58.55	63.79	85.16	45.79	36.7
17	14.2	293.68	65.51	72.13	99.75	56.45	45.59	46	8.45	360.26	58.4	63.54	84.63	45.62	36.56
18	13.73	297.63	65.17	71.87	99.64	55.81	45.05	47	8.4	361.17	58.25	63.31	84.11	45.47	36.43
19	13.29	301.47	64.83	71.59	99.5	55.19	44.52	48	8.35	362.01	58.12	63.09	83.62	45.32	36.31
20	12.88	305.18	64.49	71.29	99.33	54.52	43.96	49	8.3	362.81	57.99	62.89	83.15	45.19	36.2
21	12.51	308.76	64.18	71.0	99.12	53.87	43.41	50	8.26	363.55	57.87	62.7	82.7	45.06	36.1
22	12.16	312.21	63.88	70.73	98.86	53.23	42.86	51	8.22	364.24	57.76	62.52	82.28	44.94	36.0
23	11.84	315.53	63.59	70.47	98.55	52.6	42.33	52	8.18	364.89	57.66	62.35	81.88	44.84	35.91
24	11.54	318.72	63.29	70.16	98.19	51.98	41.81	53	8.15	365.5	57.56	62.2	81.5	44.73	35.82
25	11.26	321.78	63.0	69.87	97.78	51.68	41.57	54	8.12	366.07	57.47	62.05	81.14	44.62	35.73
26	11.0	324.71	62.72	69.58	97.33	51.26	41.22	55	8.09	366.6	57.39	61.91	80.8	44.52	35.65
27	10.77	327.52	62.43	69.23	96.83	50.86	40.89	56	8.06	367.1	57.31	61.79	80.49	44.43	35.58
28	10.55	330.19	62.16	68.89	96.28	50.47	40.57	57	8.04	367.57	57.23	61.67	80.19	44.35	35.51
29	10.34	332.74	61.91	68.58	95.7	50.1	40.26	58	8.01	368.0	57.17	61.56	79.9	44.27	35.44
30	10.15	335.17	61.64	68.25	95.08	49.74	39.96	59	7.99	368.41	57.1	61.45	79.64	44.19	35.38

Table A.112.: Fe^{7+}

Step	$\hat{E}$	$\hat{T}$	P_1	P_2	P_T	P_S	P_{AS}	Step	$\hat{E}$	$\hat{T}$	P_1	P_2	P_T	P_S	P_{AS}
2	74.08	156.9	85.64	90.16	100.0	70.53	58.09	31	12.33	310.48	64.03	70.87	98.99	54.44	43.85
3	64.01	165.64	84.02	88.35	100.0	70.55	58.09	32	12.13	312.46	63.86	70.71	98.83	54.09	43.56
4	55.5	174.58	82.34	86.52	100.0	70.53	58.07	33	11.95	314.34	63.7	70.57	98.67	53.71	43.24
5	48.38	183.68	80.62	84.74	100.0	70.48	58.01	34	11.78	316.12	63.54	70.41	98.49	53.35	42.93
6	42.53	192.89	78.9	83.02	100.0	69.77	57.33	35	11.62	317.81	63.37	70.25	98.3	53.0	42.64
7	37.57	202.16	77.2	81.4	100.0	69.11	56.71	36	11.47	319.41	63.22	70.1	98.11	52.85	42.52
8	33.45	211.42	75.57	79.93	100.0	68.35	56.0	37	11.34	320.91	63.08	69.95	97.91	52.63	42.33
9	29.94	220.6	74.05	78.63	99.99	67.48	55.19	38	11.21	322.34	62.95	69.82	97.7	52.41	42.16
10	26.96	229.65	72.65	77.47	99.99	66.51	54.3	39	11.09	323.68	62.82	69.69	97.5	52.21	42.0
11	24.43	238.5	71.39	76.47	99.99	65.43	53.32	40	10.98	324.94	62.7	69.55	97.29	52.03	41.84
12	22.27	247.09	70.27	75.61	99.99	64.19	52.2	41	10.88	326.13	62.57	69.4	97.08	51.85	41.69
13	20.43	255.37	69.28	74.87	99.99	62.9	51.05	42	10.79	327.25	62.46	69.26	96.88	51.68	41.55
14	19.62	259.37	68.83	74.54	99.99	62.39	50.6	43	10.7	328.3	62.35	69.13	96.67	51.52	41.43
15	18.86	263.28	68.41	74.23	99.99	61.9	50.18	44	10.62	329.29	62.25	69.0	96.47	51.38	41.3
16	18.17	267.09	68.01	73.94	99.98	61.41	49.77	45	10.54	330.22	62.16	68.89	96.28	51.24	41.19
17	17.52	270.79	67.64	73.68	99.97	60.92	49.35	46	10.47	331.09	62.07	68.78	96.08	51.11	41.08
18	16.92	274.38	67.29	73.43	99.96	60.43	48.93	47	10.41	331.91	61.99	68.68	95.9	50.99	40.98
19	16.37	277.86	66.96	73.19	99.94	59.97	48.54	48	10.35	332.68	61.91	68.59	95.71	50.87	40.89
20	15.86	281.23	66.64	72.97	99.92	59.44	48.09	49	10.29	333.4	61.84	68.5	95.54	50.77	40.8
21	15.4	284.47	66.34	72.75	99.89	58.92	47.65	50	10.24	334.07	61.77	68.42	95.37	50.67	40.72
22	14.97	287.6	66.05	72.53	99.85	58.41	47.22	51	10.19	334.7	61.7	68.32	95.21	50.58	40.64
23	14.58	290.61	65.78	72.33	99.81	57.92	46.8	52	10.14	335.29	61.63	68.23	95.05	50.5	40.58
24	14.22	293.5	65.53	72.14	99.75	57.43	46.39	53	10.1	335.84	61.57	68.15	94.9	50.41	40.5
25	13.89	296.27	65.29	71.96	99.68	56.96	45.99	54	10.06	336.35	61.51	68.07	94.76	50.32	40.43
26	13.58	298.93	65.07	71.79	99.6	56.5	45.6	55	10.03	336.84	61.45	68.0	94.62	50.24	40.36
27	13.29	301.46	64.83	71.59	99.5	56.06	45.23	56	9.99	337.29	61.4	67.93	94.49	50.17	40.3
28	13.02	303.88	64.61	71.39	99.4	55.63	44.86	57	9.96	337.71	61.35	67.86	94.37	50.1	40.24
29	12.77	306.19	64.4	71.21	99.27	55.22	44.51	58	9.93	338.1	61.31	67.81	94.25	50.03	40.19
30	12.55	308.39	64.21	71.03	99.14	54.82	44.18	59	9.9	338.47	61.26	67.75	94.14	49.97	40.14

Table A.113.: Fe^{8+}

Step	$\hat{E}$	$\hat{T}$	P_1	P_2	P_T	P_S	P_{AS}	Step	$\hat{E}$	$\hat{T}$	P_1	P_2	P_T	P_S	P_{AS}
2	88.35	147.02	87.48	92.18	100.0	71.26	58.7	31	14.77	289.16	65.91	72.43	99.83	59.09	47.76
3	76.33	155.17	85.96	90.51	100.0	71.37	58.78	32	14.54	290.78	65.75	72.31	99.8	58.82	47.53
4	66.3	163.49	84.42	88.79	100.0	71.47	58.85	33	14.32	292.71	65.6	72.19	99.77	58.5	47.26
5	57.82	171.97	82.83	87.05	100.0	71.53	58.89	34	14.12	294.35	65.46	72.08	99.73	58.21	47.01
6	50.66	180.54	81.21	85.34	100.0	71.55	58.89	35	13.93	295.9	65.32	71.98	99.69	57.92	46.77
7	44.79	189.15	79.59	83.71	100.0	71.09	58.44	36	13.76	297.36	65.2	71.89	99.65	57.65	46.54
8	39.83	197.74	78.0	82.16	100.0	70.56	57.94	37	13.6	298.74	65.08	71.8	99.6	57.4	46.33
9	35.66	206.26	76.46	80.74	100.0	69.94	57.35	38	13.45	300.05	64.96	71.71	99.56	57.16	46.12
10	32.15	214.65	75.02	79.45	100.0	69.24	56.7	39	13.31	301.28	64.85	71.61	99.51	56.93	45.93
11	29.16	222.84	73.69	78.33	99.99	68.44	55.96	40	13.18	302.44	64.74	71.51	99.46	56.71	45.75
12	26.61	230.79	72.48	77.34	99.99	67.49	55.09	41	13.06	303.53	64.64	71.42	99.41	56.51	45.58
13	24.45	238.43	71.4	76.47	99.99	66.49	54.19	42	12.95	304.56	64.55	71.34	99.36	56.32	45.42
14	23.48	242.13	70.91	76.09	99.99	65.98	53.72	43	12.85	305.52	64.46	71.26	99.31	56.14	45.26
15	22.6	245.74	70.44	75.73	99.99	65.46	53.25	44	12.75	306.43	64.38	71.19	99.26	55.97	45.12
16	21.77	249.25	70.01	75.41	99.99	64.93	52.78	45	12.66	307.28	64.31	71.12	99.21	55.81	44.99
17	21.01	252.66	69.6	75.1	99.99	64.4	52.3	46	12.58	308.08	64.24	71.05	99.16	55.66	44.86
18	20.31	255.97	69.21	74.81	99.99	63.87	51.83	47	12.5	308.83	64.17	71.0	99.11	55.52	44.74
19	19.66	259.17	68.85	74.55	99.99	63.37	51.37	48	12.43	309.53	64.11	70.94	99.06	55.39	44.63
20	19.05	262.27	68.52	74.31	99.99	63.1	51.16	49	12.36	310.19	64.05	70.89	99.01	55.27	44.53
21	18.5	265.26	68.2	74.08	99.98	62.68	50.81	50	12.3	310.81	64.0	70.84	98.97	55.16	44.44
22	17.98	268.14	67.9	73.87	99.98	62.27	50.46	51	12.24	311.38	63.95	70.8	98.92	55.05	44.35
23	17.5	270.91	67.63	73.67	99.97	61.87	50.12	52	12.19	311.92	63.9	70.75	98.88	54.96	44.27
24	17.06	273.56	67.37	73.48	99.96	61.48	49.79	53	12.14	312.43	63.86	70.72	98.84	54.86	44.18
25	16.65	276.11	67.12	73.31	99.95	61.1	49.47	54	12.09	312.9	63.82	70.68	98.8	54.76	44.1
26	16.27	278.55	66.89	73.15	99.94	60.74	49.16	55	12.05	313.35	63.78	70.64	98.76	54.67	44.02
27	15.91	280.88	66.68	72.99	99.92	60.38	48.86	56	12.01	313.76	63.75	70.61	98.72	54.58	43.95
28	15.59	283.11	66.47	72.85	99.9	60.04	48.57	57	11.97	314.14	63.71	70.58	98.68	54.5	43.88
29	15.29	285.23	66.27	72.7	99.88	59.71	48.29	58	11.93	314.51	63.68	70.56	98.65	54.43	43.81
30	15.02	287.24	66.09	72.56	99.86	59.39	48.02	59	11.9	314.84	63.65	70.53	98.62	54.36	43.76

Table A.114.: Fe^{9+}

Step	$\hat{E}$	$\hat{T}$	P_1	P_2	P_T	P_S	P_{AS}	Step	$\hat{E}$	$\hat{T}$	P_1	P_2	P_T	P_S	P_{AS}
2	103.5	138.87	89.02	93.77	100.0	71.83	59.17	31	17.35	271.8	67.54	73.61	99.97	62.68	50.78
3	89.2	146.52	87.57	92.28	100.0	72.02	59.32	32	17.07	273.49	67.37	73.49	99.96	62.47	50.59
4	77.42	154.35	86.12	90.68	100.0	72.19	59.46	33	16.81	275.1	67.22	73.38	99.96	62.21	50.37
5	67.62	162.31	84.64	89.04	100.0	72.35	59.58	34	16.57	276.62	67.07	73.28	99.95	61.96	50.16
6	59.32	170.35	83.13	87.38	100.0	72.5	59.69	35	16.34	278.05	66.94	73.18	99.94	61.72	49.96
7	52.3	178.43	81.61	85.76	100.0	72.56	59.73	36	16.13	279.41	66.81	73.09	99.93	61.49	49.77
8	46.49	186.49	80.09	84.2	100.0	72.27	59.44	37	15.94	280.7	66.69	73.01	99.93	61.28	49.59
9	41.62	194.48	78.6	82.74	100.0	71.85	59.03	38	15.76	281.91	66.58	72.93	99.92	61.08	49.42
10	37.49	202.33	77.17	81.38	100.0	71.36	58.56	39	15.59	283.05	66.48	72.85	99.91	60.89	49.26
11	34.04	210.0	75.81	80.15	100.0	70.78	58.01	40	15.44	284.13	66.38	72.78	99.89	60.71	49.11
12	31.1	217.42	74.56	79.06	99.99	70.05	57.33	41	15.31	285.14	66.28	72.7	99.88	60.54	48.96
13	28.58	224.57	73.42	78.11	99.99	69.27	56.62	42	15.18	286.09	66.19	72.64	99.87	60.38	48.83
14	27.47	228.02	72.9	77.67	99.99	68.87	56.26	43	15.06	286.99	66.11	72.58	99.86	60.23	48.7
15	26.44	231.38	72.4	77.27	99.99	68.46	55.88	44	14.95	287.83	66.03	72.52	99.85	60.09	48.59
16	25.49	234.66	71.93	76.88	99.99	68.05	55.51	45	14.84	288.62	65.96	72.47	99.84	59.96	48.48
17	24.61	237.84	71.48	76.53	99.99	67.64	55.13	46	14.75	289.36	65.9	72.41	99.83	59.84	48.37
18	23.79	240.92	71.07	76.22	99.99	67.22	54.76	47	14.66	290.06	65.83	72.37	99.82	59.73	48.28
19	23.04	243.91	70.68	75.91	99.99	66.84	54.4	48	14.57	290.71	65.77	72.32	99.81	59.62	48.19
20	22.34	246.79	70.31	75.64	99.99	66.36	53.98	49	14.5	291.32	65.72	72.28	99.79	59.52	48.1
21	21.7	249.58	69.97	75.38	99.99	65.89	53.56	50	14.42	291.89	65.67	72.25	99.78	59.43	48.02
22	21.1	252.26	69.65	75.14	99.99	65.43	53.15	51	14.36	292.43	65.62	72.21	99.77	59.35	47.95
23	20.55	254.83	69.34	74.91	99.99	64.99	52.75	52	14.29	292.93	65.58	72.18	99.76	59.28	47.9
24	20.03	257.3	69.06	74.7	99.99	64.55	52.36	53	14.24	293.4	65.54	72.15	99.75	59.19	47.82
25	19.56	259.67	68.8	74.52	99.99	64.31	52.16	54	14.18	293.83	65.5	72.12	99.74	59.11	47.75
26	19.12	261.94	68.55	74.34	99.99	64.01	51.91	55	14.13	294.24	65.46	72.09	99.73	59.03	47.68
27	18.71	264.11	68.32	74.17	99.99	63.72	51.66	56	14.09	294.63	65.43	72.07	99.72	58.95	47.62
28	18.33	266.18	68.11	74.01	99.98	63.45	51.43	57	14.04	294.98	65.4	72.04	99.71	58.89	47.56
29	17.98	268.14	67.9	73.87	99.98	63.18	51.2	58	14.0	295.32	65.37	72.02	99.71	58.82	47.51
30	17.65	270.02	67.71	73.73	99.97	62.93	50.98	59	13.96	295.63	65.34	72.0	99.7	58.77	47.45

Table A.115.: Fe^{10+}

Step	$\hat{E}$	$\hat{T}$	P_1	P_2	P_T	P_S	P_{AS}	Step	$\hat{E}$	$\hat{T}$	P_1	P_2	P_T	P_S	P_{AS}
2	121.48	131.03	0.0	0.0	0.0	0.0	0.0	31	20.03	257.31	69.06	74.7	99.99	65.48	53.11
3	102.76	139.23	88.95	93.71	100.0	72.53	59.75	32	19.71	258.9	68.88	74.58	99.99	65.24	52.9
4	89.01	146.64	87.55	92.25	100.0	72.77	59.94	33	19.42	260.4	68.72	74.46	99.99	65.15	52.84
5	77.67	154.17	86.15	90.72	100.0	73.0	60.12	34	19.14	261.82	68.57	74.35	99.99	64.94	52.66
6	68.22	161.77	84.74	89.15	100.0	73.26	60.33	35	18.88	263.17	68.42	74.24	99.99	64.74	52.49
7	60.22	169.41	83.31	87.57	100.0	73.46	60.48	36	18.65	264.44	68.29	74.14	99.99	64.55	52.33
8	53.44	177.02	81.88	86.03	100.0	73.55	60.55	37	18.43	265.65	68.16	74.05	99.98	64.37	52.18
9	47.78	184.56	80.45	84.57	100.0	73.38	60.38	38	18.22	266.78	68.04	73.97	99.98	64.2	52.04
10	43.07	191.98	79.07	83.18	100.0	73.06	60.05	39	18.03	267.85	67.93	73.89	99.98	64.04	51.9
11	39.06	199.21	77.73	81.91	100.0	72.65	59.65	40	17.85	268.86	67.83	73.81	99.98	63.89	51.77
12	35.69	206.21	76.47	80.75	100.0	72.09	59.12	41	17.69	269.81	67.74	73.75	99.98	63.75	51.65
13	32.83	212.93	75.31	79.7	100.0	71.49	58.57	42	17.54	270.7	67.65	73.68	99.97	63.61	51.54
14	31.56	216.18	74.77	79.23	100.0	71.18	58.28	43	17.4	271.54	67.56	73.62	99.97	63.49	51.44
15	30.39	219.35	74.25	78.8	99.99	70.86	57.98	44	17.26	272.32	67.49	73.57	99.97	63.38	51.34
16	29.3	222.43	73.76	78.38	99.99	70.54	57.69	45	17.14	273.06	67.41	73.52	99.97	63.27	51.25
17	28.3	225.42	73.29	78.0	99.99	70.22	57.39	46	17.03	273.76	67.35	73.47	99.96	63.17	51.16
18	27.37	228.32	72.85	77.63	99.99	69.89	57.09	47	16.92	274.41	67.28	73.43	99.96	63.07	51.08
19	26.51	231.13	72.43	77.29	99.99	69.6	56.82	48	16.82	275.02	67.23	73.38	99.96	62.99	51.01
20	25.72	233.84	72.04	76.98	99.99	69.2	56.46	49	16.73	275.59	67.17	73.34	99.96	62.91	50.94
21	24.98	236.46	71.67	76.68	99.99	68.81	56.11	50	16.65	276.13	67.12	73.31	99.95	62.83	50.88
22	24.3	238.97	71.33	76.42	99.99	68.42	55.76	51	16.57	276.63	67.07	73.27	99.95	62.76	50.82
23	23.67	241.39	71.01	76.17	99.99	68.05	55.43	52	16.49	277.1	67.03	73.24	99.95	62.71	50.78
24	23.09	243.71	70.7	75.93	99.99	67.69	55.1	53	16.42	277.53	66.99	73.21	99.95	62.63	50.71
25	22.55	245.94	70.42	75.72	99.99	67.33	54.78	54	16.36	277.94	66.95	73.19	99.94	62.56	50.65
26	22.05	248.06	70.15	75.52	99.99	66.99	54.48	55	16.3	278.33	66.91	73.16	99.94	62.49	50.59
27	21.58	250.1	69.91	75.33	99.99	66.66	54.18	56	16.25	278.69	66.88	73.14	99.94	62.43	50.54
28	21.15	252.04	69.67	75.16	99.99	66.35	53.9	57	16.19	279.02	66.85	73.12	99.94	62.37	50.48
29	20.75	253.88	69.45	75.0	99.99	66.05	53.63	58	16.15	279.33	66.82	73.09	99.94	62.32	50.44
30	20.38	255.64	69.25	74.84	99.99	65.76	53.36	59	16.1	279.63	66.79	73.08	99.93	62.27	50.4

Table A.116.: Fe^{11+}

Step	$\hat{E}$	$\hat{T}$	P_1	P_2	P_T	P_S	P_{AS}	Step	$\hat{E}$	$\hat{T}$	P_1	P_2	P_T	P_S	P_{AS}
2	0.0	125.23	0.0	0.0	0.0	0.0	0.0	31	22.78	244.98	70.54	75.81	99.99	68.39	55.66
3	119.06	132.0	0.0	0.0	0.0	0.0	0.0	32	22.42	246.47	70.35	75.67	99.99	68.2	55.48
4	101.17	140.02	88.8	93.56	100.0	73.25	60.34	33	22.09	247.89	70.17	75.53	99.99	67.94	55.25
5	88.1	147.18	87.45	92.15	100.0	73.54	60.57	34	21.78	249.24	70.01	75.41	99.99	67.69	55.03
6	77.34	154.41	86.1	90.67	100.0	73.88	60.85	35	21.49	250.51	69.86	75.3	99.99	67.46	54.82
7	68.34	161.67	84.75	89.17	100.0	74.19	61.1	36	21.22	251.71	69.71	75.19	99.99	67.24	54.63
8	60.71	168.91	83.41	87.68	100.0	74.41	61.27	37	20.97	252.85	69.58	75.09	99.99	67.03	54.44
9	54.23	176.07	82.06	86.22	100.0	74.52	61.35	38	20.74	253.92	69.45	74.99	99.99	66.84	54.27
10	48.78	183.11	80.73	84.84	100.0	74.52	61.35	39	20.53	254.93	69.33	74.91	99.99	66.66	54.11
11	44.28	189.97	79.44	83.55	100.0	74.18	60.99	40	20.33	255.88	69.22	74.82	99.99	66.48	53.96
12	40.44	196.61	78.2	82.36	100.0	73.76	60.59	41	20.14	256.77	69.12	74.75	99.99	66.32	53.81
13	37.17	202.99	77.05	81.27	100.0	73.3	60.15	42	19.97	257.61	69.03	74.68	99.99	66.17	53.68
14	35.75	206.07	76.5	80.77	100.0	73.06	59.93	43	19.81	258.4	68.94	74.62	99.99	66.03	53.55
15	34.43	209.07	75.97	80.3	100.0	72.82	59.7	44	19.66	259.15	68.86	74.56	99.99	65.9	53.44
16	33.21	211.99	75.47	79.84	100.0	72.57	59.47	45	19.53	259.84	68.78	74.5	99.99	65.96	53.51
17	32.08	214.82	74.99	79.42	100.0	72.32	59.23	46	19.4	260.5	68.71	74.45	99.99	65.87	53.44
18	31.04	217.57	74.54	79.04	99.99	72.07	58.99	47	19.28	261.11	68.64	74.4	99.99	65.8	53.37
19	30.08	220.23	74.11	78.68	99.99	71.86	58.79	48	19.17	261.69	68.58	74.36	99.99	65.72	53.31
20	29.18	222.79	73.7	78.34	99.99	71.52	58.49	49	19.06	262.23	68.52	74.31	99.99	65.66	53.25
21	28.35	225.27	73.31	78.02	99.99	71.19	58.19	50	18.97	262.73	68.47	74.28	99.99	65.6	53.2
22	27.58	227.65	72.95	77.71	99.99	70.86	57.89	51	18.88	263.2	68.42	74.24	99.99	65.54	53.15
23	26.87	229.93	72.61	77.44	99.99	70.55	57.61	52	18.8	263.64	68.37	74.21	99.99	65.5	53.12
24	26.21	232.13	72.29	77.18	99.99	70.24	57.33	53	18.72	264.06	68.33	74.17	99.99	65.44	53.06
25	25.61	234.23	71.99	76.93	99.99	69.94	57.06	54	18.65	264.45	68.29	74.14	99.99	65.37	53.01
26	25.04	236.24	71.7	76.7	99.99	69.66	56.8	55	18.58	264.81	68.25	74.12	99.98	65.31	52.96
27	24.52	238.16	71.44	76.5	99.99	69.38	56.56	56	18.52	265.14	68.21	74.09	99.98	65.26	52.91
28	24.03	240.0	71.19	76.31	99.99	69.12	56.32	57	18.46	265.46	68.18	74.07	99.98	65.21	52.87
29	23.58	241.74	70.96	76.13	99.99	68.86	56.09	58	18.41	265.76	68.15	74.04	99.98	65.16	52.83
30	23.17	243.4	70.74	75.97	99.99	68.62	55.87	59	18.36	266.03	68.12	74.02	99.98	65.12	52.79

Table A.117.: Fe^{12+}

Step	$\hat{E}$	$\hat{T}$	P_1	P_2	P_T	P_S	P_{AS}	Step	$\hat{E}$	$\hat{T}$	P_1	P_2	P_T	P_S	P_{AS}
2	0.0	120.17	0.0	0.0	0.0	0.0	0.0	31	25.58	234.32	71.97	76.92	99.99	70.81	57.77
3	0.0	126.65	0.0	0.0	0.0	0.0	0.0	32	25.18	235.74	71.77	76.76	99.99	70.65	57.63
4	115.98	133.26	0.0	0.0	0.0	0.0	0.0	33	24.81	237.08	71.59	76.61	99.99	70.42	57.42
5	99.04	141.1	88.6	93.35	100.0	73.99	60.95	34	24.47	238.36	71.41	76.48	99.99	70.21	57.23
6	86.73	148.01	87.3	91.98	100.0	74.4	61.28	35	24.15	239.57	71.25	76.36	99.99	70.0	57.04
7	76.62	154.94	86.0	90.56	100.0	74.8	61.61	36	23.85	240.71	71.1	76.24	99.99	69.81	56.87
8	68.13	161.85	84.72	89.13	100.0	75.12	61.87	37	23.57	241.79	70.95	76.13	99.99	69.62	56.71
9	60.92	168.69	83.45	87.72	100.0	75.35	62.05	38	23.32	242.8	70.82	76.03	99.99	69.45	56.56
10	54.79	175.41	82.19	86.35	100.0	75.48	62.15	39	23.08	243.76	70.7	75.93	99.99	69.29	56.41
11	49.6	181.95	80.95	85.07	100.0	75.49	62.15	40	22.86	244.66	70.58	75.84	99.99	69.14	56.28
12	45.33	188.29	79.75	83.87	100.0	75.15	61.8	41	22.65	245.51	70.47	75.76	99.99	69.0	56.15
13	41.69	194.37	78.62	82.76	100.0	74.81	61.47	42	22.46	246.31	70.37	75.68	99.99	68.87	56.04
14	40.07	197.3	78.08	82.24	100.0	74.63	61.3	43	22.28	247.06	70.28	75.61	99.99	68.75	55.93
15	38.57	200.16	77.56	81.74	100.0	74.45	61.13	44	22.12	247.77	70.19	75.55	99.99	68.64	55.82
16	37.2	202.94	77.06	81.28	100.0	74.26	60.95	45	21.96	248.43	70.11	75.48	99.99	68.53	55.73
17	35.94	205.64	76.57	80.84	100.0	74.07	60.76	46	21.82	249.05	70.03	75.43	99.99	68.43	55.64
18	34.78	208.25	76.11	80.43	100.0	73.88	60.58	47	21.69	249.63	69.96	75.38	99.99	68.34	55.56
19	33.71	210.78	75.68	80.03	100.0	73.73	60.43	48	21.56	250.18	69.9	75.33	99.99	68.26	55.48
20	32.72	213.22	75.26	79.66	100.0	73.45	60.17	49	21.45	250.69	69.83	75.28	99.99	68.18	55.41
21	31.79	215.58	74.87	79.32	100.0	73.17	59.92	50	21.34	251.17	69.78	75.24	99.99	68.11	55.35
22	30.94	217.84	74.49	79.0	99.99	72.89	59.67	51	21.24	251.61	69.72	75.2	99.99	68.04	55.29
23	30.15	220.02	74.14	78.7	99.99	72.62	59.42	52	21.15	252.03	69.67	75.16	99.99	68.0	55.25
24	29.42	222.1	73.81	78.43	99.99	72.36	59.19	53	21.06	252.43	69.63	75.12	99.99	67.92	55.18
25	28.74	224.1	73.49	78.17	99.99	72.11	58.96	54	20.98	252.79	69.58	75.09	99.99	67.85	55.11
26	28.11	226.01	73.2	77.92	99.99	71.87	58.74	55	20.91	253.14	69.54	75.06	99.99	67.78	55.05
27	27.52	227.84	72.92	77.69	99.99	71.64	58.53	56	20.84	253.46	69.5	75.03	99.99	67.72	55.0
28	26.98	229.58	72.66	77.48	99.99	71.42	58.33	57	20.78	253.76	69.47	75.01	99.99	67.67	54.95
29	26.48	231.24	72.42	77.28	99.99	71.2	58.13	58	20.72	254.04	69.44	74.98	99.99	67.61	54.9
30	26.01	232.82	72.19	77.1	99.99	71.0	57.95	59	20.66	254.3	69.41	74.96	99.99	67.56	54.85

Table A.118.: Fe^{13+}

Step	$\hat{E}$	$\hat{T}$	P_1	P_2	P_T	P_S	P_{AS}	Step	$\hat{E}$	$\hat{T}$	P_1	P_2	P_T	P_S	P_{AS}
2	0.0	115.71	0.0	0.0	0.0	0.0	0.0	31	28.45	224.97	73.36	78.05	99.99	72.85	59.55
3	0.0	121.93	0.0	0.0	0.0	0.0	0.0	32	28.01	226.33	73.15	77.88	99.99	72.73	59.44
4	0.0	128.28	0.0	0.0	0.0	0.0	0.0	33	27.59	227.62	72.96	77.72	99.99	72.52	59.25
5	112.56	134.71	0.0	0.0	0.0	0.0	0.0	34	27.21	228.84	72.77	77.57	99.99	72.33	59.08
6	96.6	142.37	88.36	93.1	100.0	74.84	61.65	35	26.86	229.99	72.6	77.43	99.99	72.15	58.92
7	85.1	149.02	87.11	91.77	100.0	75.32	62.05	36	26.53	231.08	72.44	77.3	99.99	71.97	58.77
8	75.7	155.65	85.87	90.42	100.0	75.73	62.38	37	26.22	232.1	72.29	77.18	99.99	71.81	58.62
9	67.74	162.2	84.66	89.06	100.0	76.06	62.64	38	25.94	233.07	72.15	77.07	99.99	71.66	58.49
10	60.98	168.63	83.46	87.73	100.0	76.3	62.83	39	25.68	233.99	72.02	76.96	99.99	71.52	58.36
11	55.22	174.9	82.28	86.46	100.0	76.42	62.92	40	25.43	234.85	71.9	76.86	99.99	71.39	58.24
12	50.33	180.97	81.13	85.26	100.0	76.34	62.86	41	25.2	235.66	71.78	76.77	99.99	71.26	58.13
13	46.29	186.79	80.03	84.15	100.0	76.09	62.59	42	24.99	236.42	71.68	76.68	99.99	71.15	58.03
14	44.51	189.6	79.51	83.62	100.0	75.96	62.46	43	24.8	237.14	71.58	76.61	99.99	71.04	57.93
15	42.86	192.33	79.0	83.12	100.0	75.83	62.33	44	24.61	237.81	71.49	76.54	99.99	70.94	57.84
16	41.33	194.99	78.5	82.65	100.0	75.69	62.2	45	24.45	238.44	71.4	76.47	99.99	70.85	57.76
17	39.92	197.57	78.03	82.19	100.0	75.56	62.06	46	24.29	239.03	71.32	76.41	99.99	70.76	57.68
18	38.62	200.07	77.57	81.76	100.0	75.41	61.92	47	24.14	239.59	71.25	76.35	99.99	70.69	57.61
19	37.41	202.49	77.14	81.35	100.0	75.32	61.82	48	24.01	240.11	71.18	76.3	99.99	70.61	57.54
20	36.31	204.83	76.72	80.97	100.0	75.08	61.6	49	23.88	240.59	71.11	76.25	99.99	70.55	57.48
21	35.3	207.08	76.32	80.61	100.0	74.84	61.38	50	23.76	241.05	71.05	76.2	99.99	70.48	57.42
22	34.36	209.24	75.94	80.27	100.0	74.6	61.16	51	23.65	241.48	71.0	76.16	99.99	70.43	57.37
23	33.49	211.32	75.58	79.95	100.0	74.38	60.96	52	23.55	241.88	70.94	76.12	99.99	70.39	57.34
24	32.68	213.31	75.25	79.64	100.0	74.16	60.76	53	23.45	242.25	70.89	76.08	99.99	70.32	57.28
25	31.93	215.22	74.93	79.37	100.0	73.95	60.56	54	23.37	242.6	70.85	76.05	99.99	70.26	57.22
26	31.24	217.05	74.62	79.11	99.99	73.74	60.37	55	23.28	242.93	70.81	76.01	99.99	70.2	57.16
27	30.59	218.79	74.34	78.87	99.99	73.55	60.19	56	23.21	243.23	70.77	75.98	99.99	70.14	57.11
28	29.99	220.46	74.07	78.65	99.99	73.36	60.02	57	23.14	243.52	70.73	75.95	99.99	70.09	57.07
29	29.44	222.04	73.82	78.44	99.99	73.18	59.86	58	23.07	243.79	70.69	75.93	99.99	70.04	57.02
30	28.93	223.54	73.58	78.24	99.99	73.01	59.7	59	23.01	244.03	70.66	75.9	99.99	70.0	56.98

Table A.119.: Fe^{14+}

Step	$\hat{E}$	$\hat{T}$	P_1	P_2	P_T	P_S	P_{AS}	Step	$\hat{E}$	$\hat{T}$	P_1	P_2	P_T	P_S	P_{AS}
2	0.0	111.73	0.0	0.0	0.0	0.0	0.0	31	31.37	216.7	74.68	79.16	99.99	74.6	61.08
3	0.0	117.73	0.0	0.0	0.0	0.0	0.0	32	30.88	218.0	74.47	78.98	99.99	74.5	60.99
4	0.0	123.85	0.0	0.0	0.0	0.0	0.0	33	30.43	219.24	74.27	78.81	99.99	74.32	60.82
5	124.02	130.05	0.0	0.0	0.0	0.0	0.0	34	30.01	220.4	74.08	78.65	99.99	74.15	60.67
6	108.99	136.3	0.0	0.0	0.0	0.0	0.0	35	29.62	221.51	73.9	78.51	99.99	73.98	60.52
7	94.05	143.76	88.1	92.83	100.0	75.77	62.42	36	29.26	222.55	73.74	78.37	99.99	73.83	60.39
8	83.41	150.13	86.9	91.55	100.0	76.25	62.81	37	28.93	223.54	73.58	78.24	99.99	73.68	60.26
9	74.69	156.43	85.72	90.25	100.0	76.66	63.15	38	28.62	224.46	73.44	78.12	99.99	73.55	60.14
10	67.27	162.61	84.58	88.98	100.0	76.99	63.41	39	28.33	225.34	73.3	78.01	99.99	73.42	60.02
11	60.97	168.64	83.46	87.73	100.0	77.21	63.59	40	28.06	226.16	73.18	77.9	99.99	73.31	59.92
12	55.6	174.47	82.36	86.54	100.0	77.22	63.59	41	27.81	226.94	73.06	77.8	99.99	73.2	59.82
13	51.02	180.06	81.3	85.44	100.0	77.18	63.55	42	27.58	227.67	72.95	77.71	99.99	73.1	59.73
14	49.03	182.76	80.8	84.91	100.0	77.15	63.52	43	27.36	228.35	72.84	77.63	99.99	73.0	59.64
15	47.22	185.39	80.3	84.41	100.0	77.01	63.37	44	27.16	229.0	72.75	77.55	99.99	72.91	59.56
16	45.55	187.94	79.82	83.93	100.0	76.92	63.27	45	26.98	229.6	72.66	77.48	99.99	72.83	59.49
17	44.01	190.42	79.36	83.47	100.0	76.83	63.17	46	26.8	230.17	72.58	77.41	99.99	72.76	59.42
18	42.58	192.82	78.91	83.03	100.0	76.73	63.07	47	26.64	230.7	72.5	77.35	99.99	72.69	59.36
19	41.25	195.14	78.48	82.62	100.0	76.68	63.01	48	26.49	231.2	72.42	77.29	99.99	72.63	59.3
20	40.03	197.38	78.06	82.23	100.0	76.47	62.82	49	26.35	231.66	72.36	77.23	99.99	72.57	59.25
21	38.89	199.54	77.67	81.85	100.0	76.27	62.63	50	26.22	232.1	72.29	77.18	99.99	72.51	59.2
22	37.84	201.62	77.3	81.49	100.0	76.07	62.45	51	26.1	232.51	72.23	77.13	99.99	72.46	59.15
23	36.88	203.61	76.94	81.17	100.0	75.88	62.27	52	25.99	232.89	72.18	77.09	99.99	72.44	59.13
24	36.0	205.52	76.59	80.86	100.0	75.69	62.1	53	25.89	233.25	72.13	77.05	99.99	72.37	59.07
25	35.18	207.36	76.27	80.57	100.0	75.52	61.93	54	25.79	233.59	72.08	77.01	99.99	72.32	59.02
26	34.42	209.11	75.97	80.29	100.0	75.34	61.77	55	25.7	233.9	72.03	76.97	99.99	72.26	58.97
27	33.71	210.78	75.68	80.03	100.0	75.18	61.62	56	25.62	234.19	71.99	76.94	99.99	72.21	58.92
28	33.06	212.37	75.41	79.79	100.0	75.02	61.48	57	25.54	234.46	71.95	76.91	99.99	72.17	58.88
29	32.45	213.89	75.15	79.56	100.0	74.87	61.34	58	25.47	234.72	71.92	76.88	99.99	72.12	58.84
30	31.89	215.33	74.91	79.35	100.0	74.73	61.2	59	25.4	234.96	71.88	76.85	99.99	72.08	58.8

Table A.120.: Fe^{15+}

Step	$\hat{E}$	$\hat{T}$	P_1	P_2	P_T	P_S	P_{AS}	Step	$\hat{E}$	$\hat{T}$	P_1	P_2	P_T	P_S	P_{AS}
2	0.0	108.16	0.0	0.0	0.0	0.0	0.0	31	34.33	209.31	75.93	80.26	100.0	76.11	62.4
3	0.0	113.96	0.0	0.0	0.0	0.0	0.0	32	33.8	210.56	75.71	80.07	100.0	76.04	62.33
4	0.0	119.86	0.0	0.0	0.0	0.0	0.0	33	33.31	211.75	75.51	79.88	100.0	75.87	62.18
5	0.0	125.85	0.0	0.0	0.0	0.0	0.0	34	32.86	212.87	75.32	79.71	100.0	75.72	62.04
6	119.32	131.89	0.0	0.0	0.0	0.0	0.0	35	32.43	213.93	75.14	79.55	100.0	75.57	61.91
7	103.16	139.04	88.99	93.74	100.0	76.16	62.74	36	32.04	214.93	74.97	79.41	100.0	75.43	61.79
8	91.51	145.18	87.83	92.55	100.0	76.71	63.19	37	31.68	215.88	74.82	79.28	100.0	75.3	61.67
9	81.75	151.26	86.69	91.32	100.0	77.19	63.58	38	31.34	216.77	74.67	79.15	99.99	75.18	61.56
10	73.68	157.22	85.58	90.09	100.0	77.6	63.92	39	31.03	217.61	74.53	79.04	99.99	75.07	61.46
11	66.81	163.03	84.51	88.89	100.0	77.9	64.16	40	30.73	218.41	74.4	78.93	99.99	74.97	61.37
12	60.96	168.65	83.46	87.73	100.0	77.97	64.22	41	30.46	219.15	74.28	78.82	99.99	74.87	61.28
13	55.98	174.04	82.44	86.63	100.0	78.02	64.25	42	30.21	219.85	74.17	78.73	99.99	74.78	61.2
14	53.77	176.63	81.95	86.11	100.0	78.02	64.25	43	29.97	220.51	74.06	78.64	99.99	74.7	61.12
15	51.72	179.16	81.47	85.61	100.0	78.02	64.24	44	29.76	221.13	73.96	78.56	99.99	74.62	61.05
16	49.84	181.63	81.01	85.13	100.0	78.01	64.23	45	29.55	221.71	73.87	78.48	99.99	74.55	60.99
17	48.16	184.01	80.56	84.67	100.0	78.0	64.22	46	29.37	222.25	73.78	78.41	99.99	74.48	60.93
18	46.6	186.32	80.12	84.24	100.0	77.86	64.06	47	29.19	222.77	73.7	78.34	99.99	74.42	60.87
19	45.16	188.56	79.7	83.82	100.0	77.86	64.04	48	29.03	223.24	73.63	78.28	99.99	74.37	60.82
20	43.82	190.72	79.3	83.42	100.0	77.68	63.87	49	28.88	223.69	73.56	78.22	99.99	74.32	60.78
21	42.59	192.79	78.92	83.04	100.0	77.51	63.71	50	28.73	224.11	73.49	78.17	99.99	74.27	60.73
22	41.45	194.79	78.54	82.68	100.0	77.34	63.56	51	28.6	224.51	73.43	78.11	99.99	74.23	60.69
23	40.39	196.71	78.18	82.34	100.0	77.18	63.41	52	28.48	224.87	73.38	78.07	99.99	74.21	60.67
24	39.4	198.55	77.85	82.02	100.0	77.02	63.26	53	28.37	225.22	73.32	78.02	99.99	74.15	60.62
25	38.49	200.32	77.53	81.72	100.0	76.87	63.12	54	28.26	225.54	73.27	77.98	99.99	74.1	60.57
26	37.65	202.0	77.23	81.43	100.0	76.73	62.99	55	28.16	225.84	73.23	77.94	99.99	74.05	60.53
27	36.88	203.61	76.94	81.17	100.0	76.59	62.86	56	28.07	226.12	73.18	77.91	99.99	74.0	60.49
28	36.17	205.14	76.66	80.92	100.0	76.46	62.73	57	27.99	226.38	73.14	77.87	99.99	73.96	60.45
29	35.51	206.6	76.4	80.69	100.0	76.34	62.62	58	27.91	226.63	73.11	77.84	99.99	73.92	60.41
30	34.9	207.99	76.16	80.47	100.0	76.22	62.51	59	27.84	226.86	73.07	77.81	99.99	73.89	60.38

Table A.121.: Fe^{16+}

Step	$\hat{E}$	$\hat{T}$	P_1	P_2	P_T	P_S	P_{AS}	Step	$\hat{E}$	$\hat{T}$	P_1	P_2	P_T	P_S	P_{AS}
2	0.0	104.93	0.0	0.0	0.0	0.0	0.0	31	37.34	202.65	77.11	81.32	100.0	77.43	63.56
3	0.0	110.54	0.0	0.0	0.0	0.0	0.0	32	36.76	203.86	76.89	81.13	100.0	77.38	63.5
4	0.0	116.26	0.0	0.0	0.0	0.0	0.0	33	36.24	205.0	76.69	80.94	100.0	77.23	63.37
5	0.0	122.06	0.0	0.0	0.0	0.0	0.0	34	35.74	206.08	76.49	80.77	100.0	77.09	63.24
6	0.0	127.91	0.0	0.0	0.0	0.0	0.0	35	35.29	207.11	76.31	80.61	100.0	76.96	63.13
7	114.79	133.76	0.0	0.0	0.0	0.0	0.0	36	34.86	208.07	76.15	80.46	100.0	76.84	63.01
8	99.8	140.71	88.67	93.42	100.0	77.1	63.52	37	34.47	208.99	75.99	80.31	100.0	76.72	62.91
9	89.1	146.58	87.56	92.27	100.0	77.65	63.97	38	34.1	209.85	75.84	80.18	100.0	76.61	62.81
10	80.18	152.35	86.49	91.09	100.0	78.13	64.36	39	33.76	210.66	75.7	80.05	100.0	76.51	62.72
11	72.75	157.96	85.44	89.94	100.0	78.5	64.66	40	33.45	211.42	75.57	79.93	100.0	76.42	62.64
12	66.41	163.39	84.44	88.82	100.0	78.64	64.77	41	33.15	212.14	75.44	79.82	100.0	76.33	62.56
13	61.01	168.6	83.47	87.74	100.0	78.74	64.85	42	32.88	212.82	75.33	79.72	100.0	76.25	62.49
14	58.62	171.11	82.99	87.23	100.0	78.78	64.88	43	32.63	213.45	75.22	79.62	100.0	76.18	62.42
15	56.4	173.55	82.53	86.73	100.0	78.81	64.91	44	32.39	214.05	75.12	79.53	100.0	76.11	62.36
16	54.35	175.93	82.09	86.25	100.0	78.84	64.92	45	32.17	214.61	75.03	79.46	100.0	76.05	62.3
17	52.46	178.23	81.65	85.8	100.0	78.86	64.93	46	31.97	215.13	74.94	79.38	100.0	75.99	62.25
18	50.71	180.47	81.22	85.36	100.0	78.87	64.94	47	31.78	215.62	74.86	79.31	100.0	75.94	62.2
19	49.12	182.62	80.82	84.94	100.0	78.93	64.99	48	31.6	216.08	74.78	79.25	100.0	75.89	62.15
20	47.68	184.71	80.43	84.54	100.0	78.74	64.8	49	31.44	216.52	74.71	79.19	99.99	75.84	62.11
21	46.34	186.71	80.05	84.16	100.0	78.59	64.66	50	31.28	216.92	74.64	79.13	99.99	75.8	62.07
22	45.11	188.64	79.69	83.8	100.0	78.45	64.53	51	31.14	217.3	74.58	79.08	99.99	75.77	62.04
23	43.96	190.5	79.34	83.46	100.0	78.32	64.4	52	31.01	217.65	74.52	79.03	99.99	75.75	62.03
24	42.9	192.27	79.01	83.13	100.0	78.19	64.28	53	30.89	217.99	74.47	78.98	99.99	75.7	61.98
25	41.91	193.97	78.69	82.83	100.0	78.06	64.16	54	30.77	218.3	74.42	78.94	99.99	75.65	61.93
26	41.0	195.6	78.39	82.54	100.0	77.94	64.04	55	30.67	218.58	74.37	78.9	99.99	75.61	61.89
27	40.15	197.15	78.1	82.27	100.0	77.83	63.94	56	30.57	218.86	74.33	78.86	99.99	75.57	61.85
28	39.36	198.63	77.83	82.01	100.0	77.72	63.83	57	30.48	219.11	74.29	78.83	99.99	75.53	61.82
29	38.63	200.04	77.58	81.76	100.0	77.62	63.73	58	30.39	219.34	74.25	78.8	99.99	75.49	61.78
30	37.96	201.38	77.34	81.53	100.0	77.52	63.64	59	30.31	219.56	74.21	78.77	99.99	75.46	61.75

Table A.122.: Fe^{17+}

Step	$\hat{E}$	$\hat{T}$	P_1	P_2	P_T	P_S	P_{AS}	Step	$\hat{E}$	$\hat{T}$	P_1	P_2	P_T	P_S	P_{AS}
2	0.0	101.99	0.0	0.0	0.0	0.0	0.0	31	40.44	196.61	78.2	82.36	100.0	78.6	64.57
3	0.0	107.43	0.0	0.0	0.0	0.0	0.0	32	39.81	197.77	77.99	82.16	100.0	78.57	64.54
4	0.0	112.98	0.0	0.0	0.0	0.0	0.0	33	39.23	198.88	77.79	81.97	100.0	78.43	64.42
5	0.0	118.61	0.0	0.0	0.0	0.0	0.0	34	38.69	199.93	77.6	81.78	100.0	78.3	64.3
6	0.0	124.28	0.0	0.0	0.0	0.0	0.0	35	38.19	200.92	77.42	81.61	100.0	78.18	64.2
7	124.27	129.95	0.0	0.0	0.0	0.0	0.0	36	37.72	201.85	77.25	81.45	100.0	78.07	64.09
8	110.55	135.6	0.0	0.0	0.0	0.0	0.0	37	37.3	202.73	77.09	81.31	100.0	77.97	64.0
9	96.67	142.34	88.36	93.11	100.0	78.05	64.31	38	36.9	203.56	76.94	81.18	100.0	77.87	63.91
10	86.87	147.92	87.31	92.0	100.0	78.59	64.75	39	36.54	204.35	76.8	81.05	100.0	77.78	63.83
11	78.77	153.36	86.3	90.88	100.0	79.03	65.1	40	36.2	205.09	76.67	80.93	100.0	77.7	63.76
12	71.94	158.62	85.32	89.8	100.0	79.22	65.26	41	35.88	205.78	76.55	80.82	100.0	77.62	63.68
13	66.12	163.66	84.39	88.76	100.0	79.39	65.39	42	35.59	206.43	76.43	80.72	100.0	77.55	63.62
14	63.54	166.09	83.93	88.26	100.0	79.45	65.44	43	35.31	207.05	76.32	80.62	100.0	77.48	63.56
15	61.15	168.45	83.49	87.77	100.0	79.52	65.49	44	35.06	207.62	76.22	80.53	100.0	77.42	63.5
16	58.94	170.75	83.06	87.3	100.0	79.57	65.53	45	34.82	208.17	76.13	80.44	100.0	77.37	63.45
17	56.9	172.99	82.64	86.85	100.0	79.62	65.57	46	34.6	208.67	76.04	80.36	100.0	77.32	63.41
18	55.02	175.15	82.23	86.41	100.0	79.66	65.6	47	34.4	209.15	75.96	80.29	100.0	77.27	63.36
19	53.27	177.23	81.84	85.99	100.0	79.75	65.68	48	34.21	209.59	75.88	80.22	100.0	77.23	63.32
20	51.65	179.25	81.45	85.6	100.0	79.66	65.6	49	34.03	210.01	75.81	80.15	100.0	77.19	63.29
21	50.16	181.19	81.09	85.22	100.0	79.58	65.53	50	33.87	210.4	75.74	80.09	100.0	77.16	63.26
22	48.82	183.06	80.74	84.85	100.0	79.51	65.47	51	33.72	210.77	75.68	80.03	100.0	77.13	63.23
23	47.58	184.85	80.4	84.51	100.0	79.32	65.28	52	33.57	211.11	75.62	79.98	100.0	77.12	63.22
24	46.44	186.57	80.07	84.19	100.0	79.21	65.17	53	33.44	211.43	75.57	79.93	100.0	77.07	63.17
25	45.38	188.22	79.77	83.88	100.0	79.11	65.07	54	33.32	211.73	75.51	79.88	100.0	77.02	63.13
26	44.39	189.79	79.47	83.59	100.0	79.01	64.98	55	33.2	212.01	75.47	79.84	100.0	76.98	63.09
27	43.48	191.29	79.2	83.31	100.0	78.92	64.89	56	33.1	212.27	75.42	79.8	100.0	76.94	63.06
28	42.63	192.72	78.93	83.05	100.0	78.83	64.8	57	33.0	212.52	75.38	79.76	100.0	76.91	63.03
29	41.85	194.08	78.67	82.81	100.0	78.75	64.72	58	32.91	212.74	75.34	79.73	100.0	76.88	63.0
30	41.12	195.38	78.43	82.58	100.0	78.67	64.65	59	32.82	212.96	75.31	79.7	100.0	76.85	62.97

Table A.123.: Fe^{18+}

Step	$\hat{E}$	$\hat{T}$	P_1	P_2	P_T	P_S	P_{AS}	Step	$\hat{E}$	$\hat{T}$	P_1	P_2	P_T	P_S	P_{AS}
2	0.0	99.3	0.0	0.0	0.0	0.0	0.0	31	43.6	191.09	79.23	83.35	100.0	79.63	65.48
3	0.0	104.58	0.0	0.0	0.0	0.0	0.0	32	42.92	192.22	79.02	83.14	100.0	79.62	65.46
4	0.0	109.98	0.0	0.0	0.0	0.0	0.0	33	42.3	193.29	78.82	82.95	100.0	79.5	65.35
5	0.0	115.45	0.0	0.0	0.0	0.0	0.0	34	41.72	194.31	78.63	82.77	100.0	79.38	65.24
6	0.0	120.96	0.0	0.0	0.0	0.0	0.0	35	41.18	195.27	78.45	82.6	100.0	79.27	65.15
7	0.0	126.47	0.0	0.0	0.0	0.0	0.0	36	40.68	196.17	78.28	82.44	100.0	79.17	65.05
8	119.15	131.96	0.0	0.0	0.0	0.0	0.0	37	40.22	197.03	78.13	82.29	100.0	79.08	64.97
9	106.66	137.37	0.0	0.0	0.0	0.0	0.0	38	39.78	197.83	77.98	82.15	100.0	78.99	64.89
10	93.83	143.88	88.08	92.81	100.0	79.01	65.1	39	39.38	198.59	77.84	82.02	100.0	78.91	64.82
11	84.89	149.15	87.08	91.75	100.0	79.5	65.5	40	39.01	199.31	77.71	81.89	100.0	78.84	64.75
12	77.55	154.25	86.13	90.7	100.0	79.75	65.69	41	38.66	199.98	77.59	81.77	100.0	78.77	64.69
13	71.31	159.14	85.22	89.7	100.0	79.96	65.86	42	38.34	200.61	77.47	81.67	100.0	78.7	64.63
14	68.53	161.5	84.79	89.21	100.0	80.05	65.94	43	38.04	201.21	77.37	81.56	100.0	78.64	64.57
15	65.97	163.8	84.36	88.73	100.0	80.14	66.01	44	37.77	201.77	77.27	81.47	100.0	78.59	64.52
16	63.6	166.03	83.94	88.27	100.0	80.22	66.07	45	37.51	202.29	77.17	81.38	100.0	78.54	64.48
17	61.41	168.19	83.54	87.83	100.0	80.29	66.13	46	37.27	202.78	77.08	81.3	100.0	78.5	64.44
18	59.38	170.29	83.15	87.4	100.0	80.36	66.18	47	37.05	203.24	77.0	81.23	100.0	78.46	64.4
19	57.51	172.31	82.76	86.98	100.0	80.49	66.29	48	36.85	203.67	76.92	81.16	100.0	78.42	64.37
20	55.77	174.27	82.4	86.58	100.0	80.4	66.21	49	36.66	204.08	76.85	81.09	100.0	78.39	64.33
21	54.17	176.15	82.04	86.21	100.0	80.32	66.15	50	36.49	204.46	76.78	81.03	100.0	78.36	64.31
22	52.68	177.96	81.7	85.85	100.0	80.26	66.09	51	36.32	204.81	76.72	80.97	100.0	78.33	64.28
23	51.3	179.7	81.37	85.51	100.0	80.21	66.05	52	36.17	205.14	76.66	80.92	100.0	78.33	64.28
24	50.03	181.36	81.06	85.18	100.0	80.17	66.01	53	36.03	205.45	76.61	80.87	100.0	78.28	64.23
25	48.89	182.96	80.76	84.87	100.0	80.14	65.99	54	35.9	205.74	76.55	80.83	100.0	78.24	64.2
26	47.83	184.48	80.47	84.58	100.0	80.12	65.97	55	35.77	206.01	76.51	80.78	100.0	78.2	64.16
27	46.85	185.94	80.19	84.31	100.0	79.89	65.73	56	35.66	206.27	76.46	80.74	100.0	78.17	64.13
28	45.95	187.33	79.93	84.05	100.0	79.82	65.66	57	35.55	206.5	76.42	80.7	100.0	78.14	64.1
29	45.1	188.65	79.69	83.8	100.0	79.75	65.6	58	35.46	206.72	76.38	80.67	100.0	78.11	64.07
30	44.32	189.9	79.45	83.57	100.0	79.69	65.54	59	35.36	206.93	76.35	80.64	100.0	78.08	64.04

Table A.124.: Fe^{19+}

Step	$\hat{E}$	$\hat{T}$	P_1	P_2	P_T	P_S	P_{AS}	Step	$\hat{E}$	$\hat{T}$	P_1	P_2	P_T	P_S	P_{AS}
2	0.0	96.82	0.0	0.0	0.0	0.0	0.0	31	46.79	186.03	80.18	84.29	100.0	80.56	66.29
3	0.0	101.97	0.0	0.0	0.0	0.0	0.0	32	46.07	187.13	79.97	84.08	100.0	80.56	66.28
4	0.0	107.22	0.0	0.0	0.0	0.0	0.0	33	45.4	188.17	79.77	83.89	100.0	80.45	66.18
5	0.0	112.54	0.0	0.0	0.0	0.0	0.0	34	44.78	189.16	79.59	83.71	100.0	80.34	66.08
6	0.0	117.9	0.0	0.0	0.0	0.0	0.0	35	44.21	190.09	79.42	83.53	100.0	80.25	66.0
7	0.0	123.27	0.0	0.0	0.0	0.0	0.0	36	43.67	190.97	79.26	83.37	100.0	80.16	65.91
8	127.87	128.61	0.0	0.0	0.0	0.0	0.0	37	43.18	191.79	79.1	83.22	100.0	80.07	65.84
9	114.52	133.87	0.0	0.0	0.0	0.0	0.0	38	42.72	192.58	78.96	83.08	100.0	79.99	65.76
10	100.89	140.16	88.78	93.53	100.0	79.38	65.41	39	42.29	193.31	78.82	82.95	100.0	79.92	65.7
11	91.32	145.29	87.81	92.53	100.0	79.92	65.85	40	41.89	194.01	78.69	82.82	100.0	79.85	65.64
12	83.23	150.24	86.88	91.52	100.0	80.21	66.08	41	41.52	194.66	78.57	82.71	100.0	79.79	65.58
13	76.56	155.0	85.99	90.55	100.0	80.47	66.29	42	41.18	195.28	78.45	82.6	100.0	79.73	65.53
14	73.59	157.29	85.56	90.08	100.0	80.59	66.39	43	40.86	195.85	78.34	82.5	100.0	79.68	65.48
15	70.85	159.52	85.15	89.62	100.0	80.7	66.47	44	40.56	196.39	78.24	82.4	100.0	79.63	65.44
16	68.32	161.69	84.75	89.17	100.0	80.8	66.56	45	40.28	196.9	78.15	82.31	100.0	79.59	65.4
17	65.98	163.79	84.37	88.73	100.0	80.89	66.63	46	40.03	197.38	78.06	82.23	100.0	79.55	65.36
18	63.81	165.82	83.98	88.31	100.0	80.98	66.71	47	39.79	197.83	77.98	82.15	100.0	79.52	65.33
19	61.81	167.79	83.62	87.91	100.0	81.15	66.84	48	39.57	198.25	77.9	82.08	100.0	79.49	65.3
20	59.95	169.69	83.26	87.52	100.0	81.06	66.77	49	39.36	198.64	77.83	82.01	100.0	79.46	65.27
21	58.23	171.52	82.91	87.14	100.0	80.99	66.71	50	39.17	199.01	77.77	81.94	100.0	79.43	65.25
22	56.64	173.28	82.58	86.79	100.0	80.93	66.65	51	38.99	199.35	77.7	81.88	100.0	79.41	65.22
23	55.17	174.97	82.27	86.44	100.0	80.88	66.61	52	38.82	199.67	77.64	81.83	100.0	79.41	65.22
24	53.81	176.59	81.96	86.12	100.0	80.84	66.58	53	38.67	199.97	77.59	81.78	100.0	79.37	65.18
25	52.54	178.14	81.66	85.81	100.0	80.82	66.55	54	38.53	200.25	77.54	81.73	100.0	79.33	65.15
26	51.37	179.62	81.38	85.52	100.0	80.8	66.54	55	38.39	200.52	77.49	81.68	100.0	79.3	65.12
27	50.28	181.03	81.12	85.25	100.0	80.79	66.53	56	38.27	200.76	77.45	81.64	100.0	79.26	65.08
28	49.3	182.38	80.87	84.99	100.0	80.79	66.53	57	38.15	200.99	77.41	81.6	100.0	79.23	65.06
29	48.4	183.66	80.63	84.74	100.0	80.8	66.54	58	38.04	201.21	77.37	81.56	100.0	79.21	65.03
30	47.57	184.88	80.39	84.51	100.0	80.6	66.33	59	37.94	201.41	77.33	81.53	100.0	79.18	65.01

Table A.125.: Fe^{20+}

Step	$\hat{E}$	$\hat{T}$	P_1	P_2	P_T	P_S	P_{AS}	Step	$\hat{E}$	$\hat{T}$	P_1	P_2	P_T	P_S	P_{AS}
2	0.0	94.53	0.0	0.0	0.0	0.0	0.0	31	50.03	181.37	81.06	85.18	100.0	81.46	67.08
3	0.0	99.55	0.0	0.0	0.0	0.0	0.0	32	49.26	182.44	80.86	84.97	100.0	81.53	67.14
4	0.0	104.66	0.0	0.0	0.0	0.0	0.0	33	48.55	183.45	80.67	84.78	100.0	81.48	67.1
5	0.0	109.85	0.0	0.0	0.0	0.0	0.0	34	47.89	184.4	80.48	84.6	100.0	81.44	67.06
6	0.0	115.08	0.0	0.0	0.0	0.0	0.0	35	47.27	185.31	80.31	84.43	100.0	81.12	66.76
7	0.0	120.31	0.0	0.0	0.0	0.0	0.0	36	46.7	186.16	80.15	84.27	100.0	81.04	66.69
8	0.0	125.51	0.0	0.0	0.0	0.0	0.0	37	46.18	186.97	80.0	84.11	100.0	80.96	66.62
9	122.47	130.65	0.0	0.0	0.0	0.0	0.0	38	45.68	187.73	79.86	83.97	100.0	80.89	66.55
10	110.38	135.67	0.0	0.0	0.0	0.0	0.0	39	45.23	188.45	79.72	83.84	100.0	80.83	66.49
11	97.84	141.72	88.48	93.23	100.0	80.3	66.17	40	44.8	189.12	79.6	83.71	100.0	80.77	66.44
12	89.16	146.55	87.57	92.27	100.0	80.63	66.43	41	44.41	189.76	79.48	83.59	100.0	80.71	66.39
13	81.87	151.17	86.71	91.33	100.0	80.93	66.67	42	44.04	190.36	79.37	83.48	100.0	80.66	66.34
14	78.71	153.4	86.3	90.87	100.0	81.07	66.79	43	43.7	190.92	79.27	83.38	100.0	80.62	66.3
15	75.8	155.57	85.89	90.43	100.0	81.2	66.89	44	43.39	191.44	79.17	83.28	100.0	80.57	66.26
16	73.1	157.68	85.49	90.0	100.0	81.32	66.99	45	43.09	191.94	79.08	83.19	100.0	80.54	66.22
17	70.6	159.73	85.11	89.57	100.0	81.44	67.09	46	42.82	192.4	78.99	83.11	100.0	80.5	66.19
18	68.29	161.71	84.75	89.16	100.0	81.55	67.18	47	42.57	192.84	78.91	83.03	100.0	80.47	66.16
19	66.16	163.62	84.4	88.77	100.0	81.74	67.33	48	42.33	193.24	78.83	82.96	100.0	80.44	66.13
20	64.18	165.47	84.05	88.39	100.0	81.66	67.27	49	42.11	193.62	78.76	82.89	100.0	80.42	66.11
21	62.35	167.25	83.72	88.02	100.0	81.59	67.21	50	41.91	193.98	78.69	82.83	100.0	80.4	66.09
22	60.65	168.96	83.4	87.67	100.0	81.54	67.16	51	41.71	194.32	78.63	82.77	100.0	80.38	66.07
23	59.08	170.6	83.09	87.33	100.0	81.49	67.12	52	41.54	194.63	78.57	82.71	100.0	80.38	66.07
24	57.63	172.18	82.79	87.01	100.0	81.45	67.09	53	41.37	194.92	78.52	82.66	100.0	80.34	66.04
25	56.28	173.69	82.51	86.7	100.0	81.43	67.06	54	41.22	195.19	78.47	82.61	100.0	80.31	66.0
26	55.03	175.13	82.24	86.41	100.0	81.41	67.05	55	41.08	195.45	78.42	82.57	100.0	80.28	65.97
27	53.88	176.5	81.98	86.14	100.0	81.4	67.04	56	40.95	195.69	78.37	82.52	100.0	80.25	65.95
28	52.8	177.81	81.73	85.88	100.0	81.41	67.04	57	40.82	195.91	78.33	82.48	100.0	80.22	65.92
29	51.81	179.06	81.49	85.63	100.0	81.42	67.05	58	40.71	196.12	78.29	82.45	100.0	80.2	65.9
30	50.88	180.24	81.27	85.4	100.0	81.43	67.06	59	40.6	196.32	78.26	82.41	100.0	80.17	65.87

Table A.126.: Fe^{21+}

Step	$\hat{E}$	$\hat{T}$	P_1	P_2	P_T	P_S	P_{AS}	Step	$\hat{E}$	$\hat{T}$	P_1	P_2	P_T	P_S	P_{AS}
2	0.0	92.41	0.0	0.0	0.0	0.0	0.0	31	53.42	177.05	81.87	86.03	100.0	82.01	67.54
3	0.0	97.3	0.0	0.0	0.0	0.0	0.0	32	52.58	178.09	81.67	85.82	100.0	82.08	67.6
4	0.0	102.3	0.0	0.0	0.0	0.0	0.0	33	51.79	179.08	81.49	85.63	100.0	82.03	67.56
5	0.0	107.36	0.0	0.0	0.0	0.0	0.0	34	51.06	180.01	81.31	85.45	100.0	81.99	67.53
6	0.0	112.46	0.0	0.0	0.0	0.0	0.0	35	50.39	180.89	81.15	85.28	100.0	81.96	67.5
7	0.0	117.57	0.0	0.0	0.0	0.0	0.0	36	49.77	181.72	80.99	85.11	100.0	81.93	67.47
8	0.0	122.64	0.0	0.0	0.0	0.0	0.0	37	49.21	182.51	80.84	84.96	100.0	81.91	67.45
9	0.0	127.65	0.0	0.0	0.0	0.0	0.0	38	48.69	183.25	80.71	84.82	100.0	81.89	67.44
10	117.67	132.56	0.0	0.0	0.0	0.0	0.0	39	48.2	183.95	80.57	84.69	100.0	81.87	67.42
11	106.75	137.33	0.0	0.0	0.0	0.0	0.0	40	47.75	184.6	80.45	84.56	100.0	81.59	67.16
12	95.22	143.12	88.22	92.95	100.0	81.01	66.75	41	47.33	185.22	80.33	84.44	100.0	81.55	67.11
13	87.35	147.63	87.37	92.05	100.0	81.35	67.02	42	46.94	185.8	80.22	84.33	100.0	81.5	67.07
14	83.89	149.8	86.96	91.61	100.0	81.5	67.15	43	46.58	186.35	80.12	84.23	100.0	81.46	67.03
15	80.8	151.92	86.57	91.18	100.0	81.65	67.27	44	46.25	186.86	80.02	84.14	100.0	81.42	67.0
16	77.93	153.97	86.19	90.76	100.0	81.8	67.39	45	45.93	187.34	79.93	84.04	100.0	81.39	66.97
17	75.28	155.97	85.81	90.35	100.0	81.93	67.5	46	45.64	187.79	79.84	83.96	100.0	81.36	66.94
18	72.83	157.9	85.45	89.95	100.0	82.06	67.6	47	45.37	188.22	79.77	83.88	100.0	81.33	66.91
19	70.56	159.76	85.1	89.57	100.0	82.28	67.78	48	45.12	188.61	79.69	83.81	100.0	81.31	66.89
20	68.46	161.56	84.77	89.19	100.0	82.2	67.72	49	44.89	188.99	79.62	83.74	100.0	81.29	66.87
21	66.52	163.3	84.46	88.84	100.0	82.14	67.66	50	44.67	189.33	79.56	83.67	100.0	81.27	66.86
22	64.72	164.96	84.14	88.49	100.0	82.08	67.61	51	44.47	189.66	79.5	83.61	100.0	81.26	66.84
23	63.05	166.56	83.84	88.16	100.0	82.04	67.58	52	44.28	189.96	79.44	83.56	100.0	81.26	66.84
24	61.5	168.1	83.56	87.84	100.0	82.0	67.55	53	44.11	190.25	79.39	83.5	100.0	81.23	66.81
25	60.07	169.57	83.28	87.54	100.0	81.98	67.53	54	43.95	190.51	79.34	83.45	100.0	81.2	66.78
26	58.74	170.97	83.02	87.26	100.0	81.96	67.51	55	43.8	190.76	79.29	83.41	100.0	81.17	66.75
27	57.51	172.31	82.76	86.98	100.0	81.96	67.51	56	43.66	191.0	79.25	83.36	100.0	81.14	66.72
28	56.37	173.59	82.52	86.72	100.0	81.96	67.51	57	43.53	191.21	79.21	83.32	100.0	81.11	66.7
29	55.31	174.8	82.3	86.48	100.0	81.97	67.51	58	43.4	191.42	79.17	83.29	100.0	81.09	66.68
30	54.33	175.95	82.08	86.24	100.0	81.99	67.52	59	43.29	191.6	79.14	83.25	100.0	81.07	66.66

Table A.127.: Fe^{22+}

Step	$\hat{E}$	$\hat{T}$	P_1	P_2	P_T	P_S	P_{AS}	Step	$\hat{E}$	$\hat{T}$	P_1	P_2	P_T	P_S	P_{AS}
2	0.0	90.43	0.0	0.0	0.0	0.0	0.0	31	56.86	173.04	82.63	86.83	100.0	82.51	67.96
3	0.0	95.21	0.0	0.0	0.0	0.0	0.0	32	55.96	174.05	82.44	86.63	100.0	82.58	68.02
4	0.0	100.09	0.0	0.0	0.0	0.0	0.0	33	55.13	175.01	82.26	86.43	100.0	82.53	67.98
5	0.0	105.04	0.0	0.0	0.0	0.0	0.0	34	54.36	175.92	82.09	86.25	100.0	82.5	67.95
6	0.0	110.02	0.0	0.0	0.0	0.0	0.0	35	53.64	176.78	81.92	86.08	100.0	82.47	67.92
7	0.0	115.01	0.0	0.0	0.0	0.0	0.0	36	52.98	177.59	81.77	85.92	100.0	82.44	67.9
8	0.0	119.97	0.0	0.0	0.0	0.0	0.0	37	52.36	178.36	81.62	85.77	100.0	82.41	67.88
9	0.0	124.86	0.0	0.0	0.0	0.0	0.0	38	51.79	179.08	81.49	85.63	100.0	82.4	67.86
10	125.05	129.66	0.0	0.0	0.0	0.0	0.0	39	51.26	179.76	81.36	85.5	100.0	82.38	67.85
11	113.48	134.32	0.0	0.0	0.0	0.0	0.0	40	50.76	180.4	81.24	85.37	100.0	82.37	67.84
12	101.35	139.93	88.82	93.57	100.0	81.36	67.04	41	50.3	181.01	81.12	85.25	100.0	82.36	67.83
13	93.01	144.33	87.99	92.72	100.0	81.73	67.34	42	49.88	181.57	81.02	85.14	100.0	82.36	67.82
14	89.32	146.45	87.59	92.29	100.0	81.9	67.48	43	49.49	182.1	80.92	85.04	100.0	82.35	67.82
15	85.9	148.52	87.2	91.87	100.0	82.07	67.61	44	49.14	182.6	80.83	84.94	100.0	82.35	67.82
16	82.82	150.52	86.83	91.47	100.0	82.23	67.74	45	48.81	183.07	80.74	84.85	100.0	82.35	67.82
17	80.01	152.47	86.47	91.07	100.0	82.38	67.87	46	48.5	183.51	80.65	84.77	100.0	82.36	67.83
18	77.42	154.35	86.12	90.68	100.0	82.53	67.99	47	48.21	183.93	80.58	84.69	100.0	82.36	67.83
19	75.01	156.17	85.77	90.31	100.0	82.77	68.19	48	47.95	184.31	80.5	84.62	100.0	82.37	67.84
20	72.79	157.93	85.44	89.95	100.0	82.7	68.13	49	47.7	184.68	80.43	84.55	100.0	82.08	67.56
21	70.73	159.62	85.13	89.6	100.0	82.63	68.07	50	47.47	185.01	80.37	84.48	100.0	82.07	67.55
22	68.82	161.25	84.83	89.26	100.0	82.58	68.03	51	47.26	185.33	80.31	84.42	100.0	82.06	67.54
23	67.06	162.81	84.55	88.94	100.0	82.54	67.99	52	47.06	185.63	80.25	84.37	100.0	82.06	67.54
24	65.42	164.31	84.27	88.63	100.0	82.51	67.97	53	46.88	185.91	80.2	84.31	100.0	82.03	67.51
25	63.9	165.74	84.0	88.33	100.0	82.48	67.95	54	46.7	186.17	80.15	84.27	100.0	82.0	67.48
26	62.5	167.11	83.74	88.05	100.0	82.47	67.93	55	46.54	186.41	80.1	84.22	100.0	81.97	67.46
27	61.19	168.41	83.5	87.78	100.0	82.46	67.93	56	46.39	186.64	80.06	84.18	100.0	81.95	67.43
28	59.98	169.66	83.27	87.52	100.0	82.46	67.93	57	46.26	186.85	80.02	84.14	100.0	81.93	67.41
29	58.86	170.84	83.04	87.28	100.0	82.47	67.93	58	46.13	187.04	79.98	84.1	100.0	81.9	67.39
30	57.82	171.97	82.83	87.05	100.0	82.49	67.95	59	46.01	187.23	79.95	84.07	100.0	81.89	67.37

Table A.128.: Fe^{23+}

Step	$\hat{E}$	$\hat{T}$	P_1	P_2	P_T	P_S	P_{AS}	Step	$\hat{E}$	$\hat{T}$	P_1	P_2	P_T	P_S	P_{AS}
2	0.0	88.58	0.0	0.0	0.0	0.0	0.0	31	60.33	169.3	83.34	87.6	100.0	82.97	68.35
3	0.0	93.26	0.0	0.0	0.0	0.0	0.0	32	59.39	170.29	83.15	87.4	100.0	83.03	68.4
4	0.0	98.03	0.0	0.0	0.0	0.0	0.0	33	58.51	171.22	82.97	87.2	100.0	82.99	68.36
5	0.0	102.87	0.0	0.0	0.0	0.0	0.0	34	57.69	172.11	82.8	87.02	100.0	82.96	68.33
6	0.0	107.74	0.0	0.0	0.0	0.0	0.0	35	56.94	172.95	82.64	86.85	100.0	82.93	68.31
7	0.0	112.62	0.0	0.0	0.0	0.0	0.0	36	56.23	173.74	82.49	86.69	100.0	82.9	68.28
8	0.0	117.47	0.0	0.0	0.0	0.0	0.0	37	55.58	174.49	82.36	86.54	100.0	82.88	68.27
9	0.0	122.26	0.0	0.0	0.0	0.0	0.0	38	54.97	175.2	82.22	86.4	100.0	82.86	68.25
10	0.0	126.95	0.0	0.0	0.0	0.0	0.0	39	54.41	175.86	82.1	86.26	100.0	82.84	68.24
11	120.28	131.51	0.0	0.0	0.0	0.0	0.0	40	53.89	176.49	81.98	86.14	100.0	82.83	68.23
12	109.87	135.9	0.0	0.0	0.0	0.0	0.0	41	53.4	177.07	81.87	86.02	100.0	82.83	68.22
13	98.74	141.26	88.57	93.32	100.0	82.07	67.63	42	52.95	177.63	81.76	85.91	100.0	82.82	68.22
14	94.83	143.33	88.18	92.91	100.0	82.26	67.78	43	52.53	178.15	81.66	85.81	100.0	82.82	68.21
15	91.22	145.35	87.8	92.51	100.0	82.44	67.93	44	52.14	178.64	81.57	85.72	100.0	82.82	68.21
16	87.89	147.31	87.43	92.12	100.0	82.62	68.07	45	51.78	179.09	81.48	85.63	100.0	82.82	68.21
17	84.8	149.21	87.07	91.73	100.0	82.79	68.21	46	51.44	179.52	81.4	85.54	100.0	82.82	68.22
18	82.05	151.05	86.73	91.36	100.0	82.95	68.34	47	51.13	179.93	81.33	85.46	100.0	82.83	68.22
19	79.51	152.83	86.41	90.99	100.0	83.22	68.56	48	50.84	180.3	81.25	85.39	100.0	82.84	68.23
20	77.16	154.54	86.08	90.64	100.0	83.15	68.5	49	50.56	180.66	81.19	85.32	100.0	82.85	68.23
21	74.99	156.19	85.77	90.3	100.0	83.09	68.45	50	50.31	180.99	81.13	85.26	100.0	82.86	68.24
22	72.97	157.78	85.47	89.98	100.0	83.04	68.41	51	50.08	181.3	81.07	85.2	100.0	82.87	68.25
23	71.11	159.31	85.19	89.66	100.0	83.0	68.37	52	49.86	181.59	81.01	85.14	100.0	82.9	68.28
24	69.38	160.77	84.92	89.36	100.0	82.96	68.35	53	49.67	181.86	80.96	85.09	100.0	82.89	68.27
25	67.78	162.17	84.67	89.07	100.0	82.94	68.33	54	49.49	182.11	80.92	85.04	100.0	82.88	68.25
26	66.29	163.5	84.42	88.79	100.0	82.93	68.32	55	49.32	182.35	80.87	84.99	100.0	82.87	68.24
27	64.91	164.78	84.18	88.53	100.0	82.92	68.31	56	49.16	182.57	80.83	84.95	100.0	82.86	68.24
28	63.64	165.99	83.95	88.28	100.0	82.92	68.31	57	49.02	182.78	80.79	84.91	100.0	82.85	68.23
29	62.45	167.15	83.73	88.04	100.0	82.93	68.32	58	48.88	182.97	80.76	84.87	100.0	82.84	68.22
30	61.35	168.25	83.53	87.81	100.0	82.95	68.33	59	48.75	183.15	80.72	84.84	100.0	82.84	68.22

Table A.129.: Fe^{24+}

Step	$\hat{E}$	$\hat{T}$	P_1	P_2	P_T	P_S	P_{AS}	Step	$\hat{E}$	$\hat{T}$	P_1	P_2	P_T	P_S	P_{AS}
2	0.0	86.85	0.0	0.0	0.0	0.0	0.0	31	63.84	165.79	83.99	88.32	100.0	83.39	68.7
3	0.0	91.43	0.0	0.0	0.0	0.0	0.0	32	62.85	166.76	83.81	88.12	100.0	83.45	68.75
4	0.0	96.1	0.0	0.0	0.0	0.0	0.0	33	61.92	167.68	83.64	87.93	100.0	83.41	68.71
5	0.0	100.84	0.0	0.0	0.0	0.0	0.0	34	61.06	168.55	83.48	87.75	100.0	83.38	68.69
6	0.0	105.61	0.0	0.0	0.0	0.0	0.0	35	60.26	169.37	83.32	87.58	100.0	83.35	68.66
7	0.0	110.39	0.0	0.0	0.0	0.0	0.0	36	59.52	170.14	83.17	87.43	100.0	83.32	68.64
8	0.0	115.14	0.0	0.0	0.0	0.0	0.0	37	58.83	170.87	83.03	87.28	100.0	83.3	68.62
9	0.0	119.82	0.0	0.0	0.0	0.0	0.0	38	58.19	171.56	82.9	87.14	100.0	83.28	68.61
10	0.0	124.41	0.0	0.0	0.0	0.0	0.0	39	57.6	172.21	82.78	87.0	100.0	83.27	68.59
11	127.16	128.87	0.0	0.0	0.0	0.0	0.0	40	57.05	172.82	82.67	86.88	100.0	83.26	68.59
12	116.18	133.17	0.0	0.0	0.0	0.0	0.0	41	56.54	173.4	82.56	86.76	100.0	83.25	68.58
13	106.82	137.29	0.0	0.0	0.0	0.0	0.0	42	56.06	173.94	82.46	86.65	100.0	83.25	68.57
14	100.4	140.41	88.73	93.48	100.0	82.59	68.06	43	55.62	174.45	82.36	86.55	100.0	83.24	68.57
15	96.6	142.38	88.36	93.1	100.0	82.79	68.22	44	55.21	174.93	82.28	86.45	100.0	83.24	68.57
16	93.08	144.3	88.0	92.72	100.0	82.98	68.37	45	54.82	175.37	82.19	86.36	100.0	83.25	68.57
17	89.83	146.15	87.64	92.35	100.0	83.16	68.52	46	54.47	175.79	82.11	86.28	100.0	83.25	68.58
18	86.82	147.95	87.31	91.99	100.0	83.34	68.67	47	54.14	176.19	82.04	86.2	100.0	83.26	68.58
19	84.06	149.69	86.98	91.64	100.0	83.63	68.9	48	53.83	176.56	81.97	86.13	100.0	83.26	68.59
20	81.58	151.37	86.67	91.29	100.0	83.56	68.84	49	53.54	176.9	81.9	86.06	100.0	83.27	68.59
21	79.29	152.98	86.38	90.96	100.0	83.5	68.8	50	53.28	177.22	81.84	85.99	100.0	83.28	68.6
22	77.17	154.54	86.08	90.64	100.0	83.45	68.76	51	53.03	177.53	81.78	85.93	100.0	83.29	68.61
23	75.2	156.03	85.8	90.34	100.0	83.41	68.72	52	52.8	177.81	81.73	85.88	100.0	83.32	68.63
24	73.38	157.46	85.53	90.04	100.0	83.38	68.7	53	52.59	178.08	81.68	85.83	100.0	83.31	68.62
25	71.69	158.83	85.28	89.76	100.0	83.36	68.68	54	52.39	178.32	81.63	85.78	100.0	83.3	68.61
26	70.12	160.13	85.04	89.49	100.0	83.35	68.67	55	52.21	178.55	81.58	85.73	100.0	83.29	68.6
27	68.67	161.38	84.81	89.23	100.0	83.34	68.66	56	52.03	178.77	81.54	85.69	100.0	83.28	68.59
28	67.32	162.57	84.59	88.99	100.0	83.35	68.66	57	51.87	178.97	81.51	85.65	100.0	83.28	68.59
29	66.08	163.7	84.38	88.75	100.0	83.35	68.67	58	51.73	179.16	81.47	85.61	100.0	83.27	68.58
30	64.92	164.77	84.18	88.53	100.0	83.37	68.68	59	51.59	179.34	81.44	85.58	100.0	83.27	68.57

Table A.130.: Fe^{25+}

Step	$\hat{E}$	$\hat{T}$	P_1	P_2	P_T	P_S	P_{AS}	Step	$\hat{E}$	$\hat{T}$	P_1	P_2	P_T	P_S	P_{AS}
2	0.0	85.23	0.0	0.0	0.0	0.0	0.0	31	67.39	162.51	84.6	89.0	100.0	83.78	69.02
3	0.0	89.71	0.0	0.0	0.0	0.0	0.0	32	66.34	163.46	84.43	88.8	100.0	83.84	69.07
4	0.0	94.29	0.0	0.0	0.0	0.0	0.0	33	65.37	164.35	84.26	88.62	100.0	83.8	69.04
5	0.0	98.93	0.0	0.0	0.0	0.0	0.0	34	64.46	165.2	84.1	88.44	100.0	83.77	69.01
6	0.0	103.61	0.0	0.0	0.0	0.0	0.0	35	63.62	166.01	83.95	88.28	100.0	83.74	68.99
7	0.0	108.29	0.0	0.0	0.0	0.0	0.0	36	62.84	166.76	83.81	88.12	100.0	83.71	68.97
8	0.0	112.94	0.0	0.0	0.0	0.0	0.0	37	62.12	167.48	83.67	87.97	100.0	83.69	68.95
9	0.0	117.53	0.0	0.0	0.0	0.0	0.0	38	61.45	168.15	83.55	87.83	100.0	83.68	68.94
10	0.0	122.03	0.0	0.0	0.0	0.0	0.0	39	60.82	168.79	83.43	87.7	100.0	83.66	68.92
11	0.0	126.4	0.0	0.0	0.0	0.0	0.0	40	60.24	169.39	83.32	87.58	100.0	83.65	68.91
12	122.56	130.61	0.0	0.0	0.0	0.0	0.0	41	59.7	169.95	83.21	87.46	100.0	83.64	68.91
13	112.71	134.65	0.0	0.0	0.0	0.0	0.0	42	59.2	170.48	83.11	87.36	100.0	83.64	68.9
14	108.35	136.59	0.0	0.0	0.0	0.0	0.0	43	58.74	170.98	83.02	87.25	100.0	83.64	68.9
15	102.03	139.59	88.89	93.64	100.0	83.11	68.48	44	58.3	171.44	82.93	87.16	100.0	83.64	68.9
16	98.32	141.47	88.53	93.28	100.0	83.31	68.65	45	57.9	171.88	82.84	87.07	100.0	83.64	68.9
17	94.9	143.29	88.19	92.92	100.0	83.51	68.81	46	57.53	172.29	82.77	86.99	100.0	83.64	68.91
18	91.74	145.05	87.85	92.57	100.0	83.7	68.97	47	57.18	172.68	82.69	86.91	100.0	83.65	68.91
19	88.81	146.75	87.53	92.23	100.0	84.0	69.21	48	56.86	173.04	82.63	86.83	100.0	83.66	68.91
20	86.1	148.39	87.22	91.9	100.0	83.94	69.16	49	56.56	173.38	82.56	86.77	100.0	83.66	68.92
21	83.63	149.98	86.93	91.58	100.0	83.88	69.11	50	56.28	173.69	82.5	86.7	100.0	83.67	68.93
22	81.4	151.5	86.65	91.27	100.0	83.84	69.08	51	56.02	173.99	82.45	86.64	100.0	83.68	68.94
23	79.33	152.95	86.38	90.97	100.0	83.8	69.05	52	55.77	174.27	82.4	86.58	100.0	83.71	68.96
24	77.42	154.35	86.12	90.68	100.0	83.77	69.02	53	55.55	174.53	82.35	86.53	100.0	83.7	68.95
25	75.64	155.69	85.86	90.41	100.0	83.75	69.0	54	55.34	174.77	82.3	86.48	100.0	83.69	68.94
26	73.99	156.97	85.62	90.14	100.0	83.74	68.99	55	55.15	174.99	82.26	86.44	100.0	83.68	68.93
27	72.47	158.19	85.4	89.89	100.0	83.73	68.99	56	54.97	175.21	82.22	86.39	100.0	83.68	68.92
28	71.05	159.35	85.18	89.65	100.0	83.73	68.99	57	54.8	175.4	82.19	86.35	100.0	83.67	68.91
29	69.74	160.46	84.98	89.42	100.0	83.74	69.0	58	54.64	175.59	82.15	86.32	100.0	83.66	68.91
30	68.52	161.51	84.78	89.21	100.0	83.76	69.01	59	54.5	175.76	82.12	86.28	100.0	83.66	68.9

Table A.131.: Fe^{26+}

Step	$\hat{E}$	$\hat{T}$	P_1	P_2	P_T	P_S	P_{AS}	Step	$\hat{E}$	$\hat{T}$	P_1	P_2	P_T	P_S	P_{AS}
2	0.0	83.7	0.0	0.0	0.0	0.0	0.0	31	70.97	159.42	85.17	89.64	100.0	84.13	69.32
3	0.0	88.1	0.0	0.0	0.0	0.0	0.0	32	69.87	160.35	85.0	89.45	100.0	84.19	69.37
4	0.0	92.58	0.0	0.0	0.0	0.0	0.0	33	68.85	161.23	84.84	89.26	100.0	84.15	69.34
5	0.0	97.13	0.0	0.0	0.0	0.0	0.0	34	67.9	162.06	84.68	89.09	100.0	84.12	69.31
6	0.0	101.72	0.0	0.0	0.0	0.0	0.0	35	67.02	162.85	84.54	88.93	100.0	84.1	69.29
7	0.0	106.31	0.0	0.0	0.0	0.0	0.0	36	66.2	163.59	84.4	88.78	100.0	84.07	69.27
8	0.0	110.87	0.0	0.0	0.0	0.0	0.0	37	65.44	164.29	84.27	88.63	100.0	84.05	69.25
9	0.0	115.37	0.0	0.0	0.0	0.0	0.0	38	64.73	164.95	84.15	88.49	100.0	84.04	69.24
10	0.0	119.78	0.0	0.0	0.0	0.0	0.0	39	64.08	165.57	84.03	88.37	100.0	84.02	69.23
11	0.0	124.07	0.0	0.0	0.0	0.0	0.0	40	63.47	166.16	83.92	88.24	100.0	84.01	69.22
12	0.0	128.2	0.0	0.0	0.0	0.0	0.0	41	62.9	166.71	83.82	88.13	100.0	84.01	69.21
13	118.66	132.16	0.0	0.0	0.0	0.0	0.0	42	62.37	167.23	83.72	88.02	100.0	84.0	69.21
14	114.07	134.06	0.0	0.0	0.0	0.0	0.0	43	61.89	167.71	83.63	87.92	100.0	84.0	69.21
15	109.84	135.92	0.0	0.0	0.0	0.0	0.0	44	61.43	168.17	83.55	87.83	100.0	84.0	69.21
16	103.62	138.81	89.03	93.79	100.0	83.62	68.9	45	61.01	168.6	83.47	87.74	100.0	84.0	69.21
17	100.03	140.59	88.69	93.45	100.0	83.83	69.08	46	60.62	169.0	83.39	87.66	100.0	84.01	69.21
18	96.71	142.32	88.37	93.11	100.0	84.03	69.24	47	60.25	169.38	83.32	87.58	100.0	84.01	69.21
19	93.63	143.99	88.05	92.78	100.0	84.35	69.5	48	59.91	169.73	83.25	87.51	100.0	84.02	69.22
20	90.79	145.59	87.75	92.46	100.0	84.29	69.45	49	59.6	170.06	83.19	87.44	100.0	84.02	69.23
21	88.16	147.14	87.46	92.15	100.0	84.24	69.41	50	59.3	170.37	83.13	87.38	100.0	84.03	69.23
22	85.72	148.63	87.18	91.85	100.0	84.19	69.37	51	59.03	170.66	83.07	87.32	100.0	84.04	69.24
23	83.5	150.06	86.91	91.56	100.0	84.16	69.34	52	58.78	170.93	83.02	87.26	100.0	84.07	69.27
24	81.49	151.43	86.66	91.28	100.0	84.13	69.32	53	58.54	171.19	82.98	87.21	100.0	84.06	69.25
25	79.63	152.74	86.42	91.01	100.0	84.11	69.3	54	58.32	171.43	82.93	87.16	100.0	84.05	69.24
26	77.9	154.0	86.18	90.75	100.0	84.1	69.29	55	58.12	171.65	82.89	87.12	100.0	84.04	69.23
27	76.3	155.19	85.96	90.51	100.0	84.09	69.29	56	57.93	171.85	82.85	87.08	100.0	84.04	69.23
28	74.81	156.33	85.74	90.27	100.0	84.09	69.29	57	57.75	172.05	82.81	87.04	100.0	84.03	69.22
29	73.43	157.41	85.54	90.05	100.0	84.1	69.3	58	57.59	172.23	82.78	87.0	100.0	84.03	69.21
30	72.16	158.44	85.35	89.84	100.0	84.12	69.31	59	57.43	172.4	82.75	86.96	100.0	84.02	69.21

Bibliography

Aschwanden, M., *Physics of the Solar Corona*, Springer-Verlag Berlin Heidelberg New York, 2004.

Berger, L., Velocity Distribution Functions of Heavy Ions in the Solar Wind at 1 AU, Ph.D. thesis, IEAP, CAU-Kiel, Germany, 2008.

Bochsler, P., F. Auchere, and R. M. Skoug, Helium-hydrogen fractionation in the solar wind - How much is due to inefficient Coulomb drag?, *SOHO-17. 10 Years of SOHO and Beyond, Proceedings of the conference held 7-12 May, 2006 at Giardini Naxos, Sicily, Italy.*, 2006.

Bodmer, R., Kollimator und Energieanalysator beim WIND-SWICS Ionen-Massenspektrometer, Master's thesis, Physical Institute, University of Bern, 1992.

Bodmer, R., and P. Bochsler, The helium isotopic ratio in the solar wind and ion fractionation in the corona by inefficient Coulomb drag, *The Astronomy and Astrophysics Review*, *337*, 921–927, 1998.

Burbidge, E., G. Burbidge, W. Fowler, and F. Hoyle, Synthesis of the Elements in Stars, *Review of Modern Physics*, *29, Number 4*, 1957.

Clayton, D., *Isotopes in the Cosmos*, Camebridge University Press, 2003.

Dobler, F., Variabilität des Si/Mg Verhältnisses im Sonnenwind mit ACE/SWICS, Master's thesis, Physikalisches Institut der Universität Bern, 2000.

Gloeckler, G., et al., The solar wind ion composition spectrometer, *A&A*, *92*(2), 267–289, 1992.

Gloeckler, G., et al., Investigation of the composition of solar and interstellar matter using solar wind and pickup ion measurements with SWICS and SWIMS on the ACE spacecraft, *Space Science Reviews*, *86*(1-4), 497–539, doi:10.1023/A:1005036131689, 1998.

Gonin, M., Ein semiempirisches Modell des Ladungsaustausches von niederenergetischen Ionen beim Durchgang durch dünne Folien, zur Eichung von isochronen Flugzeit-Massenspektrometern, Ph.D. thesis, University of Bern, 1995.

Harris, M. J., D. L. Lambert, and A. Goldman, The C-12/C-13 and O-16/O-18 ratios in the solar photosphere, *Royal Astronomical Society, Monthly Notices (ISSN 0035-8711)*, *224*, 237–255, 1987.

Hollweg, J. V., Drivers of the solar wind: then and now, *Philosophical Transactions of Royal Society A*, *364*, 505–527, 2006.

Högberg, G., H. Norden, and H. Berry, Angular distributions of ions scattered in thin carbon foils, *Nuclear Instruments and Methods*, *90*, 283–288, 1970.

Bibliography

Ipavich, F. M., L. Ma Sung, and G. Gloeckler, Measurements of energy loss of H, He, C, N, O, Ne, S, Ar, Fe, and Kr passing through thin carbon foils, *Tech. rep.*, Departement of Physics and Astronomy, University of Maryland, USA, 1982.

Kallenbach, R., et al., Isotopic composition of solar wind neon measured by CELIAS/MTOF on board SOHO, *Journal of Geophysical Research*, *102*, 26,895–26,904, 1997a.

Kallenbach, R., et al., Limits to the fractionation of isotopes in the solar wind as observed with SOHO/CELIAS/MTOF, in *Correlated Phenomena at the Sun, in the Heliosphere and in Geospace*, pp. 33 – 37, ESA SP-415, 1997b.

Kohl, J. L., et al., First results from the SOHO Ultraviolet Coronagraph Spectrometer, *Solar Physics*, *175*, 613–644, 1997.

Köten, M., Detection efficiencies for STEREO/PLASTIC and ACE/SWICS, Master's thesis, IEAP, CAU-Kiel, Germany, 2005.

Press, W. H., S. A. Teukolsky, W. T. Vetterling, and B. P. Flannery, *Numerical Recipes in C - The Art of Scientific Computing*, second ed., Cambridge University Press, 1992.

Prölls, G., *Physik des erdnahen Weltraums*, Springer, 2004.

Rothard, H., K. Kroneberger, A. Clouvas, E. Veye, P. Lorenzen, N. Keller, J. Kemmler, W. Meckbach, and K.-O. Groeneveld, Secondary electron yields from thin foils: A possible probe for the electronic stopping power of heavy ions, *Physical Review A*, *41*, 2521–2535, 1989.

Stix, M., *The Sun: An Introduction*, Springer, 2004.

Turcotte, S., and R. F. Wimmer-Schweingruber, Solar evolution/elemental segregation and possible implications for studies of interplanetary particles, *J. Geophys. Res.*, *107*, SSH 5–1, citeID 1442, DOI 10.1029/2002JA009418, 2003.

Unsöld, B.-B., A., *Der neue Kosmos*, Springer Verlag Berlin Heidelberg New York, 2005.

von Steiger, R., N. A. Schwadron, L. A. Fisk, J. Geiss, G. Gloeckler, S. Hefti, B. Wilken, R. F. Wimmer-Schweingruber, and T. H. Zurbuchen, Composition of quasi-stationary solar wind flows from Ulysses/Solar Wind Ion Composition Spectrometer, *JGR*, *105*(A12), 27,217–27,238, 2000.

Wallerstein, G., et al., Synthesis of the elements in stars: forty years in progress, *Review of Modern Physics*, *69, Number 4*, 1997.

Wiens, R., P. Bochsler, D. Burnett, and R. F. Wimmer-Schweingruber, Solar and solar-wind isotopic compositions, *Earth and Planetary Science Letters*, *222*, 697–712, 2004.

Woods, P., Carbon isotope measurements in the Solar System, 2009.

Woods, P., and K. Willacy, Carbon Isotope Fractionation in Protoplanetary Disks, *The Astrophysical Journal*, *693*, 1360–1378, 2009.

Ziegler, J., J. Biersack, and U. Littmark, The Stopping and Range of Ions in Matter, *Pergamon Press, New York, 1*, 1985.

Danksagung

Mein Dank gilt in erster Linie Prof. Dr. Robert F. Wimmer-Schweingruber für die Vergabe dieser Arbeit und die sehr gute Betreuung. Desweiteren möchte ich allen Mitgliedern der AG Wimmer danken, die Ihren Teil zu dieser Arbeit beigetragen haben. Besonders Herrn Dr. Lars Berger, Herrn Dipl. phys. Onno Kortmann, Herrn Dipl. phys. Roland Rodde und Herrn Dipl. phys. Bent Ehresmann möchte ich darüber hinaus für die Zusammenarbeit und die zahllosen Diskussionen in kleiner Runde danken. Ich danke ebenfalls der Deutschen Forschungs-Gemeinschaft und dem Land Schleswig-Holstein, die diese Arbeit finanziell unterstützt haben.

Für die seelische Unterstützung während der Promotionszeit möchte ich, ganz besonders meiner Familie, im speziellen meiner Mutter Sati Köten, allen Freunden und Bekannten, und dem gesamten Cafe de Cuba Team danken. Ich widme diese Arbeit meinem Vater Süleyman Köten (†18.06.1988).

Lebenslauf

Name:	Muharrem Köten	
Wohnort:	Alsenstr. 25, 24118 Kiel	
Geboren:	27.3.1977 in Neumünster	
Familienstand:	Ledig	
Staatsangehörigkeit:	Türkisch	

Schulbildung :	1983 - 1985	Vicelinschule, Neumünster
	1985 - 1987	Rudolf-Tonner-Schule, Neumünster
	1987 - 1996	Integrierte Gesamtschule, Neumünster-Brachenfeld
		Abschluß: Abitur

Ausbildung :	1996 - 1999	Ausbildung zum Sozialversicherungsfachangestellten bei der Deutschen Angestellten Krankenkasse
Studium :	1999 - 2005	Studium der Physik an der Christian-Albrechts Universität zu Kiel, Diplomnote : sehr gut Diplomarbeit mit dem Titel "Detection efficiencies for STEREO/PLASTIC and ACE/SWICS", Betreuer: Prof. Dr. R. F. Wimmer-Schweingruber

Berufstätigkeit :	Seit Mai 2005	Wissenschaftlicher Mitarbeiter der Arbeitsgruppe Wimmer am Institut für Experimentelle und Angewandte Physik der Christian-Albrechts Universität zu Kiel

Eidesstattliche Versicherung

Hiermit versichere ich an Eides Statt, dass ich die vorliegende Arbeit abgesehen vom Rat meiner akademischen Lehrer ohne fremde Hilfe und lediglich unter der Verwendung der angegebenen Literatur sowie den bekannten Nachschlagewerken der Naturwissenschaften angefertigt habe, und sie nach Inhalt und Form meine eigene ist. Diese Arbeit ist unter Einhaltung der Regeln guter wissenschaftlicher Praxis entstanden.
Des weiteren versichere ich, dass diese Arbeit weder ganz noch teilweise an anderer Stelle zur Prüfung vorlag. Frühere Promotionsversuche wurden von mir nicht vorgenommen.

Kiel, den _____

Muharrem Köten